UNIVERSIDAD COMPLUTENSE DE MADRID

FACULTAD DE CIENCIAS QUÍMICAS
Departamento de Química Orgánica I

TESIS DOCTORAL

FtsZ protein as a therapeutic target for the development of new antibacterial agents
FtsZ como diana terapéutica para el desarrollo de nuevos agentes antibacterianos

MEMORIA PARA OPTAR AL GRADO DE DOCTOR

PRESENTADA POR

Marta Elena Artola Pérez de Azanza

Directores

María Luz López Rodríguez
María del Mar Martín-Fontecha Corrales
Henar Vázquez Villa

Madrid, 2014

UNIVERSIDAD COMPLUTENSE DE MADRID

FACULTAD DE CIENCIAS QUÍMICAS

Departamento de Química Orgánica I

FtsZ PROTEIN AS A THERAPEUTIC TARGET FOR THE DEVELOPMENT OF NEW ANTIBACTERIAL AGENTS

FtsZ COMO DIANA TERAPÉUTICA PARA EL DESARROLLO DE NUEVOS AGENTES ANTIBACTERIANOS

PhD candidate

Marta Elena Artola Pérez de Azanza

Advisors:
Dra. María Luz López Rodríguez
Dra. María del Mar Martín-Fontecha Corrales
Dra. Henar Vázquez Villa

MADRID, 2014

“If I have seen further it is by standing on the shoulders of giants”

Isaac Newton

El presente trabajo ha sido realizado en el laboratorio de Química Médica dirigido por la ***Dra. María Luz López Rodríguez*** *en el Departamento de Química Orgánica I de la Facultad de Ciencias Químicas de la Universidad Complutense de Madrid, bajo la supervisión de las* ***Dras. Henar Vázquez Villa*** *y* ***María del Mar Martín-Fontecha Corrales*** *a quienes deseo expresar mi más profundo agradecimiento por su acogida en este grupo de investigación, por sus continuas enseñanzas a lo largo de todo este tiempo, y muy especialmente, por todo el ánimo, apoyo y confianza depositada en mí.*

Asimismo, quiero expresar mi agradecimiento:

A mis compañeros de laboratorio con los que tan buenos momentos he compartido, en especial a Nono y Carlos que me han enseñado tanto, a los que ya estaban cuando llegué y que han contribuido a crear los lazos tan importantes en el grupo, Belli, Silvia, Tania, Ángel, Marga, José, Lidia, Rocío, Moisés, Ana e Inés. A los que llegaron después y han sabido mantener el espíritu de compañerismo y de trabajo en equipo, Débora, Ainoa, Javi, Paco, Gloria, Sergio, Leticia, Nagore y Clara, sin olvidarme de la inestimable ayuda de Jorge.

Al Dr. José Manuel Andreu del Centro de Investigaciones Biológicas (CIB) del Centro Superiores de Investigaciones Científicas (CSIC) y a su grupo de investigación, en concreto a las Dras. Sonia Huecas, Laura Ruiz-Avila y Lidia Araujo y a Albert Vergoñós, por llevar a cabo la evaluación biológica de los compuestos sintetizados en esta tesis doctoral y estar siempre dispuestos a resolver mis dudas. Al Dr. Pablo Chacón y Erney Ramirez-Aportela del Instituto de Química Física "Rocasolano" del CSIC, por realizar los estudios de modelización y la dinámica molecular de los compuestos. Al Prof. Stephan Sieber de la Technische Universität München (TUM) en Munich, por su acogida en el laboratorio y sus enseñanzas en la determinación de las Concentraciones Mínimas Inhibitorias (CMI) en bacterias patógenas. Al grupo del Prof. Baran del "The Scripps Research Institute" (TSRI) en San Diego, especialmente al Dr. Christian Kuttruff, por hacerme sentir una más durante mi estancia predoctoral.

A la Dra. Beatriz de Pascual-Teresa de la Universidad San Pablo-CEU de Madrid por su atención y asesoramiento durante mis estudios de Farmacia. Al equipo de Janssen Cilag S.A., y especialmente a Luz, Han Min y Susana por animarme a emprender este camino.

A mis padres, a mis hermanos y a Francesco. Sin su apoyo y cariño no habría sido posible este trabajo. En especial a mi hermana María.

TABLE OF CONTENTS

ABBREVIATIONS AND ACRONYMS

Throughout this manuscript, abbreviations and acronyms recommended by the American Chemical Society in the Organic Chemistry and Medicinal Chemistry areas have been employed (revised in the *Journal of Organic Chemistry* and *Journal of Medicinal Chemistry* on September 2014; http://pubs.acs.org/paragonplus/submission/joceah/joceah_abbreviations.pdf and http://pubs.acs.org/paragonplus/submission/jmcmar/jmcmar_abbreviations.pdf. In addition, those indicated below have also been used.

B. subtilis	*Bacillus subtilis*
Bs-FtsZ	FtsZ of *Bacillus subtilis*
CAI	centro de asistencia a la investigación
DIPEA	diisopropylethylamine
DMBA	1,3-dimethylbarbituric acid
EGCG	(-)-epigallocatechin gallate
FASN	fatty acid synthase
FtsZ	filamenting temperature sensitive mutant Z
GFP	green fluorescent protein
MSSA	methicillin-susceptible *Staphyilococcus aureus*
NBD	nitrobenzoxadiazole
NHS	*N*-hydroxysuccinimide
Cl-NBD	4-chloro-7-nitro-2,1,3-benzoxadiazole
PAβN	phenyl-arginine-beta-naphthylamide
PODO	podophyllotoxin
PyBroP®	bromotripyrrolidinophosphonium hexafluorophosphate
SEM	standard error media
TAMRA	5-(and-6)-carboxytetramethylrhodamine
Tf_2O	trifluoromethanesulfonic anhydride

1. INTRODUCTION

Hospital and community-acquired infections associated to antibiotic resistance have become a major public concern at a time when antibacterial drug discovery efforts are declining, and the need for effective treatments against new multi-drug resistant pathogens is desperately increasing.[1] Recent studies estimate that at least 2 million people acquire serious infections in which bacteria are resistant to antibiotics[2,3] and more than 23,000 people die as a direct result of resistant bacterial infections in the United States of America (USA) each year.[4] This number is probably higher since deaths attributed to other diseases (*e.g.*, chronic obstructive pulmonary disease, human immunodeficiency virus and cancer) for which a bacterial infection is the terminal cause are not included.[5] In addition, antibacterial resistant infections cost more than 20 billion dollars to the USA healthcare system per year due to prolonged hospitalizations and costlier treatments compared to infections susceptible to antibiotics.

1.1. Antibacterial Drug Discovery

Antibacterial chemotherapy has its origin in the late 19th century with the discoveries performed by renowned scientists such as Robert Koch or Louis Pasteur and the search of Paul Ehrlich for a "magic bullet" able to selectively kill bacterial cells, which was a turning point in human history.[6] However, it was not until the discovery of sulfonamides as a chemical therapy and natural β-lactam antibiotics in the 1930s when it gave rise to the modern age of antibacterials in which rapid treatment of patients with previously mortal bacterial infections was possible (Figure 1). Over the next 40 years (1930-1970), now seen as the ''golden era'' of antibiotic research, the majority of antibiotic drug classes in use today were discovered.[7] Nonetheless, after this period, all newly approved antibiotics, except the topical drug mupirocin developed in 1985,[8] were based on medicinal chemistry programs rediscovering existing treatments with modified versions of already known scaffolds rather than novel chemical entities. This led to a period known as "innovation gap", when we dug our own grave and bacteria easily acquired resistance to all marketed antibiotics, even before the antibacterials were commercialized. Since 2000, the situation has improved and five new classes of antibiotics have been approved by the Food and Drug Administration (FDA).

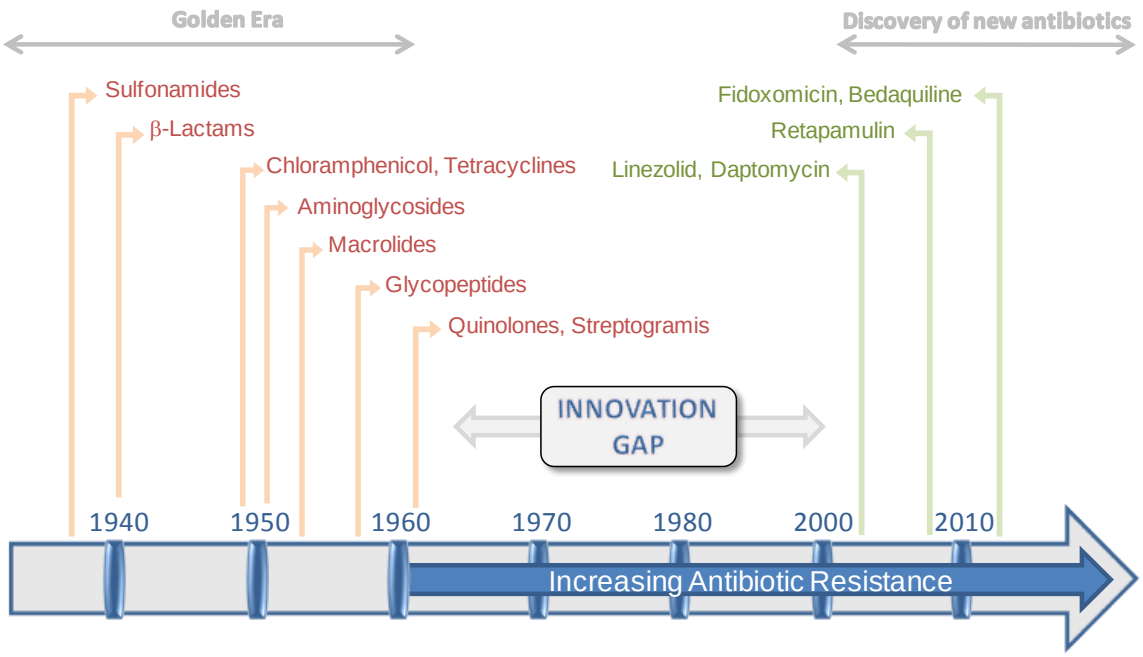

Figure 1. Innovation gap between 1962 and 2000 and antibiotic resistance.

Thus, linezolid, daptomycin, and the topical retapamulin were marketed in the first decade of the 21st century (Figure 2).[9] More recently, fidaxomicin -a macrocyclic fermentation product with a narrow spectrum for pathogenic *Clostridium difficile*- has been approved, and bedaquiline, a diarylquinoline developed by Janssen that specifically inhibits mycobacterial adenosine 5'-triphosphate synthase interfering with the bacterial energy metabolism, has also been marketed. This compound was fast tracked through clinical trials for the treatment of tuberculosis thanks to its combination with at least three drugs active against the patient's tuberculosis isolate.[10,11] However, it is worth mentioning that none of these derivatives, except bedaquiline, are truly novel antibiotics, having been discovered decades ago and rescued from failed campaigns. More importantly, all these new agents have a Gram-positive spectrum whereas Gram-negative therapies are urgently needed.

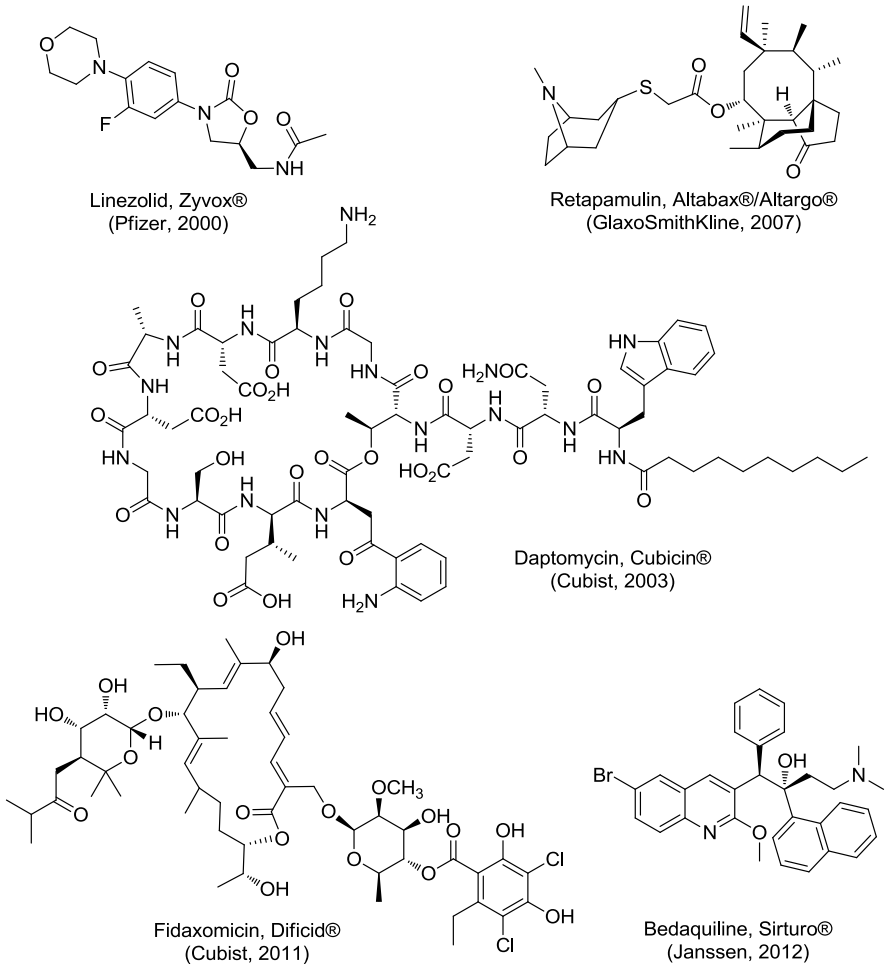

Figure 2. New antibiotics approved by the FDA since 2000.

In order to solve this global bacterial threat, pharmaceutical industry, prompted by the bacterial genome discovery in 1995, focused on the development of synthetic analogues and high tech approaches based on genomics, combinatorial chemistry, huge high-throughput screening (HTS) campaigns and rational design. However, the disappointing results led to an antibacterial crisis where only four big Pharma remain investigating in the field: AstraZeneca, Novartis, GlaxoSmithKline, and Sanofi-Aventis.[12] This crisis was caused by different reasons that have been deeply discussed.[2,13-15] First, HTS has shown to be four- to five-fold less productive than for other therapeutic targets, which has been mainly related to a wrong selection of the HTS libraries.

Noteworthy, most HTS campaigns use bacteria cultures that are kept under favorable growth conditions and hits found in such conditions may result in less active or even inactive in metabolic resting bacteria or *in vivo* models of chronic infections.[16]

Moreover, clinical trials with antibacterials are conducted in patients with drug-susceptible infections whereas antibiotics for resistant pathogens are desperately needed. All this is happening at a time when the FDA regulations are enforced and reaching phase I clinical trials is more difficult than ever. Last but not least, the return in investment is quite modest owing to short term treatment for acute infections and low drug pricing if compared to other therapeutic areas. Consequently, a large number of big pharmaceutical companies has left antibacterial research. Contrary, small companies and biotechs seem to see an opportunity in this situation and are filling the gap rescuing medicinal chemistry programs and clinical trials that have been abandoned by large companies.[17]

In order to solve the antibiotic drug discovery decline, several strategies have been proposed.[2,6,15,18] Most antibacterials were discovered at a time when few molecular and mechanism pathways were known and target based-programs have not been very successful. Therefore, more phenotypic rather than target based HTS and screenings in which bacterial penetration rules are reformulated should be implemented. In addition, driving HTS in metabolic resting stages bacteria emerges as a promising hit-discovery strategy.

Regarding the antibacterial drug discovery process itself, it presents unique challenges due to the differences between eukaryote host cells and the target bacteria cells. Indeed, finding a hit is just the beginning in a therapeutic area where one single compound must inhibit different Gram-positive and Gram-negative pathogens all with different molecular targets, permeability and metabolic pathways. Therefore, factors as bacterial cell penetration and efflux, metabolism and elimination, together with bacteria resistance must be seriously taken into consideration.[19] With respect to permeability, bacterial cell wall of Gram-positive bacteria is very different from Gram-negative in terms of structure and physical properties. Gram-negative antibacterials usually enter the cell through porins in the outer membrane followed by diffusion across cytoplasmatic membrane, and therefore are usually more hydrophilic, with limited molecular weight and high charge density compounds at physiological pH. Contrary, Gram-positive bacteria possess only a cytoplasmatic membrane, so bigger and more lipophilic agents are required to cross it by diffusion. As if all this was not enough, higher doses of antibiotics are needed in order to achieve effectiveness when compared to other drugs due to poor penetration. At these high doses, acceptable side effects and good pharmacokinetic properties must be demonstrated to allow competitive and convenient dosing profile.[15]

However, it is undisputed that the biggest problem in this area is the antimicrobial resistance, in which not only hospital but also community acquired resistances to almost every new antibiotic have been developed. As a result, we are entering a post-antibiotic era with limited treatment options for multiple bacterial infections, highlighting the urgent need for novel approaches.[20,21]

1.2. Antibacterial Targets and Resistance

Currently, commercial antibiotics inhibit a small number of targets which are involved in the synthesis of (i) the cell wall, (ii) proteins, (iii) folate or (iv) nucleic acids (Figure 3). Although there are more than fifteen different antibacterial mechanisms of action, none of them has escaped from bacterial resistance. Methicillin-resistant *Staphylococcus aureus* (MRSA) and glycopeptide resistant enterococci (GRE) are examples of Gram-positive bacteria that have already shown resistance to the last arsenal of new marketed antibiotics such as daptomycin and linezolid.[22,23] The situation is even more concerning for Gram-negative bacteria, where no new drug candidates are currently in advanced clinical development stages and multi-resistant strains have developed very effective ways to deal with the newest broad spectrum therapies.[2,24]

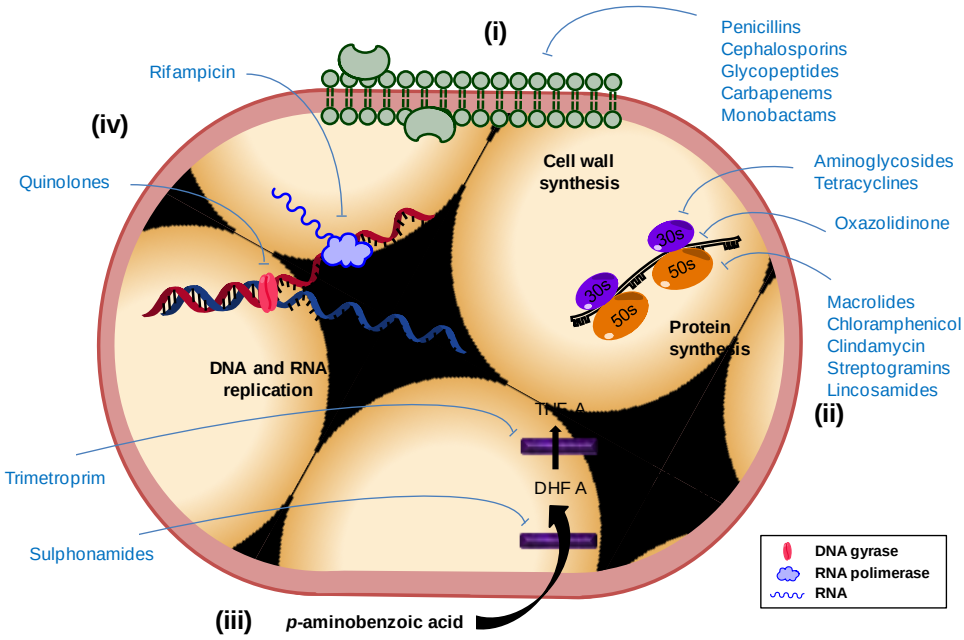

Figure 3. Antibiotics and their antibacterial targets.[15]

Although antibiotic resistance is not a new concept, the number of multidrug resistant pathogens -also colloquially known as “superbugs”-, the geographic spread and the different resistant mechanisms in single organisms are unprecedented and mounting.[25] In this sense, genetic resistance firstly arises from a chromosomal mutation followed by clonal spread or by acquisition of an antibiotic resistance gene that can be transfer from one bacterium to another through different routes such as plasmids, bacteriophages, naked DNA or transposons.[26] Additionally, many different mechanisms of antibiotic resistance have been described (Figure 4). Some target the antibiotic itself by (a) enzymatic degradation or modification, as for example β-lactamases demolish penicillins or cephalosporins. Bacteria can also (b) develop bypass pathways, (c) alter or (d) overexpress a specific intracellular target or even (e) produce new biomolecules that block the target. Furthermore, (f) a decrease membrane permeability or multidrug resistant (MDR) efflux pumps, such as the AcrAB–TolC MDR pump that effluxes linezolid, can drop dramatically the antibiotic intracellular concentration.

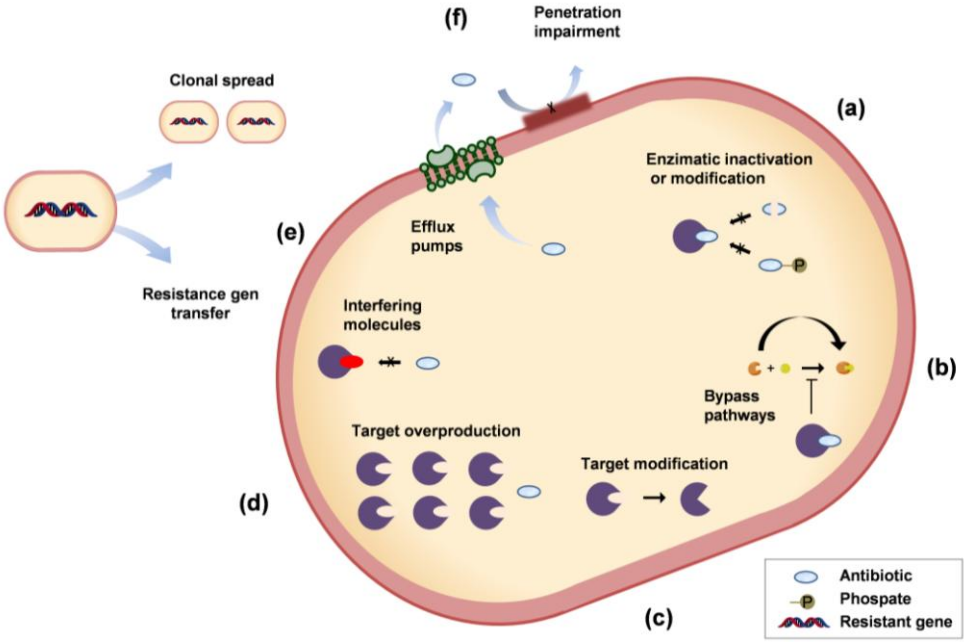

Figure 4. Antibiotic resistance and tolerance mechanisms.[15]

The use of multitarget antibiotics has proved to be very effective in avoiding resistances, and drug combinations have allowed the renaissance of several antibacterial therapies. For example, the use of clavulanic acid, a β-lactamase inhibitor, in combination to amoxicillin resulted in one of

the most popular antibiotics: Augmentine. Other researches involved the development of hybrid inhibitors which combine two different merged antibiotics, or the use of antimicrobial peptides.[27,28] Moreover, the employment of MDR efflux pumps inhibitors, such as NorA in Gram-positive or AcrAB-TolC in Gram-negavive bacteria, can restore susceptibility of antibiotics by increasing their intracellular concentrations.

Notably, one of the most asked question is whether nature has already discovered all useful antibacterial targets or if only the “low-hanging fruit” has been identified.[29] What is unquestionable is that novel mode of action (MoA) agents are urgently needed to overcome the antibiotic resistance problem. Bacteria are prompted to develop new strategies to confront antibiotics, so a multi-disciplinary approach is required and it should be continuously redefined. In summary, the key components for maintaining effective antimicrobial chemotherapy include better use of existing agents, avoiding the misuse or overuse and continuous investment in new and innovative techniques to discover antibiotics with novel MoA.[3,30]

In this context, the bacterial cell division protein Filamenting temperature-sensitive mutant Z (FtsZ), which has not been targeted yet by any commercial antibiotic, has been proposed as an attractive therapeutic target for the discovery of new antibacterial agents.[2,31-33]

1.3. FtsZ and the Divisome

Much progress towards the understanding of bacterial cell division has been made in the last decades. However, the molecular mechanisms and dynamics underlying this process are still unclear. Bacterial cytokynesis is regulated by a macromolecular machinery called the divisome, which consists of an assembly of FtsZ polymers around the cylindrical axis of the cell and more than 20 regulating proteins.[34] FtsZ exists in the bacterial cells both as monomers or highly order polymers depending on whether it is bound to guanosine 5’-triphosphate (GTP) or guanosine 5’-diphosphate (GDP) and which accessory protein is bound to it. At the earliest step of cell division, FtsZ is recruited from the cytoplasm to the division site and undergoes self-assembly by the head-to-tail association of individual subunits at mid-cell creating a GTP-hydrolytic center (Figure 5A). Thus, the GTP-binding promotes the FtsZ polymerization and formation of protofilaments with a longitudinal subunit repeated. Contrary, when GTP is hydrolyzed to GDP, the protofilament gets a curve conformation and disintegrates. In the cell division process, these protofilaments can polymerize in different shaped filaments leading to a ring-like structure known as the Z-ring (Figure 5A).[35,36] The Z-ring is a highly dynamic structure with a half time of a few seconds and there is continuous exchange of FtsZ subunits between the Z-ring and the cytoplasm.[37,38] Other bacterial

division proteins are then recruited to the Z-ring to regulate and form the divisome, a complex that finally constricts to generate the two new daughter cells (Figure 5B).

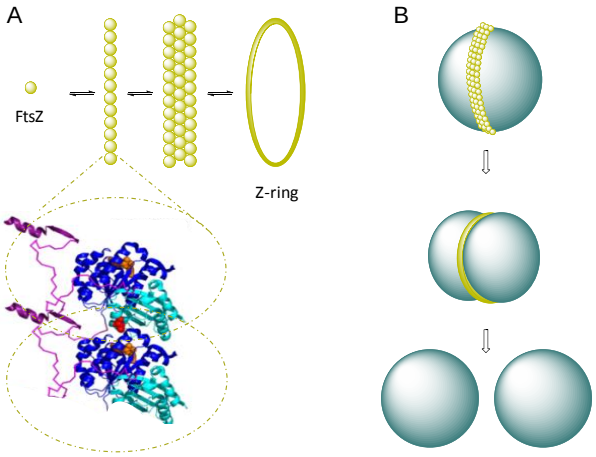

Figure 5. (A) FtsZ polymerization and Z-ring formation. (B) Bacterial division process.

FtsZ polymerization is widely regulated in space and time by placing the Z-ring in a specific place and coordinating the assembly/disassembly balance with DNA replication to ensure an equal partition into two new cells at the right time.[39] A complex regulatory network is committed to orchestrate this division process initiated by FtsZ (Figure 6). In this sense, FtsZ polymerization is closely related to Min family proteins which are responsible from placing the Z-ring at the mid cell when the bacteria is big enough to divide.[40] Then, FtsA and ZipA attach FtsZ to the cell membrane and stabilize FtsZ polymers at the membrane. Shape factors such as SepF and FzlA have an important role in regulating the highly ordered polymer structure which must progressively curve in order to encircle the cell. Furthermore, metabolic and oxidative sensors control the bacterial division depending on the environment of the cell. For example, under nutritional starvation, UgtP does not inhibit FtsZ assembly and the divisome is form earlier leading to smaller daughter cells. Although FtsZ protein is highly conserved among bacteria, its regulators are less so. In this sense, ClpX chaperone is one of the most conserved and its protease activity is responsible from FtsZ degradation.[41]

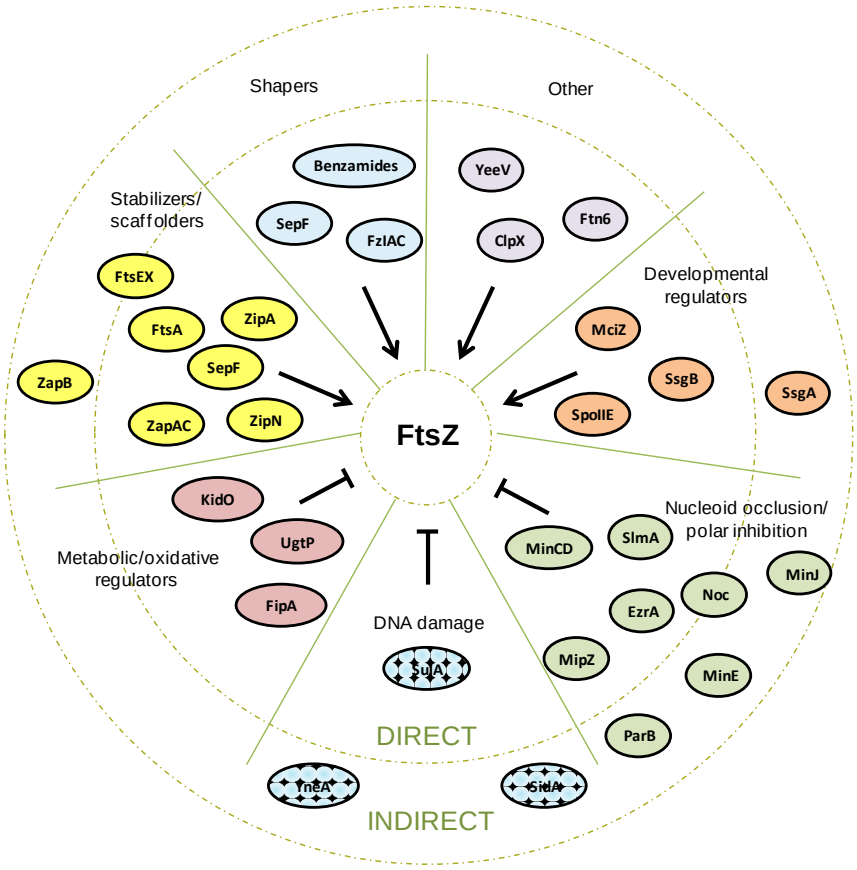

Figure 6. Direct and indirect regulators of FtsZ assembly.

From a structural point of view, FtsZ is a tubulin-like GTPase almost universally conserved throughout the bacteria. Several crystal structures of FtsZ from different bacteria and archaea have been obtained in apo form and in complex with GTP or its closest analogues, as for example *Methanocaldococcus jannaschii*[42] (*M. Jannaschii*) and *Mycobacterium tuberculosis* (*M. tuberculosis*).[43] The enzymatic pocket of this protein is composed of two globular sub-domains, N- and C-terminal regions, separated by the helix H7 as the central core helix (Figure 7).[42,44] During monomer assembling at the polymerization stage, the C-terminal GTPase-activating domain of the upper subunit contacts the nucleotide site of the subunit below by insertion of the T7 loop into the nucleotide binding site and forms the catalytic pocket, what underscores the key role of the GTP-binding site in regulating the FtsZ function. Moreover, the long cleft located between these domains constitutes an additional pocket, equivalent to the taxol binding site in tubulin, that has also been

proposed for ligand binding.[45] Although FtsZ and tubulin have only a 20% of sequence homology, they show high structure similarity. Therefore, selectivity against tubulin is an important factor in the discovery of FtsZ inhibitors. In fact, the identification of FtsZ selective inhibitors has demonstrated that it is possible to bind this protein without observing unwanted side effects through tubulin.[46]

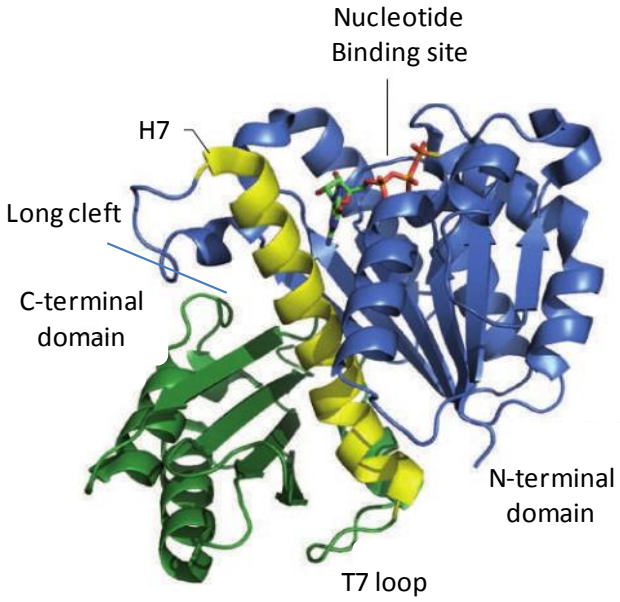

Figure 7. Crystal structure of a *Bacillus subtilis* FtsZ monomer bound to GTP-γS.

Taking into account the key role of FtsZ in the bacterial division, molecules able to inhibit its activity will eventually avoid bacterial viability and may hold promise for the development of clinically efficacious antibiotics with an unexplored MoA.

1.4. FtsZ as an Antibacterial Target

Over the last decade, several compounds have been identified as FtsZ inhibitors perturbing the protein polymerization and the GTPase activity, some of them with promising antibacterial profile.[33,47-50] The reported FtsZ inhibitors able to modulate the assembly or disassembly of the protein include natural products, compounds derived from the tubulin field, and synthetic compounds identified by HTS. However, the binding modes of most of them are still unknown.

1.4.1. Natural Products

Historically, natural products have been one of the most prolific sources of new molecular entities for drug discovery and more importantly in the case of antibiotics. Interestingly, the majority of natural products identified as FtsZ inhibitors are structures with phenolic moieties (Figure 8). Among them, viriditoxin[51] and the macrocycle chrysophaentin A[52] stand out. They act as GTPase inhibitors and block protein assembly in the 10-50 μM range. Both compounds are active against Gram-positive bacteria pathogens such as MRSA, with minimum inhibitory concentration (MIC) values of 4-8 μM in the case of viriditoxin and 2-4 μM for the chrysophaentin A. Curcumin also showed moderate effect increasing FtsZ GTPase activity (at 10-20 μM) and it was prompted to phase I clinical trials at relatively high doses (8 g/day). However, its cytotoxity through the eukaryote homologue tubulin and poor bioavailability stopped its development.[53] Another interesting natural product is the diterpenoid totarol, endowed with antibacterial activity against *M. tuberculosis* at 16 μM.[54,55] Furthermore, a family of five structurally diverse small compounds identified by HTS, zantrins Z1-Z5, inhibited FtsZ GTPase activity and induced hyperstabilization or destabilization of FtsZ protofilaments. Among them, polyphenol derivative Z1, showed the best profile with antibacterial activity against *Escherichia coli* (*E. coli)* at 20 μM and MRSA at 2.5 μM.[56] On the other hand, the two cationic alkaloids sanguinarine and berberine have also been described as FtsZ inhibitors, although the latter also showed moderate effect in tubulin.[57,58] These compounds share a polycyclic scaffold structurally different from the natural products above described, and were used as a starting point to successfully design and synthesize new inhibitors endowed with good antibacterial activity in MRSA and *Enterococcus faecalis* (*E. faecalis*).[59-63]

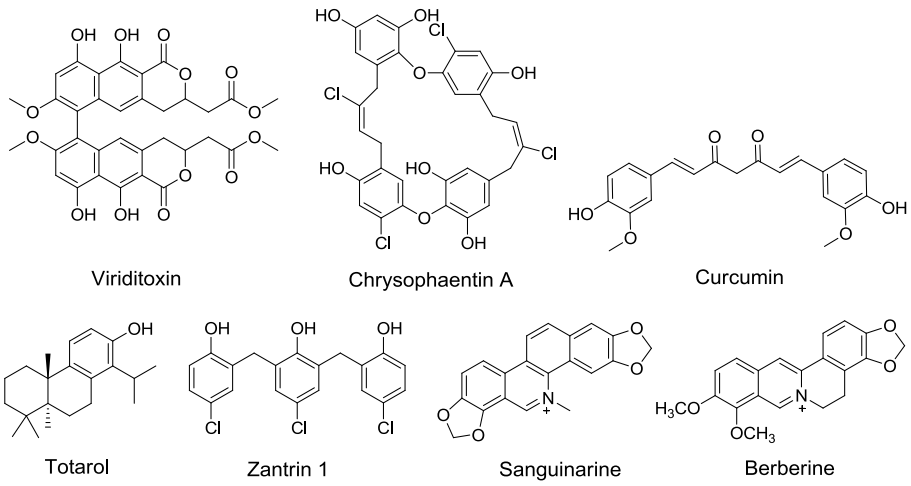

Figure 8. Natural products as FtsZ inhibitors: polyphenolic compounds and cationic alkaloids.

1.4.2. Compounds from the Tubulin Field

The development of FtsZ inhibitors based on the structure of taxol, the most potent tubulin inhibitor, has been another area of research in the identification of new antimicrobials. Hence, a screening of 120 taxanes allowed the identification of new inhibitors such as SB-RA-2001 with good antibacterial properties in *Mycobacterium* strains (MIC = 2.5-5 μM).[64,65] Further modifications led to semisynthetic taxane SB-RA-5001 with activity against drug sensitive and drug resistant *M. tuberculosis* at 1.3-2.5 μM, targeting FtsZ without appreciable cytotoxicity (IC_{50} > 80 μM) (Figure 9). Computational analysis suggested that this inhibitor binds to FtsZ in the long cleft between the C-terminal domain and helix H7.[64,65]

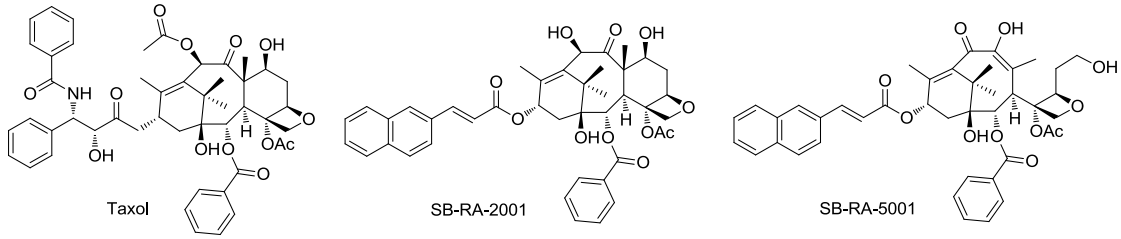

Figure 9. Taxol and its most potent FtsZ inhibitor analogues.

1.4.3. Synthetic Derivatives

One of the main strategies to alter FtsZ polymerization is to perturb the GTPase activity of the protein. Therefore, a forward approach in the development of FtsZ inhibitors has been the design and synthesis of GTP analogues. In fact, C8-substituted GTP derivatives, such as 8-bromo-GTP, inhibit FtsZ polymerization while supporting tubulin assembly, confirming that selective inhibition of the GTP-binding site of this bacterial protein is possible without unwanted side effects in eukaryotic cells (Figure 10).[46] Unfortunately, these GTP derivatives lack antibacterial activity probably due to their poor penetration through bacterial cell wall. On the other hand, a family of novel trisubstituted benzimidazoles that increase GTPase activity and disable FtsZ assembly has been developed through a medicinal chemistry program. Among them, compound 1b-G1 exhibited the best antibacterial activity in resistant strains of *M. tuberculosis* (MIC = 1 μM) although its binding site is still unknown.[66] Another interesting synthetic inhibitor identified from a screening of a 105,000 compound library by Prolysis Ltd company and further hit optimization process is PC170942, with antibacterial activity in Gram-positive bacteria [MIC = 16 μM in *Bacillus subtilis* (*B. subtilis*) and 64 μM in *Staphylococcus aureus* (*S. aureus*)].[67]

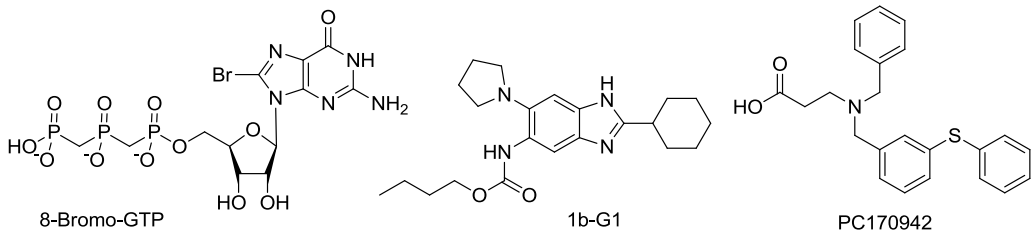

Figure 10. Synthetic FtsZ inhibitors.

Nonetheless, the biggest contribution to the synthetic inhibitors came from the development of 3-methoxybenzamide (3-MBA) derivatives (Figure 11).[68] SAR studies carried out around this scaffold have explored the influence of the halogens at positions 2 and 6, and the length of an alkyl chain in the alkoxy group, showing that fluorine atoms and a nonyl chain gave the best antibacterial activity (MIC = 1.7 μM in *S. aureus*).[69] Then, replacement of the 3-alkoxy moiety by a variety of heteroarylmethoxy substituents allowed the identification of more drug-like derivatives: PC190723 and 8j.[70,71] These compounds have potent antistaphylococcal activity [MIC (8j) = 0.7 μM and MIC (PC190723) = 2.8 μM] and although 8j showed better antibacterial activity, thiazolopyridine PC190723 exhibited better pharmacokinetic profile due to a lower plasma protein binding. Indeed, this compound is the most studied FtsZ inhibitor so far.[72,73] PC190723 is an FtsZ polymer-stabilizing agent that modulates the flexibility and assembly of the protein, inhibits the GTPase activity at 10 μM and has been characterized as a potent selective bactericide. Notably, it is the first inhibitor shown to be efficacious in an *in vivo* model of bacterial infection. A dose of 30 mg/kg of PC190723 completely protected mice inoculated with a lethal dose of *S. aureus.* One of the major drawbacks of this compound has been its lack of activity in Gram-negative bacteria probably due to its inability to target *E. coli* FtsZ itself. In this sense, Kaul and coworkers have demonstrated very recently that the co-administration of PC190723 with the efflux pump inhibitor PAβN restored antimicrobial activity in *E. coli, Klebsiella pneumonia,* and *Acinetobacter baumannii.* However, even under efflux pump inhibition conditions, its activity in Gram-negative strains is 8- to 16-fold lower than in *S. aureus*.[74]

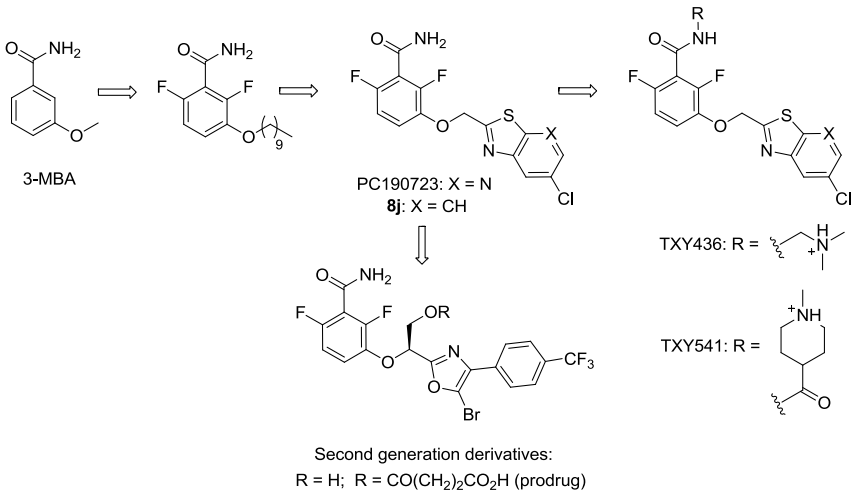

Figure 11. 3-Methoxybenzamide derivatives.

In the search of new derivatives with improved pharmacokinetic properties, two different prodrugs, TXY436 and TXY541 with higher aqueous solubility have shown efficacy in *in vivo* models of methicillin-susceptible *Staphylococcus aureus* (MSSA) and MRSA infections, and could be considered as promising agents for clinical development to treat staphylococcal infections.[75,76] Lately, a second generation of PC190723 derivatives with better metabolic stability has been described. In these compounds, the thiazolopyridine was replaced by a non-fused bicyclic scaffold and a hydroxymethylene substituent was incorporated in the pseudobencylic position (Figure 11).[77] An ester prodrug based on this new scaffold showed good *in vitro* and *in vivo* pharmacokinetic with improved solubility enabling intravenous or oral administration at higher doses of compound (5 mg/kg and 10 mg/kg, respectively). This prodrug displayed improved antibacterial potency, better resistance profile as well as efficacy in the murine thigh model of *S. aureus* infection for the first time in the case of an FtsZ inhibitor.[76,78,79]

X-ray structure of PC190723 bound to *S. aureus* FtsZ showed that this compound binds to a narrow pocket within the deep cleft formed by the C-terminal half of the H7 helix, the T7 loop, and the C-terminal four-stranded β-sheet, known as the PC binding pocket (Figure 12). It has been proposed that the interaction of the ligand in this allosteric cleft modulates the conformational switch that enables the assembly of the protein.[80] Despite the relatively high number of FtsZ inhibitors described in the literature, it is noteworthy that PC190723[81] and morpholino-GTP are the only two compounds whose binding mode to FtsZ have been revealed by X-ray crystallography. In fact, the X-ray structure of *S. aureus* FtsZ with PC190723 showed a new allosteric binding site for

small molecules. However, the lack of biological tools for the assessment of a binding constant for this newly identified druggable site hampers the possibility of carrying out HTS campaigns for this allosteric pocket and makes the development of a medicinal chemistry program a very challenging goal.

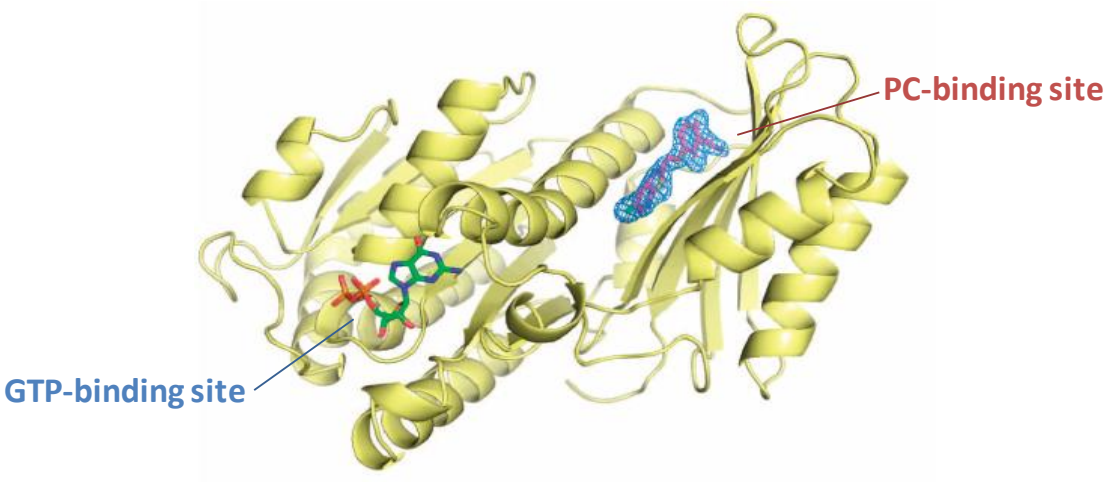

Figure 12. Crystal structure of *S. aureus* FtsZ-GDP in complex with PC190723.

In summary, the identification of FtsZ inhibitors with antibacterial properties provide a compelling rational approach for the search of new agents with novel MoA, which could contribute to fight against the virulence and the speed in which bacteria adquire resistance to recently approved antibiotics, one of the biggest threat of the health system in the 21st century.

Thus, the main objective of this work is the development of new FtsZ inhibitors with antibacterial properties in order to validate FtsZ protein as an antibacterial target. For this purpose we have focused our efforts on the identification of new compounds targeting the two druggable binding sites: the GTP- and the PC-binding pockets (Figure 12).

The development of new small molecules able to replace the natural regulator GTP and to specifically inhibit FtsZ in order to block the bacterial cell division process involves the following steps:

- Identification of hits.
- Design, synthesis, and biological evaluation of a new series of compounds. In this evaluation we will consider the assessment of the FtsZ binding affinity, the antibacterial activity and selectivity against tubulin.
- Further characterization of optimized inhibitors in terms of antibacterial properties against Gram-positive and Gram-negative pathogens, cytological profile, and mechanism of action.

Regarding the PC-binding pocket, the interesting antibacterial properties of 3-MBA derivatives such as PC190723 and the lack of a methodology to assess the binding affinity against this newly reported binding site in FtsZ prompted us to develop fluorescent probes based on this inhibitor to set up a fluorescence-based binding assay for the identification of new inhibitors. In addition, these probes could contribute to study this long cleft that seems to play a key role in FtsZ assembly, in order to get a better understanding about this dynamic process. Therefore, the second goal of this project implies the following steps:

- Design and synthesis of fluorescent derivatives based on PC190723.
- Biological evaluation and fluorescent characterization of the synthesized compounds.
- Use of the best fluorescent probes as biological tools for the study of the bacterial cell division process and for the identification of new FtsZ inhibitors by a fluorescence-based displacement assay.

2. RESULTS AND DISCUSSION

Taking into account the main objectives of this thesis, we focused on the development of FtsZ inhibitors targeting both binding sites described for the protein (Figure 13). First, we addressed the development of new small molecules able to replace the natural regulator GTP, and secondly, we designed a series of PC190723-based fluorescent probes in order to obtain biological tools for a better understanding of this allosteric binding site.

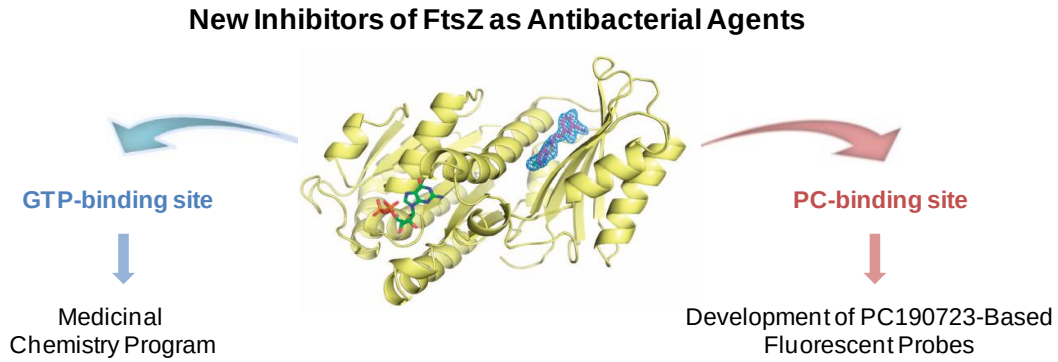

Figure 13. Dual strategy on the search of new FtsZ inhibitors.

2.1. Development of FtsZ Inhibitors Targeting the GTP-Binding Site

One of the main approaches in order to alter FtsZ polymerization is to perturb the GTPase activity of the protein with compounds able to bind the GTP-binding pocket. Despite the number of small molecules that interact with FtsZ and block bacterial cell division, the specificity and binding site on FtsZ was only established in a few cases. In fact, at the beginning of this project only C8-substituted GTP derivatives demonstrated to selectively inhibit FtsZ at the GTP-binding site.[82] Therefore, our first goal was the identification and development of non-nucleotide GTP-replacing inhibitors of FtsZ as antibacterial agents.

2.1.1. Hit Identification

In the search of new FtsZ inhibitors of the GTP-binding site, we docked our in-house library into the GTP-binding pocket of *B. subtilis* FtsZ (Bs-FtsZ) and tested the hits with the highest scores in the *mant*-GTP fluorescent anisotropy competitive assay to measure their binding affinity (dissociation equilibrium constant, K_d).[82] The best molecules obtained from this screening belonged to a series of galloyl derivatives (Table 1), which had been previously developed in our research group as anticancer fatty acid synthase (FASN) inhibitors.[83]

Table 1. FtsZ affinity and antibacterial activity of hits obtained from our in-house compound library.

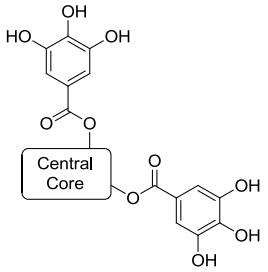

Compd	Central Core	K_d[a] (μM)	MIC (μM) *B. Subtilis*[b]	MIC (μM) MRSA USA300[c]
UCM01		12 ± 4	100	>100
UCM02 (1)		2.3 ± 0.1	100	60
UCM03		3.7 ± 0.2	50	100
UCM04		10.0 ± 0.3	100	>100
UCM05		8 ± 1	100	50
UCM06	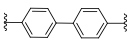	6 ± 2	50	50
UCM07		29	>400	>100

UCM08		86	>200	>100
UCM09		84	>200	>100
UCM10		33	>400	>100
UCM11		58	>500	>100
UCM12		94	>400	>100
UCM13		53	>200	>100
UCM14		11	>100	>100
UCM15 (2)	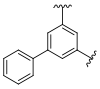	0.8 ± 0.1	40	50
UCM16		3.3	>100	>100
UCM17		5.4	100	100

[a]Affinity constant values determined in *B. subtilis* FtsZ are the mean ± SEM. [b]*B. subtilis* 168 cells. [c]MRSA USA300, *S. aureus* community acquired methicillin-resistant ATCC Nr: BAA-1556 (Institute Pasteur, France)

All these compounds share a general structure of two gallate subunits bound to a central core of differently substituted naphthalene, biphenyl, phenyl, or cyclohexane rings as well as an ethylene spacer. Among them, hits UCM02 (**1**) and UCM15 (**2**), containing a naphthalene and a biphenyl system as central scaffolds respectively, showed the highest affinities for Bs-FtsZ (K_d = 2.3 and 0.8 µM, respectively) and moderate antibacterial activity in *B. subtilis* (MIC = 100 and 40 µM, respectively) and represent the first non-nucleotide synthetic molecules that effectively compete with GTP for binding to FtsZ (Figure 14).[84]

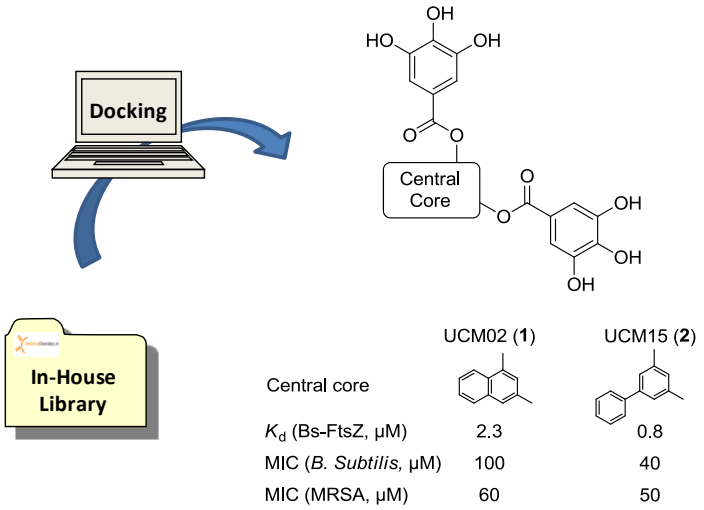

Figure 14. Hits identified from our in-house library.

Molecular dynamics (MD) simulations predicted that one of the galloyl rings of compound **1** replaces the interactions made by the phosphates of the nucleotide whereas the central core of the naphthalene and the other galloyl system overlap with the nucleobase of the GTP (Figure 15A). Further biological studies showed that hit **1** competitively inhibits the GTP-binding and perturbs normal assembly of the protein, impairing the localization of FtsZ into the Z-ring (Figure 15B). Indeed, this inhibitor induces filamentation of *B. subtilis* cells and finally blocks bacterial cell division (Figure 15C).[84]

These findings provided a compelling rationale for the development of non-nucleotide derivatives targeting the GTP-binding site as antibacterial agents and prompted us to carry out a deeper chemical exploration around these compounds, in order to obtain FtsZ inhibitors with improved antibacterial properties and to gain further insight into their mechanism of action on bacterial cells. Therefore, in this thesis, starting from inhibitors **1** and **2**, we focused our efforts on the development of new small molecules that replace the natural regulator GTP and block the bacterial cell division process by specifically inhibiting FtsZ.

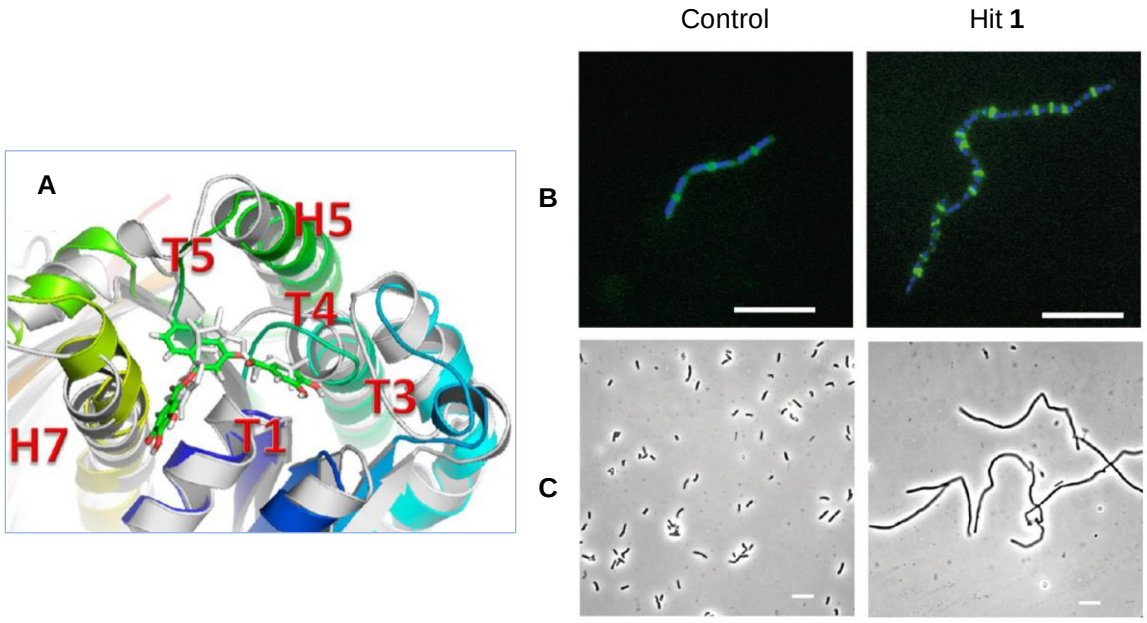

Figure 15. (A) Representative snapshot of MD simulation for the binding mode of hit **1** (green) superimposed with the GDP-bound crystallographic structure (grey). (B) *B. subtilis* cells SU570, in which the wild type *ftsZ* gene is replaced by *ftsZ-gfp*, were incubated during 1 h with hit **1** (40 µM) and visualized by fluorescent microscopy. (C) *In vitro* effects of hit **1** (50 µM) on *B. subtilis* 168 cells after 2 h of culture observed by phase-contrast microscopy. Scale bars, 10 µm.

2.1.2. Design, Synthesis, and Biological Evaluation of a New Series of Compounds

In order to carry out a structure-affinity-activity analysis around hits **1** and **2**, we focused our attention on two subunits susceptible to structural modifications: the galloyl rings and the ester bonds used as spacers. Variations in the central core were discarded since derivatives of our in-house library bearing other scaffolds displayed less affinity and/or antibacterial activity than the 1,3-naphthyl or 3,5-biphenyl counterparts (see Table 1). The structure of compound **1** was used as a starting point for chemical modifications. Thus, to study the influence of the hydroxy groups of the phenyl rings, we first considered the reduction of the number of these groups as well as their substitution pattern and their replacement by other substituents such as methoxy or chlorine, while keeping constant other parts of the molecule (**3**-**30**). In addition, monoester derivatives of hit **1** (**31** and **32**) were synthesized in order to study the influence of both phenyl rings in the binding to FtsZ and to explore the activity of possible metabolites of hit **1**. Moreover, compounds in which the ester groups were replaced by other spacers such as amides, sulfonamides and double bonds were contemplated (**33**-**36**). After the biological evaluation of this series, the best modifications obtained for hit **1** were applied to biphenyl derivative **2** and compounds having a lower number of hydroxy groups (**37**-**42**), monoesters (**43-46**) and non-ester derivatives (**47**-**50**) were synthesized (Figure 16).

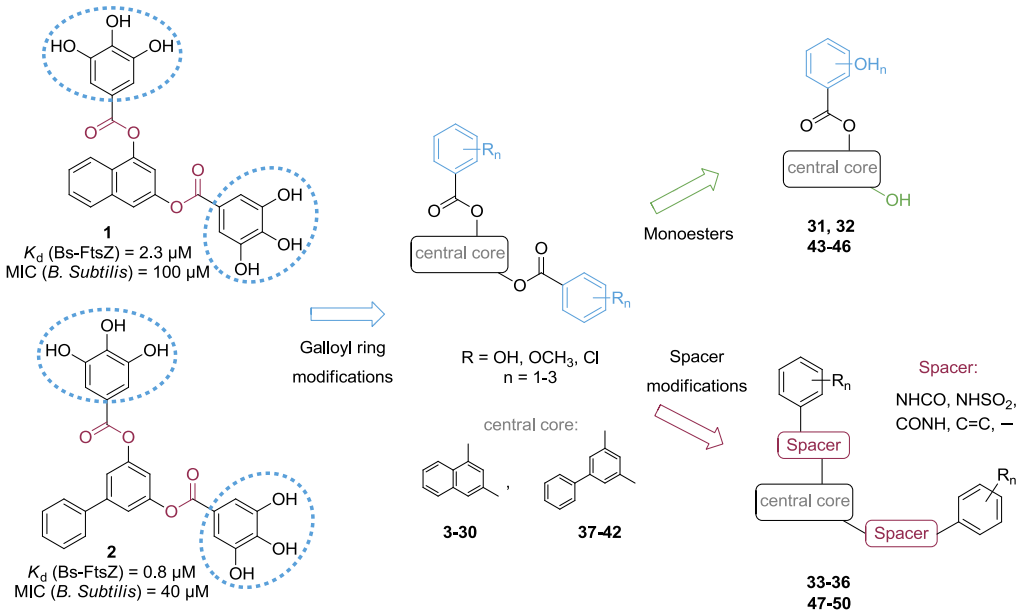

Figure 16. Design of compounds **3-50** based on hits **1** and **2**.

2.1.2.1. Series I: Naphthalene Derivatives

- Design, Synthesis, FtsZ Affinity, and Antibacterial Activity

Following the proposed structural design, in a first stage, we explored the influence of the galloyl rings in the naphthalene derivative **1**. Therefore, compounds **3**-**30** that arise from modifications of the hydroxy groups of the phenyl rings together with monoesters **31** and **32** were synthesized (Figure 17).

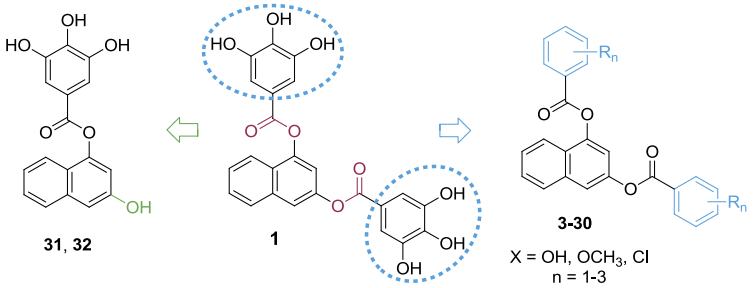

Figure 17. Designed naphthyl derivatives **3-32** targeting the GTP-binding site.

Target ester derivatives **3**-**30** were synthesized by esterification reactions of 1,3-dihydroxynaphthalene and the corresponding benzoyl chlorides **52a**-**h**. Thus, the proper (poly)hydroxybenzoic acids were initially transformed into protected benzoic acids **51a**-**f** using *tert*-butyldimethylsilyl (TBS) chloride in dimethylformamide (DMF) under microwave (MW) irradiation or conventional heating, followed by selective cleavage of the resulting silyl esters with acetic acid (Scheme 1). Both reactions were carried out in gram scale with good yields. Then, just before setting up the esterification reaction, carboxylic acids **51a**-**f**, and commercially available 3,4-dichlorobenzoic and 3,4,5-trimethoxybenzoic acids were treated with oxalyl chloride and catalytic DMF in toluene to give benzoyl chlorides **52a**-**h**.

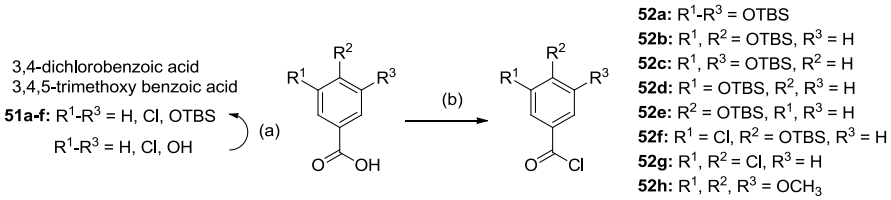

Scheme 1. Reagents and conditions: (a) (i) TBS-Cl, DIPEA, DMF, MW 100 ºC, 20 min or TBS-Cl, imidazole, DMF, rt, 18 h; (ii) CH_3CO_2H, THF, rt, 3 h, 74-81%; (b) oxalyl chloride, DMF, toluene, 50 ºC, 1 h, quantitative.

Protected diesters **53**-**58** and final compound **3**, with identical substitution at the 1 and 3 positions of the naphthalene core, were readily prepared by esterification reaction of commercially available 1,3-dihydroxynaphthalene with an excess (4 equiv) of the corresponding benzoyl chlorides **52a**-**f**,**h** in the presence of triethylamine as a base and dichloromethane (DCM) as solvent (Scheme 2). Then, TBS deprotection of the intermediate diesters **53**-**58** by treatment with hydrofluoride acid-pyridine (HF·Py) complex in tetrahydrofuran (THF) gave desired compounds **1**, **4**-**8**. Due to the high excess of acid chlorides **52a**-**f**,**h** employed in the esterification step, the corresponding acid anhydrides were obtained in some cases as by-products, which hampered the purification of the diesters and led to moderate yields.

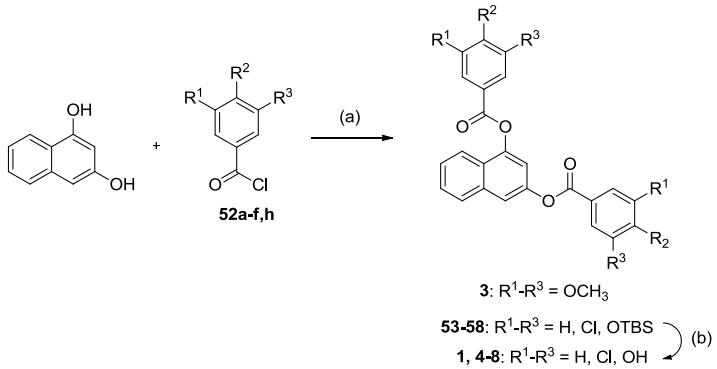

Scheme 2. Reagents and conditions: (a) Et_3N, DCM, rt, 18 h, 54-71%; (b) HF·Py, pyridine, THF, rt, 15 min, 26-88%.

For those compounds where 1,3-dihydroxynaphthalene was esterified with different benzoyl systems (**9**-**30**), the synthesis involved sequential monoesterification reactions (Scheme 3). Thus, the stoichiometry of the reaction of 1,3-dihydroxynaphthalene and benzoyl chlorides **52a,c**,**d** was adjusted to 4 equiv of 1,3-dihydroxynaphthalene and 1 equiv of acid chloride to yield the corresponding monoesters **59**-**64**. In each case, the mixture of the two possible acylated products was separated by column chromatography and each monoester was subjected to a second esterification reaction with the corresponding acid chlorides **52b**-**h** (2 equiv) to afford the protected diesters **65**-**86**, which yielded the final compound **9**-**30** after removal of the TBS groups under standard conditions.

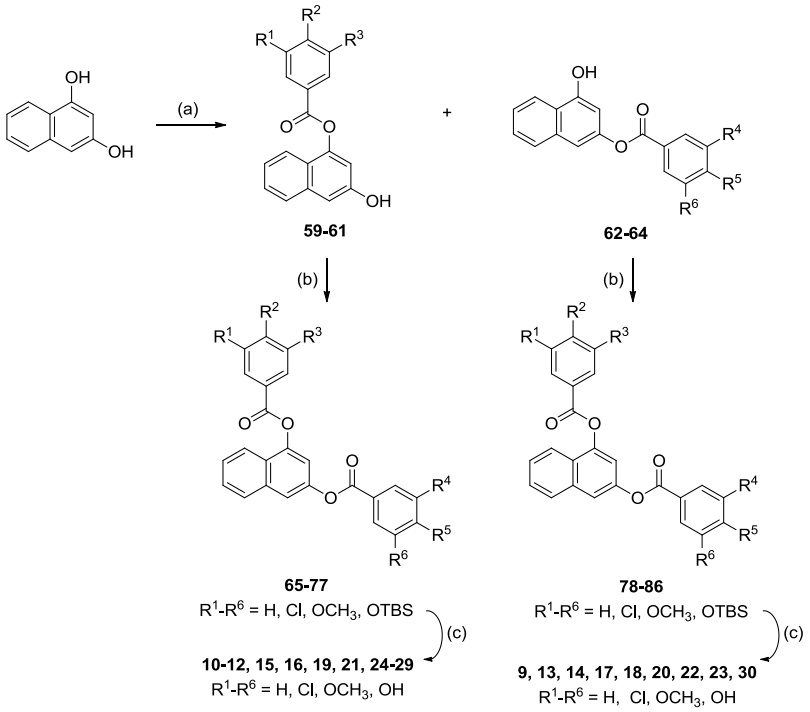

Scheme 3. Reagents and conditions: (a) **52a**,**c**, or **d** (0.25 equiv), Et_3N, DCM, rt, 18 h, 22-38%; (b) **52b**-**h** (2 equiv), Et_3N, DCM, rt, 18 h, 24-92%; (c) HF·Py, pyridine, THF, rt, 15 min, 15-92%.

Next, monoester derivatives **31** and **32** were synthesized by TBS-deprotection of intermediates **59** and **62**, respectively (Scheme 4).

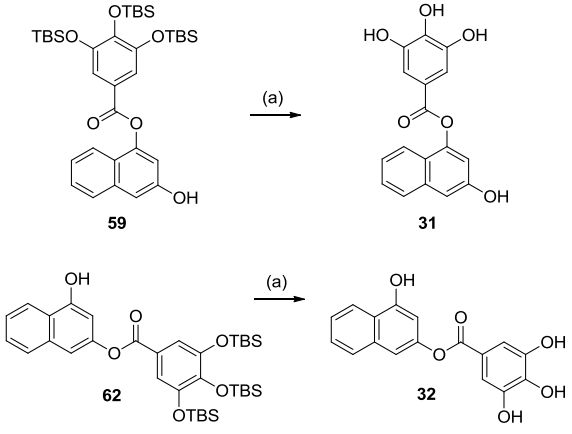

Scheme 4. Reagents and conditions: (a) HF·Py, pyridine, THF, rt, 15 min, 78 and 93%.

The synthesized compounds **3**-**32** were then evaluated using the *mant*-GTP fluorescence anisotropy competitive assay[82] to measure their binding affinities (K_d) for Bs-FtsZ (Table 2). All synthesized compounds, with the exception of the hexamethoxy derivative **3**, were able to displace *mant*-GTP, showing better affinity values (K_d = 0.7-2.2 μM) than the initial hit **1** (K_d = 2.3 μM). In the case of compound **3**, the loss of affinity (K_d > 300 μM) can be explained by the absence of free hydroxy groups, as the affinity was recovered when one of the original galloyl rings is kept (compounds **9** and **10**, K_d = 1.5 and 1.6 μM, respectively). In general, the reduction in the number of hydroxy groups on both phenyl rings improves the binding affinity and the best K_d values corresponded to derivatives having four or less hydroxy groups (compounds **24**, **28** and **29**, K_d = 0.7-0.8 μM). However, the substitution pattern of the phenyl rings did not exert a significant effect on the affinity for FtsZ. The introduction of chlorine atoms proved to be critically important for the affinity, being compounds **7**, **19**, **20**, and **25** among the best inhibitors (K_d = 0.8-0.9 μM). Moreover, the combination of hydroxy and chlorine substituents in the same phenyl ring also demonstrated to be favorable for the affinity, whereas compounds with only chlorine subtituents in one of the benzoyl rings displayed less affinity (*e.g.* **20**: K_d = 0.9 μM vs **22**: K_d = 2.0 μM). In addition, the removal of one phenyl ring proved that both hydroxyphenyl rings are important for the the binding to FtsZ, being monoesters **31**, **32** the weakest inhibitors (K_d = 26-33 μM).

The antibacterial activity of compounds **3**-**32** against *B. subtilis* and the clinically isolated MRSA USA300 −as a representative strain of community acquired resistant Gram-positive bacteria− was also assessed (Table 2). In general, all compounds showed better antibacterial activity against *B. subtilis* than the initial hit **1**, with the exception of derivatives with methoxy substituents **3**, **9**, and **10** and monoesters **31** and **32** [*e.g.* **1**: MIC (*B. subtilis*) = 100 μM vs **3** and **31**: MIC (*B. subtilis*) >200 μM]. Nonetheless, the relationship between the antibacterial activity in this strain and the number or position of the hydroxy groups remains unclear. Noteworthy, the antibacterial activity in *B. subtilis* (MIC) follows the same trend as the FtsZ affinity (K_d) within this series, which supports the role of this target in the antibacterial activity exerted by these naphthyl derivatives. Regarding the activity in MRSA, compounds bearing a galloyl subunit (**9-22**) exhibited poor antibacterial activity whereas the reduction in the number of hydroxy groups seems to be favorable in terms of potency. Thus, derivatives **6**-**8** and **25**-**30** with three or two hydroxy groups showed MIC values in MRSA ≤ 10 μM. In fact, the most potent derivatives were those with only two hydroxy groups [compounds **8**, **29** and **30**: MIC (MRSA) = 5 μM]. Moreover, the replacement of any hydroxy group by chlorine led to a remarkable improvement in the activity, reaching values of 10 μM in the case of analogues **7** and **25** [**7**: MIC (MRSA) = 10 μM vs **4**: MIC (MRSA) > 100 μM; **25**: MIC (MRSA) = 10 μM vs **24**: MIC (MRSA) = 50 μM]. As observed in *B. subtilis*, the antibacterial activity of monoesters **31** and **32** in MRSA was also reduced when compared with their corresponding diesters **1**, suggesting that both polyhydroxyphenyl subunits are required for FtsZ binding and antibacterial activity.

Table 2. FtsZ affinity and antibacterial activity of naphthalene esters **1**, **3**-**32.**

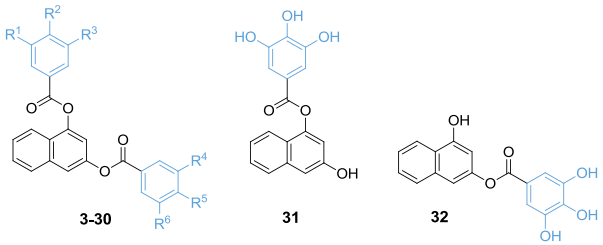

Compd	R^1	R^2	R^3	R^4	R^5	R^6	K_d[a] (µM) Bs-FtsZ	MIC (µM) *B. Subtilis*[b]	MIC (µM) MRSA[c]
1	OH	OH	OH	OH	OH	OH	2.3 ± 0.1	100	60
3	OCH_3	OCH_3	OCH_3	OCH_3	OCH_3	OCH_3	>300	>200	>100
4	OH	OH	H	OH	OH	H	1.96 ± 0.04	50	>100
5	OH	H	OH	OH	H	OH	1.6 ± 0.1	25	10
6	OH	H	H	OH	H	H	1.5 ± 0.1	15	10
7	Cl	OH	H	Cl	OH	H	0.8 ± 0.1	15	10
8	H	OH	H	H	OH	H	1.72 ± 0.02	5	5
9	OCH_3	OCH_3	OCH_3	OH	OH	OH	1.5 ± 0.2	100	100
10	OH	OH	OH	OCH_3	OCH_3	OCH_3	1.6 ± 0.3	100	100
11	OH	OH	OH	OH	OH	H	1.45 ± 0.03	50	100
12	OH	OH	OH	OH	H	OH	1.3 ± 0.1	50	100
13	OH	OH	H	OH	OH	OH	1.2 ± 0.1	25	100
14	OH	H	OH	OH	OH	OH	1.4 ± 0.2	50	100
15	OH	OH	OH	OH	H	H	2.0 ± 0.1	50	100
16	OH	OH	OH	H	OH	H	1.5 ± 0.1	50	100
17	OH	H	H	OH	OH	OH	1.3 ± 0.1	50	100
18	H	OH	H	OH	OH	OH	2.0 ± 0.1	>50	100
19	OH	OH	OH	Cl	OH	H	0.9 ± 0.2	25	50
20	Cl	OH	H	OH	OH	OH	0.9 ± 0.1	50	50
21	OH	OH	OH	Cl	Cl	H	1.1 ± 0.1	>15	24
22	Cl	Cl	H	OH	OH	OH	2.0 ± 0.1	>15	24
23	OH	OH	H	OH	H	OH	0.9 ± 0.1	>50	50
24	OH	H	OH	OH	OH	H	0.7 ± 0.2	25	50
25	OH	H	OH	Cl	OH	H	0.8 ± 0.1	25	10
26	OH	H	OH	OH	H	H	1.5 ± 0.1	20	10
27	OH	H	OH	H	OH	H	2.2 ± 0.1	>50	8
28	OH	H	H	OH	OH	H	0.7 ± 0.2	20	10
29	OH	H	H	H	OH	H	0.8 ± 0.2	5	5
30	H	OH	H	OH	H	H	1.5 ± 0.1	5	5
31	OH	OH	OH	-	-	-	26 ± 9	>200	>100
32	-	-	-	OH	OH	OH	33 ± 10	200	>100

[a]The values are the mean ± SEM. [b]*B. subtilis* 168 cells. [c]*S. aureus* community acquired methicillin resistant ATCC Nr: BAA-1556 (Institute Pasteur, France) MRSA USA300.

In order to analyze the influence of the spacer between the naphthalene central core and the polyhydroxyphenyl rings, derivatives **33**-**36** in which the ester linkers were replaced by amides, sulfonamides or alkene moieties were synthesized (Figure 18). As an initial exploration of this replacement and considering the synthetic viability, we synthesized derivatives of initial hit **1** and compound **7**, as an example of high FtsZ affinity (K_d = 0.8 µM) and good antibacterial activity [MIC (MRSA) = 10 µM] inhibitor.

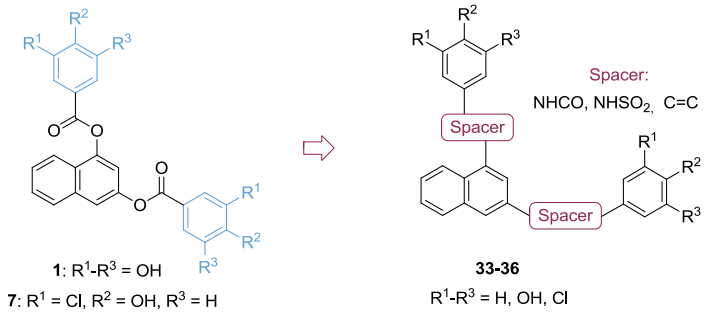

Figure 18. Spacer exploration in the naphthalene series: compounds **33**-**36**.

Synthesis of amides **33** and **35** -derived from compounds **1** and **7**, respectively- is outlined in Scheme 5. First, catalytic hydrogenation of commercially available 1,3-dinitronaphthalene afforded 1,3-diaminonaphthalene (**87**). This diamine was then treated with benzoyl chlorides **52a** or **52f** to give the final compounds **33** and **35**, after deprotection of the hydroxy groups with the HF·Py complex. In turn, sulfonamide **36** was synthesized by sulfonylation reaction of diamine **87** with 3-chloro-4-methoxybenzenesulfonyl chloride (**90**) under standard basic conditions, followed by cleavage of the methoxy groups of intermediate **91** with boron tribromide in DCM.

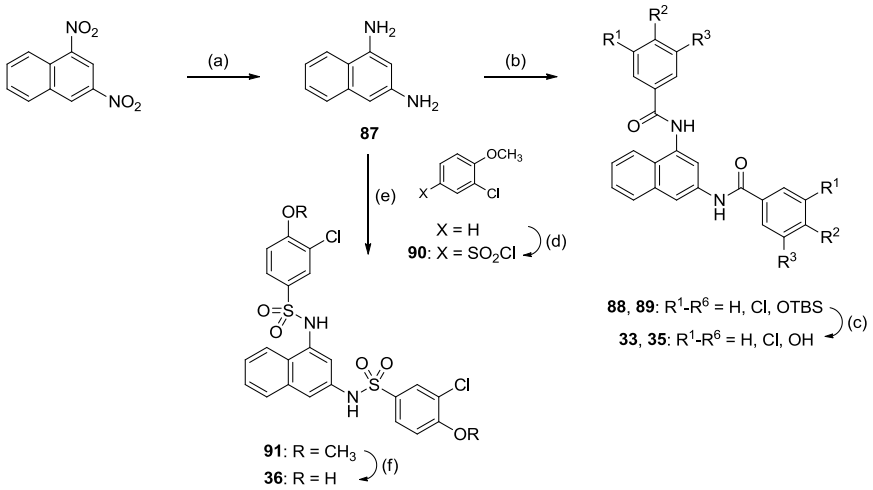

Scheme 5. Reagents and conditions: (a) H_2, 10% Pd/C, MeOH, rt, 3.5 h, 60%; (b) **52a** or **f** (4 equiv), Et_3N, DCM, rt, 18 h, 33-36%; (c) HF·Py, pyridine, THF, rt, 15 min, 75-78%; (d) $ClSO_3H$, $CHCl_3$, 0 ºC to rt, 16 h, 61%; (e) pyridine, DCM, rt, 18 h, 48%; (f) BBr_3, DCM, rt, 18 h, 38%.

Finally, alkene (1*E*,3*E*)-**34** was synthesized by Wittig reaction of the triphenylphosphonium salt **93** and aldehyde **95**, followed by Pd(0)-catalyzed deprotection of the allyl ethers using 1,3-dimethylbarbituric acid (DMBA) (Scheme 6). Thus, phosphonium salt **93** was prepared by radical bromination of 1,3-dimethylnaphthalene in the presence of *N*-bromosuccinimide (NBS) and 2,2'-azobisisobutyronitrile (AIBN), and subsequent reaction of the resulting dibromo derivative **92** with triphenylphosphine in xylene under reflux. Aldehyde **95** was obtained by *O*-allylation of methyl 3,4,5-trihydroxybenzoate and further reduction of ester **94** with sodium bis(2-methoxyethoxy)aluminumhydride (Red-Al®). Diene **96** was obtained as a mixture of (1*E*,3*E*) and (1*E*,3*Z*) isomers that could be separated by chromatography and fully characterized. However, deprotection of both isomers gave final product (1*E*,3*E*)-**34** by isomerization of the doble bond in the presence of Pd.

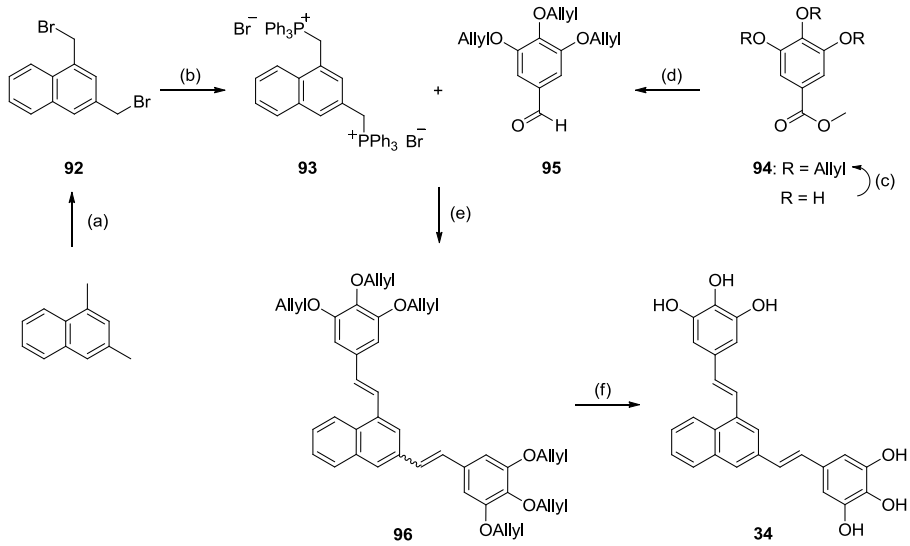

Scheme 6. Reagents and conditions: (a) NBS, AIBN, CCl_4, 90 ºC, 16 h, 73%; (b) Ph_3P, xylene, reflux, 72 h, 96%; (c) CH_2=$CHCH_2Br$, K_2CO_3, DMF, 65 ºC, 4 h, 99%; (d) Red-Al®, KO*t*-Bu, pyrrolidine, THF, 0 ºC, 10 min, 78%; (e) *n*-BuLi, THF, -78 ºC to rt, 18 h, (1*E*,3*E*) 30% and (1*E*,3*Z*) 18%; (f) DMBA, $Pd(PPh_3)_4$, DCM/MeOH, rt, 1 h, 19%.

Regarding the influence of the spacer between the naphthalene central core and the polyhydroxyphenyl subunits, the replacement of the esters by amides, sulfonamides or alquenes (**33**-**36**) did not provide an improvement in terms of binding affinity for FtsZ nor antibacterial activity in the pathogenic bacteria MRSA when compared to their parent compounds **1** and **7**, and only amide **35** showed modest affinity for FtsZ (K_d = 3.1 µM) and antibacterial activity [MIC (*B. subtilis*) = 25 µM, MIC (MRSA) = 50 µM] (Table 3).

Table 3. FtsZ affinity and antibacterial activity of compounds **33**-**36**.

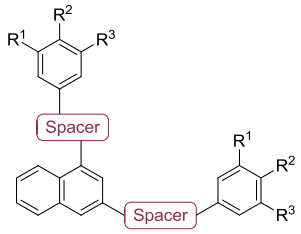

33-36

Compd	Spacer	R^1	R^2	R^3	K_d[a] (µM) Bs-FtsZ	MIC (µM) *B. subtilis*[b]	MIC (µM) MRSA[c]
1	OCO	OH	OH	OH	2.3 ± 0.1	100	50
33	NHCO	OH	OH	OH	25.0 ± 0.2	>50	>100
34	CH=CH	OH	OH	OH	8 ± 1	>20	>100
7	OCO	Cl	OH	H	0.8 ± 0.1	15	10
35	NHCO	Cl	OH	H	3.1 ± 0.5	25	50
36	$NHSO_2$	Cl	OH	H	21.3 ± 0.2	>200	>100

[a]The values are the mean ± SEM. [b]*B. subtilis* 168 cells. [c]*S. aureus* community acquired methicillin resistant ATCC Nr: BAA-1556 (Institute Pasteur, France) MRSA USA300.

- Selectivity versus Tubulin

Taken together the results obtained with compounds **3**-**36**, the new identified high-affinity inhibitors **6**, **7**, **19**-**21**, **23**-**26**, and **28**-**30** (K_d ≤ 1.5 µM) endowed with good antibacterial activity (MIC in *B. subtilis* and MRSA ≤ 50 µM) were selected to assess their FtsZ selectivity, since effective antibacterial compounds targeting FtsZ should avoid unwanted interactions with its closest eukaryotic structural homolog tubulin (Figure 19A). Thus, sedimentation assays were used to determine the effect of the compounds on FtsZ and tubulin assembly. These polymer pelleting experiments were made by sedimenting the FtsZ or tubulin polymers formed under well-controlled assembly conditions in the presence of increasing concentrations of the selected compound, GTP or GDP, and quantifying them after loading the pellets and supernatants with a time lag into polyacrylamide gel electrophoresis (Figure 19B). It is noteworthy to mention that these assays were performed at the maximal concentrations of the compounds permitted by their average solubility in the presence of each protein: 25 µM for FtsZ or 100 µM for tubulin. The inhibition percentage was determined after substracting the negative control (GDP) and it was expressed relative to the maximal polymerization induced by GTP with regeneration system (RS) by the following equation:

$$\text{FtsZ or Tubulin Inhibition } \% = 100 * \left[1 - \left(\frac{(\%pellet\ compound - \%pellet\ GDP)}{(\%pellet\ GTP - \%pellet\ GDP)}\right)\right]$$

Notwithstanding the higher sensitivity of the tubulin inhibition test compared to FtsZ inhibition assay, compounds **6**, **20**, **21**, **26**, and **30** do not inhibit tubulin polymerization, whereas **19**, **23**, **24**, and **29** are weak tubulin inhibitors (<25%) and derivatives **7**, **25**, and **28** as well as hit **1** cross-inhibit tubulin assembly (>40%). Therefore, the reduction of hydroxy groups, not only seems to be critical in terms of FtsZ affinity and antibacterial activity but also for selectivity, being hit **1** ($R^{1\text{-}6}$ = OH) the most potent tubulin inhibitor, whereas compounds **6** and **26** with only two or three hydroxy groups are the most selective. Interestingly, all derivatives that cross-inhibit tubulin assembly (**7**, **25**, and **28**) shared a 4-hydroxybenzoyl group at position 3 of the naphthalene.

Thus, compounds **6** and **26** are the most potent FtsZ inhibitors, showing 46% inhibition at 25 µM and displaying high selectivity against tubulin (0-1% tubulin inhibition at 100 µM). Their selective inhibition of FtsZ *vs* tubulin assembly is exemplified at different concentrations (5-50 µM) in Figure 19B. These inhibitors are able to reduce the percentage of Bs-FtsZ polymers with respect to the control (in the presence of GTP) in a concentration dependent manner, and prove that it is possible to selectively inhibit FtsZ assembly with synthetic GTP-replacing compounds that are inactive on tubulin polymerization.

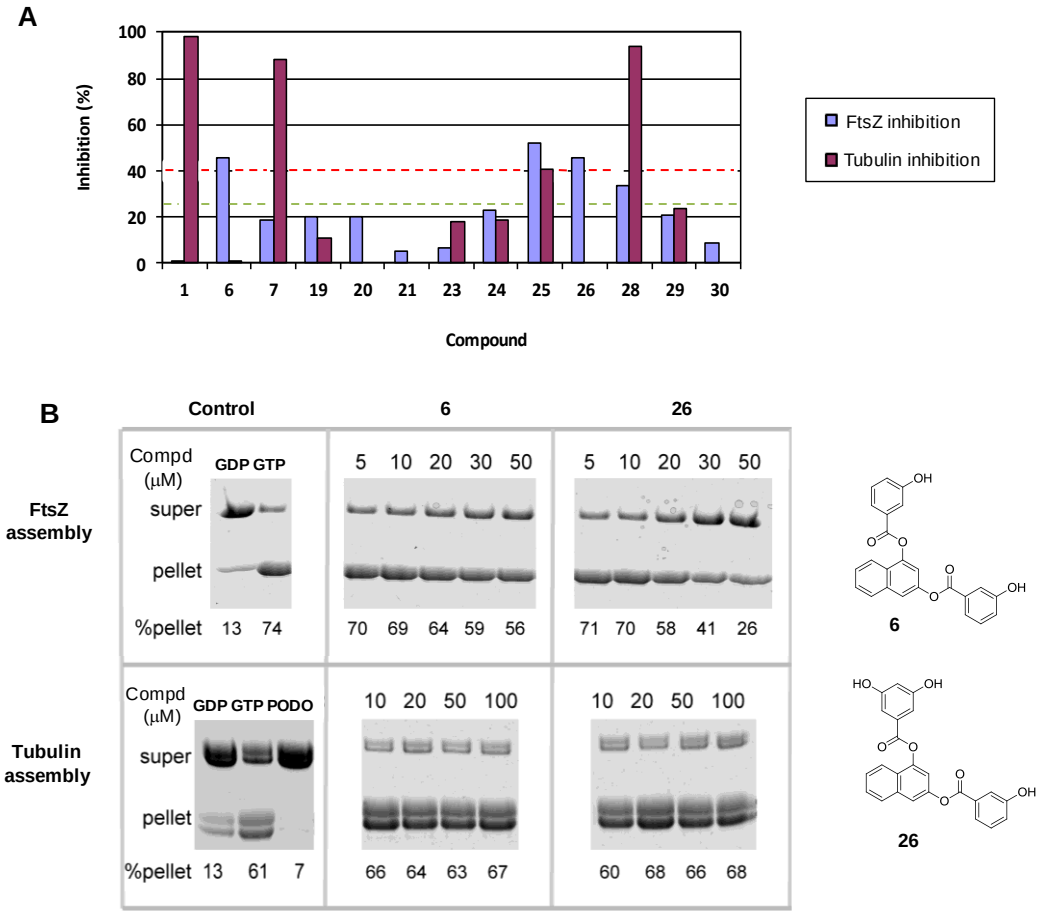

Figure 19. (A) Percentage of FtsZ (25 μM of compound) and tubulin (100 μM of compound) inhibition. (B) Effect of increasing concentrations of compounds **6** and **26** on the assembly of Bs-FtsZ (9 μM) and tubulin (15 μM). FtsZ assembly was performed with GTP regeneration system (RS). Podophyllotoxin (PODO, 50 μM) was employed as a control microtubule inhibitor in the tubulin polymerization assay.

In summary, comparing these optimized compounds with the initial hit **1**, we can infer that the hydroxy groups of the galloyl rings can be successfully reduced to obtain simpler and improved derivatives such as **6**, **26** and **29**, which combine good FtsZ inhibition, antibacterial activity and selectivity against tubulin.

2.1.2.2. Series II: Biphenyl Derivatives

- Design, Synthesis, FtsZ Affinity, and Antibacterial Activity

Considering that the reduction of hydroxy groups in the naphthalene series turned into more active and selective compounds, derivatives **37**-**42** bearing four or less hydroxy groups were considered in the study of the 3,5-biphenyl system as central core (Figure 20). In addition, monoesters **43**-**46** and compounds **47**-**50** with different spacers between the biphenyl central core and the polyhydroxyphenyl rings were also studied. In this series, replacement of hydroxy substituents by chlorine atoms was discarded due to the low FtsZ inhibition and/or the tubulin cross-inhibition observed in the naphthalene series for this modification.

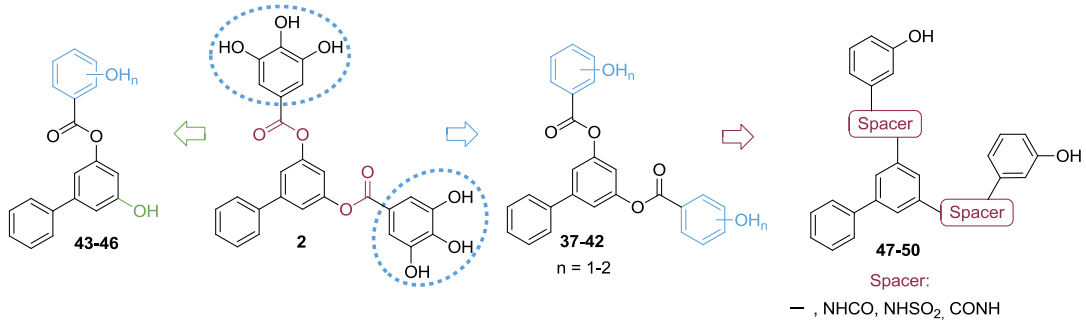

Figure 20. Designed biphenyl derivatives **37**-**50** targeting the GTP-binding site.

Symmetric diesters **2**, **40**, and **42** were synthesized by esterification of biphenyl-3,5-diol (**97**) with an excess of the corresponding benzoyl chlorides (**52a,d,e**), followed by TBS deprotection of silyl ethers **98**-**100** (Scheme 7). Diol **97** was prepared by MW-assisted Suzuki cross-coupling of 3,5-dimethoxyphenylbromide and phenylboronic acid, and subsequent methoxy deprotection with BBr_3. For non-symmetric biphenyl derivatives (**37**-**39** and **41**), the synthesis involved sequential monoesterification reactions with the appropriated benzoyl chlorides. Thus, reaction of diol **97** with 0.25 equiv of benzoyl chlorides **52b**-**e** yielded the corresponding monoesters **101**-**104**, which were used in a second esterification step with 2 equiv of acid chlorides **52c**,**d** to afford the desired final compounds **37**-**39** and **41** after removal of TBS groups under standard conditions. In addition, intermediates **101**-**104** were deprotected to afford the desired monoesters **43**-**46**.

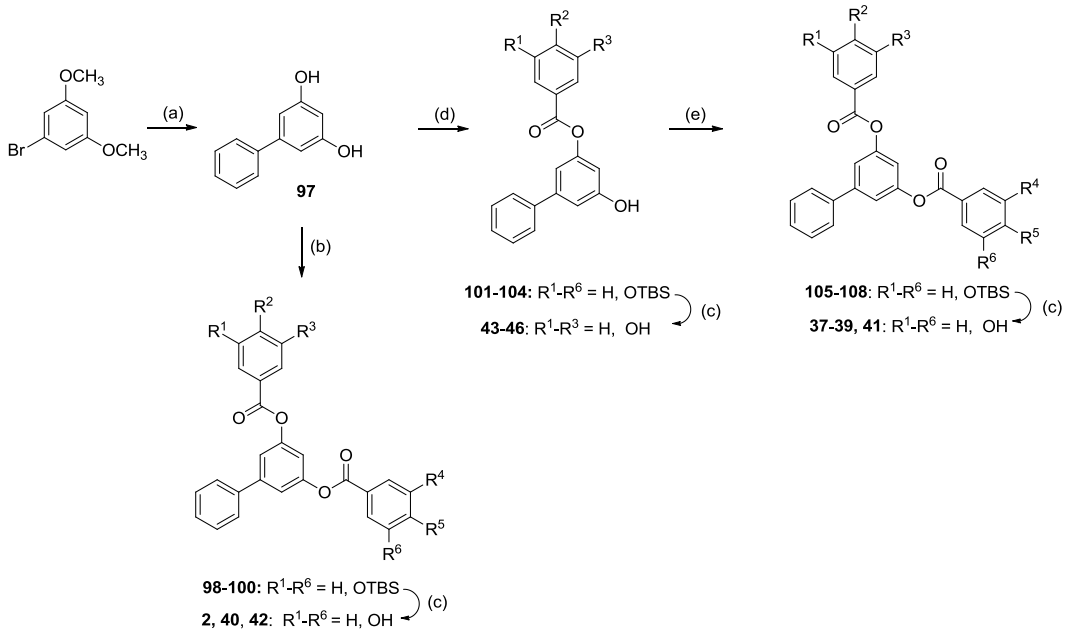

Scheme 7. Reagents and conditions: (a) (i) $PhB(OH)_2$, $Pd(PPh_3)_4$, Na_2CO_3, toluene/H_2O, MW, 150 ºC, 30 min, 75%; (ii) BBr_3, DCM, rt, 18 h, 97%; (b) **52a**,**d** or **e** (4 equiv), Et_3N, DCM, rt, 18 h, 64-87%; (c) HF·Py, pyridine, THF, rt, 15 min, 28-96%; (d) **52b**-**e** (0.25 equiv), Et_3N, DCM, rt, 18 h, 46-69%; (e) **52c** or **d** (2 equiv), Et_3N, DCM, rt, 18 h, 34-89%.

Regarding the spacer modifications, synthesis of compound **47**, in which the ester spacers were removed, was accomplished by transformation of diol **97** into the corresponding triflate, followed by Suzuki cross-coupling reaction under MW irradiation with 3-methoxyphenylboronic acid, and further methoxy deprotection of intermediate **110** with BBr_3 (Scheme 8). Amide **48** and sulfonamide **49** were synthesized from biphenyl-3,5-diamine **112**. First, Suzuki cross-coupling reaction under MW irradiation of 1-bromo-3,5-dinitrobenzene with phenylboronic acid and further catalytic reduction of biphenyl-3,5-dinitro (**111**) in anhydrous THF in the H-Cube hydrogenation system afforded biphenyl-3,5-diamine (**112**), that was transformed in situ into the corresponding amide **48** or sulfonamide **49**, due to its low chemical stability. Thus, benzoyl chloride **52d** or commercial 3-methoxybenzenesulfonyl chloride and Et_3N were added to the freshly hydrogenated solution of diamine **112** in THF to give the final compounds **48** and **49**, after TBS deprotection of diamide intermediate **113** with the HF·Py complex or methoxy deprotection of disulfonamide **114** with BBr_3. Finally, retroamide **50** which contains a reverse amide group, was synthesized by Suzuki coupling of dimethyl-5-bromoisophthalate with phenylboronic acid, followed by ester hydrolysis and further

transformation into the corresponding acid chloride **116**, whose condensation with (3-{[*tert*-butyl(dimethyl)silyl]oxy}phenyl)amine (**117**) followed by TBS deprotection afforded compound **50**.

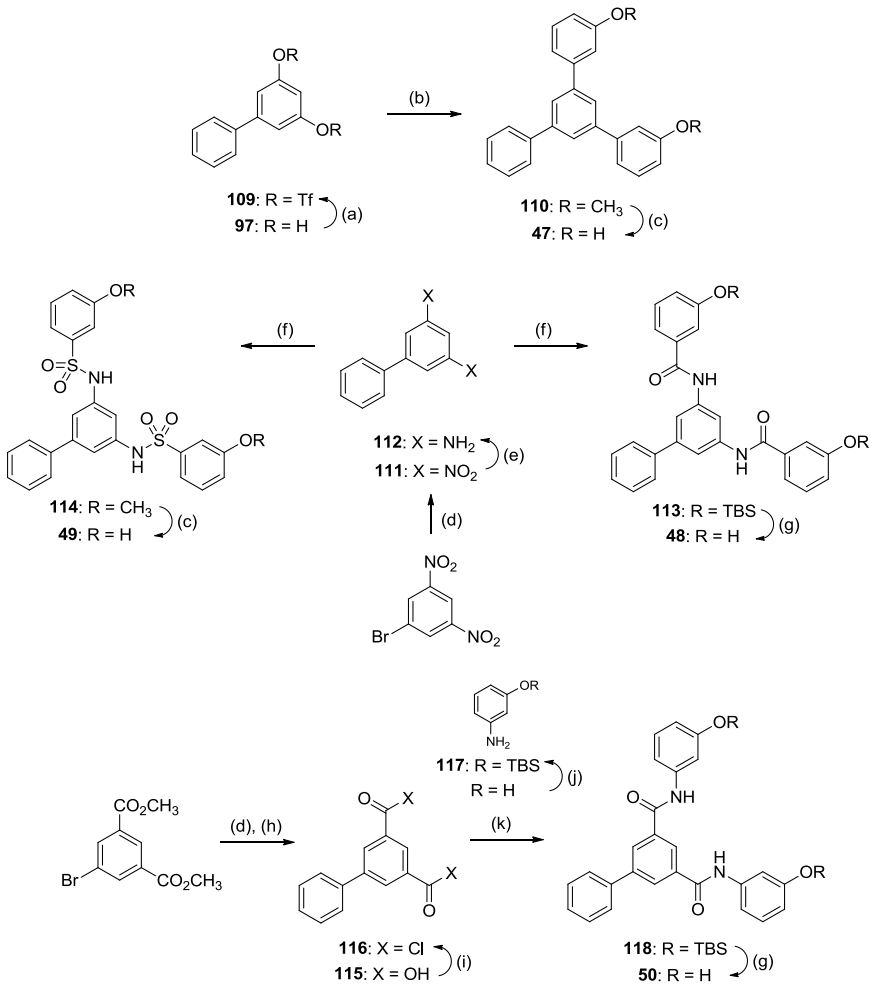

Scheme 8. Reagents and conditions: (a) trifluoromethanesulfonic anhydride, Et_3N, DCM, rt, 2.5 h, 99%; (b) 3-methoxyphenylboronic acid, $Pd(PPh_3)_4$, Na_2CO_3, toluene/EtOH/H_2O, MW, 150 ºC, 15 min, 75%; (c) BBr_3, DCM, rt, 3 h, 21-94%; (d) $PhB(OH)_2$, $Pd(PPh_3)_4$, Na_2CO_3, toluene/H_2O, MW, 150 ºC, 30 min, 83-90%; (e) H_2, 10% Pd/C, H-Cube reactor, THF, rt, 99%; (f) **52d** or 3-methoxybenzenesulfonyl chloride, Et_3N, THF, rt, 18 h, 20-45%; (g) HF·Py, pyridine, THF, rt, 15 min, 66-89%; (h) NaOH, H_2O, THF, reflux, 1.5 h, 85%; (i) $SOCl_2$, THF, reflux, 3 h, 99%; (j) TBS-Cl, imidazole, 18 h, rt, 48%; (k) Et_3N, THF, rt, 18 h, 89%.

Assessment of the binding affinities for Bs-FtsZ by the *mant*-GTP competitive assay showed that all biphenyl derivatives **37**-**50** were able to displace the nucleotide with higher affinity values than their naphthalene analogues (Table 2 and 4), confirming that the scaffold of 3,5-biphenyl is more favorable as central core than the 3,5-naphthyl system [*e.g.* K_d (**8**) = 1.72 µM vs K_d (**42**) = 0.4 µM]. Among them, diesters **37**-**42** and compound **47** showed better affinity values (K_d = 0.4-0.6 µM) than initial hit **2** (K_d = 0.8 µM) (Table 4). In general, the tendency observed in the naphthalene derivatives is repeated in this second series. Thus, the reduction in the number of hydroxy groups of both phenyl rings improves the binding affinity for the GTP-binding site of FtsZ [K_d (**37**-**42**) = 0.4-0.6 µM]. Although 1 or 2 hydroxy groups in each phenyl ring seems to be the optimal number of these substituents for FtsZ affinity, their position still did not exert a significant effect. This may be due to the flexibility of the FtsZ nucleotide binding loops. Removal of one of the polyhydroxybenzoate rings in the biphenyl derivatives demonstrated once again that both subunits are important for the binding, since monoesters **43**-**46** have ten-fold reduced affinity (K_d = 3.3-5.3 µM). The biological evaluation of non-ester analogues **47**-**50** showed that they keep micromolar affinity for FtsZ (K_d = 0.5-8.3 µM) and proves that modifications in the spacers of this new identified chemotype are tolerated. Notably, derivative **47** maintains the high FtsZ affinity of its parent compound **40** [K_d (**47**) = K_d (**40**) = 0.5 µM].

In order to assess their antibacterial activity, compounds **37**-**50** were tested against *B. subtilis* and MRSA USA300 (Table 4). In general, diesters **37**-**42** showed MIC values in the micromolar range and the reduction in the number of hydroxy groups was also favorable in terms of potency, as previously observed for FtsZ affinity. In fact, the most potent derivatives were **39**-**42** with only two or three hydroxy groups [MIC (MRSA) = 5-7 µM]. On the other hand, removal of one of the polyhydroxybenzoyl subunits led to a reduction in the antibacterial potency [*e.g.* MIC (MRSA, **40**, **42**) = 5-7 µM vs MIC (MRSA, **45**, **46**) = 50 µM]. Antibacterial evaluation of non-esters **47**-**50** showed that they also exert antimicrobial activity [MIC (*B.subtilis*) = 5-50 µM, MIC (MRSA) = 3-50 µM]. Interestingly, submicromolar high-affinity compound **47** displays the best antibacterial activity against MRSA (MIC = 3 µM) within analyzed compounds.

Table 4. FtsZ affinity and antibacterial activity of compounds **2, 37-50.**

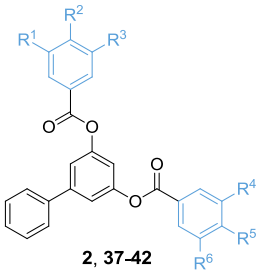

2, 37-42

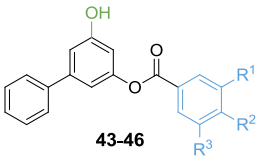

43-46

Compd	R^1	R^2	R^3	R^4	R^5	R^6	K_d[a] (µM) Bs-FtsZ	MIC (µM) *B. Subtilis*[b]	MIC (µM) MRSA[c]
2	OH	OH	OH	OH	OH	OH	0.8 ± 0.1	40	50
37	OH	OH	H	OH	H	OH	0.4 ± 0.1	15	50
38	OH	OH	H	OH	H	H	0.4 ± 0.1	15	50
39	OH	H	OH	OH	H	H	0.5 ± 0.1	5	5
40	OH	H	H	OH	H	H	0.5 ± 0.1	5	7
41	OH	H	H	H	OH	H	0.6 ± 0.1	10	5
42	H	OH	H	H	OH	H	0.4 ± 0.1	2.5	5
43	OH	OH	H	-	-	-	5.3 ± 1.0	75	50
44	OH	H	OH	-	-	-	5.3 ± 1.0	50	50
45	OH	H	H	-	-	-	3.8 ± 0.8	50	50
46	H	OH	H	-	-	-	3.3 ± 0.6	50	50

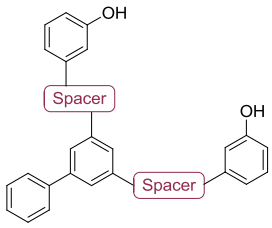

47-50

Compd	Spacer	K_d[a] (µM) Bs-FtsZ	MIC (µM) *B. Subtilis*[b]	MIC (µM) MRSA[c]
47	-	0.5 ± 0.1	5	3
48	NHCO	4.3 ± 1.0	25	50
49	$NHSO_2$	4.8 ± 0.5	50	50
50	CONH	8.3 ± 1.4	50	50

[a]The values are the mean ± SEM. [b]*B. subtilis* 168 cells. [c]*S. aureus* community acquired methicillin resistant ATCC Nr: BAA-1556 (Institute Pasteur, France) MRSA USA300.

- Selectivity versus Tubulin

Next, we studied the effects on FtsZ polymerization and tubulin assembly of high-affinity inhibitors **37**-**42** (K_d ≤ 0.6 μM), compound **45**, as a monoester example, and non-ester analogues **47**-**50** (Figure 21A). In general, all derivatives were found to inhibit the GTP-induced assembly of FtsZ more effectively than their parent compound **2** in this *in vitro* assay, being **45**, **47**-**50** the most potent compounds with inhibition percentages higher than 50% at 25 μM. Interestingly, biphenyl derivatives showed higher FtsZ inhibition and better selectivity against tubulin polymerization than the naphthene analogues. In fact, only **39**, **45** and **49** showed significant inhibition of tubulin assembly at 100 μM.

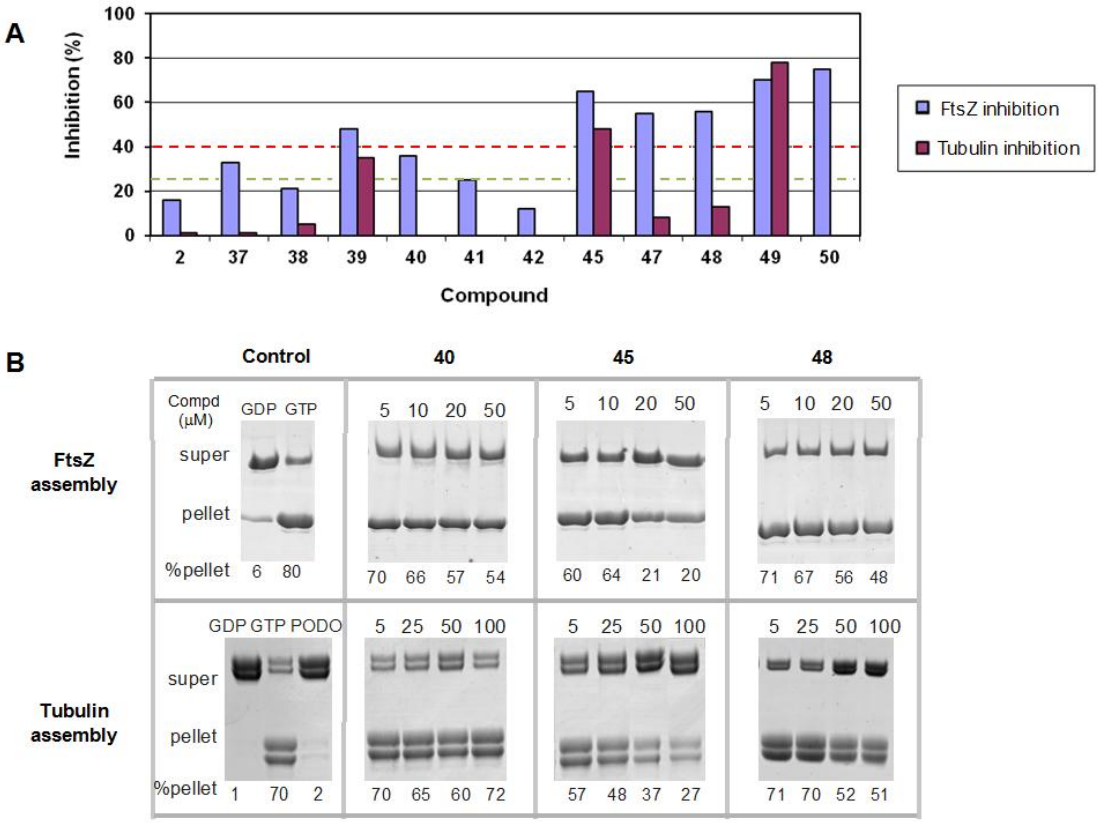

Figure 21. (A) Percentage of FtsZ and tubulin inhibition at 25 and 100 μM of compound respectively. (B) Effect of increasing concentrations of compounds **40**, **45**, and **48** on the assembly of Bs-FtsZ (9 μM) and tubulin (15 μM). FtsZ assembly was performed with GTP regeneration system (RS). PODO (50 μM) was employed as a control microtubule inhibitor in the tubulin polymerization assay.

The inhibition of FtsZ vs tubulin assembly is also exemplified at increasing concentrations of the three structurally diverse compounds **40**, **45** and **48** (Figure 21B). Thus, it can be observed how derivatives **40** and **48** inhibit to different extent FtsZ assembly at 5-50 μM range (Figure 21A), whereas they lack any significant effect on tubulin assembly up to 50 μM (Figure 21B).

Comparing these optimized compounds with the initial hit **2**, we can infer that the hydroxy groups of the galloyl rings can be also reduced to obtain simpler and improved biphenyl derivatives such as **40**-**42**, and the ester spacer can be successfully removed (compound **47**) or replaced by an amide (compound **48**). These compounds, together with naphthyl derivatives **6**, **26** and **29** could be considered as antibacterial candidates that combine good FtsZ inhibition, antibacterial activity and selectivity against tubulin.

2.1.3. Further Characterization of Optimized Inhibitors in Terms of Antibacterial Properties, Cytological Profile, and Mechanism of Action

- Antibacterial Activity in a Panel of Pathogenic Bacteria

Taken together the results obtained with compounds **1**-**50**, the new identified high-affinity inhibitors **6**, **26**, **29**, and **40**-**42** (K_d ≤ 1.5 μM) endowed with good antibacterial activity (MIC in *B. subtilis* and MRSA ≤ 20 μM) and selectivity against tubulin, together with monoester **45** and non-ester analogues **47** and **48**, were selected for further studies. Hits **1** and **2** were also included for comparative purpose. First, their microbiological profile on a broader panel of antibiotic-resistant Gram-positive and Gram-negative pathogenic bacteria was assessed (Table 5).

Table 5. Antibacterial activity pathogenic bacteria of selected compounds.

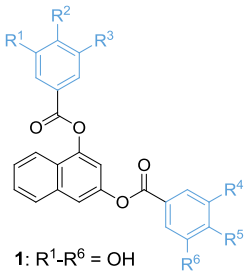

1: R^1-R^6 = OH
6: R^1, R^3 , R^4 = OH
26: R^1, R^5 = OH
29: R^2, R^4 = OH

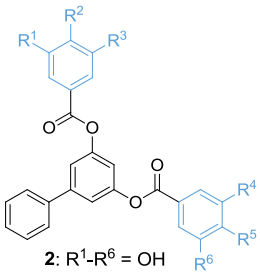

2: R^1-R^6 = OH
40: R^1, R^4 = OH
41: R^1, R^5 = OH
42: R^2, R^5 = OH

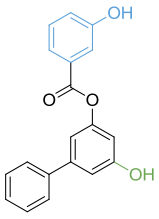

45

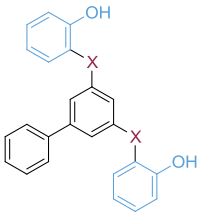

47: X = —
48: X = NHCO

Compound	K_d[a] FtsZ (μM)	MIC (μM)				
		MRSA Mu50[b]	*E. faecalis*[c]	*L. monoc.*[d]	*P. aerug.*[e]	*E. coli*[f]
1	2.3 ± 0.1	80	>100	50	100	>100
6	1.5 ± 0.1	10	50	50	>100	>100
26	1.5 ± 0.1	10	50	10	>100	>100
29	0.8 ± 0.2	5	50	5	>100	>100
2	0.8 ± 0.1	50	>100	50	50	50
40	0.5 ± 0.1	7	50	7	>50	>100
41	0.6 ± 0.3	5	50	5	>50	>100
42	0.4 ± 0.1	5	50	5	>50	>100
45	3.8 ± 0.8	50	50	50	>50	>100
47	0.5 ± 0.1	3	>100	5	>50	>100
48	4.3 ± 1.0	50	>100	50	>50	>100

[a]The values are the mean ± SEM. [b]Methicillin, ampicillin and kanamycin resistant Mu50/ATCC 700699 (Institute Pasteur, France). [c]*Enterococcus faecalis,* gentamicin and vancomycin resistant V583 ATCC700802 (sequenced strain). [d]*Listeria monocytogenes,* EGDe (sequenced strain). [e]*Pseudomonas aeruginosa,* imipenem resistant PAO1 (sequenced strain). [f]*Escherichia coli*, UTI89 from cystitis infection (sequenced strain).

In general, all tested compounds inhibited the growth of Gram-positive resistant pathogenic bacteria such as MRSA (MIC = 3-50 μM) and *Listeria monocytogenes* (*L. monoc*., MIC = 5-50 μM), being derivatives **6**, **26**, **29**, **40**-**42**, and **45** also able to inhibit *E. faecalis* growth at 50 μM. Regarding Gram-negative bacteria, although initial biphenyl hit **2** showed moderate activity in

resistant *Pseudomonas aeruginosa* (*P. aerug.*, MIC = 50 µM) and *E. coli* (MIC = 50 µM), none of its derivatives affected the growth of Gram-negative pathogens at the assayed concentration (100 µM), which indicates that removal of hydroxy groups was detrimental for the antibacterial activity against these strains.

With the aim of determining whether the new identified inhibitors were stable in the whole bacteria assay, stability of representative compounds **40**, **47**, and **48** in bacterial culture of *B. subtilis* was assessed and they were not appreciably hydrolyzed after 18 h (90% remaining compound quantified by HPLC).

- Cytological Profile and Mode of Action

In order to identify the most effective bacterial division blockers among the selected compounds, we examined their effects on the cell division of wild type *B. subtilis* 168 and on the FtsZ subcellular localization in *B. subtilis* SU570, a strain that has FtsZ fused to a green fluorescent protein (FtsZ-GFP) as the only FtsZ protein.

Cytological profiling of the nucleoid, membrane shape and membrane permeability by fluorescence microscopy has been recently shown to uniquely distinguish the mode of action of antibiotics targeting the major types of bacterial biosynthetic pathways (DNA, RNA, protein, peptidoglycan and lipid) and subclasses among them, which permits to identify the mode of action of new antibiotics.[85,86] Following this trend, we have characterized the cellular effects of our most effective FtsZ inhibitors (**29**, **40** and **41**) and the structurally representative compounds **45**, **47**, and **48**. Cells of wild type *B. subtilis* 168 exposed to each of these compounds were longer than control cells (Figure 22). Among them, derivative **40** exhibited the clearest effect as bacterial division blocker. The phenotype of cells treated with biphenyl **40** (4 µM) consisted of the longest filamentous undivided cells. Long filaments were also observed with the amide linker analogue **48** (12 µM) and weaker effects were found with **41** (5 µM) and monoester **45** (25 µM) as well as with the naphthyl compound **29** (5 µM).

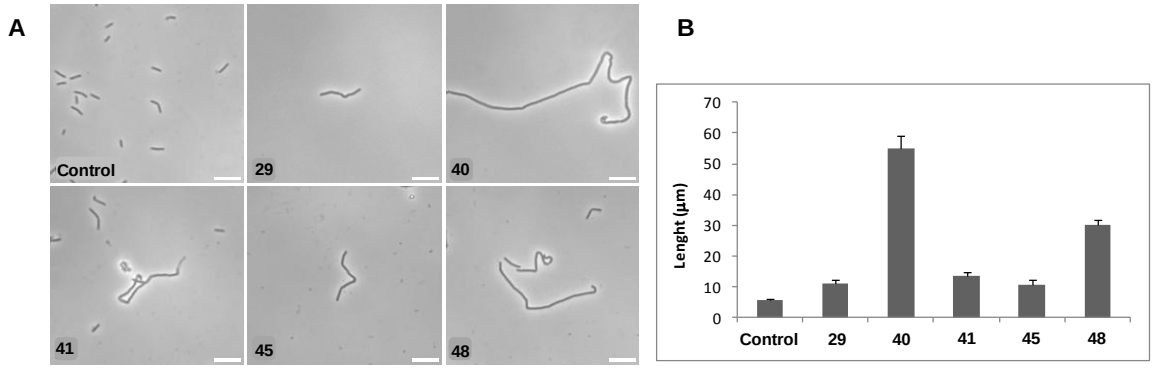

Figure 22. Cell division effect of FtsZ inhibitors. (A) *B. subtilis* 168 incubated during 3 h with FtsZ inhibitors **29** (5 µM), **40** (4 µM), **41** (5 µM), **45** (25 µM), and **48** (12 µM) and observed by phase contrast microscopy. (B) *B. subtilis* 168 cell length. Scale bar: 10 µm.

Interestingly, compound **47** inhibited bacterial viability without showing a clear effect on the Z-ring, which could suggest an alternative mechanism of action.

Moreover, each of these compounds impaired the normal assembly of FtsZ-GFP into the mid-cell Z-ring prior to division of *B. subtilis* SU570 at concentrations near their MIC values, further supporting FtsZ targeting. The observed effects consisted of a reduction in the proportion of cells with normal Z-rings at division sites with respect to controls and FtsZ delocalization into characteristic punctuate *foci* along the bacterial cells in less than 1 h (Figure 23). Z-rings along the filamented cells were very frequently observed abnormally close to each other with compounds **29**, **40**, **41**, and **48**. FtsZ-GFP *foci* were more abundant in cells treated with compounds **29** and **40**, and by contrast, fewer Z-rings and *foci* were observed in cells treated with compound **45**.

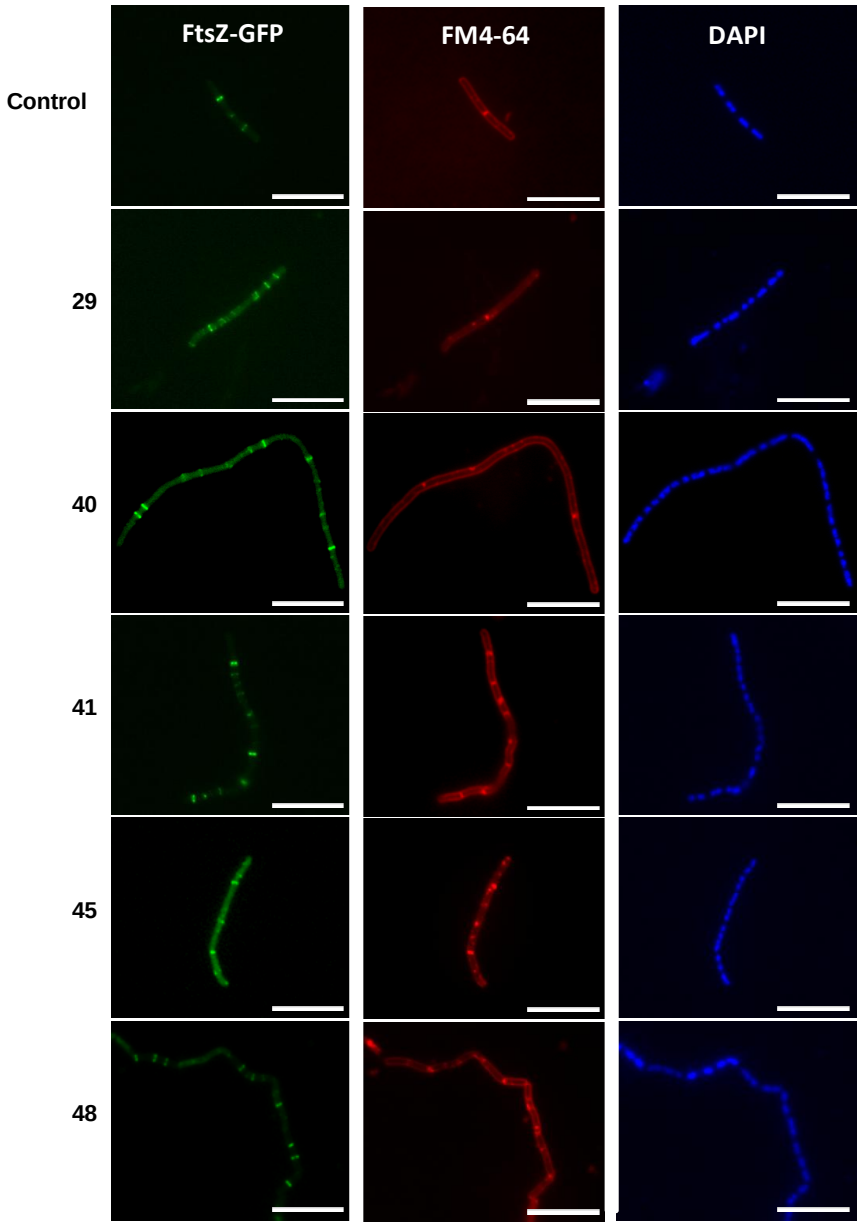

Figure 23. Effect of FtsZ inhibitors on FtsZ subcellular localization. Cells of *B. subtilis* SU570 (FtsZ-GFP) were incubated during 1 h with **29** (5 µM), **40** (3 µM), **41** (2 µM), **45** (25 µM), and **48** (12 µM). FtsZ-GFP membrane stained with FM4-64 and DNA stained with DAPI were visualized through their corresponding channels with a fluorescence microscope. Scale bar: 10 µm.

The impairment of the cell division ring was also reflected in an abnormal nucleoid morphology. Thus, cells treated with the FtsZ inhibitors **29**, **40**, **41**, **45**, and **48** showed nucleoids with a fragmenting appearance, in contrast with the control cells (Figure 23, DAPI column). In many cases, the regions of the nucleoid constriction corresponded with Z-rings or FtsZ *foci*, whereas in other zones FtsZ-GFP accumulation was not observed, which could match with previous division sites where the Z-ring has already disappeared. Membranes were visualized in the same *B. subtilis* SU570 cells treated with the vital stain FM4-64. In this case, and in addition to the plasma membrane marking the cell contour and division septa, frequent extra membrane accumulations and patches were observed, some of them coinciding with FtsZ *foci*. These observations suggest that these FtsZ inhibitors induce abortive division sites and plasma membrane lesions. These effects are similar to those reported for the most studied bacterial cell division inhibitor PC190723,[72,73,87] which targets another FtsZ binding site.[81] PC190723 (22 µM), when compared with inhibitor **40**, also induced the formation of membrane patches that overlap with the characteristic FtsZ *foci* along the undivided cellular filaments (Figure 24).

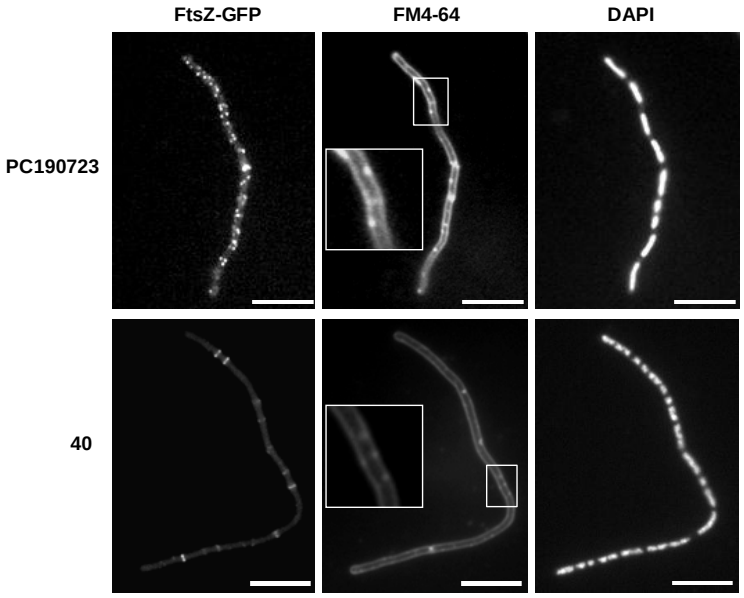

Figure 24. Cells of *B. subtilis* SU570 were incubated with PC190723 (22 µM, 1 h) or **40** (3 µM, 3 h). FtsZ-GFP, membrane stained with FM4-64 and DNA stained with DAPI were visualized. Membrane patches were observed in both, cells treated with PC190723 and with **40**. Insets show the magnification image of a specific region of the cell containing membrane patches. Scale bar: 10 µm.

All together, these studies show that, with the exception of the high affinity derivative **47** that seems to exert the inhibition of the bacterial cell division through a different mechanism, the majority of the compounds under study inhibit bacterial cell division by disrupting FtsZ assembly and impairment of the Z-ring. Among them, derivative **40** stands out as the most effective bacterial cell division inhibitor.

In summary, in the first part of this thesis we have reported a series of new compounds targeting the GTP-binding site of FtsZ (**3**-**50**) starting from hits **1** and **2** obtained from the screening of our in-house library. Assessment of their K_d values, as a measure of the direct interaction of these derivatives with the GTP-binding site of FtsZ from *B. subtilis*, along with their *in vitro* antibacterial activity against a panel of pathogenic bacteria and selectivity towards tubulin, has allowed us to identify potent and selective FtsZ inhibitors. The cytological effects of these new GTP-replacing FtsZ inhibitors mainly consist of Z-ring impairment and FtsZ delocalization into punctuate *foci*, which presumably lead to the observed inhibition of cell division. These studies led to the identification of biphenyl derivative **40** as the most effective FtsZ inhibitor and bacterial cell division blocker, with a K_d value in *B. subtilis* FtsZ of 0.5 μM, good antibacterial activity in Gram-positive pathogenic bacteria [MIC (MRSA) = 5 μM] and selectivity vs tubulin, followed by the naphthyl derivative **29.** Promising biphenyl fragment **45** and amide **48** also emerge as more effective FtsZ inhibitors than the initial hits **1** and **2**. Overall, these inhibitors contribute to expand the scarce number of GTP-mimetics available and provide a compelling rationale for the development of antibacterial agents with novel modes of action (Figure 25).

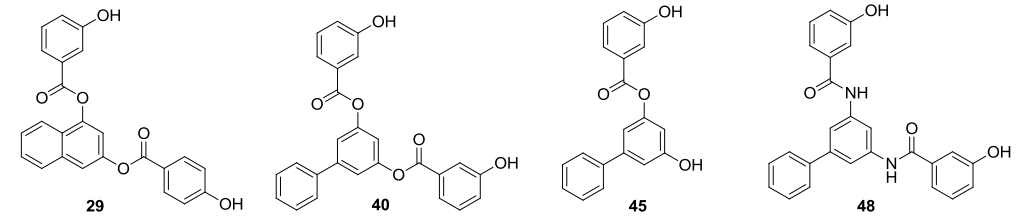

Figure 25. New FtsZ inhibitors targeting the GTP-binding site.

2.2. Development of Fluorescent Probes for the PC190723 Binding Site of FtsZ

Among the FtsZ inhibitors described so far, PC190723 is the most studied compound and its co-crystalization with FtsZ has allowed the identification of a long cleft as a new allosteric druggable site in the protein. In addition, its analogue **8j** has also been characterized as a potent FtsZ inhibitor, with higher FtsZ affinity and antibacterial activity.[71,72] However, the lack of a binding assay to assess the affinity of small molecules for this long cleft makes difficult the development of new FtsZ inhibitors addressing this new binding site. Indeed, only phenotypic experiments such as polymer pelleting assays have been used in order to identify new inhibitors. Therefore, fluorescent derivatives of PC/**8j** could be used as valuable tools to set up a fluorescence-based assay for the identification of FtsZ inhibitors by screening libraries of compounds against this newly identified binding site.

2.2.1. Design, Synthesis and Characterization of Fluorescent Compounds

An extensive SAR of benzamide derivatives perfomed by Prolisis[70,71] has shown that the 3-methoxybenzamide is the minimal structural feature for the molecular recognition by FtsZ. Therefore, we have designed fluorescent derivatives based on PC/**8j** that contain the benzamide subunit following two different approaches: (i) attachment of a fluorophore to the structure of **8j** through a rigid linker, such as an alkyne moiety, or a flexible aliphatic chain (**119**-**122**), and (ii) substitution of the heterocyclic subunit of PC/**8j** by a fluorescent tag (**123**-**125**). With respect to the fluorescent tag, we selected small fluorophores such as nitrobenzoxadiazole (NBD), a coumarin derivative, and dansyl (Figure 26).

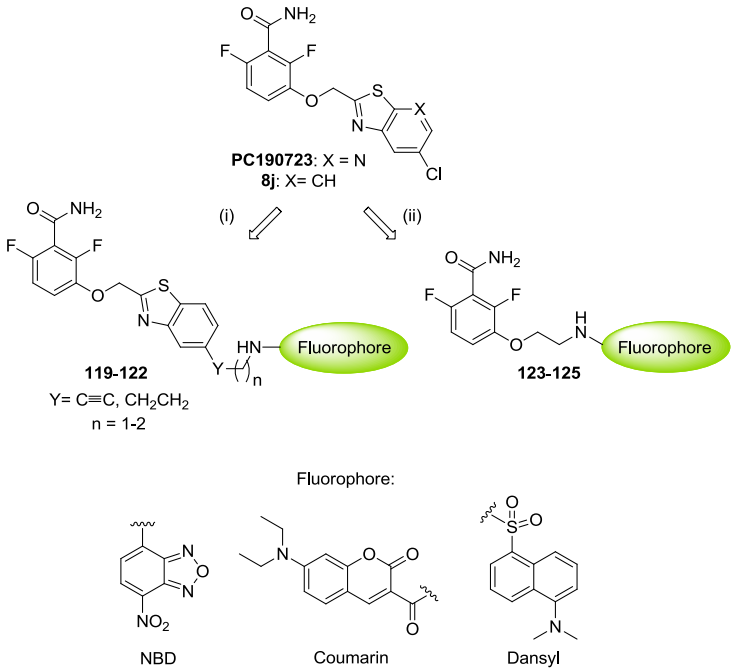

Figure 26. Initial design of PC190723/**8j**-based fluorescent probes.

Since the fluorescent assays will need a non-fluorescent substrate able to replace the fluorescent probe to confirm the interaction with the PC-binding site, we selected PC190723 for this purpose and carried out its synthesis following the synthetic route previously described in the literature (Scheme 9).[71] Thus, conversion of commercially available 2,6-difluoro-3-methoxybenzoic acid into its corresponding amide **126**, followed by methoxy deprotection with BBr_3 afforded 2,6-difluoro-3-hydroxybenzamide (**127**) in gram scale. On the other hand, the synthesis of the heterocyclic subunit started with the transformation of commercial 5-chloro-3-nitropyridin-2-ol into the bromo derivative **128**, followed by reduction of the nitro group to afford 3-aminopyridine **129** that was then condensed with benzyloxyacetyl chloride to give amide **130**. Intermediate **130** was cyclized with Lawesson's reagent and the obtained benzylether **131** was deprotected and transformed into bromo derivative **133** by reaction of the resulting alcohol **132** with NBS. Finally, Williamson alkylation of phenol **127** with **133** afforded PC190723.

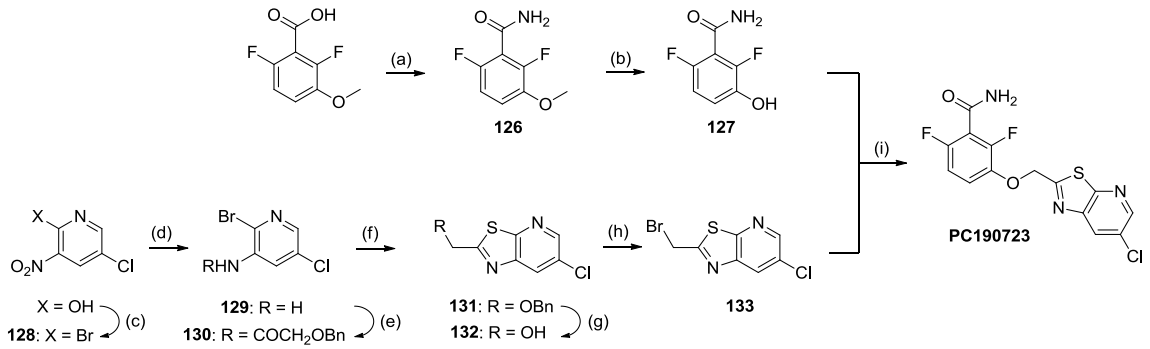

Scheme 9. Reagents and conditions: (a) i) $SOCl_2$, toluene, reflux, 5 h, quantitative; ii) NH_4OH, THF, rt, 16 h, 80%; (b) BBr_3, DCM, rt, 3 days, 79 %; (c) PBr_3, toluene/DMF, 130 ºC, 3 h, 42%; (d) $SnCl_2 \cdot H_2O$, HCl, Et_2O, 50 ºC, 30 min, 98%; (e) benzyloxyacetyl chloride, Et_3N, DCM, rt, 14 h, 80 %; (f) Lawesson's reagent, toluene, 120 ºC, 3 h, 79%; (g) BBr_3, DCM, rt, 2 h, 88%; (h) NBS, Ph_3P, DCM, rt, 2.5 h, 68%; (i) K_2CO_3, NaI, DMF, rt, 16 h, 33%.

Regarding the first series of derivatives **119**-**122**, in which the fluorophores were attached to **8j** by an alkyne or aliphatic chain, their synthesis was conceived by functionalization of **8j** with an alkynyl amine and subsequent nucleophylic substitution reaction with the corresponding fluorophore (dansyl, coumarin or NBD) (Figure 27). Hydrogenation of the triple bond present in these derivatives will afford compounds bearing a more flexible aliphatic chain as spacer.

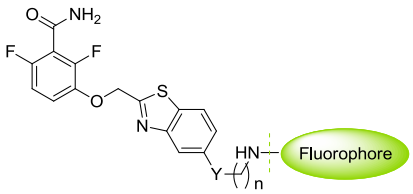

119: Y = C≡C, n = 1, Fluorophore = dansyl
120: Y = C≡C, n = 1, Fluorophore = coumarin
121: Y = C≡C, n = 2, Fluorophore = NBD
122: Y = CH_2CH_2, n = 1, Fluorophore = dansyl

Figure 27. Compounds **119**-**122**.

Thus, synthesis of propargylic amine **138** was carried out starting from commercial 5-bromo-2-methyl-1,3-benzothiazole. Its bromination with NBS and AIBN in CCl_4 followed by nucleophilic substitution of the bromo derivative **134** with hydroxybenzamide **127** gave the bromo aromatic intermediate **135** (Scheme 10).[71] Then, Sonogashira coupling of **135** with protected propargylamine **136** was carried out under thermal conditions using $PdCl_2(PPh_3)_2$ as catalyst to obtain the corresponding coupling product **137** in 58% yield. This yield was improved by the use of $Pd(PPh_3)_4$

and MW irradiation, affording the protected amine **137** in 86%, which was deprotected to obtain the intermediate amine **138**. Coupling of **138** with the three different fluorophores properly functionalized: dansyl chloride, 7-(diethylaminocoumarin)-3-carboxylic acid and 4-chloro-7-nitrobenzofurazan (Cl-NBD) yielded dansyl and coumarin derivatives **119** and **120**, respectively. Unfortunately, the low conversion (<5%) of the reaction of **138** with Cl-NBD did not allow the isolation of the desired NBD derivative (Scheme 10).

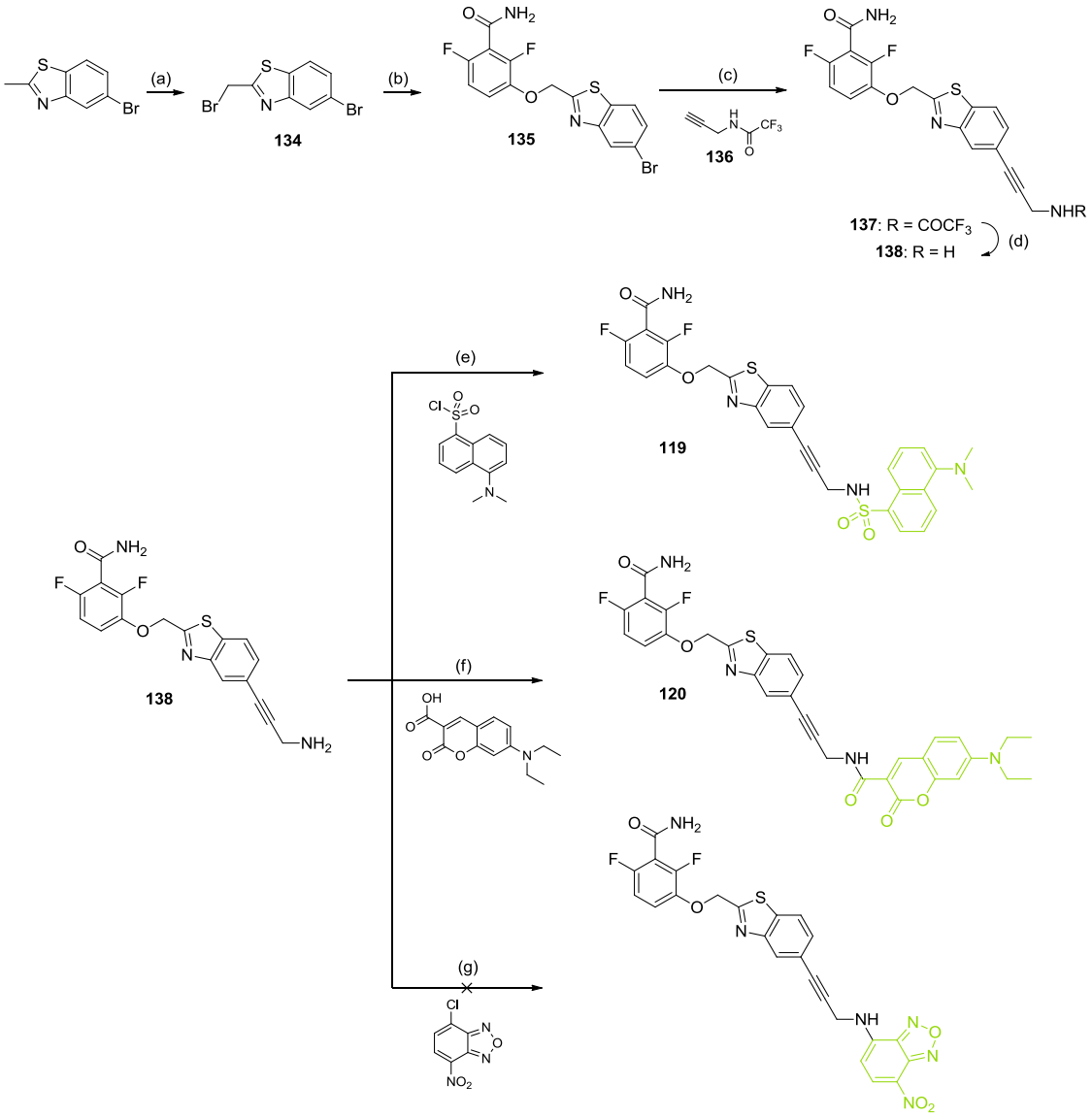

Scheme 10. Reagents and conditions: (a) NBS, AIBN, CCl_4, 90 ºC, 3 h, 13%; (b) **127**, K_2CO_3, DMF, rt, 16 h, 82%; (c) $Pd(PPh_3)_4$, CuI, Et_3N, DMF, MW, 100 ºC, 45 min, 86%; (d) NH_4OH, MeOH, rt, 17 h, 99%; (e) Et_3N, DCM/DMF, rt, 24 h, 28%; (f) PyBroP®, DIPEA, DMF, rt, 4 h, 5%; (g) Et_3N, DCM/DMF, rt, 24 h.

Therefore, for the synthesis of the NBD derivative we considered the possibility of synthesizing the NBD fluorophore functionalized with a terminal alkyne in order to perform a Sonogashira

coupling with the scaffold of **8j**. Thus, alkyne **139** was synthesized by reaction of propargylamine with Cl-NBD in the presence of Et_3N in gram scale, but the Sonogashira reation with bromo derivative **135** did not give the corresponding desired product (Scheme 11). Instead, 4-amino-NBD was mainly isolated from the reaction crude, as the result of the propargyl cleavage in **139** promoted by the palladium catalyst. In an attempt to avoid this spontaneous cleavage, we proposed the synthesis of an NBD derivative with an additional methylene group in the alkyl chain. Hence, alkyne **140** was obtained from 3-butyn-1-amine and Cl-NBD in the presence of DIPEA and then coupled with bromo derivative **135** to afford NBD-functionalized compound **121** in 77% yield (Scheme 12).

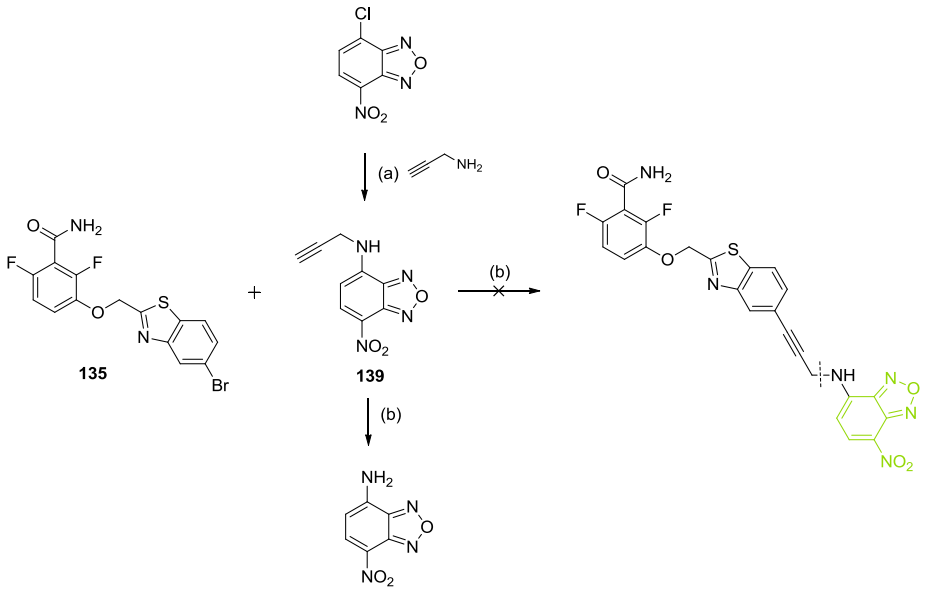

Scheme 11. Reagents and conditions: (a) Et_3N, MeCN, rt, 2 h, 35%; (b) $Pd(PPh_3)_4$, CuI, Et_3N, DMF, MW, 100 ºC, 1 h.

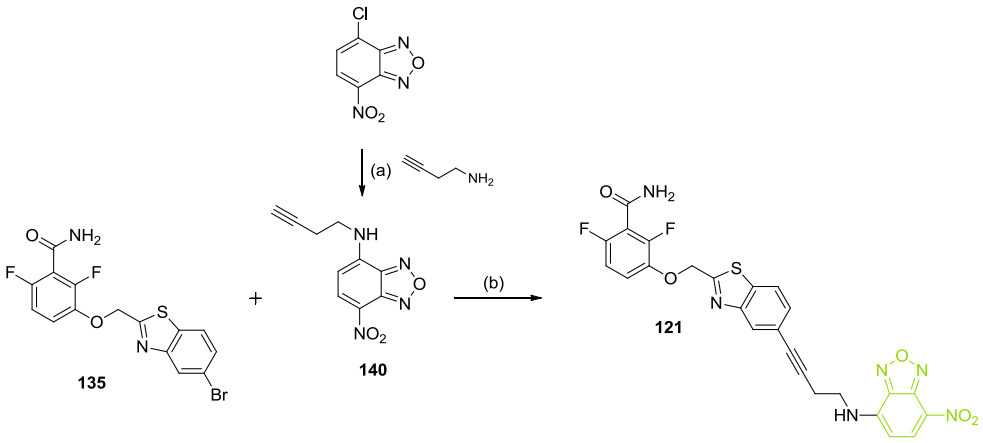

Scheme 12. Reagents and conditions: (a) DIPEA, MeOH, rt, 15 h, 77%; (b) $Pd(PPh_3)_4$, CuI, Et_3N, DMF, MW, 100 ºC, 1 h, 41%.

To study the influence of a more flexible chain, alkyne **137** was hydrogenated to afford aliphatic amide **141** in the presence of Raney-Ni as a catalyst. It is noteworthy that although the hydrogenation took place in low yield (22%), this catalyst allowed us to obtain the desired product **141** since the use of palladium promotes the cleavage of the molecule through the pseudobencylic position to yield the corresponding hydroxybenzamide. Finally, coupling of the deprotected amine **142** with dansyl chloride afforded the desired product **122** (Scheme 13).

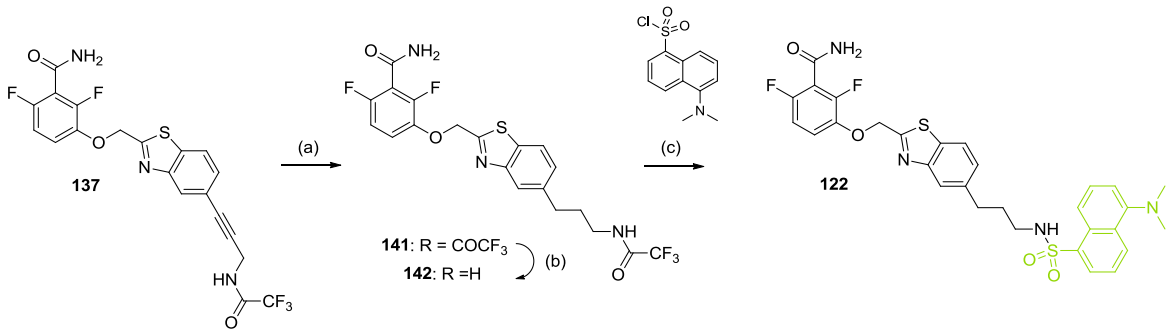

Scheme 13. Reagents and conditions: (a) H_2, Ra-Ni, THF/MeOH, rt, 3 h, 22%; (b) NH_4OH, MeOH, rt, 17 h, 99%; (c) Et_3N, DCM/DMF, rt, 24 h, 26%.

With respect to derivatives **123**-**125**, in which the heterocyclic subunit of PC was replaced by a fluorescent tag, an ethyl chain was chosen as spacer between the benzamide moiety and the fluorophore. These new probes were synthesized by reaction of the corresponding alkyl amine and the fluorophores. Thus, Mitsunobu reaction of phenol **127** with hydroxyethylphthalimide followed by

removal of the protecting group with hydrazine afforded amine **144**, which was further treated with the different fluorophores to give fluorescent derivatives **123**-**125** (Scheme 14).

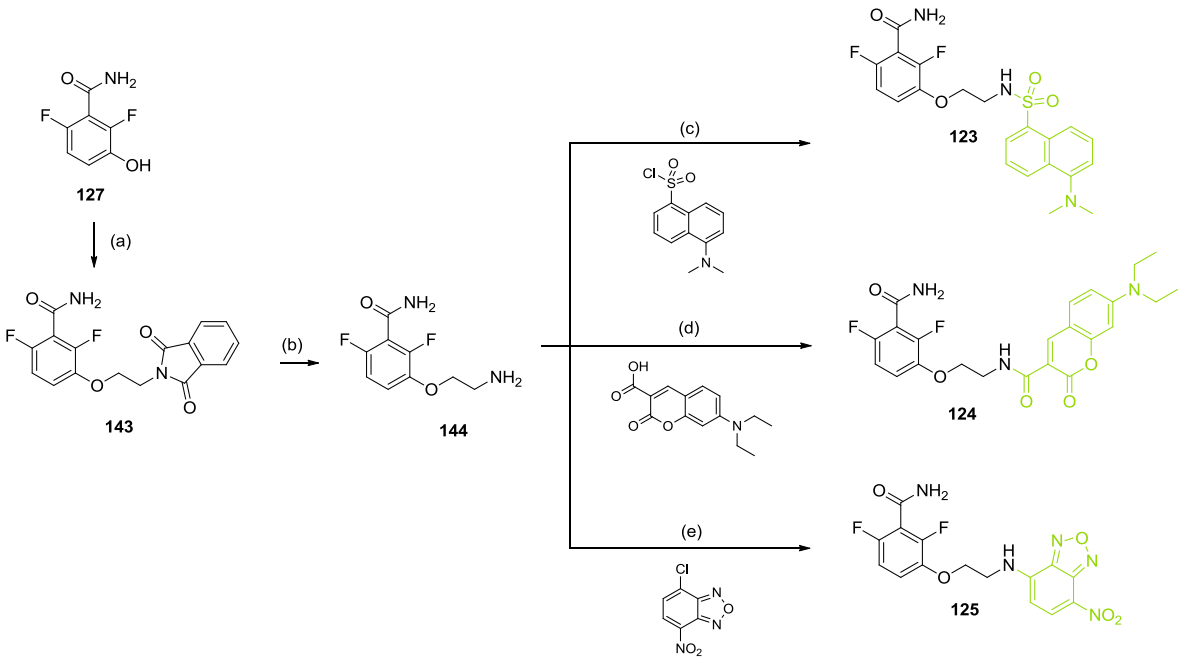

Scheme 14. Reagents and conditions: (a) *N*-(2-hydroxyethyl)phthalimide, DEAD, Ph_3P, THF, reflux, 24 h, 67%; (b) $N_2H_4 \cdot H_2O$, EtOH, reflux, 2 h, 67%; (c) Et_3N, DCM/DMF, rt, 24 h, 8%; (d) PyBroP®, DIPEA, DMF, rt, 4 h, 27%; (e) Et_3N, DMF, rt, 20 h, 13%.

Once all fluorescent compounds were synthesized, we assessed their fluorescent properties in order to evaluate their potential as chemical probes. In theory, a good candidate for a FtsZ fluorescent probe based on PC190723 should show a significant modification in the emission fluorescence spectrum [wavelength (λ) and/or emission intensity (I_{em})] or in the fluorescence anisotropy values (r) in the presence of the protein, that could be then restored to the initial values by displacement with the parent compound PC190723. Therefore, fluorescence emission spectra and anisotropy of compounds **119**-**125** (10 μM) were first registered employing an excitation wavelength corresponding to the maximum absortion of each compound in Hepes buffer at pH 6.8 and 25 ºC. Then, Bs-FtsZ (10 μM) in Hepes buffer, the slowly hydrolizable GTP analogue GMPCPP (0.1 mM) and $MgCl_2$ (10 mM) were subsequently added to set up the polymerization conditions.

Finally, PC190723 or **8j** (10 μM) was added in order to displace and revert the possible effect of the fluorescent probes.

In general, fluorescence emission spectra of these probes did not show significant changes under FtsZ polymerization conditions as it is exemplified in Figure 28 for compound **125**.

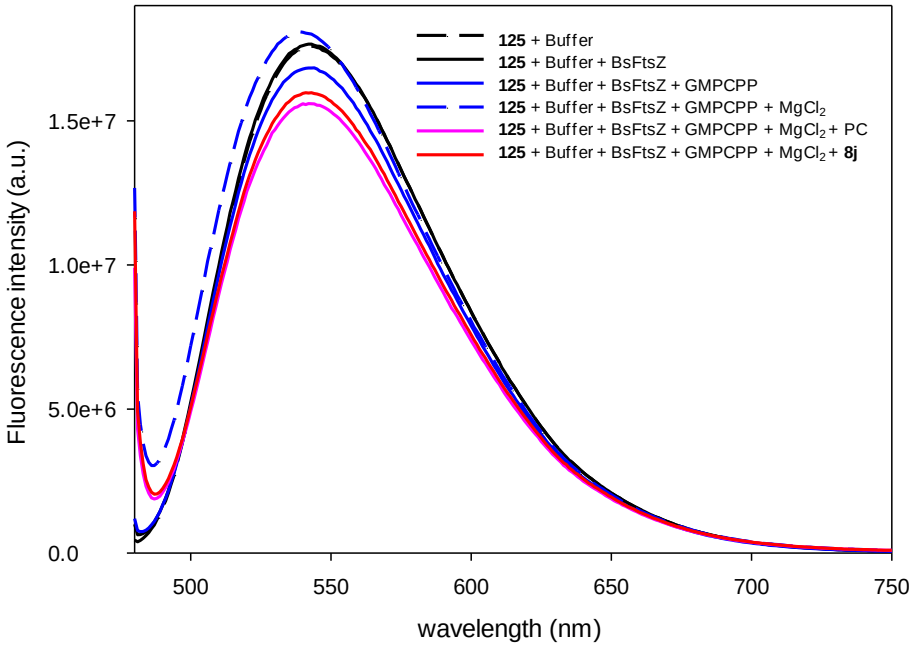

Figure 28. Emission spectra of compound **125** at λ_{exc} = 474 nm.

Regarding the anisotropy values, derivatives **119** and **120** did not undergo any significant variation after addition of the protein, nucleotide and $MgCl_2$, when compared with their basal values [*e.g.* **119** (alone): r = 0.083 vs **119** (under FtsZ polymerization): r = 0.084) (Table 7). Compounds **121** and **122** presented a high basal anisotropy which suggests the aggretation of these compounds in buffer solution (Table 7) [*e.g.* **121**: r = 0.130 vs **122**: r = 0.154].

Table 7. Anisotropy (r) values of fluorescent derivatives **119-122**.

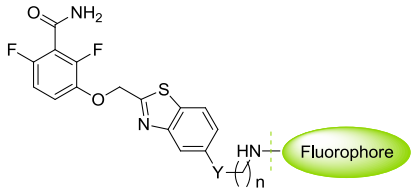

119: Y = C≡C, n = 1, Fluorophore = dansyl
120: Y = C≡C, n = 1, Fluorophore = coumarin
121: Y = C≡C, n = 2, Fluorophore = NBD
122: Y = CH_2CH_2, n = 1, Fluorophore = dansyl

Conditions	119	120	121	122
Compound (10 µM)	0.083	0.017	0.130	0.154
+ Bs-FtsZ (10 µM)	0.085	0.017	0.203	0.164
+ GMPCPP (0.1 mM)	0.086	0.016	0.246	0.171
+ $MgCl_2$ (10 mM)	0.084	0.022	0.248	0.188
+ PC190723 (10 µM)	0.079	0.032	0.328	0.158

The fluorescent assays of compounds **123**-**125**, in which the heteroaromatic subunit of PC/**8j** was replaced by a fluorophore, showed no significant changes in their emission spectra under polymerization conditions. However, fluorescence anisotropy of NBD derivative **125** was increased when $MgCl_2$ was added (highlighted in red in Table 8) and the polymerization was initiated (basal: r = 0.035; polymerization: r = 0.086). This effect was reverted after addition of PC190723 (r = 0.036, highlighted in blue), which indicates that this fluorescent compound binds to the protein at the same binding site that its parent compound (Table 8). In addition, anisotropy changes were not observed in control experiments without protein, confirming that the specific binding of the compound to FtsZ is responsible for the changes in anisotropy.

Table 8. Anisotropy values (r) of fluorescent derivatives **123**-**125**.

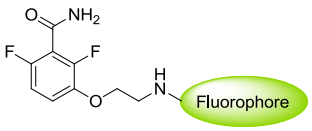

123: Fluorophore = dansyl
124: Fluorophore = coumarin
125: Fluorophore = NBD

	123	**124**	**125**
Compound (10 µM)	0.012	0.125	0.026
+ Bs-FtsZ (10 µM)	0.036	0.133	0.034
+ GMPCPP (0.1 mM)	0.049	0.139	0.035
+ $MgCl_2$ (10 mM)	0.115	0.149	0.086
+ PC190723 (10 µM)	0.151	0.106	0.036
Compound + GMPCPP	0.012	0.100	0.026
Compound + $MgCl_2$	0.036	0.120	0.034
Compound + PC190723	0.049	0.110	0.035
Mixture without Bs-FtsZ	0.115	0.140	0.038

Taking into account the positive results obtained with derivative **125**, we selected this compound to study the influence of the spacer between the difluorobenzamide and the fluorophore by increasing the length of the alkyl chain (**145**-**147**). Moreover, bearing in mind that 2,6-difluoro-3-nonyloxybenzamide is a potent inhibitor of FtsZ,[69] we considered that the introduction of an aliphatic chain in the spacer of **125** could increase FtsZ affinity. Thus, compound **148**, having an octyl chain in the linker, was also synthesized.

At this point, fluorophores for super-resolution microscopy such as 4-(and-5)-carboxytetramethylrhodamine (TAMRA) and ATTO 565 were also taken into account.[88] Super-resolution imaging with available small organic fluorophores remains challenging. New fluorescent probes bearing photoswichable fluorophores with high intensity contrast between on and off states, together with high extinction coefficients and quantum yields are needed to visualize dynamic processes in living cells. In this sense, we conceived the synthesis of compounds based on PC/**8j** (**149**-**150**) functionalized with TAMRA and ATTO 565 in order to obtain probes with optimized fluorescent properties for the study of the bacterial division process (Figure 29).

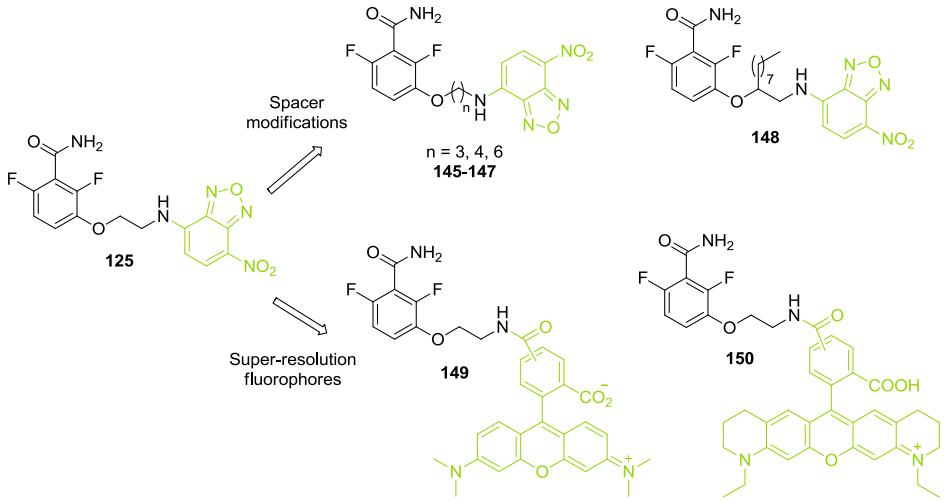

Figure 29. Design of new fluorescent probes **145**-**150** based on compound **125**.

Regarding the spacer modifications of **125**, Williamson alkylation of phenol **127** with different *N*-protected bromo aliphatic alkylamines afforded derivatives **151**, **152** and **155**. These intermediate amines were deprotected and coupled with Cl-NBD to afford the desired final compounds **145**-**147** (Scheme 15).

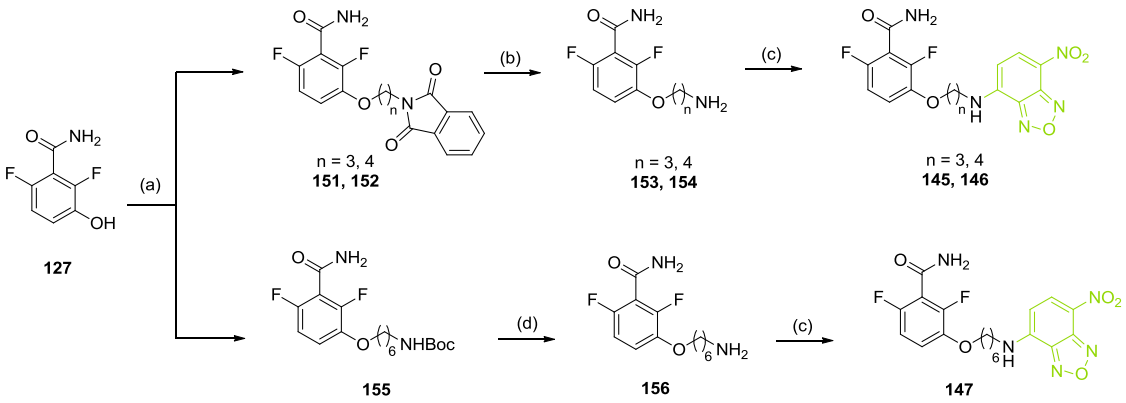

Scheme 15. Reagents and conditions: (a) *N*-(3-bromopropyl)-, *N*-(4-bromobutyl)phthalimide, or 6-bromo-*N*-Boc-1-hexanamine, K_2CO_3, NaI, DMF, rt, 16 h, 57-87%; (b) $N_2H_4 \cdot H_2O$, EtOH, reflux, 2 h, 55-64%; (c) Cl-NBD, DIPEA, DMF, rt, 16 h, 4-11%; (d) TFA, DCM, rt, 1 h, 99%.

For the synthesis of **148**, dibromoderivative **157** was obtained by treatment of *tert*-butyl carbamate with bromine in the presence of potassium carbonate at room temperature (Scheme 16).[89] Then, addition of **157** to 1-decene in an anti-Markovnikov fashion, followed by reduction with aqueous Na_2SO_3 afforded the desired bromo intermediate **158**. Finally, Williamson alkylation of phenol **127** with **158**, subsequent Boc removal and reaction of the resulting amine **160** with Cl-NBD gave final compound **148**.

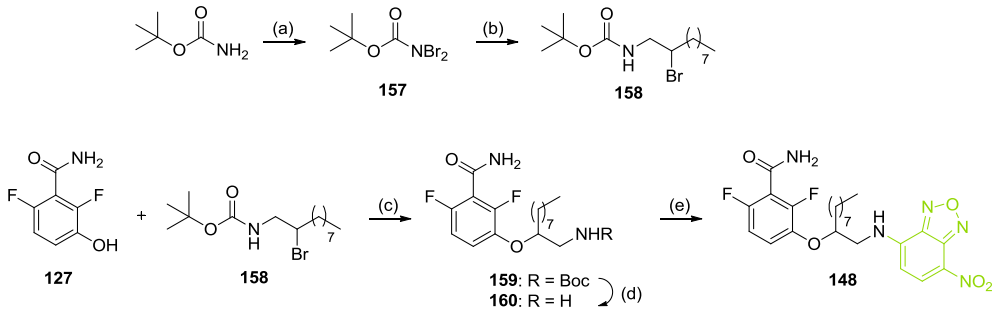

Scheme 16. Reagents and conditions: (a) Br_2, K_2CO_3, H_2O, rt, 2 h, 79%; (b) i) 1-decene, DCM, reflux, 3 h; ii) 12% aq. Na_2SO_3, 5-10 ºC, 15 min, 56%; (c) K_2CO_3, NaI, DMF, rt, 16 h, 23%; (d) TFA, DCM, rt, 1 h, 99%; (e) Cl-NBD, Et_3N, DMF, rt, 16 h, 11%.

The TAMRA and ATTO 565 fluorescent derivatives **149** and **150** were synthesized by reaction of amine **144** with the *N*-hydroxysuccinimide (NHS) esters of the corresponding fluorophore under basic conditions (Scheme 17).

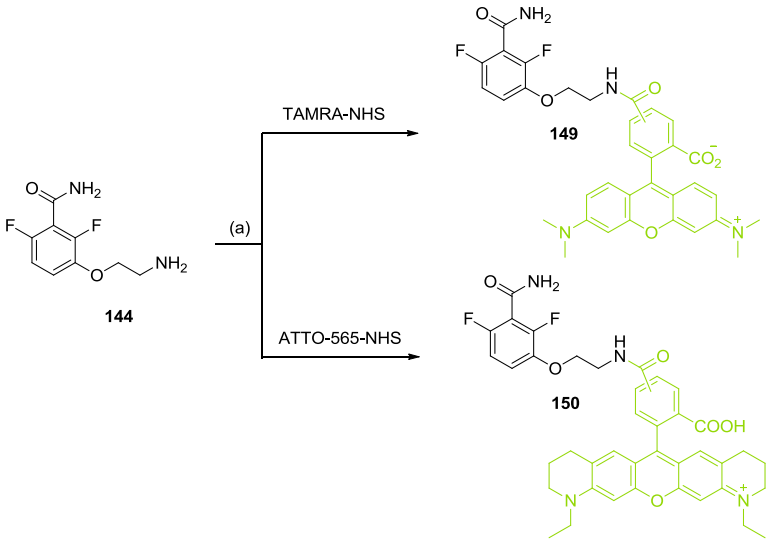

Scheme 17. Reagents and conditions: (a) Et_3N, DMF, rt, 4 h, 66, 99%.

Finally, methylamino-NBD **161** was considered as a negative control in order to discard possible interactions of the fluorophore with FtsZ. This compound was synthesized by reaction of methylamine hydrochloride with Cl-NBD in MeOH (Scheme 18).[90]

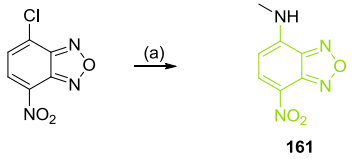

Scheme 18. Reagents and conditions: (a) i) $CH_3NH_2 \cdot HCl$, MeOH, 75 ºC, 30 min; ii) 0.75 M aq. $NaHCO_3$, 0 ºC, 1 h, 66%.

In order to evaluate these new synthesized fluorescent derivatives **145**-**150**, fluorescence emission spectra and anisotropy spectra were registered in the previously described experimental conditions. Once again, there were no significant fluorescence changes in the emission spectra (λ, I_{em}) of the analized compounds under polymerization conditions. However, anisotropy of NBD derivatives **145**-**147** was increased in the presence of FtsZ, the nucleotide and $MgCl_2$, and the initial values were restored by displacement with inhibitor PC190723 (Table 9, **125** was included for comparison). In the case of probe **148**, it showed the highest increase in the anisotropy under polymerization conditions but this value was not reverted when PC190723 was added. This last result suggests that this compound could be aggregated in the presence of the protein due to the

long hydrophobic chain or might exhibit a high affinity binding, and therefore it was not considered as a useful fluorescent probe for a FtsZ displacement assay. Regarding TAMRA and ATTO-565 derivatives **149** and **150**, no anisotropy changes were observed under polymerization conditions. Finally, as it was expected, control compound **161** did not exhibit any change in the fluorescence emission spectrum nor in anisotropy and could be used as a negative control.

Table 9. Anisotropy values (r) of fluorescent derivatives **125**, **145**-**150** and **161**.

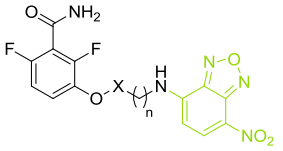

125, **145-147**: X = CH_2, n = 1, 2, 3, 5
148: X = $CH(CH_2)_7CH_3$, n = 1

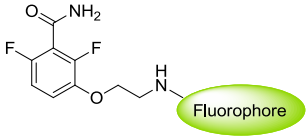

149: Fluorophore = TAMRA
150: Fluorophore = ATTO-565

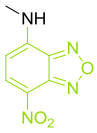

161

	125	**145**	**146**	**147**	**148**	**149**	**150**	**161**
Compound (10 µM)	0.026	0.038	0.032	0.030	0.045	0.030	0.019	0.014
+ Bs-FtsZ (10 µM)	0.034	0.042	0.035	0.042	0.130	0.031	0.025	0.016
+ GMPCPP (0.1 mM)	0.035	0.040	0.039	0.042	0.186	0.030	0.022	0.017
+ $MgCl_2$ (10 mM)	0.086	0.078	0.078	0.127	0.317	0.032	0.025	0.017
+ PC190723 (10 µM)	0.036	0.057	0.046	0.067	0.324	0.030	0.023	0.019
+ PC190723*	0.026	0.046	0.032	0.046	0.322	0.030	0.019	-
Compound + GMPCPP	0.034	0.038	0.028	0.038	0.053	0.029	0.019	-
Compound + $MgCl_2$	0.035	0.033	0.027	0.033	0.054	0.030	0.020	-
Compound + PC190723	0.038	0.032	0.028	0.032	0.052	0.030	0.020	-
Mixture without Bs-FtsZ	0.026	0.035	0.027	0.035	0.052	**-**	**-**	-

* Additional 10 µM of PC190723 was added. Final concentration of 20 µM.

In summary, NBD derivatives **125**, **145**-**147** stand out as useful fluorescent probes since they showed significant changes in the anisotropy values under FtsZ polymerization conditions. Therefore, they were selected for further biological evaluation.

2.2.2. Biological Evaluation of Selected Fluorescent Compounds

First, the effect of the new synthesized probes **125**, **145**-**147** in the FtsZ polymerization process was determined by polymer pelleting assay, showing that these derivatives alter the FtsZ polymerization in a concentration depending manner. Compounds **125**, **145** and **146** act as FtsZ

stabilizing agents like their parent compound PC190723, increasing the pellet percentage with respect to the control. This stabilizing effect is exemplified in Figure 30 for compounds **125** and **146**.

Contrary, derivative **147**, in which the alkyl chain was elongated to six methylene units, reduces the pellet percentage of FtsZ with respect to the control, acting as an inhibitor of the polymerization instead of stabilizing the protofilaments. Polymer pelleting assay also showed that derivative **148** was able to stabilize FtsZ polymers at lower concentrations than derivative **125**. As it is shown in Figure 30, compound **148** increased the polymer concentration up to 91% at 10 μM whereas derivative **125** only exhibited 77% of pellet at the same concentration.

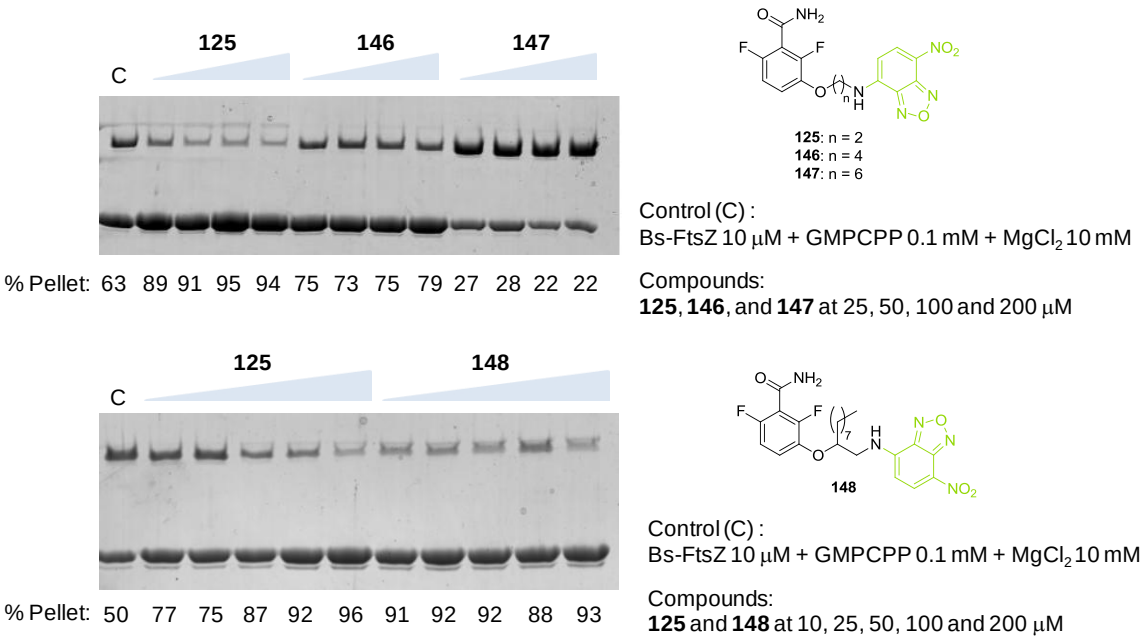

Figure 30. Polymer pelleting assays in the presence of **125**, **146**-**148**.

Therefore, the best candidates to be used as fluorescent probes to set up a displacement binding assay against the PC-binding site would be the NBD derivatives **125** and **145**-**147**. In order to evaluate the potential of these probes, displacement anisotropy curves were performed. Starting from a solution of polymerized FtsZ (5 μM) in the presence of GMPCPP (0.1 mM), $MgCl_2$ (10 mM) and the corresponding fluorescent probe (5 μM), increasing concentrations of the inhibitor PC190723 were subsequently added until the anisotropy recovered the basal value of the free compound (Figure 31). As it is shown in the graph, anisotropy values decreased with the increasing concentrations of PC190723 in all cases, confirming the suitability of these NBD derivatives as

fluorescent probes. Although the biggest difference between the bound and unbound state was observed with derivative **147**, this inhibitor had shown a different phenotytic pattern in the polymer pelleting assay. In addition, compound **145** exibited the lower anisotropy difference between the bound and unbound state. Therefore, derivatives **125** and **146** were selected to carry out a fluorescence-based displacement assay to screen a library of already described FtsZ inhibitors that do not target the GTP-binding site and a series of hits from a commercial library that has already been docked to the PC-binding pocket. This assay is currently on going in the laboratory and it will allow the assessment of the binding constants for the PC-binding site and therefore the possibility of performing an HTS in order to identify new FtsZ inhibitors targeting this allosteric binding site.

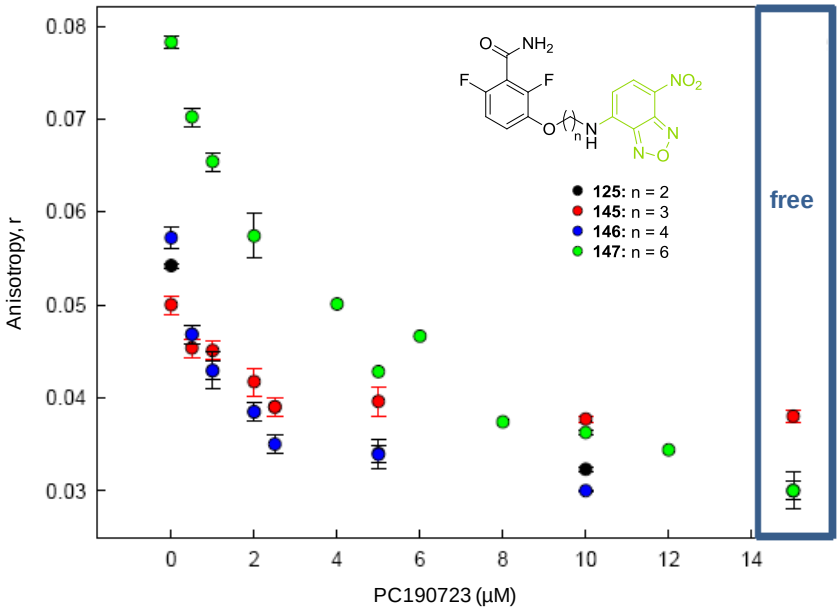

Figure 31. Displacement curves of fluorescent probes **125** and **145**-**147** by PC190723.

Finally, in order to confirm whether selected fluorescent probes would enable the visualization of FtsZ in cells, allowing the monitorization of the division process, we carried out *in vivo* studies of the probes at different concentrations with *B. subtilis* cells. Interestingly, probes **125** and **145**-**147** at concentrations lower than 50 µM were able to stain FtsZ protein in *B. subtilis* without affecting bacterial cell division process (Figure 32A). The fluorescence disappears by addition of PC190723 (25 µM) and consequent displacement of the fluorescent probes, which demonstrates the specificity of the staining (Figure 32B). Moreover, at higher concentration (200 µM) the probes enabled not only to label the cells but also to alter FtsZ polymerization (Figure 32C). As a negative control,

fluorescence was not observed with NBD derivative **161** and cells were not affected by this compound.

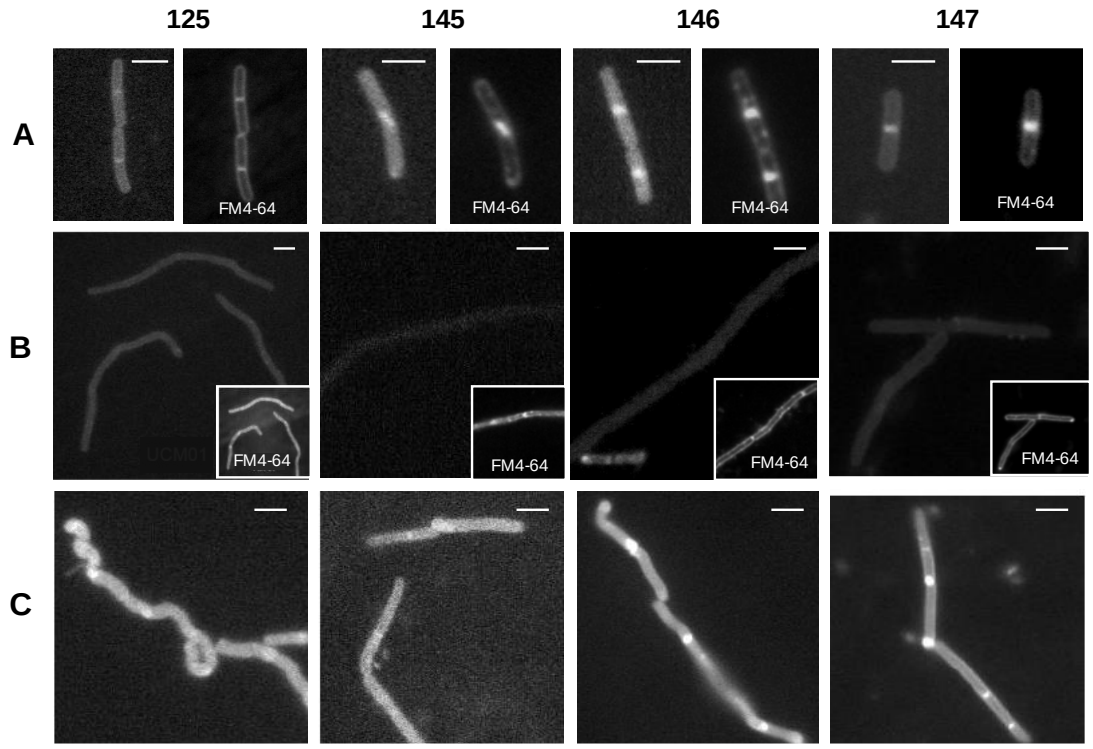

Figure 32. *In vivo* studies of fluorescent probes **125** and **145**-**147** in *B. subtilis*. (A) Labeling of FtsZ with the probes at 50 µM and visualization by fluorescent microscopy. (B) To assess specificity, cells were labeled under previous conditions and PC190723 (25 µM) was then added. (C) Fluorescent filamentous cells were observed at 200 µM of compound.

In summary, in the second part of this project we have developed the fluorescent probes **125**, and **145**-**147** which represent, to the best of our knowledge, the first probes targeting the new binding site identified for PC190723. These compounds can be used depending on their concentration for the visualization of the bacterial cell division and to study the role of FtsZ in this process, or as biological tools for the screening and identification of new hits for the PC-binding site, which will allow the discovery of new allosteric inhibitors of FtsZ.

3. CONCLUSIONS

The present work was aimed at the search of small molecules targeting FtsZ protein as antibacterial agents. To achieve this goal our efforts have being focused on the two druggable binding sites identified for the protein: i) the orthosteric GTP-binding pocket and ii) the allosteric PC-binding site.

Concerning the GTP-binding site, we have developed a series of compounds able to replace the natural regulator GTP and to specifically inhibit FtsZ. These inhibitors perturb protein assembly and block bacterial cytokinesis. Furthermore, they display high antibacterial activity against multidrug-resistant Gram-positive pathogenic bacteria. Among them, biphenyl **40** stands out as the most promising FtsZ inhibitor, with good affinity (K_d = 0.5 µM) and antibacterial activity [MIC (MRSA) = 7 µM], and selectivity against tubulin. This compound together with **29**, **45**, and **48**, acts as an effective FtsZ assembly modifier and leads to filamentous undivided cells, finally disrupting bacterial viability.

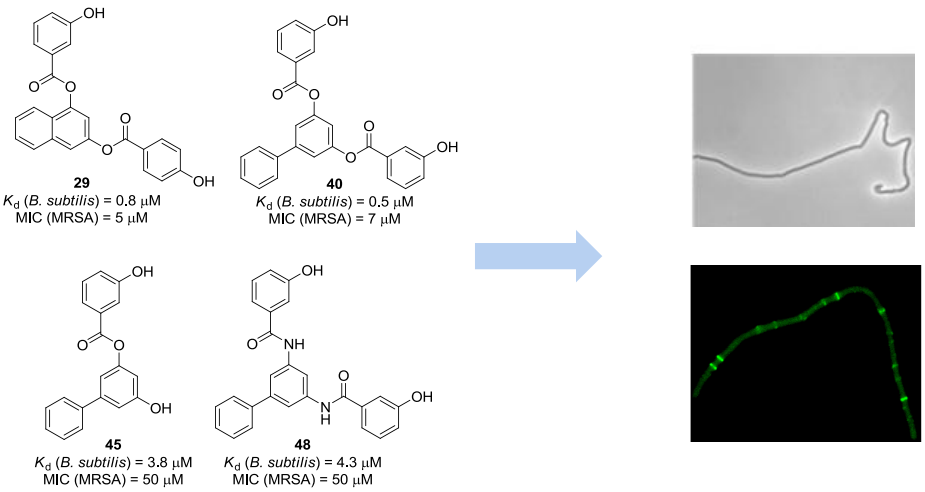

Regarding the PC-binding site, we have developed the first fluorescent derivatives of PC190723 as chemical probes for the study of FtsZ. Among synthesized compounds, NBD derivatives **125**, **145**-**147** have been used to set up a fluorescence-based displacement assay that will allow the identification of new allosteric inhibitors of FtsZ. These compounds have demonstrated to be valuable tools for the *in vivo* labeling of FtsZ.

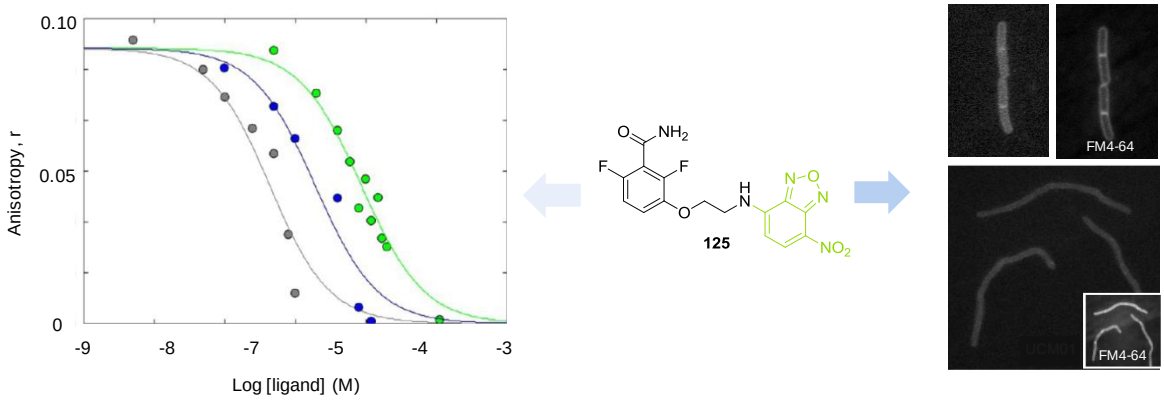

Overall, the new non-nucleotide GTP-replacing compounds synthesized in this work contribute to expand the scarce number of GTP mimetics available and provide a compelling rationale for the development of antibacterial agents with novel modes of action. Moreover, we described the first small molecule fluorescent probes for the visualization of the Z-ring targeting the allosteric PC-binding site. These probes should provide key insights towards the understanding of the role of FtsZ in the bacterial division process.

4. EXPERIMENTAL PART

4.1. Chemistry

Unless stated otherwise, starting materials, reagents and solvents were purchased as high-grade commercial products from Sigma-Aldrich, ABCR, Acros, Lancaster, Invitrogen, ATTO-TEC or Scharlab and were used without further purification. Tetrahydrofuran (THF) and dichloromethane (DCM) were either distilled from sodium benzophenone ketyl and calcium hydride respectively, or dried using a Pure Solv^{TM} Micro 100 Liter solvent purification system. Triethylamine and pyridine were dried over potassium hydroxide and distilled before using. Analitical thin-layer chromatography (TLC) was run on Merck silica gel plates (Kieselgel 60 F-254) with detection by UV light (254 nm), ninhydrin solution, or 10% phosphomolybdic acid solution in EtOH. Flash chromatography was performed on a Varian 971-FP flash purification system using silica gel cartridges (Varian, particle size 50 μm). All compounds were obtained as oils, except for those whose melting points (mp) are indicated, which were solids. Mp (uncorrected) were determined on a Stuart Scientific electrothermal apparatus. Infrared (IR) spectra were measured on a Shimadzu-8300 or Bruker Tensor 27 instrument equipped with a Specac ATR accessory of 5200-650 cm^{-1} transmission range; frequencies (ν) are expressed in cm^{-1}. Nuclear magnetic resonance (NMR) spectra were recorded on a Bruker Avance III 700 MHz (^{1}H, 700 MHz; ^{13}C, 175 MHz), Bruker Avance 500 MHz (^{1}H, 500 MHz; ^{13}C, 125 MHz) or Bruker DPX 300 MHz (^{1}H, 300 MHz; ^{13}C, 75 MHz) instrument at room temperature at the Universidad Complutense de Madrid (UCM) NMR core facility. Chemical shifts (δ) are expressed in parts per million relative to internal tetramethylsilane; coupling constants (J) are in hertz (Hz). The following abbreviations are used to describe peak patterns when appropriate: s (singlet), d (doublet), t (triplet), q (quartet), qt (quintet), m (multiplet), br (broad), app (apparent). 2D NMR experiments (heteronuclear multiple quantum correlation [HMQC] and heteronuclear multiple bond correlation [HMBC]) of representative compounds were carried out to assign protons and carbons of the new structures and the following abbreviations have been used for the peak assignment: gal. (gallic acid), eud. (eudesmic acid), prot. (protocatechuic acid), α-res. (α-resorcylic acid), *m*-sal. (*m*-salicylic acid), *p*-sal. (*p*-salicylic acid), Clbenz. (3-chloro-4-hydroxybenzoic acid), Cl2benz. (3,4-dichlorobenzoic acid), naph. (naphthalene), biph. (biphenyl), coum. (coumarin), DS (dansyl), NBD (nitrobenzoxadiazole) and pht. (phthalimide) (see Figure 33).

Mass spectrometry (MS) was carried out on a Bruker LC-Esquire spectrometer in electrospray ionization (ESI) mode at the UCM's mass spectrometry core faciliy. High performance liquid chromatography coupled to mass spectrometry (HPLC-MS) analysis was performed using an Agilent 1200LC-MSD VL instrument. LC separation was achieved with an Zorbax Eclipse XDB-C18 column (5 μm, 4.6 mm x 150 mm) for naphthalene derivatives and a Zorbax SB-C3 column (5 μm, 2.1 mm x 50 mm) for biphenyl derivatives, both together with a guard column (5 μm, 4.6 mm x 12.5 mm). The gradient mobile phases consisted of A (95:5 water/MeOH) and B (5:95 water/MeOH) with 0.1% ammonium hydroxide and 0.1% formic acid as the solvent modifiers. MS analysis was performed with an ESI source. The capillary voltage was set to 3.0 kV and the fragmentor voltage was set at 72 eV. The drying gas temperature was 350 ºC, the drying gas flow was 10 L/min, and the nebulizer pressure was 20 psi. Spectra were acquired in positive or negative ionization mode from 100 to 1200 *m/z* and in UV-mode at four different wavelengths (210, 230, 254, and 280 nm). Elemental analyses (C, H, N, S) were obtained on a LECO CHNS-932 apparatus at the UCM and the Universidad Autónoma de Madrid analysis services and were within ±0.5% of the theoretical values, confirming a purity of at least 95% of all tested compounds.

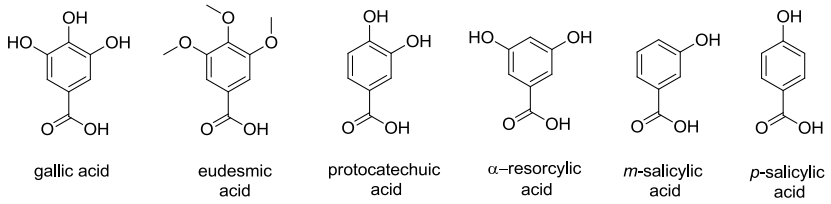

Figure 33. Common names used for the peak assignment.

4.1.1. Synthesis of Intermediates 51a-f, 52a-h, and 97

General Procedure for the Synthesis of Carboxylic Acids 51a-f. Method A: A mixture of the corresponding carboxylic acid (1 equiv), imidazole (2.4 equiv/hydroxy group) and *tert*-butyldimethylsilyl (TBS) chloride (1.4 equiv/hydroxy group) was dissolved in anhydrous DMF (3.4 mL/mmol acid) under an argon atmosphere. The reaction mixture was stirred overnight at room temperature. Method B: A mixture of the corresponding carboxylic acid (1 equiv), DIPEA (3 equiv), and TBS-Cl (1.4 equiv/hydroxy group) was dissolved in anhydrous DMF (2.0 mL/mmol acid) under an argon atmosphere. The reaction mixture was heated in the microwave at 100 ºC for 20 min.

For both methods, a 1 M aqueous solution of H_3PO_4 was added to the reaction mixture and it was extracted with hexane. The organic layer was washed with saturated aqueous solutions of $NaHCO_3$ and NaCl, dried (Na_2SO_4) and the solvent was evaporated under reduced pressure. The residue was dried under high vacuum to obtain the corresponding silyl esters as colourless oils which were used in the next step without further purification.

Silyl esters were treated with water (3.0 mL/mmol), AcOH (9.0 mL/mmol) and THF (6.0 mL/mmol) and stirred for 3 h at room temperature. The reaction mixture was extracted with DCM, and the organic phase was washed with water and saturated aqueous solutions of $NaHCO_3$ and NaCl, and dried (Na_2SO_4). The solvent was evaporated under reduced pressure. The resulting oil was purified by chromatography using DCM as eluent to afford pure **51a-f**.

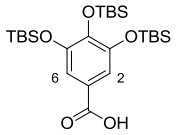

51a

3,4,5-Tris{[*tert*-butyl(dimethyl)silyl]oxy}benzoic acid (51a). Obtained from galic acid (3.0 g, 18 mmol) by method A in 84% yield. mp 238-239 ºC (Lit.[91] 223-224 °C); IR (ATR) ν 3461 (OH), 1697 (C=O), 1575 (Ar), 1078 (C-O); ^{1}H NMR (300 MHz, $CDCl_3$) δ 0.17 (s, 6H, $(CH_3)_2Si$), 0.27 (s, 12H, $2(CH_3)_2Si$), 0.97 (s, 18H, $2(CH_3)_3CSi$), 1.02 (s, 9H, $(CH_3)_3CSi$), 7.31 (s, 2H, H_2, H_6); ^{13}C NMR (75 MHz, $CDCl_3$) δ −3.8 ($(CH_3)_2Si$), −3.5 ($2(CH_3)_2Si$), 17.8 ($(CH_3)_3\underline{C}Si$), 18.0 ($2(CH_3)_3\underline{C}Si$), 26.2 ($3(\underline{C}H_3)_3CSi$), 116.2 (C_2H, C_6H), 121.2 (C_1), 144.2 (C-O), 148.2 (2C-O), 172.2 (C=O). The spectroscopic data are in agreement with those previously described.[91]

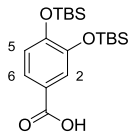

51b

3,4-Bis{[*tert*-butyl(dimethyl)silyl]oxy}benzoic acid (51b). Obtained from protocatechuic acid (4.0 g, 26 mmol) by method B in 81% yield. mp 154-157 ºC; IR (ATR) ν 1690 (C=O), 1598 (Ar); ^{1}H NMR (300 MHz, $CDCl_3$) δ 0.23 (s, 6H, $(CH_3)_2Si$), 0.24 (s, 6H, $(CH_3)_2Si$), 0.99 (s, 9H, $(CH_3)_3CSi$), 1.00 (s, 9H, $(CH_3)_3CSi$), 6.87 (d, *J* = 8.3, 1H, H_5), 7.57 (d, *J* = 2.0, 1H, H_2), 7.61 (dd, *J* = 8.3, 2.2, 1H, H_6); ^{13}C NMR (75 MHz, $CDCl_3$) δ −4.1, −4.0 ($2(CH_3)_2Si$), 18.5 ($2(CH_3)_3\underline{C}Si$), 25.9 ($2(\underline{C}H_3)_3CSi$), 120.6, 122.5 (2CH), 122.8 (C_1), 124.5 (CH), 146.8, 152.5 (2C-O), 172.0 (C=O); ESI-MS 406.1 $(M+Na)^+$.

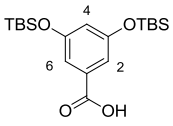

51c

3,5-Bis{[*tert*-butyl(dimethyl)silyl]oxy}benzoic acid (51c). Obtained from α-resorcilic acid (2.1 g, 14 mmol) by method A in 76% yield. mp 188-192 ºC; IR (ATR) ν 1692 (C=O), 1593 (Ar), 1171 (C-O); ^{1}H NMR (300 MHz, $CDCl_3$) δ 0.25 (s, 12H, 2$(CH_3)_2$Si), 1.01 (s, 18H, 2$(CH_3)_3$CSi), 6.63 (d, *J* = 2.3, 1H, H_4), 7.17 (d, *J* = 2.3, 2H, H_2, H_6); ^{13}C NMR (75 MHz, $CDCl_3$) δ −4.3 (2$(CH_3)_2$Si), 18.8 (2$(CH_3)_3\underline{C}$Si), 25.9 (2$(\underline{C}H_3)_3$CSi), 115.4 (C_2H, C_6H), 114.4 (C_4H), 133.4 (C_1), 157.5 (2C-O), 167.1 (C=O). The spectroscopic data are in agreement with those previously described.[92]

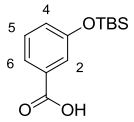

51d

3-{[*tert*-Butyl(dimethyl)silyl]oxy}benzoic acid (51d). Obtained from *m*-salicylic acid (3.0 g, 22 mmol) by method B in 67% yield. mp 96-97 ºC; IR (ATR) ν 1685 (CO), 1581, 1471 (Ar); ^{1}H NMR (300 MHz, $CDCl_3$) δ 0.22 (s, 6H, $(CH_3)_2$Si), 1.00 (s, 9H, $(CH_3)_3$CSi), 7.09 (ddd, *J* = 8.1, 2.6, 1.1 Hz, 1H, H_4), 7.33 (t, *J* = 7.9 Hz, 1H, H_5), 7.57 (dd, *J* = 2.5, 1.5 Hz, 1H, H_2), 7.72 (dt , *J* = 7.8, 1.3 Hz, 1H, H_6); ^{13}C NMR (75 MHz, $CDCl_3$) δ −4.3 ($(CH_3)_2$Si), 18.4 ($(CH_3)_3\underline{C}$Si), 25.8 ($(\underline{C}H_3)_3$CSi), 121.6, 123.4, 125.9, 129.7 (4CH), 130.7 (C_1), 155.9 (C-O), 172.1 (C=O); ESI-MS 250.8 $(M-H)^-$. The spectroscopic data are in agreement with those previously described.[93]

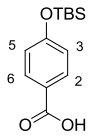

51e

4-{[*tert*-Butyl(dimethyl)silyl]oxy}benzoic acid (51e). Obtained from *p*-salicylic acid (3.0 g, 22 mmol) by method B in 74% yield. mp 108-111 ºC; IR (ATR) ν 1675 (C=O), 1597, 1510, 1422 (Ar); ^{1}H NMR (300 MHz, $CDCl_3$) δ 0.24 (s, 6H, $(CH_3)_2$Si), 0.99 (s, 9H, $(CH_3)_3$CSi), 6.89 (d, *J* = 8.7 Hz, 2H, H_3, H_5), 8.02 (d, *J* = 8.7 Hz, 2H, H_2, H_6); ^{13}C NMR (75 MHz, $CDCl_3$) δ −4.2 ($(CH_3)_2$Si), 18.4 ($(CH_3)_3\underline{C}$Si), 25.7 ($(\underline{C}H_3)_3$CSi), 120.1 (C_3H, C_5H), 122.4 (C_1), 132.5 (C_2H, C_6H), 161.0 (C-O), 172.2 (C=O); ESI-MS 250.8 $(M-H)^-$. The spectroscopic data are in agreement with those previously described.[94]

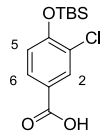

51f

4-{[*tert*-Butyl(dimethyl)silyl]oxy}-3-chlorobenzoic acid (51f). Obtained from 3-chloro-4-hydroxybenzoic acid (5.0 g, 29 mmol) by method A in 74% yield. mp 106-107 ºC; IR (ATR) ν 1693 (C=O), 1596 (Ar); ^{1}H NMR (300 MHz, $CDCl_3$) δ 0.27 (s, 6H, $(CH_3)_2Si$), 1.04 (s, 9H, $(CH_3)_3CSi$), 6.93 (d, *J* = 8.5, 1H, H_5), 7.90 (dd, *J* = 8.5, 2.2, 1H, H_6), 8.13 (d, *J* = 2.1, 1H, H_2); ^{13}C NMR (75 MHz, $CDCl_3$) δ −4.2 ($(CH_3)_2Si$), 18.5 ($(CH_3)_3\underline{C}Si$), 25.7 ($(\underline{C}H_3)_3CSi$), 120.3 (CH), 123.2, 126.1 (C_1,C_3), 130.3, 132.8 (2CH), 156.8 (C-O), 170.9 (C=O); ESI-MS 309.0 $(M+Na)^+$.

General Procedure for the Synthesis of Acid Chlorides 52a-h. To a solution of the corresponding carboxylic acid **51a**-**f**, commercial 3,4-dichlorobenzoic acid or 3,4,5-trimethoxybenzoic acid (1 equiv) and a catalytic amount of anhydrous DMF in dry toluene (1 mL/mmol) under an argon atmosphere, oxalyl chloride (1.5 equiv) was added dropwise. The reaction mixture was stirred at 50 ºC for 1 h. Once at room temperature, the mixture was decanted and the solvent was evaporated under reduced pressure to afford the corresponding acid chloride in quantitative yield as a solid that was used in the next step without further purification.

The following acid chlorides were synthesized:

3,4,5-tris{[*tert*-butyl(dimethyl)silyl]oxy}benzoyl chloride (**52a**)
3,4-bis{[*tert*-butyl(dimethyl)silyl]oxy}benzoyl chloride (**52b**)
3,5-bis{[*tert*-butyl(dimethyl)silyl]oxy}benzoyl chloride (**52c**)
3-{[*tert*-butyl(dimethyl)silyl]oxy}benzoyl chloride (**52d**)
4-{[*tert*-butyl(dimethyl)silyl]oxy}benzoyl chloride (**52e**)
4-{[*tert*-butyl(dimethyl)silyl]oxy}-3-chlorobenzoyl chloride (**52f**)
3,4-dichlorobenzoyl chloride (**52g**)
3,4,5-trimethoxybenzoyl chloride (**52h**)

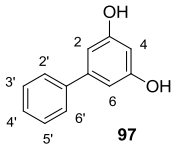

97

Biphenyl-3,5-diol (97). The reaction was performed in batches of 500 mg of starting material. A suspension of 3,5-dimethoxyphenylbromide (500 mg, 2.3 mmol), phenylboronic acid (337 mg, 2.8 mmol), Na_2CO_3 (732 mg, 6.9 mmol) and $Pd(PPh_3)_4$ (133 mg, 0.12 mmol) in a 5:3 mixture of toluene

and water (16 mL) under an argon atmosphere was heated at 150 ºC in the microwave for 30 min. Afterward, the reaction mixture was extracted with ethyl acetate and the organic phase was dried (Na_2SO_4) and concentrated under reduced pressure. The crude was purified by chromatography (from hexane to DCM) to afford 3,5-dimethoxybiphenyl in 75% yield, which was used in the next step without further purification. R_f (hexane/DCM, 1:1) 0.57; mp 62-64 ºC; IR (ATR) ν 1598, 1462 (Ar).; ^{1}H NMR (300 MHz, $CDCl_3$) δ 3.75 (s, 6H, $2CH_3O$), 6.39 (t, J = 2.3 Hz ,1H, H_4), 6.65 (d, J = 2.3 Hz, 2H, H_2, H_6), 7.26 (t, J = 7.2 Hz, 1H, $H_{4'}$), 7.30-7.37 (m, 2H, $H_{3'}$, $H_{5'}$), 7.47-7.51 (m, 2H, $H_{2'}$, $H_{6'}$); ^{13}C NMR (75 MHz, $CDCl_3$) δ 55.5 ($2CH_3$), 99.4 (C_4H), 105.6 (C_2H, C_6H), 127.3 ($C_{2'}H$, $C_{6'}H$), 127.7 ($C_{4'}H$), 128.8 ($C_{3'}H$, $C_{5'}H$), 141.3, 143.6 ($2C_{biph.}$), 161.2 (2C-OH); ESI-MS 215.1 $(M+H)^+$.

3,5-Dimethoxybiphenyl (730 mg, 3.1 mmol) was dissolved in anhydrous DCM (14 mL) under an argon atmosphere and BBr_3 (0.8 mL, 8.2 mmol) was added dropwise at -20 ºC. The mixture was then warmed up to room temperature and stirred overnight. Then, the reaction was quenched with 1 M HCl (0.8 mL) at 0 ºC and extracted with ethyl acetate (3 x 10 mL). The organic layers were dried (Na_2SO_4) and concentrated under reduced pressure, and the crude was purified by chromatography (from DCM to DCM/MeOH, 95:5) to afford intermediate **97** in 97% yield. R_f (DCM/MeOH, 98:2) 0.41; mp 157-159 ºC; IR (ATR) ν 3379 (OH), 1609, 1481, 1434 (Ar); ^{1}H NMR (300 MHz, acetone-d_6) δ 6.28 (t, J = 2.2, 1H, H_4), 6.53 (d, J = 2.2, 2H, H_2, H_6), 7.23 (t, J = 7.2, 1H, $H_{4'}$), 7.29-7.35 (m, 2H, $H_{3'}$, $H_{5'}$), 7.44-7.49 (m, 2H, $H_{2'}$, $H_{6'}$), 8.27 (br s, 2H, 2OH); ^{13}C NMR (75 MHz, acetone-d_6) δ 102.6 (C_4H), 106.4 (C_2H, C_6H), 127.6 ($C_{2'}H$, $C_{6'}H$), 128.2 ($C_{4'}H$), 129.6 ($C_{3'}H$, $C_{5'}H$), 142.1, 144.1 ($2C_{biph.}$), 159.8 (2C-OH); ESI-MS 187.1 $(M+H)^+$.

4.1.2 Synthesis of 1-32 and 37-46

General Procedure for the Synthesis of Final Compound 3 and Protected Diesters 53-58 and 98-100. To a solution of 1,3-dihydroxynaphthalene or **97** (1 equiv) and triethylamine (4 equiv) in anhydrous DCM (10 mL/mmol acid chloride **52**) under an argon atmosphere, a solution of the corresponding acid chloride **52a**-**f**,**h** (4 equiv) in anhydrous DCM (2 mL/mmol) was added dropwise and the reaction mixture was stirred at room temperature overnight. Then, the mixture was washed with a saturated aqueous solution of $NaHCO_3$ and with water. The organic layer was dried (Na_2SO_4) and the solvent was evaporated under reduced pressure. The crude was purified by chromatography (from hexane to DCM) to afford final compound **3** or the corresponding diesters **53**-**58** and **98-100**.

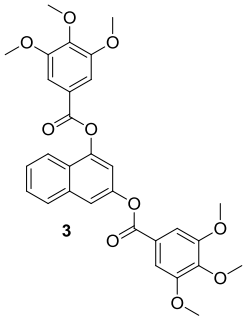

3

Naphthalene-1,3-diyl bis(3,4,5-trimethoxybenzoate) (3). Obtained from 1,3-dihydroxynaphthalene (87 mg, 0.54 mmol) and acid chloride **52h** (500 mg, 2.2 mmol) in 69% yield. R_f (DCM) 0.20; mp 139-140 ºC; IR (ATR) ν 1735 (C=O), 1590, 1503, 1460 (Ar); ^{1}H NMR (300 MHz, $CDCl_3$) δ 3.96 (s, 6H, $2CH_3$), 3.97 (s, 3H, CH_3), 3.98 (s, 6H, $2CH_3$), 3.99 (s, 3H, CH_3), 7.34 (d, J = 2.2, 1H, $CH_{naph.}$), 7.48-7.60 (m, 6H, $2CH_{naph.}$, $4CH_{eud.}$), 7.68 (d, J = 2.0, 1H, $CH_{naph.}$), 7.90 (d, J = 7.7, 1H, $CH_{naph.}$), 7.95 (d, J = 8.1, 1H, $CH_{naph.}$); ^{13}C NMR (75 MHz, $CDCl_3$) δ 56.5 ($2CH_3$), 56.6 ($2CH_3$), 61.1, 61.2 ($2CH_3$), 107.7 ($2CH_{eud.}$), 107.8 ($2CH_{eud.}$), 114.6, 117.2, 121.6 ($3CH_{naph.}$), 124.0, 124.3 ($2C_{eud.}$), 125.5 ($C_{naph.}$), 126.5, 127.5, 128.1 ($3CH_{naph.}$), 134.6 ($C_{naph.}$), 135.2, 143.2 ($2C\text{-}O_{eud.}$), 147.7, 148.1 ($2C\text{-}O_{naph.}$), 153.3 ($2C\text{-}O_{eud.}$), 153.4 ($2C\text{-}O_{eud.}$), 164.7, 164.9 (2C=O); ESI-MS 566.2 $(M+NH_4)^+$; elemental analysis (calcd., found for $C_{30}H_{28}O_{10}$): C (65.69, 65.40), H, (5.15, 5.12).

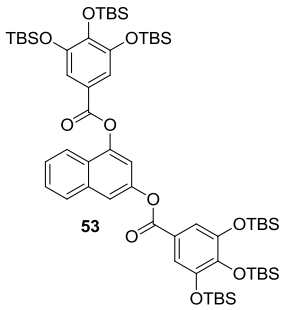

53

Naphthalene-1,3-diyl bis(3,4,5-tris{[*tert*-butyl(dimethyl)silyl]oxy}benzoate) (53). Obtained from 1,3-dihydroxynaphthalene (71 mg, 0.44 mmol) and acid chloride **52a** (935 mg, 1.8 mmol) in 71% yield. R_f (hexane/DCM, 6:4) 0.41; mp 198-200 ºC; IR (ATR) ν 1740 (C=O), 1577 (Ar), 1088 (C-O); ^{1}H NMR (300 MHz, $CDCl_3$) δ 0.19 (s, 6H, $(CH_3)_2$Si *para*), 0.21 (s, 6H, $2(CH_3)_2$Si *para*), 0.28 (s, 12H, $2(CH_3)_2$Si *meta*), 0.29 (s, 12H, $2(CH_3)_2$Si *meta*), 0.98 (s, 18H, $2(CH_3)_3$CSi *meta*), 0.99 (s, 18H, $2(CH_3)_3$CSi *meta*), 1.02 (s, 9H, $(CH_3)_3$CSi *para*), 1.04 (s, 9H, $(CH_3)_3$CSi *para*), 7.40 (d, J = 2.3, 1H, $CH_{naph.}$), 7.42 (s, 2H, $2CH_{gal.}$), 7.45-7.49 (m, 4H, $2CH_{gal.}$, $2CH_{naph.}$), 7.63 (d, J = 2.0, 1H, $CH_{naph.}$), 7.85-7.90 (m, 1H, $CH_{naph.}$), 7.97-8.01 (m, 1H, $CH_{naph.}$); ^{13}C NMR (75 MHz, $CDCl_3$) δ −3.6 ($(CH_3)_2$Si *para*), −3.7 ($(CH_3)_2$Si *para*), −3.7 ($4(CH_3)_2$Si *meta*), 18.5 ($2(CH_3)_3\underline{C}$Si), 18.8 ($2(CH_3)_3\underline{C}$Si), 18.9

(2(CH_3)$_3$CSi), 26.1 (2(CH_3)$_3$CSi *para*), 26.2 (4(CH_3)$_3$CSi *meta*), 114.4 ($CH_{naph.}$), 116.1 (4$CH_{gal.}$), 116.6 ($CH_{naph.}$), 120.8, 121.0 (2$C_{gal.}$), 121.5 ($CH_{naph.}$), 125.3 ($C_{naph.}$), 126.0, 127.1, 127.8 (3$CH_{naph.}$), 134.3 ($C_{naph.}$), 144.1, 144.2 (2$C_{gal.}$), 147.5, 148.1 (2C-$O_{naph.}$), 148.7, 148.8 (4C-$O_{gal.}$), 164.4, 164.8 (2C=O).

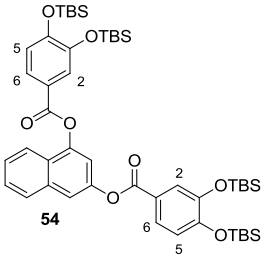

54

Naphthalene-1,3-diyl bis(3,4-bis{[*tert*-butyl(dimethyl)silyl]oxy}benzoate) (54). Obtained from 1,3-dihydroxynaphthalene (58 mg, 0.36 mmol) and acid chloride **52b** (520 mg, 1.3 mmol) in 63% yield. R_f (hexane/DCM, 1:1) 0.56; mp 131-133 ºC; IR (ATR) ν 1737 (C=O), 1599 (Ar); ^{1}H NMR (300 MHz, $CDCl_3$) δ 0.26 (s, 6H, (CH_3)$_2$Si), 0.27 (s, 12H, 2(CH_3)$_2$Si), 0.28 (s, 6H, (CH_3)$_2$Si), 1.02 (s, 18H, 2(CH_3)$_3$CSi), 1.02 (s, 9H, (CH_3)$_3$CSi), 1.03 (s, 9H, (CH_3)$_3$CSi), 6.96 (d, *J* = 8.4, 1H, H_5), 6.97 (d, *J* = 8.4, 1H, H_5), 7.36 (d, *J* = 2.2, 1H, $CH_{naph.}$), 7.42-7.60 (m, 2H, 2$CH_{naph.}$), 7.64 (d, *J* = 1.7, 1H, H_2), 7.70 (d, *J* = 2.2, 1H, H_2), 7.75 (dd, *J* = 8.4, 2.2, 1H, H_6), 7.79 (d, *J* = 8.4, 1H, H_6), 7.81-7.92 (m, 2H, 2$CH_{naph.}$), 7.97 (d, *J* = 7.7, 1H, $CH_{naph.}$); ^{13}C NMR (75 MHz, $CDCl_3$) δ −4.1 (2(CH_3)$_2$Si), −4.0 (2(CH_3)$_2$Si), 18.5 (2(CH_3)$_3$CSi), 18.6 (2(CH_3)$_3$CSi), 25.9 (4(CH_3)$_3$CSi), 114.5, 116.7 (2$CH_{naph.}$), 120.7, 120.8 (2$CH_{prot.}$), 121.6 ($CH_{naph.}$), 122.1, 122.4 (2$C_{prot.}$), 122.8 (2$CH_{prot.}$), 124.4, 124.6 (2$CH_{prot.}$), 125.3 ($C_{naph.}$), 126.1, 127.2, 127.9 (3$CH_{naph.}$), 134.4 ($C_{naph.}$), 147.0, 147.1 (2C-$O_{prot.}$), 147.6, 148.1 (2C-$O_{naph.}$), 152.5, 152.7 (2C-$O_{prot.}$), 164.5, 164.8 (2C=O); ESI-MS 911.5 $(M+Na)^+$.

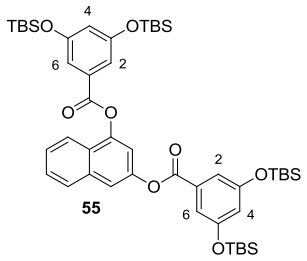

55

Naphthalene-1,3-diyl bis(3,5-bis{[*tert*-butyl(dimethyl)silyl]oxy}benzoate) (55). Obtained from 1,3-dihydroxynaphthalene (21 mg, 0.13 mmol) and acid chloride **52c** (210 mg, 0.52 mmol) in 55% yield. R_f (hexane/DCM, 1:1) 0.56; mp 131-133 ºC; IR (ATR) ν 1745 (C=O), 1590 (Ar); ^{1}H NMR (300 MHz, $CDCl_3$) δ 0.24 (s, 12H, 2(CH_3)$_2$Si), 0.25 (s, 12H, 2(CH_3)$_2$Si), 1.00 (s, 18H, 2(CH_3)$_3$CSi), 1.01 (s, 18H, 2(CH_3)$_3$CSi), 6.61 (t, *J* = 2.3, 1H, H_4), 6.65 (t, *J* = 2.3, 1H, H_4), 7.31 (d, *J* = 2.3, 2H, H_2,

H_6), 7.37 (t, *J* = 2.2, 1H, $CH_{naph.}$), 7.40 (d, *J* = 2.3, 2H, H_2, H_6), 7.47-7.58 (m, 2H, $2CH_{naph.}$), 7.67 (d, *J* = 2.0, 1H, $CH_{naph.}$), 7.88 (d, *J* = 7.4, 1H, $CH_{naph.}$), 7.95 (d, *J* = 7.8, 1H, $CH_{naph.}$); ^{13}C NMR (75 MHz, $CDCl_3$) δ –4.0 ($4(CH_3)_2Si$), 18.6 ($4(CH_3)_3\underline{C}Si$), 26.1 ($4(\underline{C}H_3)_3CSi$), 114.7 ($CH_{naph.}$), 115.5 ($2CH_{α\text{-}res.}$), 115.6 ($2CH_{α\text{-}res.}$), 117.3, 118.1 ($2CH_{naph.}$), 121.9 ($2CH_{α\text{-}res.}$), 125.6 ($C_{naph.}$), 126.6, 127.7, 128.3 ($3CH_{naph.}$), 131.1, 131.3 ($2C_{α\text{-}res.}$), 134.7 ($C_{naph.}$), 147.8, 148.3 ($2C\text{-}O_{naph.}$), 157.3 ($2C\text{-}O_{α\text{-}res.}$), 157.8 ($2C\text{-}O_{α\text{-}res.}$), 164.9, 165.2 (2C=O); ESI-MS 911.4 $(M+Na)^+$.

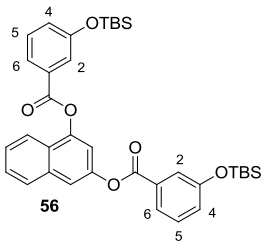

56

Naphthalene-1,3-diyl bis(3-{[*tert*-butyl(dimethyl)silyl]oxy}benzoate) (56). Obtained from 1,3-dihydroxynaphthalene (60 mg, 0.37 mmol) and acid chloride **52d** (410 mg, 1.5 mmol) as an oil in 61% yield. R_f (hexane/DCM, 2:8) 0.91; IR (ATR) ν 1744 (C=O), 1593, 1480 (Ar); ^{1}H NMR (300 MHz, $CDCl_3$) δ 0.26 (s, 6H, $(CH_3)_2Si$), 0.27 (s, 6H, $(CH_3)_2Si$), 1.01 (s, 9H, $(CH_3)_3CSi$), 1.02 (s, 9H, $(CH_3)_3CSi$), 7.13 (ddd, *J* = 8.1, 2.5, 0.9, 1H, H_4), 7.17 (ddd, *J* = 8.1, 2.5, 0.9, 1H, H_4), 7.39 (d, *J* = 1.8, 1H, $CH_{naph.}$), 7.40 (t, *J* = 7.9, 1H, H_5), 7.43 (t, *J* = 7.9, 1H, H_5), 7.48-7.59 (m, 2H, $2CH_{naph.}$), 7.68-7.69 (m, 2H, H_2, $CH_{naph.}$), 7.77 (app t, *J* = 2.0, 1H, H_2), 7.85 (dt, *J* = 7.9, 1.3, 1H, H_6), 7.89 (d, *J* = 7.5, 1H, $CH_{naph.}$), 7.92-7.99 (m, 2H, H_6, $CH_{naph.}$); ^{13}C NMR (75 MHz, $CDCl_3$) δ −4.2 ($2(CH_3)_2Si$), 18.4 ($2(CH_3)_3\underline{C}Si$), 25.8 ($2(\underline{C}H_3)_3CSi$), 114.5, 117.0 ($2CH_{naph.}$), 121.6, 121.7, 121.8 ($2CH_{m\text{-}sal.}$, $CH_{naph.}$), 123.4, 123.5 ($2CH_{m\text{-}sal.}$), 125.4 ($C_{naph.}$), 125.8, 126.0 ($2CH_{m\text{-}sal.}$), 126.4, 127.4, 128.1 ($3CH_{naph.}$), 129.8, 130.0 ($2CH_{m\text{-}sal.}$), 130.6, 130.8 ($2C_{m\text{-}sal.}$), 134.5 ($C_{naph.}$), 147.6, 148.1 ($2C\text{-}O_{naph.}$), 156.1, 156.2 ($2C\text{-}O_{m\text{-}sal.}$), 164.7, 165.0 (2C=O); ESI-MS 651.4 $(M+Na)^+$.

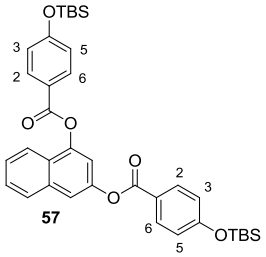

57

Naphthalene-1,3-diyl bis(4-{[*tert*-butyl(dimethyl)silyl]oxy}benzoate) (57). Obtained from 1,3-dihydroxynaphthalene (67 mg, 0.42 mmol) and acid chloride **52e** (450 mg, 1.7 mmol) as an oil in 58% yield. R_f (hexane/DCM, 2:8) 0.58; IR (ATR) ν 1738 (C=O), 1636, 1509 (Ar); ^{1}H NMR (300

MHz, $CDCl_3$) δ 0.27 (s, 6H, $(CH_3)_2Si$), 0.29 (s, 6H, $(CH_3)_2Si$), 1.01 (s, 9H, $(CH_3)_3CSi$), 1.02 (s, 9H, $(CH_3)_3CSi$), 6.95 (d, *J* = 8.8, 2H, H_3, H_5), 6.99 (d, *J* = 8.8, 2H, H_3, H_5), 7.35 (d, *J* = 2.2, 1H, $CH_{naph.}$), 7.46-7.56 (m, 2H, $2CH_{naph.}$), 7.65 (d, *J* = 2.0, 1H, $CH_{naph.}$), 7.87 (d, *J* = 7.4, 1H, $CH_{naph.}$), 7.96 (d, *J* = 8.0, 1H, $CH_{naph.}$), 8.14 (d, *J* = 8.8, 2H, H_2, H_6), 8.23 (d, *J* = 8.8, 2H, H_2, H_6); ^{13}C NMR (75 MHz, $CDCl_3$) δ −4.2 ($2(CH_3)_2Si$), 18.4 ($2(CH_3)_3\underline{C}Si$), 25.8 ($2(\underline{C}H_3)_3CSi$), 114.6, 116.9 ($2CH_{naph.}$), 120.3 ($2CH_{p\text{-}sal.}$), 120.4 ($2CH_{p\text{-}sal.}$), 121.7 ($C_{p\text{-}sal.}$), 122.1 ($CH_{naph.}$), 122.4 ($C_{p\text{-}sal.}$), 125.4 ($C_{naph.}$), 126.2, 127.3, 128.0 ($3CH_{naph.}$), 132.5 ($2CH_{p\text{-}sal.}$), 132.6 ($2CH_{p\text{-}sal.}$), 134.5 ($C_{naph.}$), 147.7, 148.2 ($2C\text{-}O_{naph.}$), 161.0, 161.1 ($2C\text{-}O_{p\text{-}sal.}$), 164.7, 164.9 (2C=O); ESI-MS 626.8 $(M-H)^-$.

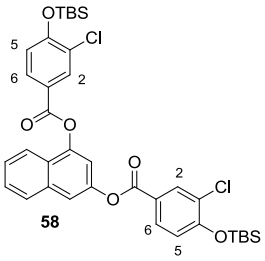

58

Naphthalene-1,3-diyl bis(4-{[*tert*-butyl(dimethyl)silyl]oxy}-3-chlorobenzoate) (58). Obtained from 1,3-dihydroxynaphthalene (66 mg, 0.41 mmol) and acid chloride **52f** (500 mg, 1.6 mmol) in 54% yield. R_f (hexane/DCM, 1:1) 0.50; mp 69-72 ºC; IR (ATR) ν 1741 (C=O), 1594, 1500 (Ar); ^{1}H NMR (300 MHz, $CDCl_3$) δ 0.30 (s, 6H, $(CH_3)_2Si$), 0.32 (s, 6H, $(CH_3)_2Si$), 1.06 (s, 9H, $(CH_3)_3CSi$), 1.07 (s, 9H, $(CH_3)_3CSi$), 6.99 (d, *J* = 8.5, 1H, H_5), 7.03 (d, *J* = 8.5, 1H, H_5), 7.34 (d, *J* = 2.1, 1H, $CH_{naph.}$), 7.47-7.58 (m, 2H, $CH_{naph.}$), 7.66 (d, *J* = 2.2, 1H, $CH_{naph.}$), 7.88 (d, *J* = 7.5, 1H, $CH_{naph.}$), 7.94 (d, *J* = 8.1, 1H, $CH_{naph.}$), 8.03 (dd, *J* = 8.5, 2.2, 1H, H_6), 8.11 (dd, *J* = 8.5, 2.2, 1H, H_6), 8.26 (d, *J* = 2.2, 1H, H_2), 8.34 (d, *J* = 2.2, 1H, H_2); ^{13}C NMR (75 MHz, $CDCl_3$) δ −4.2, −4.1 ($2(CH_3)_2Si$), 18.5 ($2(CH_3)_3\underline{C}Si$), 25.7 ($2(\underline{C}H_3)_3CSi$), 114.4, 117.0 ($2CH_{naph.}$), 120.4, 120.5 ($2CH_{Clbenz.}$), 121.6 ($CH_{naph.}$), 123.0, 123.3 ($2C_{Clbenz.}$), 125.3 ($C_{naph.}$), 126.3 ($2C_{Clbenz.}$), 126.4, 127.5, 128.1 ($3CH_{naph.}$), 130.3, 130.4, 132.7, 132.8 ($4CH_{Clbenz.}$), 134.5 ($C_{naph.}$), 147.5, 147.9 ($2C\text{-}O_{naph.}$), 156.7, 156.9 ($2C\text{-}O_{Clbenz.}$), 163.7, 163.9 (2C=O); ESI-MS 580.8 $(M-TBS)^-$.

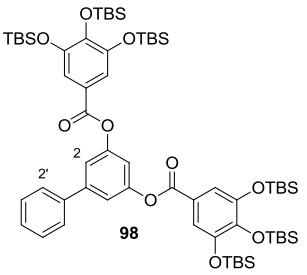

98

Biphenyl-3,5-diyl bis(3,4,5-tris{[*tert*-butyl(dimethyl)silyl]oxy}benzoate (98). Obtained from **97** (102 mg, 0.55 mmol) and acid chloride **52a** (1.2 g, 2.2 mmol) as an oil in 87% yield. R_f (hexane/DCM, 1:1) 0.74; IR (ATR) ν 1739 (C=O), 1578, 1487, 1428 (Ar); ^{1}H NMR (300 MHz, $CDCl_3$) δ 0.17 (s, 12H, 2(CH_3)$_2$Si *para*), 0.26 (s, 24H, 4(CH_3)$_2$Si *meta*), 0.97 (s, 36H, 4(CH_3)$_3$CSi *meta*), 1.01 (s, 18H, 2(CH_3)$_3$CSi *para*), 7.11 (t, *J* = 2.1, 1H, C_4H), 7.34 (d, *J* = 2.1, 2H, H_2, H_6), 7.36-7.38 (m, 5H, 4$CH_{gal.}$, $H_{4'}$), 7.61 (t, *J* = 7.2, 2H, $H_{3'}$, $H_{5'}$), 7.61 (d, *J* = 6.9, 2H, $H_{2'}$, $H_{6'}$); ^{13}C NMR (75 MHz, $CDCl_3$) δ −3.7 (2(CH_3)$_2$Si *para*), −3.5 (4(CH_3)$_2$Si *meta*), 18.7 (2(CH_3)$_3$CSi *para*), 19.0 (4(CH_3)$_3$CSi *meta*), 26.2 (2(CH_3)$_3$CSi *para*), 26.3 (4(CH_3)$_3$CSi *meta*), 114.8 (C_4H), 116.3 (4$CH_{gal.}$), 118.1 (C_2H, C_6H), 121.0 (2$C_{gal.}$), 127.4 ($C_{2'}$H, $C_{6'}$H), 128.1 ($C_{4'}$H), 129.0 ($C_{3'}$H, $C_{5'}$H), 139.7, 143.5 (2$C_{biph.}$), 144.2 (2C-$O_{biph.}$), 148.8 (4C-$O_{gal.}$), 152.0 (2C-$O_{gal.}$), 164.8 (2C=O); ESI-MS 1198.5 $(M+Na)^+$.

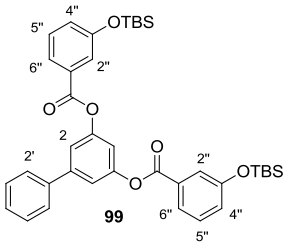

99

Biphenyl-3,5-diyl bis(3-{[*tert*-butyl(dimethyl)silyl]oxy}benzoate) (99). Obtained from **97** (50 mg, 0.27 mmol) and acid chloride **52d** (292 mg, 1.1 mmol) as an oil in 77% yield. R_f (DCM) 0.92; IR (ATR) ν 1743 (C=O), 1593, 1482, 1463, 1439 (Ar), 1282 (C–O); ^{1}H NMR (300 MHz, $CDCl_3$) δ 0.26 (s, 12H, 2(CH_3)$_2$Si), 1.02 (s, 18H, 2(CH_3)$_3$CSi), 7.13 (ddd, *J* = 8.1, 2.5, 0.9, 2H, 2$H_{4''}$), 7.18 (t, *J* = 2.1, 1H, H_4), 7.36-7.42 (m, 5H, H_2, H_6, $H_{4'}$, 2$H_{5''}$), 7.45 (t, *J* = 7.2, 2H, $H_{3'}$, $H_{5'}$), 7.63 (d, *J* = 7.0, 2H, $H_{2'}$, $H_{6'}$), 7.67 (t, *J* = 2.0, 2H, 2$H_{2''}$), 7.83 (dt, *J* = 7.8, 1.3, 2H, 2$H_{6''}$); ^{13}C NMR (75 MHz, $CDCl_3$) δ −4.3 (2(CH_3)$_2$Si), 18.4 (2(CH_3)$_3$CSi), 25.8 (2(CH_3)$_3$CSi), 114.6 (C_4H), 118.2 (C_2H, C_6H), 121.7 (2$CH_{m\text{-sal.}}$), 123.4 (2$CH_{m\text{-sal.}}$), 125.9 (2$CH_{m\text{-sal.}}$), 127.4 ($C_{2'}$H, $C_{6'}$H), 128.2 ($C_{4'}$H), 129.0 ($C_{3'}$H, $C_{5'}$H), 129.8 (2$CH_{m\text{-sal.}}$), 130.7 (2$C_{m\text{-sal.}}$), 139.6, 143.7 (2$C_{biph.}$), 151.8 (2C-$O_{biph.}$), 156.1 (2C-$O_{m\text{-sal.}}$), 164.8 (2C=O); ESI-MS 418.9 $[M-(C_{13}H_{19}O_2Si)]^-$.

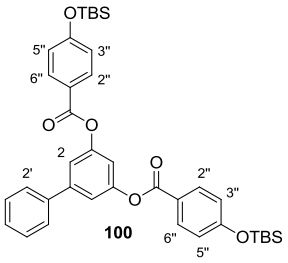

100

Biphenyl-3,5-diyl bis(4-{[*tert*-butyl(dimethyl)silyl]oxy}benzoate) (100). Obtained from **97** (60 mg, 0.32 mmol) and acid chloride **52e** (350 mg, 1.3 mmol) as an oil in 64% yield. R_f (hexane/DCM, 6:4) 0.26; IR (ATR) ν 1732 (C=O), 1601, 1509 (Ar), 1264 (C-O); ^{1}H NMR (300 MHz, $CDCl_3$) δ 0.26 (s, 12H, 2$(CH_3)_2$Si), 1.01 (s, 18H, 2$(CH_3)_3$CSi), 6.93 (d, J = 8.6, 4H, 2$H_{3''}$, 2$H_{5''}$), 7.13 (t, J = 2.0, 1H, H_4), 7.32-7.49 (m, 5H, H_2, H_6, $H_{3'}$, $H_{4'}$, $H_{5'}$), 7.61 (d, J = 7.1, 2H, $H_{2'}$, $H_{6'}$), 8.11 (d, J = 8.6, 4H, 2$H_{2''}$, 2$H_{6''}$); ^{13}C NMR (75 MHz, $CDCl_3$) δ −4.2 (2$(CH_3)_2$Si), 18.4 (2$(CH_3)_3\underline{C}$Si), 25.7 (2$(\underline{C}H_3)_3$CSi), 114.8 (C_4H), 118.1 (C_2H, C_6H), 120.3 (4$CH_{p\text{-sal.}}$), 122.3 (2$C_{p\text{-sal.}}$), 127.4 ($C_{2'}$H, $C_{6'}$H), 128.1 ($C_{4'}$H), 129.0 ($C_{3'}$H, $C_{5'}$H), 132.5 (4$CH_{p\text{-sal.}}$), 141.3, 144.0 (2$C_{biph.}$), 151.8 (4C-O), 159.2 (2C=O); ESI-MS 677.2 $(M+Na)^+$.

General Procedure for the Synthesis of Protected Monoesters 59-64 and 101-104. To a solution of 1,3-dihydroxynaphthalene or **97** (4 equiv) and triethylamine (4 equiv) in anhydrous DCM (10 mL/mmol acid chloride **52**) under an argon atmosphere, a solution of the corresponding acid chloride **52a,c,d** (1 equiv) in anhydrous DCM (2 mL/mmol) was added dropwise. The reaction mixture was stirred at room temperature overnight. Then, the mixture was washed with a saturated aqueous solution of $NaHCO_3$ and with water, the organic layer was dried (Na_2SO_4) and concentrated under reduced pressure. The crude was purified by chromatography (from hexane to DCM) to afford the corresponding monoesters **59-64** or **101-104**.

3-Hydroxy-1-naphthyl 3,4,5-tris{[(*tert*-butyl(dimethyl)silyl]oxy}benzoate (59) and 4-hydroxy-2-naphthyl 3,4,5-tris{[(*tert*-butyl(dimethyl)silyl]oxy}benzoate (62). Obtained from 1,3-dihydroxynaphthalene (625 mg, 3.9 mmol) and acid chloride **52a** (500 mg, 0.94 mmol).

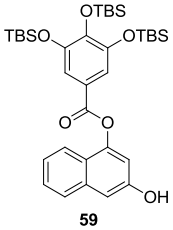

59

59: 33% yield; R_f (hexane/DCM, 2:8) 0.51; mp 158-160 ºC; IR (ATR) ν 3398 (OH), 1736 (C=O), 1577, 1490, 1428 (Ar); ^{1}H NMR (300 MHz, $CDCl_3$) δ 0.22 (s, 6H, $(CH_3)_2$Si *para*), 0.30 (s, 12H, 2$(CH_3)_2$Si *meta*), 1.00 (s, 18H, 2$(CH_3)_3$CSi *meta*), 1.05 (s, 9H, $(CH_3)_3$CSi *para*), 6.89 (d, *J* = 2.1, 1H, $CH_{naph.}$), 7.06 (d, *J* = 2.3, 1H, $CH_{naph.}$), 7.26-7.35 (m, 1H, $CH_{naph.}$), 7.37-7.43 (m, 1H, $CH_{naph.}$), 7.53-7.55 (m, 3H, 2$CH_{gal.}$, $CH_{naph.}$), 7.85 (d, *J* = 8.3, 1H, $CH_{naph.}$); ^{13}C NMR (75 MHz, $CDCl_3$) δ –3.8 ($(CH_3)_2$Si *para*), –3.6 (2$(CH_3)_2$Si *meta*), 18.6 ($(CH_3)_3\underline{C}$Si *para*), 18.9 (2$(CH_3)_3\underline{C}$Si *meta*), 26.2 (3($\underline{C}H_3)_3$CSi), 107.9, 111.1 (2$CH_{naph.}$), 116.3 (2$CH_{gal.}$), 120.7 ($C_{gal.}$), 121.2 ($CH_{naph.}$), 122.4 ($C_{naph.}$), 123.9, 126.6, 127.0 (3$CH_{naph.}$), 135.3 ($C_{naph.}$), 144.4, 147.7 (2C-$O_{naph.}$), 148.9 (2C-$O_{gal.}$ *meta*), 153.4 (C-$O_{gal.}$ *para*), 165.2 (C=O); ESI-MS 653.0 $(M-H)^-$.

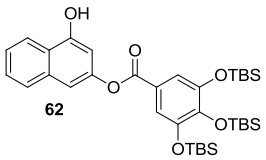

62

62: 38% yield; R_f (hexane/DCM, 2:8) 0.20; mp 169-170 ºC; IR (ATR) ν 3381 (OH), 1741 (C=O), 1581, 1488, 1429 (Ar); ^{1}H NMR (300 MHz, $CDCl_3$) δ 0.22 (s, 6H, $(CH_3)_2$Si *para*), 0.31 (s, 12H, 2$(CH_3)_2$Si *meta*), 1.00 (s, 18H, 2$(CH_3)_3$CSi *meta*), 1.06 (s, 9H, $(CH_3)_3$CSi *para*), 6.73 (d, *J* = 2.0, 1H, $CH_{naph.}$), 6.96 (s, 1H, OH), 7.23 (d, *J* = 1.9, 1H, $CH_{naph.}$), 7.27-7.34 (m, 1H, $CH_{naph.}$), 7.44-7.49 (m, 3H, 2$CH_{gal.}$, $CH_{naph.}$), 7.50 (d, *J* = 8.2, 1H, $CH_{naph.}$), 7.89 (d, *J* = 8.3, 1H, $CH_{naph.}$); ^{13}C NMR (75 MHz, $CDCl_3$) δ −3.4 ($(CH_3)_2$Si *para*), −3.1 (2$(CH_3)_2$Si *meta*), 19.0 ($(CH_3)_3\underline{C}$Si *para*), 19.3 (2$(CH_3)_3\underline{C}$Si *meta*), 26.5 (($\underline{C}H_3)_3$CSi *para*), 26.6 (2($\underline{C}H_3)_3$CSi *meta*), 104.9, 110.9 (2$CH_{naph.}$), 116.6 (2$CH_{gal.}$), 121.3 ($C_{gal.}$), 122.5 ($CH_{naph.}$), 123.5 ($C_{naph.}$), 125.0, 127.4, 127.6 (3$CH_{naph.}$), 134.9 ($C_{naph.}$), 144.8 149.0 (2C-$O_{naph.}$), 149.2 (2C-$O_{gal.}$ *meta*), 153.7 (C-$O_{gal.}$ *para*), 166.6 (C=O); ESI-MS 653.3 $(M-H)^-$.

3-Hydroxy-1-naphthyl 3,5-bis{[*tert*-butyl(dimethyl)silyl]oxy}benzoate (60) and 4-hydroxy-2-naphthyl 3,5-bis{[*tert*-butyl(dimethyl)silyl]oxy}benzoate (63). Obtained from 1,3-dihydroxynaphthalene (1.6 g, 10 mmol) and acid chloride **52c** (1.0 g, 2.5 mmol).

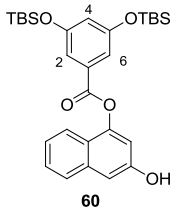

60

60: 24% yield; R_f (DCM) 0.42; mp 123-124 ºC; IR (ATR) ν 3391 (OH), 1713 (C=O), 1588 (Ar); ^{1}H NMR (300 MHz, $CDCl_3$) δ 0.29 (s, 12H, 2$(CH_3)_2$Si), 1.04 (s, 18H, 2$(CH_3)_3$CSi), 6.70 (t, *J* = 2.2, 1H,

CH_4), 6.89 (d, *J* = 2.2, 1H, $CH_{naph.}$), 7.03 (d, *J* = 2.2, 1H, $CH_{naph.}$), 7.29-7.43 (m, 2H, $2CH_{naph.}$), 7.45 (d, *J* = 2.4, 2H, H_2, H_6), 7.45 (d, *J* = 8.1, 1H, $CH_{naph.}$), 7.54 (d, *J* = 8.1, 1H, $CH_{naph.}$); ^{13}C NMR (75 MHz, $CDCl_3$) δ −3.9 ($2(CH_3)_2Si$), 18.7 ($2(CH_3)_3\underline{C}Si$), 26.1 ($2(\underline{C}H_3)_3CSi$), 108.6, 111.6 ($2CH_{naph.}$), 115.7 ($2CH_{α\text{-}res.}$), 118.4 ($CH_{α\text{-}res.}$), 121.5 ($CH_{naph.}$), 122.5 ($C_{naph.}$), 124.3, 127.1, 127.4 ($3CH_{naph.}$), 131.1 ($C_{α\text{-}res.}$), 135.7 ($C_{naph.}$), 147.9, 153.9 ($2C\text{-}O_{naph.}$), 157.4 ($2C\text{-}O_{α\text{-}res.}$), 165.9 (C=O); ESI-MS 547.3 $(M+Na)^+$.

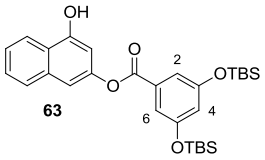

63

63: 22% yield; R_f (DCM) 0.59; mp 133-134 ºC; IR (ATR) ν 3417 (OH), 1717 (C=O), 1589, 1471 (Ar); ^{1}H NMR (300 MHz, $CDCl_3$) δ 0.23 (s, 12H, $2(CH_3)_2Si$), 0.99 (s, 18H, $2(CH_3)_3CSi$), 6.63 (t, *J* = 2.3, 1H, H_4), 7.17 (d, *J* = 1.9, 1H, $CH_{naph.}$), 7.19-7.24 (m, 2H, $2CH_{naph.}$), 7.35 (d, *J* = 2.3, 2H, H_2, H_6), 7.38-7.40 (m, 1H, $CH_{naph.}$), 7.67 (d, *J* = 8.2, 1H, $CH_{naph.}$), 7.78 (d, *J* = 8.4, 1H, $CH_{naph.}$); ^{13}C NMR (75 MHz, $CDCl_3$) δ −3.9 ($2(CH_3)_2Si$), 18.7 ($2(CH_3)_3\underline{C}Si$), 26.2 ($2(\underline{C}H_3)_3CSi$), 104.7, 110.9 ($2CH_{naph.}$), 115.7 ($2CH_{α\text{-}res.}$), 118.3 ($CH_{α\text{-}res.}$), 122.6 ($CH_{naph.}$), 123.7 ($C_{naph.}$), 125.1, 127.5, 127.6 ($3CH_{naph.}$), 131.4 ($C_{α\text{-}res.}$), 134.9 ($C_{naph.}$), 148.7, 154.0 ($2C\text{-}O_{naph.}$), 157.8 ($2C\text{-}O_{α\text{-}res.}$), 166.9 (C=O); ESI-MS 547.3 $(M+Na)^+$.

3-Hydroxy-1-naphthyl 3-{[*tert*-butyl(dimethyl)silyl]oxy}benzoate (61) and 4-hydroxy-2-naphthyl 3-{[*tert*-butyl(dimethyl)silyl]oxy}benzoate (64) Obtained from 1,3-dihydroxynaphthalene (2.8 g, 18 mmol) and acid chloride **52d** (1.2 g, 4.4 mmol) as oils.

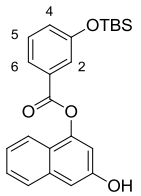

61

61: 27% yield; R_f (hexane/DCM, 2:8) 0.21; IR (ATR) ν 3406 (OH), 1731 (C=O), 1594, 1478 (Ar); ^{1}H NMR (300 MHz, $CDCl_3$) δ 0.27 (s, 6H, $(CH_3)_2Si$), 1.03 (s, 9H, $(CH_3)_3CSi$), 5.67 (br s, 1H OH), 6.95 (d, *J* = 2.2, 1H, $CH_{naph.}$), 7.03 (d, *J* = 2.3, 1H, $CH_{naph.}$), 7.18 (ddd, *J* = 8.1, 2.5, 1.0, 1H, H_4), 7.32 (ddd, *J* = 8.1, 6.8, 1.2, 1H, $CH_{naph.}$), 7.39-7.47 (m, 2H, $CH_{naph.}$, H_5), 7.59 (d, *J* = 8.2, 1H, $CH_{naph.}$), 7.78 (t, *J* = 2.0, 1H, H_2), 7.82 (d, *J* = 8.4, 1H, $CH_{naph.}$), 7.95 (dt, *J* = 7.8, 1.3, 1H, H_6); ^{13}C NMR (75 MHz, $CDCl_3$) δ −4.2 ($(CH_3)_2Si$), 18.4 ($(CH_3)_3\underline{C}Si$), 25.8 ($(\underline{C}H_3)_3CSi$), 108.3, 111.1, 121.3 ($3CH_{naph.}$), 121.9 ($CH_{m\text{-}sal.}$), 122.4 ($C_{naph.}$), 123.5 ($CH_{m\text{-}sal.}$), 124.2 ($CH_{naph.}$), 126.1 ($CH_{m\text{-}sal.}$), 126.8,

127.2 (2$CH_{naph.}$), 130.0 ($CH_{m\text{-}sal.}$), 130.5 ($C_{m\text{-}sal.}$), 135.4 ($C_{naph.}$), 147.7, 153.3 (2C-$O_{naph.}$), 156.2 (C-$O_{m\text{-}sal.}$), 165.5 (C=O); ESI-MS 393.0 $(M-H)^-$.

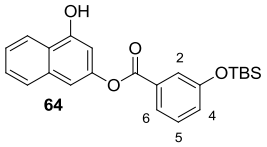

64

64: 26% yield; R_f (hexane/DCM, 2:8) 0.40; IR (ATR) ν 3387 (OH), 1712 (C=O), 1590, 1480 (Ar); ^{1}H NMR (300 MHz, $CDCl_3$) δ 0.25 (s, 6H, $(CH_3)_2Si$), 1.02 (s, 9H, $(CH_3)_3CSi$), 6.34 (br s, 1H, OH), 6.69 (d, *J* = 2.1, 1H, $CH_{naph.}$), 7.14 (ddd, *J* = 8.1, 2.5, 0.9, 1H, H_4), 7.24 (d, *J* = 1.9, 1H, $CH_{naph.}$), 7.35 (ddd, *J* = 8.3, 6.9, 1.2, 1H, $CH_{naph.}$), 7.40 (t, *J* = 8.0, 1H, H_5), 7.47 (ddd, *J* = 8.2, 6.9, 1.2, 1H, $CH_{naph.}$), 7.70 (t, *J* = 2.0, 1H, H_2), 7.75 (d, *J* = 8.2, 1H, $CH_{naph.}$), 7.86 (dt, *J* = 7.8, 1.3, 1H, H_6), 7.93 (d, *J* = 8.3, 1H, $CH_{naph.}$); ^{13}C NMR (75 MHz, $CDCl_3$) δ −4.3 ($(CH_3)_2Si$), 18.4 ($(CH_3)_3\underline{C}Si$), 25.8 ($(\underline{C}H_3)_3CSi$), 104.5, 111.1 (2$CH_{naph.}$), 121.8 ($CH_{m\text{-}sal.}$), 122.1 ($CH_{naph.}$), 123.1 ($C_{naph.}$), 123.5 ($CH_{m\text{-}sal.}$), 125.0 ($CH_{naph.}$), 125.9 ($CH_{m\text{-}sal.}$), 127.3, 127.5 (2$CH_{naph.}$), 129.8 ($CH_{m\text{-}sal.}$), 130.8 ($C_{m\text{-}sal.}$), 134.7 ($C_{naph.}$), 148.5, 153.2 (2C-$O_{naph.}$), 156.1 (C-$O_{m\text{-}sal.}$), 166.1 (C=O); ESI-MS 393.0 $(M-H)^-$.

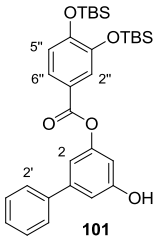

101

5-Hydroxybiphenyl-3-yl 3,4-bis{[*tert*-butyl(dimethyl)silyl]oxy}benzoate (101). Obtained from **97** (901 mg, 4.8 mmol) and acid chloride **52b** (481 mg, 1.2 mmol) as an oil in 47% yield. R_f (DCM) 0.78; IR (ATR) ν 3404 (OH), 1707 (C=O), 1511, 1466, 1421 (Ar), 1301 (C-O); ^{1}H NMR (300 MHz, $CDCl_3$) δ 0.24 (s, 6H, $(CH_3)_2Si$), 0.26 (s, 6H, $(CH_3)_2Si$), 1.01 (s, 18H, 2$(CH_3)_3CSi$), 5.32 (s, 1H, OH), 6.70 (t, *J* = 2.1, 1H, H_4), 6.92 (d, *J* = 8.4, 1H, $H_{5''}$), 6.94 (t, *J* = 1.7, 1H, H_6), 7.00 (t, *J* = 1.7, 1H, H_2), 7.32-7.44 (m, 3H, $H_{3'}$, $H_{4'}$, $H_{5'}$), 7.56 (d, *J* = 7.0, 2H, $H_{2'}$, $H_{6'}$), 7.67 (d, *J* = 2.1, 1H, $H_{2''}$), 7.72 (dd, *J* = 8.4, 2.2, 1H, $H_{6''}$); ^{13}C NMR (75 MHz, $CDCl_3$) δ −3.9, −4.0 (2$(CH_3)_2Si$), 18.6, 18.7 (2$(CH_3)_3\underline{C}Si$), 25.9, 26.0 (2$(\underline{C}H_3)_3CSi$), 108.5 (C_4H), 112.3 (C_6H), 112.6 (C_2H), 120.8 ($C_{5''}H$), 122.3 ($C_{prot.}$), 123.0 ($C_{2''}H$), 124.7 ($C_{6''}H$), 127.2 ($C_{2'}H$, $C_{6'}H$), 127.8 ($C_{4'}H$), 128.8 ($C_{3'}H$, $C_{5'}H$), 140.2, 143.8 (2$C_{biph.}$), 147.1, 152.1 (2C-$O_{prot.}$), 152.8 (C-$O_{biph.}$), 157.3 (C-OH), 165.8 (C=O); ESI-MS 573.2 $(M+Na)^+$.

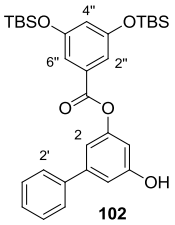

102

5-Hydroxybiphenyl-3-yl 3,5-bis{[*tert*-butyl(dimethyl)silyl]oxy}benzoate (102). Obtained from **97** (126 mg, 0.68 mmol) and acid chloride **52c** (68 mg, 0.17 mmol) as an oil in 69% yield. R_f (DCM) 0.71; IR (ATR) ν 3410 (OH), 1714 (C=O), 1449, 1336 (Ar), 1170 (C-O); ^{1}H NMR (300 MHz, $CDCl_3$) δ 0.24 (s, 12H, 2$(CH_3)_2$Si), 1.00 (s, 18H, 2$(CH_3)_3$CSi), 5.40 (s, 1H, OH), 6.61 (t, *J* = 2.3, 1H, $H_{4''}$), 6.70 (t, *J* = 2.1, 1H, H_4), 6.95 (t, *J* = 1.8, 1H, H_6), 7.01 (t, *J* = 1.7, 1H, H_2), 7.29 (d, *J* = 2.3, 2H, $H_{2''}$, $H_{6''}$), 7.32-7.44 (m, 3H, $H_{3'}$, $H_{4'}$, $H_{5'}$), 7.55 (dd, *J* = 8.2, 1.3, 2H, $H_{2'}$, $H_{6'}$); ^{13}C NMR (75 MHz, $CDCl_3$) δ −4.2 (2$(CH_3)_2$Si), 18.4 (2$(CH_3)_3\underline{C}$Si), 25.8 (2$(\underline{C}H_3)_3$CSi), 108.3 (C_4H), 112.1 (C_6H), 113.1 (C_2H), 115.3 (2$CH_{\alpha\text{-res.}}$), 117.8 ($CH_{\alpha\text{-res.}}$), 127.3 ($C_{2'}$H, $C_{6'}$H), 128.0 ($C_{4'}$H), 128.9 ($C_{3'}$H, $C_{5'}$H), 131.2 ($C_{\alpha\text{-res.}}$), 140.1, 144.0 (2$C_{biph.}$), 152.2 (C-$O_{biph.}$), 156.8 (C-OH), 156.9 (2C-$O_{\alpha\text{-res.}}$), 165.1 (C=O); ESI-MS 549.2 $(M-H)^-$.

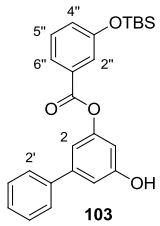

103

5-Hydroxybiphenyl-3-yl 3-{[*tert*-butyl(dimethyl)silyl]oxy}benzoate (103). Obtained from **97** (701 mg, 3.8 mmol) and acid chloride **52d** (255mg, 0.94 mmol) as an oil in 46% yield. R_f (DCM) 0.20; IR (ATR) ν 3407 (OH), 1713 (C=O), 1596, 1483, 1435 (Ar), 1285 (C-O); ^{1}H NMR (300 MHz, $CDCl_3$) δ 0.25 (s, 6H, $(CH_3)_2$Si), 1.02 (s, 9H, $(CH_3)_3$CSi), 6.69 (t, *J* = 2.2, 1H, H_4), 6.93 (t, *J* = 1.9, 1H, H_6), 7.00 (t, *J* = 1.7, 1H, H_2), 7.14 (ddd, *J* = 8.1, 2.5, 0.9, 1H, $H_{4''}$), 7.30-7.43 (m, 4H, $H_{3'}$, $H_{4'}$, $H_{5'}$, $H_{5''}$), 7.53 (dd, *J* = 8.1, 1.4, 2H, $H_{2'}$, $H_{6'}$), 7.67 (t, *J* = 2.0, 1H, $H_{2''}$), 7.83 (dt, *J* = 7.7, 1.4, 1H, $H_{6''}$); ^{13}C NMR (75 MHz, $CDCl_3$) δ −4.3 ($(CH_3)_2$Si), 18.3 ($(CH_3)_3\underline{C}$Si), 25.8 ($(\underline{C}H_3)_3$CSi), 108.3 (C_4H), 112.3 (C_6H), 112.7 (C_2H), 121.7 ($CH_{m\text{-sal.}}$), 123.4 ($CH_{m\text{-sal.}}$), 125.9 ($CH_{m\text{-sal.}}$), 127.2 ($C_{2'}$H, $C_{6'}$H), 127.9 ($C_{4'}$H), 128.9 ($C_{3'}$H, $C_{5'}$H), 129.8 ($CH_{m\text{-sal.}}$), 130.7 ($C_{m\text{-sal.}}$), 140.0, 143.9 (2$C_{biph.}$), 152.0 (C-$O_{biph.}$), 156.0 (C-$O_{m\text{-sal.}}$), 157.0 (C-OH), 165.7 (C=O); ESI-MS 418.9 $(M-H)^-$.

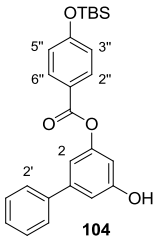

104

5-Hydroxybiphenyl-3-yl 4-{[*tert*-butyl(dimethyl)silyl]oxy}benzoate (104). Obtained from **97** (566 mg, 3.0 mmol) and 4-{[*tert*-butyl(dimethyl)silyl]oxy}benzoyl chloride **52e** (206 mg, 0.76 mmol) as an oil in 52% yield. R_f (DCM) 0.21; IR (ATR) ν 3450 (OH), 1732 (C=O), 1601, 1509 (Ar), 1263 (C-O); ^{1}H NMR (300 MHz, $CDCl_3$) δ 0.26 (s, 6H, $(CH_3)_2Si$), 1.01 (s, 9H, $(CH_3)_3CSi$), 6.70 (t, *J* = 2.1, 1H, H_4), 6.91-6.96 (m, 3H, H_6, $H_{3''}$, $H_{5''}$), 7.00 (t, *J* = 1.7, 1H, H_2), 7.32-7.37 (m, 1H, $H_{4'}$), 7.42 (t, *J* = 7.2, 2H, $H_{3'}$, $H_{5'}$), 7.56 (d, *J* = 6.9, 2H, $H_{2'}$, $H_{6'}$), 8.11 (d, *J* = 8.7, 2H, $H_{2''}$,$H_{6''}$); ^{13}C NMR (75 MHz, $CDCl_3$) δ −4.2 ($(CH_3)_2Si$), 18.4 ($(CH_3)_3\underline{C}Si$), 25.7 ($(\underline{C}H_3)_3CSi$), 108.4 (C_4H), 112.0 (C_6H), 113.2 (C_2H), 120.3 ($2CH_{p\text{-sal.}}$), 122.4 ($C_{p\text{-sal.}}$), 127.3 ($C_{2'}H$, $C_{6'}H$), 127.9 ($C_{4'}H$), 128.9 ($C_{3'}H$, $C_{5'}H$), 132.5 ($2CH_{p\text{-sal.}}$), 140.1, 143.9 ($2C_{biph.}$), 152.3 (C-O), 156.8 (2C-O), 161.0 (C=O); ESI-MS 418.9 $(M-H)^-$.

General Procedure for the Synthesis of Protected Diesters 65-86 and 105-108. To a solution of monoester **59**-**64** or **101-104** (1 equiv) and triethylamine (2 equiv) in anhydrous DCM (10 mL/mmol acid chloride **52**) under an argon atmosphere, a solution of the corresponding acid chloride **52b-h** (2 equiv) in anhydrous DCM (2 mL/mmol) was added dropwise and the reaction mixture was stirred at room temperature overnight. Then, the mixture was washed with a saturated aqueous solution of $NaHCO_3$ and with water, and the organic layer was dried (Na_2SO_4) and concentrated under reduced pressure. The crude was purified by chromatography (from hexane to DCM) to afford the title diesters **65-86** or **105-108**.

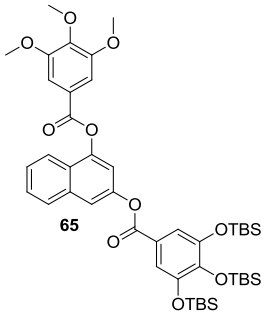

65

4-[(3,4,5-Trimethoxybenzoyl)oxy]-2-naphthyl 3,4,5-tris{[*tert*-butyl(dimethyl)silyl]oxy} benzoate (65). Obtained from monoester **62** (200 mg, 0.31 mmol) and acid chloride **52h** (140 mg, 0.62 mmol) in 91% yield. R_f (hexane/DCM, 2:8) 0.30; mp 167-169 ºC; IR (ATR) ν 1734 (C=O),

1585, 1495, 1466 (Ar); ^{1}H NMR (300 MHz, $CDCl_3$) δ 0.18 (s, 6H, $(CH_3)_2$Si *para)*, 0.27 (s, 12H, 2$(CH_3)_2$Si *meta*), 0.97 (s, 18H, 2$(CH_3)_3$CSi *meta*), 0.99 (s, 9H, $(CH_3)_3$CSi *para*), 3.97 (s, 6H, 2CH_3O *meta*), 3.98 (s, 3H, CH_3O *para*), 7.33 (d, *J* = 2.1, 1H, $CH_{naph.}$), 7.41 (s, 2H, 2$CH_{gal.}$), 7.45-7.56 (m, 2H, 2$CH_{naph.}$), 7.57 (s, 2H, 2$CH_{eud.}$), 7.66 (d, *J* = 2.0, 1H, $CH_{naph.}$), 7.87-7.92 (m, 2H, 2$CH_{naph.}$); ^{13}C NMR (75 MHz, $CDCl_3$) δ −3.7 ($(CH_3)_2$Si *para*), −3.5 (2$(CH_3)_2$Si *meta*), 18.7 ($(CH_3)_3$CSi *para*), 19.0 (2$(CH_3)_3$CSi *meta*), 26.3 ($(CH_3)_3$CSi *para*), 26.4 (2$(CH_3)_3$CSi *meta*), 56.5 (2CH_3O *meta*), 61.2 (CH_3O *para*), 107.8 (2$CH_{eud.}$), 114.7 ($CH_{naph.}$), 116.3 (2$CH_{gal.}$), 117.1 ($CH_{naph.}$), 121.0 ($C_{gal.}$), 121.6 ($CH_{naph.}$), 124.1, 125.3 ($C_{eud.}$, $C_{naph.}$), 126.3, 127.4, 128.1 (3$CH_{naph.}$), 134.6 ($C_{naph.}$), 143.3, 144.3 (2C-$O_{naph.}$), 147.6, 148.3 (2C-O *para*), 148.9 (2C-$O_{gal.}$ *meta*), 153.4 (2C-$O_{eud.}$ *meta*), 164.7, 164.9 (2C=O); ESI-MS 847.0 $(M-H)^-$.

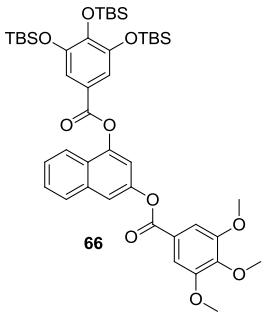

66

3-[(3,4,5-Trimethoxybenzoyl)oxy]-1-naphthyl 3,4,5-tris{[*tert*-butyl(dimethyl)silyl]oxy} benzoate (66). Obtained from monoester **59** (95 mg, 0.15 mmol) and acid chloride **52h** (67 mg, 0.29 mmol) in 82% yield. R_f (hexane/DCM, 2:8) 0.44; mp 197-198 ºC; IR (ATR) ν 1735 (C=O), 1598, 1495, 1464 (Ar); ^{1}H NMR (300 MHz, $CDCl_3$) δ 0.19 (s, 6H, $(CH_3)_2$Si *para)*, 0.29 (s, 12H, 2$(CH_3)_2$Si *meta*), 0.98 (s, 18H, 2$(CH_3)_3$CSi *meta*), 1.02 (s, 9H, $(CH_3)_3$CSi *para*), 3.95 (s, 6H, 2CH_3O *meta*), 3.96 (s, 3H, CH_3O *para*), 7.40 (d, *J* = 2.1, 1H, $CH_{naph.}$), 7.49 (s, 2H, 2$CH_{gal./eud.}$), 7.50 (s, 2H, 2$CH_{gal./eud.}$), 7.51-7.58 (m, 2H, 2$CH_{naph.}$), 7.64 (d, *J* = 1.9, 1H, $CH_{naph.}$), 7.88 (d, *J* = 7.4, 1H, $CH_{naph.}$), 8.02 (d, *J* = 8.0, 1H, $CH_{naph.}$); ^{13}C NMR (75 MHz, $CDCl_3$) δ −3.7 ($(CH_3)_2$Si *para*), −3.4 (2$(CH_3)_2$Si *meta*), 18.7 ($(CH_3)_3$CSi *para*), 19.0 (2$(CH_3)_3$CSi *meta*), 26.3 ($(CH_3)_3$CSi *para*), 26.4 (2$(CH_3)_3$CSi *meta*), 56.5 (2CH_3O *meta*), 61.2 (CH_3O *para*), 107.8 (2$CH_{eud.}$), 114.4 ($CH_{naph.}$), 116.3 (2$CH_{gal.}$), 116.8 ($CH_{naph.}$), 120.8 ($C_{gal.}$), 121.7 ($CH_{naph.}$), 124.4, 125.5 ($C_{eud.}$, $C_{naph.}$), 126.3, 127.4, 128.0 (3$CH_{naph.}$), 134.5 ($C_{naph.}$), 143.3, 144.3 (2C-$O_{naph.}$), 147.8, 148.1 (2C-O *para*), 149.0 (2C-$O_{eud.}$ *meta*), 153.3 (2C-$O_{gal.}$ *meta*), 164.6, 164.9 (2C=O); ESI-MS 847.0 $(M-H)^-$.

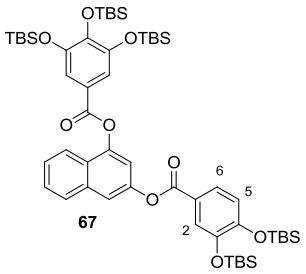

67

3-[(3,4-Bis{[*tert*-butyl(dimethyl)silyl]oxy}benzoyl)oxy]-1-naphthyl 3,4,5-tris{[*tert*-butyl (dimethyl)silyl]oxy}benzoate (67). Obtained from monoester **59** (490 mg, 0.75 mmol) and acid chloride **52b** (670 mg, 1.7 mmol) as an oil in 82% yield. R_f (hexane/DCM, 3:7) 0.37; ^{1}H NMR (300 MHz, $CDCl_3$) δ 0.27 (s, 6H, $(CH_3)_2Si$), 0.35 (s, 12H, $2(CH_3)_2Si$), 0,36 (s, 12H, $2(CH_3)_2Si$), 1.06 (s, 18H, $2(CH_3)_3CSi$), 1.10 (s, 27H, $3(CH_3)_3CSi$), 7.05 (d, J = 8.4, 1H, H_5), 7.47 (d, J = 2.1, 1H, $CH_{naph.}$), 7.52-7.58 (m, 3H, $2CH_{gal.}$, $CH_{naph.}$), 7.71 (d, J = 1.8, 1H, $CH_{naph.}$), 7.89-7.95 (m, 4H, $2CH_{naph.}$, H_2, H_6), 8.05 (d, J = 7.8, 1H, $CH_{naph.}$); ^{13}C NMR (75 MHz, $CDCl_3$) δ −4.1 ($(CH_3)_2Si$), −4.0 ($2(CH_3)_2Si$), −3.9 ($(CH_3)_2Si$), −3.6 ($(CH_3)_2Si$), 18.4 ($2(CH_3)_3\underline{C}Si$), 18.5 ($(CH_3)_3\underline{C}Si$), 18.8 ($2(CH_3)_3\underline{C}Si$), 25.8 ($(\underline{C}H_3)_3CSi$), 25.9 ($2(\underline{C}H_3)_3CSi$), 26.1 ($(\underline{C}H_3)_3CSi$), 26.2 ($(\underline{C}H_3)_3CSi$), 114.4 ($CH_{naph.}$), 116.1 ($2CH_{gal.}$), 116.6 ($CH_{naph.}$), 120.7 ($CH_{prot.}$), 121.0 ($C_{gal.}$), 121.5 ($CH_{naph.}$), 122.1 ($C_{prot.}$), 122.8, 124.5 ($2CH_{prot.}$), 125.2 ($C_{naph.}$), 126.0, 127.1, 127.8 ($3CH_{naph.}$), 134.3 ($C_{naph.}$), 144.0 ($C\text{-}O_{gal.}$ *para*), 147.0 ($C\text{-}O_{prot.}$), 147.5, 148.1 ($2C\text{-}O_{naph.}$), 148.6 ($2C\text{-}O_{gal.}$ *meta*), 152.6 ($C\text{-}O_{prot.}$), 164.3, 164.6 (2C=O); ESI-MS 1041.6 $(M+Na)^+$.

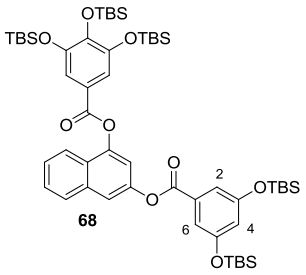

68

3-[(3,5-Bis{[*tert*-butyl(dimethyl)silyl]oxy}benzoyl)oxy]-1-naphthyl 3,4,5-tris{[*tert*-butyl (dimethyl)silyl]oxy}benzoate (68). Obtained from monoester **59** (190 mg, 0.29 mmol) and acid chloride **52c** (230 mg, 0.58 mmol) in 90% yield. R_f (hexane/DCM, 4:6) 0.35; mp 67-71 ºC; IR (ATR) ν 1743 (C=O), 1588 (Ar); ^{1}H NMR (300 MHz, $CDCl_3$) δ 0.21 (s, 6H, $(CH_3)_2Si$), 0.25 (s, 12H, $2(CH_3)_2Si$), 0.29 (s, 12H, $2(CH_3)_2Si$), 0.99 (s, 18H, $2(CH_3)_3CSi$), 1.02 (s, 18H, $2(CH_3)_3CSi$), 1.04 (s, 9H, $(CH_3)_3CSi$), 6.62 (t, J = 2.3, 1H, H_4), 7.32 (d, J = 2.3, 2H, H_2, H_6), 7.41 (d, J = 2.1, 1H, $CH_{naph.}$), 7.48-7.58 (m, 4H, $2CH_{naph.}$, $2CH_{gal.}$), 7.65 (d, J = 1.8, 1H, $CH_{naph.}$), 7.88 (d, J = 7.4, 1H, $CH_{naph.}$), 8.01 (d, J = 7.8, 1H, $CH_{naph.}$); ^{13}C NMR (75 MHz, $CDCl_3$) δ −4.4 ($(CH_3)_2Si$ *para*), −3.8 ($2(CH_3)_2Si$

meta), −3.6 (2(CH_3)$_2$Si *meta*), 18.3 ((CH_3)$_3$CSi *para*), 18.6 (2(CH_3)$_3$CSi *meta*), 18.9 (2(CH_3)$_3$CSi *meta*), 25.7 ((CH_3)$_3$CSi *para*), 26.1 (2(CH_3)$_3$CSi *meta*), 26.2 (2(CH_3)$_3$CSi *meta*), 114.3 ($CH_{naph.}$), 115.2 (2$CH_{α\text{-}res.}$), 116.2 (2$CH_{gal.}$), 116.2, 117.7 (2$CH_{naph.}$), 120.7 ($C_{gal.}$), 121.5 ($CH_{α\text{-}res.}$), 125.4 ($C_{naph.}$), 126.1, 127.2, 127.9 (3$CH_{naph.}$), 131.0 ($C_{α\text{-}res.}$), 134.3 ($C_{naph.}$), 144.3 (C-$O_{gal.}$ *para*), 147.6, 148.0 (2C-$O_{naph.}$), 148.8 (2C-$O_{gal.}$ *meta*), 156.8 (2C-$O_{α\text{-}res.}$), 164.4, 164.8 (2C=O); ESI-MS 1041.6 $(M+Na)^+$.

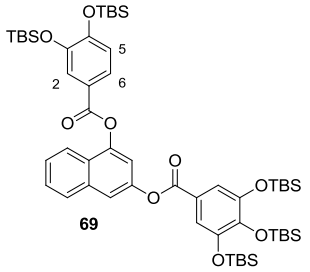

69

4-[(3,4-Bis{[*tert*-butyl(dimethyl)silyl]oxy}benzoyl)oxy]-2-naphthyl 3,4,5-tris{[*tert*-butyl (dimethyl)silyl]oxy}benzoate (69). Obtained from monoester **62** (490 mg, 0.75 mmol) and acid chloride **52b** (670 mg, 1.7 mmol) as an oil in 92% yield. R_f (hexane/DCM, 4:6) 0.39; ^{1}H NMR (300 MHz, $CDCl_3$) δ 0.25 (s, 6H, (CH_3)$_2$Si), 0.30 (s, 6H, (CH_3)$_2$Si), 0.31 (s, 6H, (CH_3)$_2$Si), 0.33 (s, 12H, 2(CH_3)$_2$Si), 1.03 (s, 18H, 2(CH_3)$_3$CSi), 1.05 (s, 9H, (CH_3)$_3$CSi), 1.06 (s, 9H, (CH_3)$_3$CSi), 1.08 (s, 9H, (CH_3)$_3$CSi), 6.98 (d, *J* = 8.4, 1H, H_5), 7.46 (d, *J* = 2.1, 1H, $CH_{naph.}$), 7.49-7.59 (m, 4H, 2$CH_{gal.}$, 2$CH_{naph.}$), 7.67 (d, *J* = 2.1, 1H, $CH_{naph.}$), 7.76 (d, *J* = 2.1, 1H, H_2), 7.81 (dd, *J* = 8.3, 2.0, 1H, H_6), 7.89 (dd, *J* = 7.1, 1.7, 1H, $CH_{naph.}$), 8.04 (d, *J* = 7.5, 1H, $CH_{naph.}$); ^{13}C NMR (75 MHz, $CDCl_3$) δ −3.6 ((CH_3)$_2$Si), −3.5 ((CH_3)$_2$Si), −3.3 ((CH_3)$_2$Si), −3.1 (2(CH_3)$_2$Si), 18.9 ((CH_3)$_3$CSi), 19.0 (2(CH_3)$_3$CSi), 19.3 (2(CH_3)$_3$CSi), 26.1 ((CH_3)$_3$CSi), 26.3 ((CH_3)$_3$CSi), 26.4 ((CH_3)$_3$CSi), 26.6 ((CH_3)$_3$CSi), 26.7 ((CH_3)$_3$CSi), 114.9 ($CH_{naph.}$), 116.6 (2$CH_{gal.}$), 117.1 ($CH_{naph.}$), 121.1 ($CH_{prot.}$), 121.2 ($C_{gal.}$), 121.9 ($CH_{naph.}$), 122.8 ($C_{prot.}$), 123.3, 124.9 (2$CH_{prot.}$), 125.7 ($C_{naph.}$), 126.5, 127.6, 128.3 (3$CH_{naph.}$), 134.8 ($C_{naph.}$), 144.7 (C-$O_{gal.}$ *para*), 147.4 (C-$O_{prot.}$), 147.9, 148.5 (2C-$O_{naph.}$), 149.2 (2C-$O_{gal.}$ *meta*), 152.9 (C-$O_{prot.}$), 164.8, 165.2 (2C=O); ESI-MS 1041.6 $(M+Na)^+$.

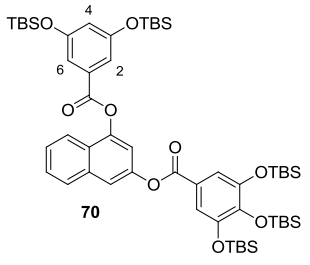

70

4-[(3,5-Bis{[*tert*-butyl(dimethyl)silyl]oxy}benzoyl)oxy]-2-naphthyl 3,4,5-tris{[*tert*-butyl (dimethyl)silyl]oxy}benzoate (70). Obtained from monoester **62** (190 mg, 0.29 mmol) and acid chloride **52c** (230 mg, 0.58 mmol) in 91% yield. R_f (hexane/DCM, 4:6) 0.41; mp 149-151 ºC; IR (ATR) ν 1743 (C=O), 1588 (Ar); ^{1}H NMR (300 MHz, $CDCl_3$) δ 0.19 (s, 6H, $(CH_3)_2$Si *para*), 0.27 (s, 12H, 2$(CH_3)_2$Si *meta*), 0.28 (s, 12H, 2$(CH_3)_2$Si *meta*), 0.98 (s, 9H, $(CH_3)_3$CSi *para*), 1.01 (s, 18H, 2$(CH_3)_3$CSi *meta*), 1.02 (s, 18H, 2$(CH_3)_3$CSi *meta*), 6.66 (t, *J* = 2.3, 1H, H_4), 7.37 (d, *J* = 2.1, 1H, $CH_{naph.}$), 7.41 (d, *J* = 2.3, 2H, H_2, H_6), 7.42 (s, 2H, 2$CH_{gal.}$), 7.47-7.57 (m, 2H, 2$CH_{naph.}$), 7.65 (d, *J* = 1.8, 1H, $CH_{naph.}$), 7.88 (d, *J* = 7.4, 1H, $CH_{naph.}$), 7.95 (d, *J* = 7.9, 1H, $CH_{naph.}$); ^{13}C NMR (75 MHz, $CDCl_3$) δ −4.3 ($(CH_3)_2$Si *para*), −3.8 (2$(CH_3)_2$Si *meta*), −3.6 (2$(CH_3)_2$Si *meta*), 15.2 ($(CH_3)_3$CSi *para*, 2$(CH_3)_3$CSi *meta*), 16.0 (2$(CH_3)_3$CSi *meta*), 25.7 ($(CH_3)_3$CSi *para*), 26.1 (2$(CH_3)_3$CSi *meta*), 26.4 (2$(CH_3)_3$CSi *meta*), 114.5 ($CH_{naph.}$), 115.2 (2$CH_{α\text{-}res.}$), 116.2 (2$CH_{gal.}$), 116.9, 117.8 (2$CH_{naph.}$), 121.0 ($C_{gal.}$), 121.5 ($CH_{α\text{-}res.}$), 125.2 ($C_{naph.}$), 126.2, 127.2, 127.9 (3$CH_{naph.}$), 130.8 ($C_{α\text{-}res.}$), 134.4 ($C_{naph.}$), 144.1 (C-$O_{gal.}$ *para*), 147.4, 148.2 (2C-$O_{naph.}$), 148.7 (2C-$O_{gal.}$ *meta*), 156.9 (2C-$O_{α\text{-}res.}$), 164.5, 164.8 (2C=O); ESI-MS 1041.6 $(M+Na)^+$.

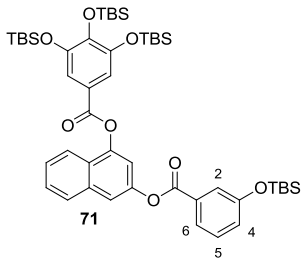

71

3-[(3-{[*tert*-Butyl(dimethyl)silyl]oxy}benzoyl)oxy]-1-naphthyl 3,4,5-tris{[*tert*-butyl (dimethyl)silyl]oxy}benzoate (71). Obtained from monoester **59** (200 mg, 0.31 mmol) and acid chloride **52d** (210 mg, 0.76 mmol) as an oil in 44% yield. R_f (hexane/DCM, 1:1) 0.40; IR (ATR) ν 1741 (C=O), 1581, 1485 (Ar); ^{1}H NMR (300 MHz, $CDCl_3$) δ 0.20 (s, 6H, $(CH_3)_2$Si *para)*, 0.25 (s, 6H, $(CH_3)_2$Si *meta)*, 0.29 (s, 12H, 2$(CH_3)_2$Si *meta*), 0.98 (s, 18H, 2$(CH_3)_3$CSi *meta*), 1.02 (s, 9H, $(CH_3)_3$CSi meta/*para*), 1.03 (s, 9H, $(CH_3)_3$CSi meta/*para*), 7.13 (ddd, *J* = 8.0, 2.5, 1.0, 1H, H_4), 7.39 (t, *J* = 7.9, 1H, H_5), 7.41 (d, *J* = 2.0, 1H, $CH_{naph.}$), 7.47-7.58 (m, 4H, 2$CH_{gal.}$, 2$CH_{naph.}$), 7.65 (d, *J* = 2.0, 1H, $CH_{naph.}$), 7.68 (t, *J* = 2.0, 1H, H_2), 7.84 (dt, *J* = 7.9, 1.3, 1H, H_6), 7.88 (dd, *J* = 7.9, 1.3, 1H, $CH_{naph.}$), 8.01 (dd, *J* = 8.0, 1.3, 1H, $CH_{naph.}$); ^{13}C NMR (75 MHz, $CDCl_3$) δ −4.3 ($(CH_3)_2$Si *meta*), −3.7 ($(CH_3)_2$Si *para*), −3.5 (2$(CH_3)_2$Si *meta*), 18.4 ($(CH_3)_3$CSi *meta*), 18.7 ($(CH_3)_3$CSi *para*), 19.0 (2$(CH_3)_3$CSi *meta*), 25.8 ($(CH_3)_3$CSi *meta*), 26.3 ($(CH_3)_3$CSi *para*), 26.4 (2$(CH_3)_3$CSi *meta*), 114.4 ($CH_{naph.}$), 116.3 (2$CH_{gal.}$), 116.7 ($CH_{naph.}$), 120.8 ($C_{gal.}$), 121.7 ($CH_{m\text{-}sal.}$), 121.9 ($CH_{naph.}$), 123.4 ($CH_{m\text{-}sal.}$), 125.5 ($C_{naph.}$), 125.8 ($CH_{m\text{-}sal.}$), 126.6, 127.4, 128.0 (3$CH_{naph.}$), 129.8 ($CH_{m\text{-}sal.}$), 130.8 ($C_{m\text{-}sal.}$), 134.4 ($C_{naph.}$), 144.4 (C-$O_{gal.}$ *para*), 147.7, 148.0 (2C-$O_{naph.}$), 148.9 (2C-$O_{gal.}$ *meta*), 156.1 (C-$O_{m\text{-}sal.}$), 164.5, 165.1 (2C=O); ESI-MS 911.5 $(M+Na)^+$.

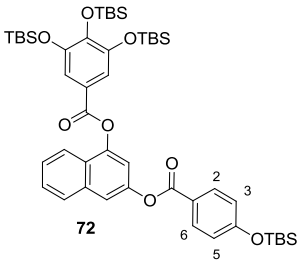

72

3-[(4-{[*tert*-Butyl(dimethyl)silyl]oxy}benzoyl)oxy]-1-naphthyl 3,4,5-tris{[*tert*-butyl(dimethyl)silyl]oxy} benzoate (72). Obtained from monoester **59** (200 mg, 0.31 mmol) and acid chloride **52e** (210 mg, 0.76 mmol) as an oil in 55% yield. R_f (hexane/DCM, 1:1) 0.87; IR (ATR) ν 1740 (C=O), 1601, 1501 (Ar); ^{1}H NMR (300 MHz, $CDCl_3$) δ 0.19 (s, 6H, $(CH_3)_2$Si *para*), 0.27 (s, 6H, $(CH_3)_2$Si *para*), 0.28 (s, 12H, 2$(CH_3)_2$Si *meta*), 0.98 (s, 18H, 2$(CH_3)_3$CSi *meta*), 1.01 (s, 9H, $(CH_3)_3$CSi *para*), 1.03 (s, 9H, $(CH_3)_3$CSi *para*), 6.94 (d, *J* = 8.7, 2H, H_3, H_5), 7.40 (d, *J* = 2.2, 1H, $CH_{naph.}$), 7.43-7.58 (m, 2H, 2$CH_{naph.}$), 7.49 (s, 2H, 2$CH_{gal.}$), 7.63 (d, *J* = 2.3, 1H, $CH_{naph.}$), 7.87 (d, *J* = 7.4, 1H, $CH_{naph.}$), 8.00 (d, *J* = 7.9, 1H, $CH_{naph.}$), 8.13 (d, *J* = 8.7, 2H, H_2, H_6); ^{13}C NMR (75 MHz, $CDCl_3$) δ −4.2, −3.7 (2$(CH_3)_2$Si *para*), −3.4 (2$(CH_3)_2$Si *meta*), 18.4, 18.7 (2$(CH_3)_3$CSi *para*), 19.0 (2$(CH_3)_3$CSi *meta*), 25.8, 26.3 (2$(CH_3)_3$CSi *para*), 26.4 (2$(CH_3)_3$CSi *meta*), 114.5 ($CH_{naph.}$), 116.3 (2$CH_{gal.}$), 116.8 ($CH_{naph.}$), 120.3 (2$CH_{p\text{-}sal.}$), 120.9 ($C_{gal.}$), 121.6 ($CH_{naph.}$), 122.4 ($C_{p\text{-}sal.}$), 125.4 ($C_{naph.}$), 126.2, 127.3, 128.0 (3$CH_{naph.}$), 132.5 (2$CH_{p\text{-}sal.}$), 134.5 ($C_{naph.}$), 144.4 (C-$O_{gal.}$ *para*), 147.7, 148.2 (2C-$O_{naph.}$), 148.9 (2C-$O_{gal.}$ *meta*), 161.0 (C-$O_{p\text{-}sal.}$), 164.5, 165.0 (2C=O); ESI-MS 911.5 $(M+Na)^+$.

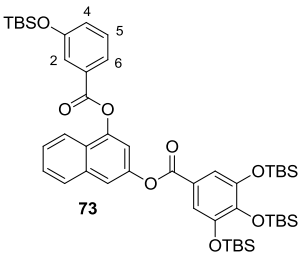

73

4-[(3-{[*tert*-Butyl(dimethyl)silyl]oxy}benzoyl)oxy]-2-naphthyl 3,4,5-tris{[*tert*-butyl(dimethyl)silyl]oxy}benzoate (73). Obtained from monoester **62** (100 mg, 0.15 mmol) and acid chloride **52d** (83 mg, 0.30 mmol) as an oil in 66% yield. R_f (hexane/DCM, 1:1) 0.47; IR (ATR) ν 1790 (C=O), 1582, 1484 (Ar); ^{1}H NMR (300 MHz, $CDCl_3$) δ 0.18 (s, 6H, $(CH_3)_2$Si *para*), 0.26 (s, 6H, $(CH_3)_2$Si *meta*), 0.27 (s, 12H, 2$(CH_3)_2$Si *meta*), 0.97 (s, 18H, 2$(CH_3)_3$CSi *meta*), 1.01 (s, 9H, $(CH_3)_3$CSi *meta/para*), 1.02 (s, 9H, $(CH_3)_3$CSi *meta/para*), 7.17 (ddd, *J* = 8.1, 2.5, 1.0, 1H, H_4), 7.37 (d, *J* = 2.1, 1H, $CH_{naph.}$), 7.41 (s, 2H, 2$CH_{gal.}$), 7.43 (t, *J* = 8.0, 1H, H_5), 7.45-7.57 (m, 2H, 2$CH_{naph.}$),

7.65 (d, *J* = 1.9, 1H, $CH_{naph.}$), 7.76 (t, *J* = 2.0, 1H, H_2), 7.88 (d, *J* = 8.0, 1H, $CH_{naph.}$), 7.93 (dt, *J* = 7.8, 1.3, 1H, H_6), 7.95 (d, *J* = 8.0, 1H, $CH_{naph.}$); ^{13}C NMR (75 MHz, $CDCl_3$) δ −4.2 ($(CH_3)_2$Si *meta*), −3.7 ($(CH_3)_2$Si *para*), −3.5 ($2(CH_3)_2$Si *meta*), 18.4 ($(CH_3)_3\underline{C}$Si *meta*), 18.7 ($(CH_3)_3\underline{C}$Si *para*), 19.0 ($2(CH_3)_3\underline{C}$Si *meta*), 25.8 ($(\underline{C}H_3)_3$CSi *meta*), 26.4 ($(\underline{C}H_3)_3$CSi *para*), 26.5 ($2(\underline{C}H_3)_3$CSi *meta*), 114.6 ($CH_{naph.}$), 116.3 ($2CH_{gal.}$), 117.0 ($CH_{naph.}$), 121.0 ($C_{gal.}$), 121.5 ($CH_{m\text{-}sal.}$), 121.7, 123.4 ($CH_{m\text{-}sal.}$, $CH_{naph.}$), 125.2 ($C_{naph.}$), 125.9 ($CH_{m\text{-}sal.}$), 126.2, 127.4, 128.0 ($3CH_{naph.}$), 130.0 ($CH_{m\text{-}sal.}$), 130.6 ($C_{m\text{-}sal.}$), 134.5 ($C_{naph.}$), 144.3 (C-$O_{gal.}$ *para*), 147.5, 148.3 (2C-$O_{naph.}$), 148.8 (2C-$O_{gal.}$ *meta*), 156.2 (C-$O_{m\text{-}sal.}$), 164.8, 164.9 (2C=O); ESI-MS 911.5 $(M+Na)^+$.

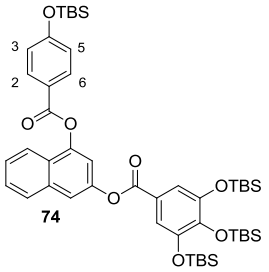

74

4-[(4-{[*tert*-Butyl(dimethyl)silyl]oxy}benzoyl)oxy]-2-naphthyl 3,4,5-tris{[*tert*-butyl (dimethyl)silyl]oxy} benzoate (74). Obtained from monoester **62** (100 mg, 0.15 mmol) and acid chloride **52e** (83 mg, 0.30 mmol) as an oil in 71% yield. R_f (hexane/DCM, 2:8) 0.88; IR (ATR) ν 1741 (C=O), 1601, 1477 (Ar); ^{1}H NMR (300 MHz, $CDCl_3$) δ 0.17 (s, 6H, $(CH_3)_2$Si *para)*, 0.27 (s, 12H, $2(CH_3)_2$Si *meta*), 0.29 (s, 6H, $(CH_3)_2$Si *para)*, 0.97 (s, 18H, $2(CH_3)_3$CSi *meta*), 1.02 (s, 9H, $(CH_3)_3$CSi *para*), 1.03 (s, 9H, $(CH_3)_3$CSi *para*), 6.98 (d, *J* = 8.8, 2H, H_3, H_5), 7.34 (d, *J* = 2.2, 1H, $CH_{naph.}$), 7.41 (s, 2H, $2CH_{gal.}$), 7.43-7.58 (m, 2H, $2CH_{naph.}$), 7.64 (d, *J* = 1.9, 1H, $CH_{naph.}$), 7.87 (d, *J* = 8.6, 1H, $CH_{naph.}$), 7.95 (d, *J* = 8.0, 1H, $CH_{naph.}$), 8.22 (d, *J* = 8.8, 2H, H_2, H_6); ^{13}C NMR (75 MHz, $CDCl_3$) δ −4.2, −3.7 ($2(CH_3)_2$Si *para*), −3.5 ($2(CH_3)_2$Si *meta*), 18.4, 18.7 ($2(CH_3)_3\underline{C}$Si *para*), 19.0 ($2(CH_3)_3\underline{C}$Si *meta*), 25.8, 26.3 ($2(\underline{C}H_3)_3$CSi *para*), 26.4 ($2(\underline{C}H_3)_3$CSi *meta*), 114.6 ($CH_{naph.}$), 116.3 ($2CH_{gal.}$), 116.9 ($CH_{naph.}$), 120.4 ($2CH_{p\text{-}sal.}$), 121.1 ($C_{gal.}$), 121.7 ($C_{p\text{-}sal.}$), 122.1 ($CH_{naph.}$), 125.4 ($C_{naph.}$), 126.2, 127.3, 128.0 ($3CH_{naph.}$), 132.6 ($2CH_{p\text{-}sal.}$), 134.5 ($C_{naph.}$), 144.2 (C-$O_{gal.}$ *para*), 147.7, 148.3 (2C-$O_{naph.}$), 148.8 (2C-$O_{gal.}$ *meta*), 161.2 (C-$O_{p\text{-}sal.}$), 164.8, 164.9 (2C=O); ESI-MS 911.4 $(M+Na)^+$.

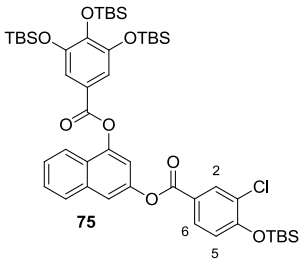

75

3-[(4-{[*tert*-Butyl(dimethyl)silyl]oxy}-3-chlorobenzoyl)oxy]-1-naphthyl 3,4,5-tris{[*tert*-butyl(dimethyl)silyl] oxy}benzoate (75). Obtained from monoester **59** (200 mg, 0.31 mmol) and acid chloride **52f** (190 mg, 0.61 mmol) in 58% yield. R_f (hexane/DCM, 2:8) 0.72; mp 135-136 ºC; IR (ATR) ν 1741 (C=O), 1586, 1493 (Ar); ^{1}H NMR (300 MHz, $CDCl_3$) δ 0.21 (s, 6H, $(CH_3)_2$Si *para*), 0.30 (s, 12H, 2$(CH_3)_2$Si *meta*), 0.31 (s, 6H, $(CH_3)_2$Si *para*), 0.99 (s, 18H, 2$(CH_3)_3$CSi *meta*), 1.04 (s, 9H, $(CH_3)_3$CSi *para*), 1.07 (s, 9H, $(CH_3)_3$CSi *para*), 7.00 (d, *J* = 8.5, 1H, H_5), 7.41 (d, *J* = 2.1, 1H, $CH_{naph.}$), 7.47-7.59 (s, 4H, 2$CH_{naph.}$, 2$CH_{gal.}$), 7.65 (d, *J* = 1.5, 1H, $CH_{naph.}$), 7.88 (d, *J* = 8.0, 1H, $CH_{naph.}$), 7.99-8.06 (m, 2H, $CH_{naph.}$, H_6), 8.27 (d, *J* = 2.1, 1H, H_2); ^{13}C NMR (75 MHz, $CDCl_3$) δ −4.1, −3.7 (2$(CH_3)_2$Si *para*), −3.4 (2$(CH_3)_2$Si *meta*), 18.5, 18.7 (2$(CH_3)_3$CSi *para*), 19.0 (2$(CH_3)_3$CSi *meta*), 25.7, 26.3 (2$(CH_3)_3$CSi *para*), 26.4 (2$(CH_3)_3$CSi *meta*), 114.3 ($CH_{naph.}$), 116.3 (2$CH_{gal.}$), 116.7 ($CH_{naph.}$), 120.4 ($CH_{Clbenz.}$), 120.8 ($C_{gal.}$), 121.7 ($CH_{naph.}$), 123.3 ($C_{Clbenz.}$), 125.5 ($C_{naph.}$), 126.3 ($CH_{naph.}$, $C_{Clbenz.}$), 127.4, 128.0 (2$CH_{naph.}$), 130.3, 132.8 (2$CH_{Clbenz.}$), 134.4 ($C_{naph.}$), 144.4 (C-$O_{gal.}$ *para*), 147.7, 147.9 (2C-$O_{naph.}$), 148.9 (2C-$O_{gal.}$ *meta*), 156.7 (C-$O_{Clbenz.}$), 164.0, 164.5 (2C=O); ESI-MS 945.3 $(M+Na)^+$.

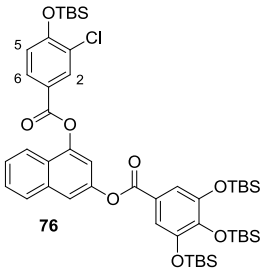

76

4-[(4-{[*tert*-Butyl(dimethyl)silyl]oxy}-3-chlorobenzoyl)oxy]-2-naphthyl 3,4,5-tris{[*tert*-butyl(dimethyl)silyl] oxy}benzoate (76). Obtained from monoester **62** (200 mg, 0.31 mmol) and acid chloride **52f** (190 mg, 0.61 mmol) in 57% yield. R_f (hexane/DCM, 2:8) 0.92; mp 76-78 ºC; IR (ATR) ν 1742 (C=O), 1586, 1491 (Ar); ^{1}H NMR (300 MHz, $CDCl_3$) δ 0.18 (s, 6H, $(CH_3)_2$Si *para*), 0.28 (s, 12H, 2$(CH_3)_2$Si *meta*), 0.32 (s, 6H, $(CH_3)_2$Si *para*), 0.98 (s, 18H, 2$(CH_3)_3$CSi *meta*), 1.02 (s, 9H, $(CH_3)_3$CSi *para*), 1.08 (s, 9H, $(CH_3)_3$CSi *para*), 7.03 (d, *J* = 8.5, 1H, H_5), 7.34 (d, *J* = 2.1, 1H, $CH_{naph.}$), 7.41 (s, 2H, 2$CH_{gal.}$), 7.46-7.57 (m, 2H, 2$CH_{naph.}$), 7.66 (d, *J* = 1.6, 1H, $CH_{naph.}$), 7.88 (d, *J* =

7.9, 1H, $CH_{naph.}$), 7.92 (d, *J* = 7.8, 1H, $CH_{naph.}$), 8.11 (dd, *J* = 8.5, 2.2, 1H, H_6), 8.34 (d, *J* = 2.1, 1H, H_2); ^{13}C NMR (75 MHz, $CDCl_3$) δ −4.1, −3.7 ($2(CH_3)_2$Si *para*), −3.5 ($2(CH_3)_2$Si *meta*), 18.6, 18.7 ($2(CH_3)_3\underline{C}$Si *para*), 19.0 ($2(CH_3)_3\underline{C}$Si *meta*), 25.7, 26.3 ($2(\underline{C}H_3)_3$CSi *para*), 26.4 ($2(\underline{C}H_3)_3$CSi *meta*), 114.6 ($CH_{naph.}$), 116.3 ($2CH_{gal.}$), 117.1 ($CH_{naph.}$), 120.5 ($CH_{Clbenz.}$), 121.1 ($C_{gal.}$), 121.6 ($CH_{naph.}$), 123.0 ($C_{Clbenz.}$), 125.2 ($C_{naph.}$), 126.3 ($CH_{naph.}$), 126.4 ($C_{Clbenz.}$), 127.4, 128.1 ($2CH_{naph.}$), 130.4, 132.8 ($2CH_{Clbenz.}$), 134.5 ($C_{naph.}$), 144.3 (C-$O_{gal.}$ *para*), 147.4, 148.2 (2C-$O_{naph.}$), 148.8 (2C-$O_{gal.}$ *meta*), 156.9 (C-$O_{Clbenz.}$), 163.8, 164.9 (2C=O); ESI-MS 807.1 $(M-TBS)^-$.

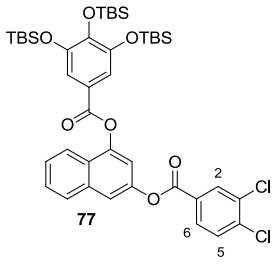

77

3-[(3,4-Dichlorobenzoyl)oxy]-1-naphthyl 3,4,5-tris{[*tert*-butyl(dimethyl)silyl]oxy} benzoate (77). Obtained from monoester **59** (325 mg, 0.50 mmol) and acid chloride **52g** (208 mg, 0.99 mmol) in 48% yield. R_f (hexane/DCM, 1:1) 0.53; mp 162-164 ºC; IR (ATR) ν 1743 (C=O), 1578, 1486 (Ar); ^{1}H NMR (300 MHz, $CDCl_3$) δ 0.20 (s, 6H, $(CH_3)_2$Si *para*), 0.29 (s, 12H, $2(CH_3)_2$Si *meta*), 0.98 (s, 18H, $2(CH_3)_3$CSi *meta*), 1.03 (s, 9H, $(CH_3)_3$CSi *para*), 7.41 (d, *J* = 2.1, 1H, $CH_{naph.}$), 7.50-7.59 (m, 4H, $2CH_{naph.,}$ $2CH_{gal.}$), 7.62 (d, *J* = 8.4, 1H, H_5), 7.65 (d, *J* = 1.8, 1H, $CH_{naph.}$), 7.88 (d, *J* = 7.5, 1H, $CH_{naph.}$), 7.98-8.07 (m, 2H, $CH_{naph.}$, H_6), 8.32 (d, *J* = 1.9, 1H, H_2); ^{13}C NMR (75 MHz, $CDCl_3$) δ −3.7 ($(CH_3)_2$Si *para*), −3.4 ($2(CH_3)_2$Si *meta*), 18.7 ($(CH_3)_3\underline{C}$Si *para*), 19.0 ($2(CH_3)_3\underline{C}$Si *meta*), 26.3 ($(\underline{C}H_3)_3$CSi *para*), 26.4 ($2(\underline{C}H_3)_3$CSi *meta*), 114.0 ($CH_{naph.}$), 116.3 ($2CH_{gal.}$), 116.6 ($CH_{naph.}$), 120.7 ($C_{gal.}$), 121.7 ($CH_{naph.}$), 125.6 ($C_{naph.}$), 126.5, 127.6, 128.1 ($3CH_{naph.}$), 129.4 ($C_{Cl2benz.}$, $CH_{Cl2benz.}$), 131.0, 132.2 ($2CH_{Cl2benz.}$), 133.5 ($C_{Cl2benz.}$), 134.4 ($C_{naph.}$), 138.7 ($C_{Cl2benz.}$), 144.5 (C-$O_{gal.}$ *para*), 147.6, 147.8 (2C-$O_{naph.}$), 149.0 (2C-$O_{gal.}$ *meta*), 163.4, 164.5 (2C=O).

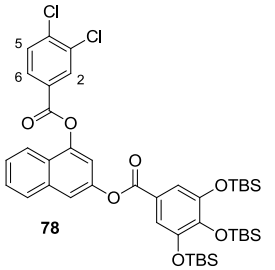

78

4-[(3,4-Dichlorobenzoyl)oxy]-2-naphthyl 3,4,5-tris{[*tert*-butyl(dimethyl)silyl]oxy} benzoate (78). Obtained from monoester **62** (305 mg, 0.47 mmol) and acid chloride **52g** (195 mg,

0.93 mmol) in 74% yield. R_f (hexane/DCM, 1:1) 0.60; mp 63-65 ºC; IR (ATR) ν 1744 (C=O), 1578, 1485 (Ar); ^{1}H NMR (300 MHz, $CDCl_3$) δ 0.17 (s, 6H, $(CH_3)_2$Si *para*), 0.27 (s, 12H, 2$(CH_3)_2$Si *meta*), 0.97 (s, 18H, 2$(CH_3)_3$CSi *meta*), 1.01 (s, 9H, $(CH_3)_3$CSi *para*), 7.35 (d, *J* = 2.2, 1H, $CH_{naph.}$), 7.40 (s, 2H, $2CH_{gal.}$), 7.48-7.58 (m, 2H, $2CH_{naph.}$), 7.66 (d, *J* = 8.4, 1H, H_5), 7.67 (d, *J* = 2.2, 1H, $CH_{naph.}$), 7.86-7.90 (m, 2H, $2CH_{naph.}$), 8.14 (dd, *J* = 8.4, 2.0, 1H, H_6), 8.40 (d, *J* = 1.9, 1H, H_2); ^{13}C NMR (75 MHz, $CDCl_3$) δ −3.7 ($(CH_3)_2$Si *para*), −3.5 (2$(CH_3)_2$Si *meta*), 18.7 ($(CH_3)_3\underline{C}$Si *para*), 19.0 (2$(CH_3)_3\underline{C}$Si *meta*), 26.3 ($(\underline{C}H_3)_3$CSi *para*), 26.4 (2$(\underline{C}H_3)_3$CSi *meta*), 114.6 ($CH_{naph.}$), 116.3 ($2CH_{gal.}$), 117.4 ($CH_{naph.}$), 121.0 ($C_{gal.}$), 121.3 ($CH_{naph.}$), 125.0 ($C_{naph.}$), 126.5, 127.5, 128.2 ($3CH_{naph.}$), 129.1 ($C_{Cl2benz.}$), 129.5, 131.1, 132.3 ($3CH_{Cl2benz.}$), 133.7 ($C_{Cl2benz.}$), 134.5 ($C_{naph.}$), 138.9 ($C_{Cl2benz.}$), 144.4 (C-$O_{gal.}$ *para*), 147.1, 148.2 (2C-$O_{naph.}$), 148.9 (2C-$O_{gal.}$ *meta*), 163.2, 164.9 (2C=O); ESI-MS 677.4 $((M-COC_6H_3Cl_2)+Na)^+$.

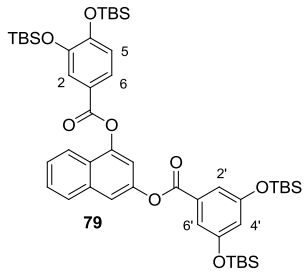

79

3-[(3,5-Bis{[*tert*-butyl(dimethyl)silyl]oxy}benzoyl)oxy]-1-naphthyl 3,4-bis{[*tert*-butyl (dimethyl)silyl]oxy}benzoate (79). Obtained from monoester **63** (400 mg, 0.76 mmol) and acid chloride **52b** (670 mg, 1.7 mmol) as an oil in 85% yield. R_f (hexane/DCM, 3:7) 0.43; ^{1}H NMR (300 MHz, $CDCl_3$) δ 0.33 (s, 12H, 2$(CH_3)_2$Si), 0.36 (s, 12H, 2$(CH_3)_2$Si), 1.09 (s, 18H, 2$(CH_3)_3$CSi *meta*), 1.10 (s, 9H, $(CH_3)_3$CSi *para/meta*), 1.11 (s, 9H, $(CH_3)_3$CSi *para/meta*), 6.73 (t, *J* = 2.3, 1H, $H_{4'}$), 7.06 (d, *J* = 8.4, 1H, H_5), 7.45 (d, *J* = 2.1, 2H, $H_{2'}$, $H_{6'}$), 7,50 (d, *J* = 2.1, 1H, $CH_{naph.}$), 7.51-7.60 (m, 2H, $2CH_{naph.}$), 7.73 (d, *J* = 1.8, 1H, $CH_{naph.}$), 7.91-7.97 (m, 3H, H_2, H_6, $CH_{naph.}$), 8.08 (d, *J* = 7.8, 1H, $CH_{naph.}$); ^{13}C NMR (75 MHz, $CDCl_3$) δ −4.4 ($(CH_3)_2$Si *para/meta*), −4.2 ($(CH_3)_2$Si *para/meta*), −4.1 (2$(CH_3)_2$Si *meta*), 18.1 ($(CH_3)_3\underline{C}$Si *para*), 18.4 (3$(CH_3)_3\underline{C}$Si *meta*), 25.6 ($(\underline{C}H_3)_3$CSi *para/meta*), 25.8 ($(\underline{C}H_3)_3$CSi *para/meta*), 25.9 (2$(\underline{C}H_3)_3$CSi *meta*), 114.2 ($CH_{naph.}$), 115.0 ($2CH_{α\text{-}res.}$), 116.5 ($CH_{naph.}$), 117.5 ($CH_{α\text{-}res.}$), 120.7 ($CH_{prot.}$), 121.4 ($C_{prot.}$), 122.0 ($CH_{naph.}$), 122.7, 124.5 ($2CH_{prot.}$), 125.3 ($C_{naph.}$), 126.1, 127.2, 127.8 ($3CH_{naph.}$), 130.9 ($C_{α\text{-}res.}$), 134.2 ($C_{naph.}$), 147.0, 147.5, 147.8 (2C-$O_{naph.}$, C-$O_{prot.}$), 152.6, (C-$O_{prot.}$), 156.7 (2C-$O_{α\text{-}res.}$), 164.2, 164.6 (2C=O); ESI-MS 911.4 $(M+Na)^+$.

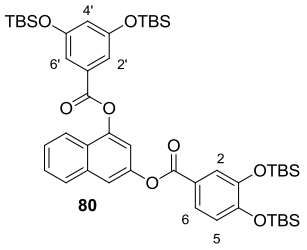

80

4-[(3,5-Bis{[*tert*-butyl(dimethyl)silyl]oxy}benzoyl)oxy]-2-naphthyl 3,4-bis{[*tert*-butyl (dimethyl)silyl]oxy}benzoate (80). Obtained from monoester **60** (400 mg, 0.76 mmol) and acid chloride **52b** (670 mg, 1.7 mmol) as an oil in 86% yield. R_f (hexane/DCM, 3:7) 0.34; ^{1}H NMR (300 MHz, $CDCl_3$) δ 0.27 (s, 18H, 3$(CH_3)_2$Si *meta*), 0.28 (s, 6H, $(CH_3)_2$Si *para*), 1.03 (s, 36H, 4$(CH_3)_3$CSi *para,meta*), 6.67 (t, *J* = 2.4, 1H, $H_{4'}$), 6.95 (d, *J* = 8.4, 1H, H_5), 7.38 (d, *J* = 2.1, 2H, $H_{2'}$, $H_{6'}$), 7.42 (d, *J* = 2.1, 1H, $CH_{naph.}$), 7.48-7.58 (m, 2H, 2$CH_{naph.}$), 7.66 (d, *J* = 2.1, 1H, $CH_{naph.}$), 7.72 (d, *J* = 2.1, 1H, H_2), 7.77 (dd, *J* = 8.4, 2.1, 1H, H_6), 7.88 (d, *J* = 7.8, 1H, $CH_{naph.}$), 7.97 (d, *J* = 7.8, 1H, $CH_{naph.}$); ^{13}C NMR (75 MHz, $CDCl_3$) δ −4.4 (2$(CH_3)_2$Si *meta*), −4.1 ($(CH_3)_2$Si *para/meta*), −4.0 ($(CH_3)_2$Si *para/meta*), 18.2 (2$(CH_3)_3$CSi *meta*), 18.4 ($(CH_3)_3$CSi *para/meta*), 18.5 ($(CH_3)_3$CSi *meta/para*), 25.6 (2$(CH_3)_3$CSi *meta*), 25.8 ($(CH_3)_3$CSi *para/meta*), 25.9 ($(CH_3)_3$CSi *para/meta*), 114.4 ($CH_{naph.}$), 115.1 (2$CH_{α\text{-}res.}$), 116.8 ($CH_{naph.}$), 117.8 ($CH_{α\text{-}res.}$), 120.6 ($CH_{prot.}$), 121.4 ($CH_{naph.}$), 122.3 ($C_{prot.}$), 122.7, 124.4 (2$CH_{prot.}$), 125.1 ($C_{naph.}$), 126.1, 127.2, 127.9 (3$CH_{naph.}$), 130.7 ($C_{α\text{-}res.}$), 134.3 ($C_{naph.}$), 146.9, 147.3, 148.0 (2C-$O_{naph.}$, C-$O_{prot.}$), 152.5 (C-$O_{prot.}$), 156.9 (2C-$O_{α\text{-}res.}$), 164.4, 164.7 (2C=O); ESI-MS 889.4 $(M+H)^+$.

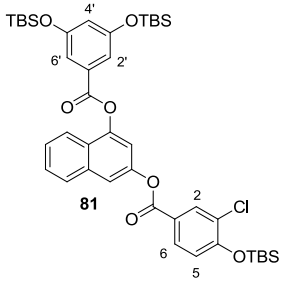

81

4-[(3,5-Bis{[*tert*-butyl(dimethyl)silyl]oxy}benzoyl)oxy]-2-naphthyl 4-{[*tert*-butyl (dimethyl)silyl]oxy}-3-chlorobenzoate (81). Obtained from monoester **60** (150 mg, 0.29 mmol) and acid chloride **52f** (175 mg, 0.57 mmol) in 24% yield. R_f (DCM) 0.77; mp 65-67 ºC; IR (ATR) ν 1739 (C=O), 1592, 1448 (Ar); ^{1}H NMR (300 MHz, $CDCl_3$) δ 0.26 (s, 12H, 2$(CH_3)_2$Si *meta)*, 0.31 (s, 6H, $(CH_3)_2$Si *para*), 1.02 (s, 18H, 2$(CH_3)_3$CSi *meta*), 1.07 (s, 9H, $(CH_3)_3$CSi *para*), 6.66 (t, *J* = 2.3,

1H, $H_{4'}$), 6.99 (d, *J* = 8.5, 1H, H_5), 7.37 (d, *J* = 2.2, 1H, $CH_{naph.}$), 7.41 (d, *J* = 2.3, 2H, $H_{2'}$, $H_{6'}$), 7.46-7.57 (m, 2H, $2CH_{naph.}$), 7.66 (d, *J* = 2.0, 1H, $CH_{naph.}$), 7.88 (d, *J* = 7.7, 1H, $CH_{naph.}$), 7.96 (d, *J* = 8.0, 1H, $CH_{naph.}$), 8.03 (dd, *J* = 8.5, 2.2, 1H, H_6), 8.26 (d, *J* = 2.2, 1H, H_2); ^{13}C NMR (75 MHz, $CDCl_3$) δ −4.2 ($2(CH_3)_2Si$ *meta*), −4.1 ($(CH_3)_2Si$ *para*), 18.4 ($2(CH_3)_3\underline{C}Si$ *meta*), 18.6 ($(CH_3)_3\underline{C}Si$ *para*), 25.7 ($(\underline{C}H_3)_3CSi$ *para*), 25.8 ($2(\underline{C}H_3)_3CSi$ *meta*), 114.4 ($CH_{naph.}$), 115.3 ($2CH_{\alpha\text{-res.}}$), 116.9 ($CH_{naph.}$), 118.0 ($CH_{\alpha\text{-res.}}$), 120.4 ($CH_{Clbenz.}$), 121.6 ($CH_{naph.}$), 123.2 ($C_{\alpha\text{-res.}}$), 125.4 ($C_{Clbenz.}$), 126.3 ($C_{naph.}$), 126.4, 127.5, 128.1 ($3CH_{naph.}$), 130.3 ($CH_{Clbenz.}$), 130.8 ($C_{ClBenz.}$), 132.8 ($CH_{Clbenz.}$), 134.5 ($C_{naph.}$), 147.6, 147.9 ($2C\text{-}O_{naph.}$), 156.8 ($C\text{-}O_{Clbenz.}$), 157.1 ($2C\text{-}O_{\alpha\text{-res.}}$), 163.9, 164.6 (2C=O); ESI-MS 816.4 $(M+Na)^+$.

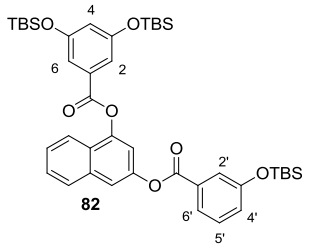

82

3-[(3-{[*tert*-Butyl(dimethyl)silyl]oxy}benzoyl)oxy]-1-naphthyl 3,5-bis{[*tert*-butyl (dimethyl)silyl]oxy}benzoate (82). Obtained from monoester **60** (200 mg, 0.38 mmol) and acid chloride **52d** (210 mg, 0.76 mmol) as an oil in 70% yield. R_f (Hexane/DCM, 1:1) 0.46; IR (ATR) ν 1744 (C=O), 1591, 1447 (Ar); ^{1}H NMR (300 MHz, $CDCl_3$) δ 0.25 (s, 6H, $(CH_3)_2Si$), 0.26 (s, 12H, $2(CH_3)_2Si$), 1.01 (s, 27H, $3(CH_3)_3CSi$), 6.65 (t, *J* = 2.3, 1H, H_4), 7.13 (ddd, *J* = 8.1, 2.5, 1.0, 1H, $H_{4'}$), 7.36-7.42 (m, 4H, $CH_{naph.}$, $H_{5'}$, H_2, H_6), 7.48-7.58 (m, 2H, $2CH_{naph.}$), 7.67-7.69 (m, 2H, $CH_{naph.}$, $H_{2'}$), 7.84 (dt, *J* =7.7, 1.3, 1H, $H_{6'}$), 7.89 (d, *J* = 7.8, 1H, $CH_{naph.}$), 7.96 (d, *J* = 7.9, 1H, $CH_{naph.}$); ^{13}C NMR (75 MHz, $CDCl_3$) δ −4.3 ($(CH_3)_2Si$), −4.2 ($2(CH_3)_2Si$), 18.4 ($3(CH_3)_3\underline{C}Si$), 25.8 ($3(\underline{C}H_3)_3CSi$), 114.5 ($CH_{naph.}$), 115.3 ($2CH_{\alpha\text{-res.}}$), 117.0 ($CH_{naph.}$), 118.0 ($CH_{\alpha\text{-res.}}$), 121.6, 121.7 ($CH_{m\text{-sal.}}$, $CH_{naph.}$), 123.4 ($CH_{m\text{-sal.}}$), 125.4 ($C_{naph.}$), 125.8 ($CH_{m\text{-sal.}}$), 126.4, 127.4, 128.1 ($3CH_{naph.}$), 129.8 ($CH_{m\text{-sal.}}$), 130.7, 130.8 ($C_{\alpha\text{-res.}}$, $C_{m\text{-sal.}}$), 134.5 ($C_{naph.}$), 147.6, 148.0 ($2C\text{-}O_{naph.}$), 156.1 ($C\text{-}O_{m\text{-sal.}}$), 157.0 ($2C\text{-}O_{\alpha\text{-res.}}$), 164.6, 165.0 (2C=O); ESI-MS 781.0 $(M+Na)^+$.

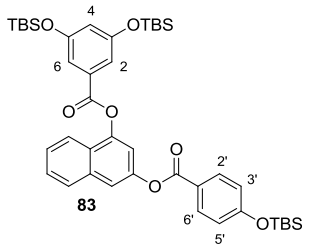

83

3-[(4-{[*tert*-Butyl(dimethyl)silyl]oxy}benzoyl)oxy]-1-naphthyl 3,5-bis{[*tert*-butyl(dimethyl)silyl]oxy} benzoate (83). Obtained from monoester **60** (200 mg, 0.38 mmol) and acid chloride (**52e**, 210 mg, 0.76 mmol) in 62% yield. R_f (hexane/DCM, 1:1) 0.42; mp 128-129 ºC; IR (ATR) ν 1742 (C=O), 1595, 1453 (Ar); ^{1}H NMR (300 MHz, $CDCl_3$) δ 0.26 (s, 12H, 2(CH_3)$_2$Si *meta*), 0.27 (s, 6H, (CH_3)$_2$Si *para*), 1.01 (s, 27H, 3(CH_3)$_3$CSi), 6.66 (t, *J* = 2.3, 1H, H_4), 6.95 (d, *J* = 8.8, 2H, $H_{3'}$, $H_{5'}$), 7.37 (d, *J* = 2.2, 1H, $CH_{naph.}$), 7.40 (d, *J* = 2.2, 2H, H_2, H_6), 7.47-7.58 (m, 2H, 2$CH_{naph.}$), 7.66 (d, *J* = 2.0, 1H, $CH_{naph.}$), 7.88 (d, *J* = 7.9, 1H, $CH_{naph.}$), 7.95 (d, *J* = 7.9, 1H, $CH_{naph.}$), 8.14 (d, *J* = 8.8, 2H, $H_{2'}$, $H_{6'}$); ^{13}C NMR (75 MHz, $CDCl_3$) δ −4.3 (2(CH_3)$_2$Si *meta*), -4.2 ((CH_3)$_2$Si *para*), 18.3 (2(CH_3)$_3$CSi *meta*), 18.4 ((CH_3)$_3$CSi *para*), 25.7 ((CH_3)$_3$CSi *para*), 25.8 (2(CH_3)$_3$CSi *meta*), 114.6 ($CH_{naph.}$), 115.3 (2$CH_{α\text{-}res.}$), 117.0 ($CH_{naph.}$), 118.0 ($CH_{α\text{-}res.}$), 120.3 (2$CH_{p\text{-}sal.}$), 121.6 ($CH_{naph.}$), 122.3 ($C_{p\text{-}sal.}$), 125.3 ($C_{naph.}$), 126.3, 127.4, 128.0 (3$CH_{naph.}$), 130.8 ($C_{α\text{-}res.}$), 132.5 (2$CH_{p\text{-}sal.}$), 134.5 ($C_{naph.}$), 147.5, 148.1 (2C-$O_{naph.}$), 157.0 (2C-$O_{α\text{-}res.}$), 161.0 (C-$O_{p\text{-}sal.}$), 164.6, 165.0 (2C=O); ESI-MS 781.0 $(M+Na)^+$.

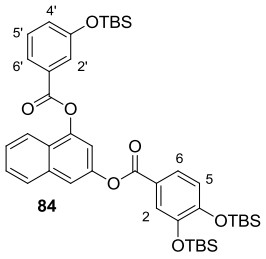

84

4-[(3-{[*tert*-Butyl(dimethyl)silyl]oxy}benzoyl)oxy]-2-naphthyl 3,4-bis{[*tert*-butyl (dimethyl)silyl]oxy} benzoate (84). Obtained from monoester **61** (150 mg, 0.38 mmol) and acid chloride **52b** (305 mg, 0.76 mmol) as an oil in 43% yield. R_f (hexane/DCM, 1:1) 0.40; IR (ATR) ν 1739 (C=O), 1594, 1511 (Ar); ^{1}H NMR (300 MHz, $CDCl_3$) δ 0.26 (s, 6H, (CH_3)$_2$Si), 0.27 (s, 6H, (CH_3)$_2$Si), 0.28 (s, 6H, (CH_3)$_2$Si), 1.02 (s, 27H, 3(CH_3)$_3$CSi), 6.94 (d, *J* = 8.4, 1H, H_5), 7.17 (dd, *J* = 8.1, 2.6, 1H, $H_{4'}$), 7.37 (d, *J* = 2.1, 1H, $CH_{naph.}$), 7.43 (t, *J* = 7.9, 1H, $H_{5'}$), 7.46-7.58 (m, 2H, 2$CH_{naph.}$), 7.66 (d, *J* = 2.0, 1H, $CH_{naph.}$), 7.71 (d, *J* = 2.1, 1H, H_2), 7.74-7.79 (m, 2H, $H_{2'}$, H_6), 7.88 (d, *J* = 7.7, 1H, $CH_{naph.}$), 7.92-7.97 (m, 2H, $CH_{naph.}$, $H_{6'}$); ^{13}C NMR (75 MHz, $CDCl_3$) δ −4.3, −4.0, −3.9 (3(CH_3)$_2$Si), 18.4, 18.6, 18.7 (3(CH_3)$_3$CSi), 25.8, 26.0, 26.1 (3(CH_3)$_3$CSi), 114.6, 117.1 (2$CH_{naph.}$), 120.8 ($CH_{prot.}$), 121.6 ($CH_{naph.}$), 121.8 ($CH_{m\text{-}sal.}$), 122.5 ($C_{prot.}$), 122.9, 123.5 ($CH_{m\text{-}sal.}$, $CH_{prot.}$), 124.6 ($CH_{prot.}$), 125.3 ($C_{naph.}$), 126.0 ($CH_{m\text{-}sal.}$), 126.3, 127.4, 128.1 (3$CH_{naph.}$), 130.0 ($CH_{m\text{-}sal.}$), 130.5 ($C_{m\text{-}sal.}$), 134.5 ($C_{naph.}$), 147.1 (C-$O_{prot.}$), 147.5, 148.2 (2C-$O_{naph.}$), 152.6 (C-$O_{prot.}$), 156.2 (C-$O_{m\text{-}sal.}$), 164.8, 164.9 (2C=O); ESI-MS 781.0 $(M+Na)^+$.

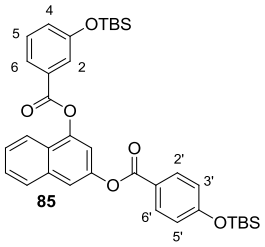

85

3-[(4-{[*tert*-Butyl(dimethyl)silyl]oxy}benzoyl)oxy]-1-naphthyl 3-{[*tert*-butyl(dimethyl)silyl]oxy}benzoate (85). Obtained from monoester **61** (150 mg, 0.38 mmol) and acid chloride **52e** (210 mg, 0.76 mmol) as an oil in 84% yield. R_f (hexane/DCM, 1:1) 0.38; IR (ATR) ν 1740 (C=O), 1599, 1507 (Ar); ^{1}H NMR (300 MHz, $CDCl_3$) δ 0.26 (s, 6H, $(CH_3)_2$Si *meta*), 0.27 (s, 6H, $(CH_3)_2$Si *para*), 1.02 (s, 9H, $(CH_3)_3$CSi), 1.03 (s, 9H, $(CH_3)_3$CSi), 6.95 (d, *J* = 8.8, 2H, $H_{3'}$, $H_{5'}$), 7.17 (ddd, *J* = 8.1, 2.5, 1.0, 1H, H_4), 7.38 (d, *J* = 2.2, 1H, $CH_{naph.}$), 7.43 (t, *J* = 7.9, 1H, H_5), 7.47-7.58 (m, 2H, $2CH_{naph.}$), 7.66 (d, *J* = 2.0, 1H, $CH_{naph.}$), 7.77 (app t, *J* = 2.0, 1H, H_2), 7.88 (d, *J* = 7.8, 1H, $CH_{naph.}$), 7.92-7.98 (m, 2H, $CH_{naph.}$, H_6), 8.15 (d, *J* = 8.8, 2H, $H_{2'}$, $H_{6'}$); ^{13}C NMR (75 MHz, $CDCl_3$) δ −4.3 ($(CH_3)_2$Si), −4.2 ($(CH_3)_2$Si), 18.3 ($(CH_3)_3\underline{C}$Si), 18.4 ($(CH_3)_3\underline{C}$Si), 25.7 ($(\underline{C}H_3)_3$CSi), 25.8 ($(\underline{C}H_3)_3$CSi), 114.6, 117.0 ($2CH_{naph.}$), 120.3 ($2CH_{p\text{-}sal.}$), 121.6, 121.8 ($CH_{naph.}$, $CH_{m\text{-}sal.}$), 122.3 ($C_{p\text{-}sal.}$), 123.5 ($CH_{m\text{-}sal.}$), 125.3 ($C_{naph.}$), 126.0 ($CH_{m\text{-}sal.}$), 126.3, 127.4, 128.1 ($3CH_{naph.}$), 130.0 ($CH_{m\text{-}sal.}$), 130.6 ($C_{m\text{-}sal.}$), 132.5 ($2CH_{p\text{-}sal.}$), 134.5 ($C_{naph.}$), 147.5, 148.1 ($2C\text{-}O_{naph.}$), 156.2 ($C\text{-}O_{m\text{-}sal.}$), 161.0 ($C\text{-}O_{p\text{-}sal.}$), 164.7, 164.9 (2C=O); ESI-MS 651.0 $(M+Na)^+$.

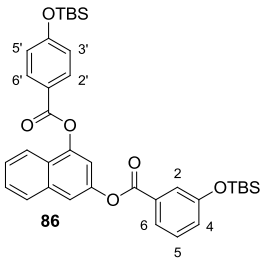

86

4-[(4-{[*tert*-Butyl(dimethyl)silyl]oxy}benzoyl)oxy]-2-naphthyl 3-{[*tert*-butyl(dimethyl)silyl]oxy}benzoate (86). Obtained from monoester **64** (150 mg, 0.38 mmol) and acid chloride **52e** (210 mg, 0.76 mmol) as an oil in 85% yield. R_f (hexane/DCM, 1:1) 0.38; IR (ATR) ν 1741 (C=O), 1599, 1509 (Ar); ^{1}H NMR (300 MHz, $CDCl_3$) δ 0.25 (s, 6H, $(CH_3)_2$Si), 0.29 (s, 6H, $(CH_3)_2$Si), 1.01 (s, 9H, $(CH_3)_3$CSi), 1.02 (s, 9H, $(CH_3)_3$CSi), 6.99 (d, *J* = 8.7, 2H, $H_{3'}$, $H_{5'}$), 7.13 (ddd, *J* = 8.1, 2.5, 0.9, 1H, H_4), 7.36-7.41 (m, 2H, $CH_{naph.}$, H_5), 7.46-7.57 (m, 2H, $2CH_{naph.}$), 7.67-7.69 (m, 2H, $CH_{naph.}$, H_2), 7.83-7.89 (m, 2H, $CH_{naph.}$, H_6), 7.97 (d, *J* = 8.1, 1H, $CH_{naph.}$), 8.23 (d, *J* = 8.7, 2H, $H_{2'}$, $H_{6'}$); ^{13}C NMR (75 MHz, $CDCl_3$) δ −4.3 ($(CH_3)_2$Si), −4.2 ($(CH_3)_2$Si), 18.3 ($(CH_3)_3\underline{C}$Si), 18.4 ($(CH_3)_3\underline{C}$Si), 25.7 ($(\underline{C}H_3)_3$CSi), 25.8 ($(\underline{C}H_3)_3$CSi), 114.5, 116.9 ($2CH_{naph.}$), 120.1 ($CH_{m\text{-}sal.}$), 120.4 ($2CH_{p\text{-}sal.}$), 121.7

($CH_{naph.}$), 122.1 ($C_{p\text{-}sal.}$), 123.4 ($CH_{m\text{-}sal.}$), 125.5 ($C_{naph.}$), 125.8 ($CH_{m\text{-}sal.}$), 126.3, 127.4, 128.1 ($3CH_{naph.}$), 129.8 ($CH_{m\text{-}sal.}$), 130.8 ($C_{m\text{-}sal.}$), 132.6 ($2CH_{p\text{-}sal.}$), 134.5 ($C_{naph.}$), 147.7, 148.0 (2C-$O_{naph.}$), 156.1 (C-$O_{m\text{-}sal.}$), 161.2 (C-$O_{p\text{-}sal.}$), 164.7, 165.0 (2C=O); ESI-MS 651.0 $(M+Na)^+$.

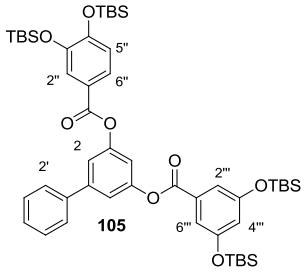

5-[(3,5-Bis{[*tert*-butyl(dimethyl)silyl]oxy}benzoyl)oxy]biphenyl-3-yl 3,4-bis{[*tert*-butyl (dimethyl)silyl]oxy}benzoate (105). Obtained from monoester **101** (168 mg, 0.31 mmol) and acid chloride **52c** (245 mg, 0.61 mmol) as an oil in 34% yield. R_f (hexane/DCM, 6:4) 0.74; IR (ATR) ν 1743 (C=O), 1591, 1447 (Ar), 1198, 1169 (C-O); ^{1}H NMR (300 MHz, $CDCl_3$) δ 0.23 (s, 12H, $2(CH_3)_2$Si *meta*), 0.24 (s, 6H, $(CH_3)_2$Si *meta/para*), 0.26 (s, 6H, $(CH_3)_2$Si *meta/para*), 1.00 (s, 18H, $2(CH_3)_3$CSi *meta*), 1.01 (s, 18H, $2(CH_3)_3$CSi *meta, para*), 6.60 (t, *J* = 2.2, 1H, $H_{4'''}$), 6.92 (d, *J* = 8.4, 1H, $H_{5''}$), 7.13 (t, *J* = 2.1, 1H, H_4), 7.28 (d, *J* = 2.2, 2H, $H_{2'''}$, $H_{6'''}$), 7.36 (d, *J* = 2.1, 2H, H_2, H_6), 7.39-7.46 (m, 3H, $H_{3'}$, $H_{4'}$, $H_{5'}$), 7.61 (d, *J* = 7.1, 2H, $H_{2'}$, $H_{6'}$), 7.67 (d, *J* = 2.1, 1H, $H_{2''}$), 7.72 (dd, *J* = 8.4, 2.2, 1H, $H_{6''}$); ^{13}C NMR (75 MHz, $CDCl_3$) δ −4.2 ($2(CH_3)_2$Si), −4.0, −3.9 ($2(CH_3)_2$Si), 18.2 ($2(CH_3)_3\underline{C}$Si), 18.4, 18.5 ($2(CH_3)_3\underline{C}$Si), 25.8 ($2(\underline{C}H_3)_3$CSi), 26.0, 26.1 ($2(\underline{C}H_3)_3$CSi), 114.7 (C_4H), 115.5 ($2CH_{\alpha\text{-}res.}$), 117.8, 118.0, 118.3 (C_2H, C_6H, $CH_{\alpha\text{-}res.}$), 120.8 ($CH_{prot.}$), 122.4 ($C_{prot.}$), 122.9, 124.6 ($2CH_{prot}$), 127.4 ($C_{2'}$H, $C_{6'}$H), 128.1 ($C_{4'}$H), 129.0 ($C_{3'}$H, $C_{5'}$H), 131.0 ($C_{\alpha\text{-}res.}$), 139.6, 143.6 ($2C_{biph.}$), 147.1, 151.8, 152.0, 152.9 (2C-$O_{prot.}$, 2C-$O_{biph.}$), 156.9 (2C-$O_{\alpha\text{-}res.}$), 164.7 (2C=O); ESI-MS 934.4 $(M+Na)^+$.

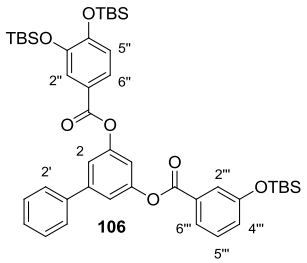

5-[(3-{[*tert*-Butyl(dimethyl)silyl]oxy}benzoyl)oxy]biphenyl-3-yl 3,4-bis{[*tert*-butyl (dimethyl)silyl]oxy}benzoate (106). Obtained from monoester **101** (256 mg, 0.47 mmol) and acid chloride **52d** (252 mg, 0.93 mmol) as an oil in 89% yield. R_f (hexane/DCM, 9:1) 0.14; IR (ATR) ν

1740 (C=O), 1510, 1465, 1440, 1418 (Ar); ^{1}H NMR (300 MHz, $CDCl_3$) δ 0.27, 0.28, 0.29 (s, 18H, 3$(CH_3)_2$Si), 1.03 (s, 18H, 2$(CH_3)_3$CSi *meta*), 1.04 (s, 9H, $(CH_3)_3$CSi *para*), 6.95 (d, *J* = 8.4, 1H, $H_{4'''}$), 7.14 (ddd, *J* = 8.2, 2.4, 0.8, 1H, $H_{5''}$), 7.18 (t, *J* = 2.0, 1H, H_4), 7.36-7.48 (m, 6H, H_2, H_6, $H_{3'}$, $H_{4'}$, $H_{5'}$, $H_{5'''}$), 7.64 (d, *J* = 7.1, 2H, $H_{2'}$, $H_{6'}$), 7.69 (t, *J* = 1.9, 1H, $H_{2'''}$), 7.72 (d, *J* = 1.9, 1H, $H_{2''}$), 7.77 (dd, *J* = 8.4, 2.1, 1H, $H_{6''}$), 7.85 (d, *J* = 7.8, 1H, $H_{6'''}$); ^{13}C NMR (75 MHz, $CDCl_3$) δ −4.3, −4.0, −3.9 (3$(CH_3)_2$Si), 18.4, 18.6, 18.7 (3$(CH_3)_3$CSi), 25.8, 26.0, 26.1 (3$(CH_3)_3$CSi), 114.7 (C_4H), 118.0, 118.2 (C_2H, C_6H), 120.8 ($CH_{prot.}$),121.7 ($CH_{m\text{-}sal.}$), 122.4 ($C_{prot.}$), 122.9 ($CH_{prot.}$), 123.4 ($CH_{m\text{-}sal.}$), 124.5 ($CH_{prot.}$), 125.8 ($CH_{m\text{-}sal.}$), 127.4 ($C_{2'}$H, $C_{6'}$H), 128.2 ($C_{4'}$H), 129.0 ($C_{3'}$H, $C_{5'}$H), 129.8 ($CH_{m\text{-}sal.}$), 130.8 ($C_{m\text{-}sal.}$), 139.7, 143.7 (2$C_{biph.}$), 147.1, 151.8, 152.0, 152.7 (2C-$O_{prot.}$, 2C-$O_{biph.}$), 156.1 (C-$O_{m\text{-}sal.}$), 164.6, 164.8 (2C=O); ESI-MS 807.4 $(M+Na)^+$.

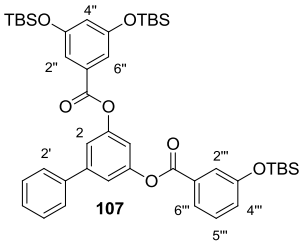

5-[(3-{[*tert*-Butyl(dimethyl)silyl]oxy}benzoyl)oxy]biphenyl-3-yl 3,5-bis{[*tert*-butyl (dimethyl)silyl]oxy}benzoate (107). Obtained from monoester **103** (101 mg, 0.24 mmol) and acid chloride **52c** (193 mg, 0.48 mmol) as an oil in 61% yield. R_f (hexane/DCM, 6:4) 0.28; ^{1}H NMR (300 MHz, $CDCl_3$) δ 0.24 (s, 12H, 2$(CH_3)_2$Si), 0.25 (s, 6H, $(CH_3)_2$Si), 1.00 (s, 18H, 2$(CH_3)_3$CSi), 1.01 (s, 9H, $(CH_3)_3$CSi), 6.61 (t, *J* = 2.3, 1H, $H_{4''}$), 7.12 (ddd, *J* = 8.2, 2.5, 1.0, 1H, $H_{4'''}$), 7.16 (t, *J* = 2.1, 1H, H_4), 7.30 (d, *J* = 2.3, 2H, $H_{2''}$, $H_{6''}$), 7.33-7.41 (m, 4H, H_2, H_6, $H_{4'}$, $H_{5'''}$), 7.45 (t, *J* = 7.2, 2H, $H_{3'}$, $H_{5'}$), 7.62 (d, *J* = 6.9, 2H, $H_{2'}$, $H_{6'}$), 7.66 (t, *J* = 2.0, 1H, $H_{2'''}$), 7.82 (dt, *J* = 7.8, 1.3, 1H, $H_{6'''}$); ^{13}C NMR (75 MHz, $CDCl_3$) δ −4.3 (3$(CH_3)_2$Si), 18.4 (3$(CH_3)_3$CSi), 25.8 (3$(CH_3)_3$CSi), 114.6 (C_4H), 115.3 (2$CH_{\alpha\text{-}res.}$), 117.8, 118.1, 118.2 (C_2H, C_6H, $CH_{\alpha\text{-}res.}$), 121.7 ($CH_{m\text{-}sal.}$), 123.4, 125.9 (2$CH_{m\text{-}sal.}$), 127.4 ($C_{2'}$H, $C_{6'}$H), 128.2 ($C_{4'}$H), 129.0 ($CH_{\alpha\text{-}res.}$, $CH_{m\text{-}sal.}$), 129.8 ($CH_{m\text{-}sal.}$), 130.7, 131.0 ($C_{\alpha\text{-}res.}$, $C_{m\text{-}sal.}$), 139.6, 143.7 (2$C_{biph.}$), 151.8 (2C-$O_{biph.}$), 156.1 (C-$O_{m\text{-}sal.}$), 156.9 (2C-$O_{\alpha\text{-}res.}$), 164.7, 164.8 (2C=O); ESI-MS 807.4 $(M+Na)^+$.

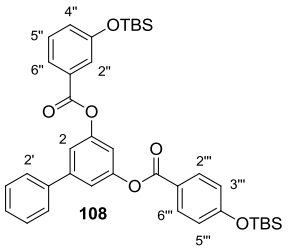

5-[(4-{[*tert*-Butyl(dimethyl)silyl]oxy}benzoyl)oxy]biphenyl-3-yl 3-{[*tert*-butyl(dimethyl) silyl]oxy}benzoate (108). Obtained from monoester **104** (110 mg, 0.26 mmol) and acid chloride **52d** (142 mg, 0.52 mmol) as an oil in 61% yield. R_f (hexane/DCM, 1:1) 0.45; IR (ATR) ν 1739 (C=O), 1600, 1508 (Ar), 1281, 1256 (C-O); ^{1}H NMR (300 MHz, $CDCl_3$) δ 0.25 (s, 6H, $(CH_3)_2Si$), 0.27 (s, 6H, $(CH_3)_2Si$), 1.01 (s, 9H, $(CH_3)_3CSi$), 1.02 (s, 9H, $(CH_3)_3CSi$), 6.95 (d, *J* = 8.8, 2H, $H_{3'''}$, $H_{5'''}$), 7.13 (ddd, *J* = 8.1, 2.5, 0.9, 1H, $H_{4''}$), 7.16 (t, *J* = 2.1, 1H, H_4), 7.34-7.42 (m, 4H, H_2, H_6, $H_{4'}$, $H_{5''}$), 7.45 (t, *J* = 7.2, 2H, $H_{3'}$, $H_{5'}$), 7.62 (d, *J* = 7.1, 2H, $H_{2'}$, $H_{6'}$), 7.67 (t, *J* = 2.0, 1H, $H_{2''}$), 7.83 (dt, *J* = 7.8, 1.3, 1H, $H_{6''}$), 8.13 (d, *J* = 8.7, 2H, $H_{2'''}$, $H_{6'''}$); ^{13}C NMR (75 MHz, $CDCl_3$) δ −4.3, −4.2 ($2(CH_3)_2Si$), 18.3, 18.4 ($2(CH_3)_3\underline{C}Si$), 25.7, 25.8 ($2(\underline{C}H_3)_3CSi$), 114.7 (C_4H), 118.0, 118.2 (C_2H, C_6H), 120.3 ($2CH_{p\text{-sal.}}$),121.7 ($CH_{m\text{-sal.}}$), 122.3 ($C_{p\text{-sal.}}$), 123.4, 125.8 ($2CH_{m\text{-sal.}}$), 127.4 ($C_{3'}H$, $C_{5'}H$), 128.2 ($C_{4'}H$), 129.0 ($C_{2'}H$, $C_{6'}H$), 129.8 ($CH_{m\text{-sal.}}$), 130.7 ($C_{m\text{-sal.}}$), 132.5 ($2CH_{p\text{-sal.}}$), 139.6, 143.7 ($2C_{biph.}$), 151.8, 151.9 ($2C\text{-}O_{biph.}$), 156.1 ($C\text{-}O_{p\text{-sal.}}$), 161.0 ($C\text{-}O_{m\text{-sal.}}$), 164.7, 164.8 (2C=O); ESI-MS 677.3 $(M+Na)^+$.

General Procedure for the Synthesis of Final Compounds 1, 2, 4-32 and 37-46. To a solution of the corresponding TBS derivative **53-59**, **62**, **65-86** or **98-108** in a mixture of pyridine (0.96 mL/mmol of TBS group) and anhydrous THF (2 mL/mmol of TBS group) under an argon atmosphere, HF·pyridine complex (0.96 mL/mmol of TBS group) was added and the reaction mixture was stirred at room temperature. After the disappearance of the starting material (TLC analysis, approx. 15 min), the reaction was diluted with water (50 mL) and the mixture was extracted with ethyl acetate. The organic layer was washed with a saturated aqueous solution of $CuSO_4$, water and dried (Na_2SO_4). The solvent was evaporated under reduced pressure and the resulting solid was recrystallized from DCM/MeOH or purified by chromatography (from DCM to DCM/MeOH, 95:5; R_f is specified) to afford the corresponding pure final compound.

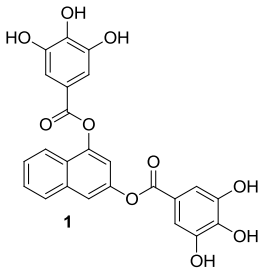

1

Naphthalene-1,3-diyl bis(3,4,5-trihydroxybenzoate) (**1**). Obtained from silyl ether **53** (300 mg, 0.39 mmol) in 65% yield. mp 163-164 ºC (Lit.[95] 163-164 ºC); IR (ATR) ν 3385 (OH), 1709 (C=O), 1608 (Ar); ^{1}H NMR (300 MHz, CD_3OD) δ 7.18-7.27 (m, 3H, $2CH_{gal.}$, $CH_{naph.}$), 7.34 (s, 2H, $2CH_{gal.}$), 7.45-7.65 (m, 3H, $3CH_{naph.}$), 7.88-7.96 (m, 2H, $2CH_{naph.}$); ^{13}C NMR (75 MHz, CD_3OD) δ 109.7, 109.8 ($4CH_{gal.}$), 114.7, 116.8 ($2CH_{naph.}$), 119.1, 119.4 ($2C_{gal.}$), 121.4 ($CH_{naph.}$), 125.6 ($C_{naph.}$),

126.3, 127.4, 128.0 (3$CH_{naph.}$), 134.8 ($C_{naph.}$), 139.7, 139.9 (2C-$O_{gal.}$), 145.8, 145.9 (4C-$O_{gal.}$), 148.1, 148.6 (2C-$O_{naph.}$), 165.7, 165.9 (2C=O); ESI-MS 462.7 $(M–H)^-$. The spectroscopic data are in agreement with those previously described.[95]

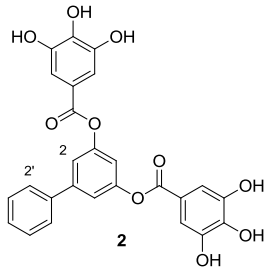

2

Biphenyl-3,5-diyl bis(3,4,5-trihydroxybenzoate) (2). Obtained from silyl ether **98** (626 mg, 0.53 mmol) in 28% yield. mp 205-207 ºC; R_f (hexane/ethyl acetate/acetic acid, 7:3:0.01) 0.40; IR (ATR) ν 3356 (OH), 1692 (C=O), 1612, 1536, 1454 (Ar), 1195 (C-O); ^{1}H NMR (300 MHz, acetone-d_6) δ 7.21 (s, 1H, H_4), 7.31 (s, 4H, 4$CH_{gal.}$), 7.40 (t, J = 7.3, 1H, $H_{4'}$), 7.47-7.52 (m, 4H, H_2, H_6, $H_{3'}$, $H_{5'}$), 7.74-7.78 (m, 2H, $H_{2'}$, $H_{6'}$), 8.32 (br s, 1H, OH), 8.46 (br s, 4H, 4OH), 8.54 (br s, 1H, OH); ^{13}C NMR (75 MHz, acetone-d_6) δ 110.5 (4$CH_{gal.}$), 115.9 (C_4H), 118.5 (C_2H, C_6H), 120.6 (2$C_{gal.}$), 127.8 ($C_{2'}$H, $C_{6'}$H), 129.0 ($C_{4'}$H), 129.9 ($C_{3'}$H, $C_{5'}$H), 139.7 (2C-$O_{biph.}$), 140.1, 143.8 (2$C_{biph.}$), 146.3 (4C-$O_{gal.}$), 153.2 (2C-$O_{gal.}$), 165.2 (2C=O); ESI-MS 488.7 $(M–H)^-$; elemental analysis (calcd., found for $C_{26}H_{18}O_{10}·3H_2O$): C (57.36, 57.76), H (4.44, 4.20).

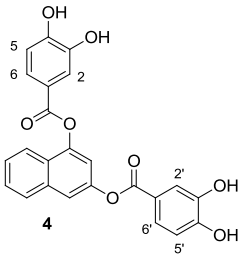

4

Naphthalene-1,3-diyl bis(3,4-dihydroxybenzoate) (4). Obtained from silyl ether **54** (168 mg, 0.39 mmol) in 26% yield. mp 79-81 ºC; IR (ATR) ν 3423 (OH), 1712 (C=O), 1603 (Ar); ^{1}H NMR (300 MHz, CD_3OD) δ 6.90 (d, J = 8.2, 1H, H_5), 6.94 (d, J = 8.3, 1H, $H_{5'}$), 7.29 d (d, J = 2.1, 1H, $CH_{naph.}$), 7.50-7.75 (m, 7H, 3$CH_{naph.}$, H_2, H_6, $H_{2'}$, $H_{6'}$), 7.89-7.97 (m, 2H, 2$CH_{naph.}$); ^{13}C NMR (75 MHz, CD_3OD) δ 115.8 ($CH_{naph.}$), 116.2, 116.4 (2$CH_{prot.}$), 117.9 ($CH_{naph.}$), 118.0 (2$CH_{prot.}$), 121.3, 121.6 (2$C_{prot.}$), 122.4 ($CH_{naph.}$), 124.6, 124.7 (2$CH_{prot.}$), 126.6 ($C_{naph.}$), 127.4, 128.4, 129.0 (3$CH_{naph.}$), 135.8 ($C_{naph.}$), 146.5, 146.7 (2C-$O_{prot.}$), 149.1, 149.6 (2C-$O_{naph.}$), 152.7, 152.9 (2C-$O_{prot.}$), 166.6, 166.7

(2C=O); ESI-MS 454.9 $(M+Na)^+$; elemental analysis (calcd., found for $C_{24}H_{16}O_8 \cdot 2H_2O$): C (61.54, 61.19), H (4.30, 4.03).

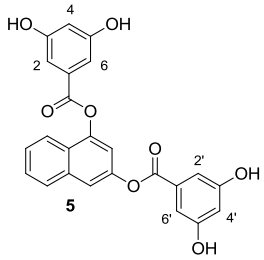

5

Naphthalene-1,3-diyl bis(3,5-dihydroxybenzoate) (5). Obtained from silyl ether **55** (140 mg, 0.32 mmol) in 52% yield. mp 167-169 ºC; IR (ATR) ν 3386 (OH), 1710 (C=O), 1603 (Ar); ^{1}H NMR (300 MHz, CD_3OD) δ 6.58 (t, *J* = 2.3, 1H, H_4), 6.62 (t, *J* = 2.3, 1H, $H_{4'}$), 7.15 (d, *J* = 2.3, 2H, H_2, H_6), 7.23 (d, *J* = 2.4, 2H, $H_{2'}$, $H_{6'}$), 7.34 (d, *J* = 2.2, 1H, $CH_{naph.}$), 7.54-7.60 (m, 2H, $2CH_{naph.}$), 7.71 (d, *J* = 2.0, 1H, $CH_{naph.}$), 7.90-7.99 (m, 2H, $2CH_{naph.}$); ^{13}C NMR (75 MHz, CD_3OD) δ 109.0 ($2CH_{α\text{-}res.}$), 109.3 ($4CH_{α\text{-}res.}$), 115.4, 117.9, 122.2 ($3CH_{naph.}$), 126.4 ($C_{naph.}$), 127.4, 128.4, 128.9 ($3CH_{naph.}$), 131.7, 132.1 ($2C_{α\text{-}res.}$), 135.7 ($C_{naph.}$), 148.8, 149.3 (2C-$O_{naph.}$), 160.0 (2C-$O_{α\text{-}res.}$), 160.1 (2C-$O_{α\text{-}res.}$), 166.3, 166.5 (2C=O); ESI-MS 454.8 $(M+Na)^+$; elemental analysis (calcd., found for $C_{24}H_{16}O_8 \cdot 3/2H_2O$): C (62.75, 62.25), H (4.17, 4.02).

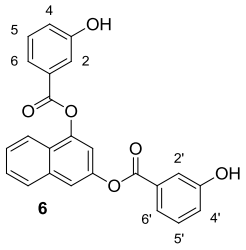

6

Naphthalene-1,3-diyl bis(3-hydroxybenzoate) (6). Obtained from silyl ether **56** (187 mg, 0.30 mmol) in 75% yield. R_f (DCM/MeOH, 95:5) 0.33; mp 91-93 ºC; IR (ATR) ν 3410 (OH), 1720 (C=O), 1595, 1492 (Ar); ^{1}H NMR (300 MHz, acetone-d_6) δ 7.21 (ddd, *J* = 8.6, 2.5, 1.0, 1H, H_4), 7.25 (ddd, *J* = 8.6, 2.5, 1.0, 1H, $H_{4'}$), 7.45 (t, *J* = 8.0, 1H, H_5), 7.49 (t, *J* = 8.0, 1H, $CH_{5'}$), 7.54 (d, *J* = 2.3, 1H, $CH_{naph.}$), 7.56-7.67 (m, 2H, $2CH_{naph.}$), 7.70 (app t, *J* = 2.0, 1H, H_2), 7.74 (dt, *J* = 7.7, 1.2 1H, H_6), 7.78 (app t, *J* = 2.0, 1H, $H_{2'}$), 7.81-7.84 (m, 2H, $H_{6'}$, $CH_{naph.}$), 7.99-8.06 (m, 2H, $2CH_{naph.}$), 8.95 (br s, 2H, 2OH); ^{13}C NMR (75 MHz, acetone-d_6) δ 115.8 ($CH_{naph.}$), 117.3, 117.4 ($2CH_{m\text{-}sal.}$), 117.9 ($CH_{naph.}$), 121.9 ($CH_{m\text{-}sal.}$), 122.1 ($2CH_{m\text{-}sal.}$), 122.1 ($CH_{m\text{-}sal.}$), 122.3 ($CH_{naph.}$), 126.2 ($C_{naph.}$), 127.4, 128.4, 128.8 ($3CH_{naph.}$), 130.9, 131.1 ($2CH_{m\text{-}sal.}$), 131.3, 131.6 ($2C_{m\text{-}sal.}$), 135.3 ($C_{naph.}$), 148.6, 149.2

(2C-$O_{naph.}$), 158.6, 158.7 (2C-$O_{m\text{-}sal.}$), 165.3, 165.5 (2C=O); ESI-MS 399.0 $(M-H)^-$; elemental analysis (calcd., found for $C_{24}H_{16}O_6 \cdot 1/2H_2O$): C (70.41, 70.54), H (4.19, 4.23).

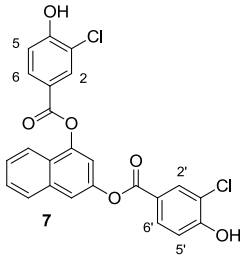

7

Naphthalene-1,3-diyl bis(3-chloro-4-hydroxybenzoate) (7). Obtained from silyl ether **58** (153 mg, 0.13 mmol) in 88% yield. R_f (DCM) 0.14; mp 217-219 ºC; IR (ATR) ν 3371 (OH), 1728 (C=O), 1595, 1505 (Ar); ^{1}H NMR (300 MHz, acetone-d_6) δ 7.22 (d, J = 8.5, 1H, H_5), 7.26 (d, J = 8.6, 1H $H_{5'}$), 7.50 (d, J = 2.1, 1H, $CH_{naph.}$), 7.55-7.66 (m, 2H, 2$CH_{naph.}$), 7.81 (d, J = 2.0, 1H, $CH_{naph.}$), 7.98-8.07 (m, 3H, 2$CH_{naph.}$, H_6), 8.14 (dd, J = 8.6, 2.1, 1H, $H_{6'}$), 8.20 (d, J = 2.1, 1H, H_2), 8.28 (d, J = 2.1, 1H, $H_{2'}$), 8.59 (s, 2H, 2OH); ^{13}C NMR (75 MHz, acetone-d_6) δ 115.7, 117.6, 117.7, 117.8 (2$CH_{naph.}$, 2$CH_{Clbenz.}$), 121.5, 121.7 (2$C_{Clbenz.}$), 122.3 ($CH_{naph.}$), 122.4, 122.7 (2$C_{Clbenz.}$), 126.2 ($C_{naph.}$), 127.3, 128.3, 128.8 (3$CH_{naph.}$), 131.5, 131.6, 133.0, 133.1 (4$CH_{Clbenz.}$), 135.3 ($C_{naph.}$), 148.5, 149.1 (2C-$O_{naph.}$), 158.9, 159.0 (2C-$O_{Clbenz.}$), 164.2, 164.3 (2C=O); ESI-MS 467.0 $(M-H)^-$; elemental analysis (calcd., found for $C_{24}H_{14}Cl_2O_6 \cdot 1/2H_2O$): C (60.67, 60.27), H (3.61, 3.16).

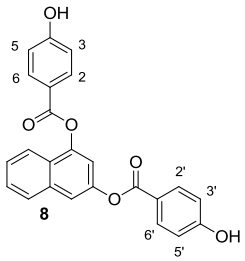

8

Naphthalene-1,3-diyl bis(4-hydroxybenzoate) (8). Obtained from silyl ether **57** (120 mg, 0.19 mmol) in 86% yield. R_f (DCM/MeOH, 95:5) 0.38; mp 269-270 ºC (decomposed); IR (ATR) ν 3369 (OH), 1708 (C=O), 1600, 1513 (Ar); ^{1}H NMR (300 MHz, acetone-d_6) δ 7.03 (d, J = 8.8, 2H, H_3, H_5), 7.08 (d, J = 8.8, 2H, $H_{3'}$, $H_{5'}$), 7.46 (d, J = 2.2, 1H, $CH_{naph.}$), 7.53-7.65 (m, 2H, 2$CH_{naph.}$), 7.78 (d, J = 2.0, 1H, $CH_{naph.}$), 7.98 (d, J = 8.2, 1H, $CH_{naph.}$), 8.02 (d, J = 7.4, 1H, $CH_{naph.}$), 8.12 (d, J = 8.8, 2H, H_2, H_6), 8.21 (d, J = 8.8, 2H, $H_{2'}$, $H_{6'}$), 9.45 (br s, 2H, 2OH); ^{13}C NMR (75 MHz, acetone-d_6) δ 115.9 ($CH_{naph.}$), 116.4 (2$CH_{p\text{-}sal.}$), 116.5 (2$CH_{p\text{-}sal.}$), 117.6 ($CH_{naph.}$), 121.1, 121.4 (2$C_{p\text{-}sal.}$), 122.3 ($CH_{naph.}$), 126.2 ($C_{naph.}$), 127.1, 128.2, 128.7 (3$CH_{naph.}$), 133.3 (2$CH_{p\text{-}sal.}$), 133.4 (2$CH_{p\text{-}sal.}$), 135.3

($C_{naph.}$), 148.7, 149.3 (2C-$O_{naph.}$), 163.4, 163.6 (2C-$O_{p\text{-}sal.}$), 165.1, 165.2 (2C=O); ESI-MS 398.5 $(M-H)^-$; elemental analysis (calcd., found for $C_{24}H_{16}O_6 \cdot 1/4H_2O$): C (71.19, 71.24), H (4.11, 4.24).

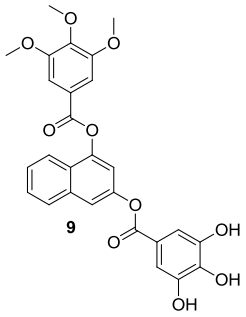

4-[(3,4,5-Trimethoxybenzoyl)oxy]-2-naphthyl 3,4,5-trihydroxybenzoate (9). Obtained from silyl ether **65** (240 mg, 0.28 mmol) in 32% yield. R_f (DCM/ethyl acetate, 1:1) 0.65; mp 104-105 ºC; IR (ATR) ν 3400 (OH), 1730 (C=O), 1596, 1505, 1460 (Ar); ^{1}H NMR (300 MHz, acetone-d_6) δ 3.88 (s, 3H, CH_3 *para)*, 3.96 (s, 6H, $2CH_3$ *meta*), 7.34 (s, 2H, $2CH_{gal.}$), 7.45 (d, *J* = 2.2, 1H, $CH_{naph.}$), 7.52-7.67 (m, 4H, $2CH_{naph.}$, $2CH_{eud.}$), 7.77 (d, *J* = 2.0, 1H, $CH_{naph.}$), 7.97 (d, *J* = 8.2, 1H, $CH_{naph.}$), 8.02 (d, *J* = 7.7, 1H, $CH_{naph.}$); ^{13}C NMR (75 MHz, acetone-d_6) δ 56.8 ($2CH_3$ *meta*), 60.8 (CH_3 *para*), 108.6 ($2CH_{eud.}$), 110.6 ($2CH_{gal.}$), 115.9, 117.8 ($2CH_{naph.}$), 120.7 ($C_{gal.}$), 122.4 ($CH_{naph.}$), 124.8 ($C_{naph.}$), 126.1 ($C_{eud.}$), 127.2, 128.2, 128.8 ($3CH_{naph.}$), 135.3 ($C_{naph.}$), 139.7 (C-$O_{eud.}$ *para*), 144.3 (C-$O_{gal.}$ *para*), 146.3 (2C-$O_{eud.}$ *meta*), 148.6, 149.4 (2C-$O_{naph.}$), 154.5 (2C-$O_{gal.}$ *meta*) , 165.1, 165.4 (2C=O); ESI-MS 505.0 $(M-H)^-$; elemental analysis (calcd., found for $C_{27}H_{22}O_{10} \cdot 1/2H_2O$): C (62.91, 62.57), H (4.50, 4.84).

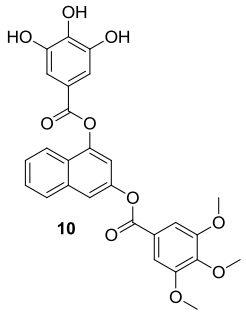

3-[(3,4,5-Trimethoxybenzoyl)oxy]-1-naphthyl 3,4,5-trihydroxybenzoate (10). Obtained from silyl ether **66** (101 mg, 0.12 mmol) in 58% yield. R_f (DCM/ethyl acetate, 1:1) 0.60; mp 172-173 ºC; IR (ATR) ν 3390 (OH), 1728 (C=O), 1599, 1460 (Ar); ^{1}H NMR (300 MHz, acetone-d_6) δ 3.85 (s, 3H, CH_3 *para)*, 3.95 (s, 6H, $2CH_3$ *meta*), 7.42 (s, 2H, $2CH_{gal.}$), 7.45 (d, *J* = 2.2, 1H, $CH_{naph.}$), 7.54 (s, 2H, $2CH_{eud.}$), 7.55-7.67 (m, 2H, $2CH_{naph.}$), 7.78 (d, *J* = 1.9, 1H, $CH_{naph.}$), 7.99 (dd, *J* = 8.2, 1.4, 1H,

$CH_{naph.}$), 8.03 (dd, *J* = 8.2, 1.1, 1H, $CH_{naph.}$), 8.37 (br s, 1H, OH *para*), 8.48 (br s, 2H, 2OH *meta*); ^{13}C NMR (75 MHz, acetone-d_6) δ 56.7 ($2CH_3$ *meta*), 60.8 (CH_3 *para*), 108.4 ($2CH_{gal.}$), 110.6 ($2CH_{eud.}$), 115.7, 117.6 ($2CH_{naph.}$), 120.3 ($C_{eud.}$), 122.3 ($CH_{naph.}$), 125.1 ($C_{naph.}$), 126.3 ($C_{gal.}$), 127.2, 128.3, 128.8 ($3CH_{naph.}$), 135.3 ($C_{naph.}$), 144.2 (2C-O *para*), 146.4 (2C-O *meta*), 148.8, 149.2 (2C-$O_{naph.}$), 154.4 (2C-O *meta*), 165.1, 165.2 (2C=O); ESI-MS 505.1 $(M-H)^-$; elemental analysis (calcd., found for $C_{27}H_{22}O_{10}\cdot 1/2H_2O$): C (62.91, 62.57), H (4.50, 4.70).

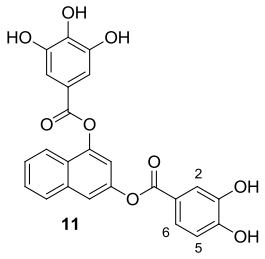

11

3-[(3,4-Dihydroxybenzoyl)oxy]-1-naphthyl 3,4,5-trihydroxybenzoate (11). Obtained from silyl ether **67** (143 mg, 0.32 mmol) in 83% yield. mp 148 ºC (decomposed); IR (ATR) ν 3324 (OH), 1703 (C=O), 1607 (Ar); ^1H NMR (300 MHz, acetone-d_6) δ 7.05 (d, *J* = 8.8, 1H, H_5), 7.33 (s, 2H, $2CH_{gal.}$), 7.43 (d, *J* = 2.2, 1H, $CH_{naph.}$), 7.51-7.67 (m, 2H, $2CH_{naph.}$), 7.75 (d, *J* = 2.0, 1H, $CH_{naph.}$), 7.66-7.81 (m, 2H, H_2, H_6), 7.92-8.06 (m, 2H, $2CH_{naph.}$), 8.32 (br s, 1H, OH), 8.45 (br s, 2H, 2OH), 8.61 (br s, 1H, OH), 8.95 (br s, 1H, OH); ^{13}C NMR (75 MHz, acetone-d_6) δ 110.6 ($2CH_{gal.}$), 115.9, 116.3, 117.6, 117.8 ($2CH_{naph.}$, $2CH_{prot.}$), 120.7 ($C_{gal.}$), 121.5 ($C_{prot.}$), 122.3 ($CH_{naph.}$), 124.5 ($CH_{prot.}$), 126.2 ($C_{naph.}$), 127.1, 128.2, 128.8 ($3CH_{naph.}$), 135.3 ($C_{naph.}$), 139.8 (C-$O_{gal.}$ *para*), 146.1(2C-$O_{gal.}$ *meta*), 146.3 (C-$O_{prot.}$), 148.8, 149.5 (2C-$O_{naph.}$), 152.0 (C-$O_{prot.}$), 165.2, 165.4 (2C=O); ESI-MS 447.0 $(M-H)^-$; elemental analysis (calcd., found for $C_{24}H_{16}O_9\cdot 3/2H_2O$): C (60.63, 60.30), H (4.03, 4.05).

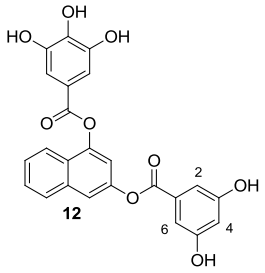

12

3-[(3,5-Dihydroxybenzoyl)oxy]-1-naphthyl 3,4,5-trihydroxybenzoate (12). Obtained from silyl ether **68** (160 mg, 0.36 mmol) in 91% yield. mp 175-177 ºC; IR (ATR) ν 3367 (OH), 1698 (C=O), 1605 (Ar); ^1H NMR (300 MHz, acetone-d_6) δ 6.73 (t, *J* = 2.3, 1H, H_4), 7.30 (d, *J* = 2.3, 1H,

$CH_{naph.}$), 7.33 (s, 2H, $2CH_{gal.}$), 7.47 (d, *J* = 2.3, 1H, $CH_{naph.}$), 7.56-7.65 (m, 2H, $2CH_{naph.}$), 7.77 (d, *J* = 2.0, 2H, H_2, H_6), 7.97 (d, *J* = 7.8, 1H, $CH_{naph.}$), 8.03 (d, *J* = 7.8, 1H, $CH_{naph.}$), 8.31 (br s, 1H, OH), 8.43 (br s, 2H, 2OH), 8.81 (br s, 2H, 2OH); ^{13}C NMR (75 MHz, acetone-d_6) δ 108.8 ($CH_{α\text{-}res.}$), 109.2 ($2CH_{α\text{-}res.}$), 110.6 ($2CH_{gal.}$), 115.7, 117.5 ($2CH_{naph.}$), 120.4 ($C_{gal.}$), 122.3 ($CH_{naph.}$), 126.3 ($C_{naph.}$), 127.2, 128.2, 128.8 ($3CH_{naph.}$), 132.2 ($C_{α\text{-}res.}$), 135.3 ($C_{naph.}$), 139.8 (C-$O_{gal.}$ *para*), 146.4 (2C-$O_{gal.}$ *meta*), 148.8, 149.2 (2C-$O_{naph.}$), 159.7 (2C-$O_{α\text{-}res.}$), 165.4 (2C=O); ESI-MS 447.1 $(M-H)^-$; elemental analysis (calcd., found for $C_{24}H_{16}O_9 \cdot 2H_2O$): C (59.51, 59.36), H (4.16, 3.98).

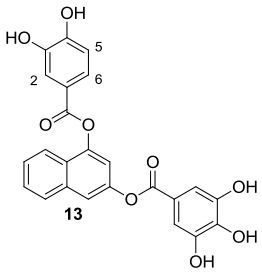

13

4-[(3,4-Dihydroxybenzoyl)oxy]-2-naphthyl 3,4,5-trihydroxybenzoate (13). Obtained from silyl ether **69** (240 mg, 0.54 mmol) in 78% yield. mp 140 ºC (decomposed); IR (ATR) ν 3401 (OH), 1709 (C=O), 1606 (Ar); ^{1}H NMR (300 MHz, acetone-d_6) δ 7.02 (d, *J* = 8.7, 1H, H_5), 7.42 (s, 2H, $2CH_{gal.}$), 7.43 (d, *J* = 2.2, 1H, $CH_{naph.}$), 7.57-7.63 (m, 2H, $2CH_{naph.}$), 7.68-7.71 (m, 2H, H_2, H_6), 7.76 (d, *J* = 2.0, 1H, $CH_{naph.}$), 7.97 (d, *J* = 7.9, 1H, $CH_{naph.}$), 8.02 (d, *J* = 7.3, 1H, $CH_{naph.}$), 8.33 (br s, 1H, OH), 8.47 (br s, 2H, OH), 8.52 (br s, 1H, OH), 8.87 (br s, 1H, OH); ^{13}C NMR (75 MHz, acetone-d_6) δ 110.7 ($2CH_{gal.}$), 115.9, 116.2, 117.7, 117.8 ($2CH_{naph.}$, $2CH_{prot.}$), 120.4 ($C_{gal.}$), 121.8 ($C_{prot.}$), 122.3 ($CH_{naph.}$), 124.3 ($CH_{prot.}$), 126.2 ($C_{naph.}$), 127.1, 128.2, 128.8 ($3CH_{naph.}$), 135.3 ($C_{naph.}$), 140.0 (C-$O_{gal.}$ *para*), 146.3 (2C-$O_{gal.}$ *meta*), 146.5 (C-$O_{prot.}$), 148.8, 149.4 (2C-$O_{naph.}$), 151.8 (C-$O_{prot.}$), 165.2, 165.3 (2C=O); ESI-MS 447.0 $(M-H)^-$; elemental analysis (calcd., found for $C_{24}H_{16}O_9 \cdot H_2O$): C (61.81, 61.42), H (3.89, 3.80).

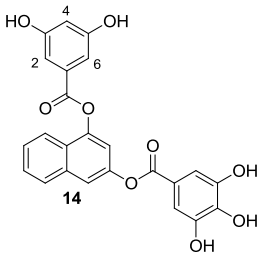

14

4-[(3,5-Dihydroxybenzoyl)oxy]-2-naphthyl 3,4,5-trihydroxybenzoate (14). Obtained from silyl ether **70** (121 mg, 0.27 mmol) in 84% yield. mp 176-178 ºC; IR (ATR) ν 3464 (OH), 1695 (C=O), 1605 (Ar); ^{1}H NMR (300 MHz, acetone-d_6) δ 6.73 (t, *J* = 2.3, 1H, H_4), 7.31 (d, *J* = 2.3, 2H,

H_2, H_6), 7.34 (s, 2H, $2CH_{gal.}$), 7.47 (d, *J* = 2.1, 1H, $CH_{naph.}$), 7.55-7.65 (m, 2H, $2CH_{naph.}$), 7.76 (d, *J* = 1.9, 1H, $CH_{naph.}$), 7.96- 8.04 (m, 2H, $2CH_{naph.}$), 8.26 (br s, 1H, OH), 8.39 (br s, 2H, OH), 8.78 (br s, 2H, OH); ^{13}C NMR (75 MHz, acetone-d_6) δ 109.1 ($CH_{α\text{-}res.}$), 109.4 ($2CH_{α\text{-}res.}$), 110.6 ($2CH_{gal.}$), 115.9, 117.8 ($2CH_{naph.}$), 120.7 ($C_{gal.}$), 122.2 ($CH_{naph.}$), 126.0 ($C_{naph.}$), 127.2, 128.3, 128.8 ($3CH_{naph.}$), 131.9 ($C_{α\text{-}res.}$), 135.4 ($C_{naph.}$), 139.8 (C-$O_{gal.}$ *para*), 146.3 (2C-$O_{gal.}$ *meta*), 148.5, 149.4 (2C-$O_{naph.}$), 159.9 (2C-$O_{α\text{-}res.}$), 165.3, 165.4 (2C=O); ESI-MS 447.0 $(M-H)^-$; elemental analysis (calcd., found for $C_{24}H_{16}O_9 \cdot 3/2\ H_2O$): C (60.63, 60.56), H (4.03, 3.93).

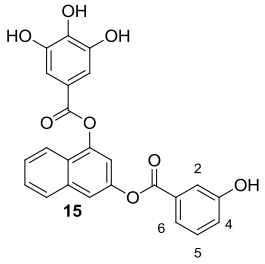

3-[(3-Hydroxybenzoyl)oxy]-1-naphthyl 3,4,5-trihydroxybenzoate (15). Obtained from silyl ether **71** (119 mg, 0.13 mmol) in 28% yield. R_f (DCM/MeOH, 95:5) 0.33; mp 117-119 ºC; IR (ATR) ν 3005 (OH), 1713 (C=O); ^{1}H NMR (300 MHz, acetone-d_6) δ 7.21 (ddd, *J* = 8.1, 2.6, 1.0, 1H, H_4), 7.42-7.48 (m, 4H, $2CH_{gal.}$, $CH_{naph.}$, H_5), 7.55-7.66 (m, 2H, $2CH_{naph.}$), 7.69 (dd, *J* = 2.2, 1.6, 1H, H_2), 7.73 (dt, *J* = 7.7, 1.3, 1H, H_6), 7.80 (d, *J* = 2.0, 1H, $CH_{naph.}$), 7.99 (d, *J* = 8.2, 1H, $CH_{naph.}$), 8.03 (d, *J* = 8.2, 1H, $CH_{naph.}$), 8.59 (br s, 4H, 4OH); ^{13}C NMR (75 MHz, acetone-d_6) δ 110.6 ($2CH_{gal.}$), 115.7 ($CH_{naph.}$), 117.3, 117.6 ($CH_{naph.}$, $CH_{m\text{-}sal.}$), 120.3 ($C_{gal.}$), 121.8, 122.1, 122.3 ($CH_{naph.}$, $2CH_{m\text{-}sal.}$), 126.3 ($C_{naph.}$), 127.2, 128.3, 128.8 ($3CH_{naph.}$), 130.9 ($CH_{m\text{-}sal.}$), 131.6 ($C_{m\text{-}sal.}$), 135.3 ($C_{naph.}$), 139.9 (C-$O_{gal.}$ *para*), 146.4 (2C-$O_{gal.}$ *meta*), 148.8, 149.2 (2C-$O_{naph.}$), 158.6 (C-$O_{m\text{-}sal.}$), 165.2, 165.4 (2C=O); ESI-MS 431.0 $(M-H)^-$; elemental analysis (calcd., found for $C_{24}H_{16}O_8 \cdot H_2O$): C (64.00, 64.02), H (4.03, 4.18).

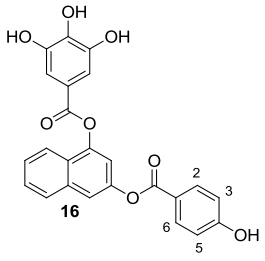

3-[(4-Hydroxybenzoyl)oxy]-1-naphthyl 3,4,5-trihydroxybenzoate (16). Obtained from silyl ether **72** (149 mg, 0.17 mmol) in 53% yield. R_f (DCM/MeOH, 95:5) 0.18; mp 134 ºC (decomposed); IR (ATR) ν 3330 (OH), 1712 (C=O), 1607, 1513 (Ar); ^{1}H NMR (300 MHz, acetone-d_6) δ 7.03 (d, *J* =

8.8, 2H, H_3, H_5), 7.42 (s, 2H, $2CH_{gal.}$), 7.45 (d, *J* = 2.2, 1H, $CH_{naph.}$), 7.54-7.65 (m, 2H, $2CH_{naph.}$), 7.77 (d, *J* = 2.1, 1H, $CH_{naph.}$), 7.97 (d, *J* = 7.8, 1H, $CH_{naph.}$), 8.01 (d, *J* = 7.8, 1H, $CH_{naph.}$), 8.12 (d, *J* = 8.8, 2H, H_2, H_6), 8.49 (br s, 4H, 4OH); ^{13}C NMR (75 MHz, acetone-d_6) δ 110.6 ($2CH_{p\text{-}sal.}$), 115.8 ($CH_{naph.}$), 116.4 ($2CH_{gal.}$), 117.6 ($CH_{naph.}$), 120.3 ($C_{gal.}$), 121.4 ($C_{p\text{-}sal.}$), 122.3 ($CH_{naph.}$), 126.2 ($C_{naph.}$), 127.1, 128.2, 128.7 ($3CH_{naph.}$), 133.3 ($2CH_{p\text{-}sal.}$), 135.3 ($C_{naph.}$), 139.9 (C-$O_{gal.}$ *para*), 146.4 (2C-$O_{gal.}$ *meta*), 148.7, 149.4 (2C-$O_{naph.}$), 150.6 (C-$O_{p\text{-}sal.}$), 163.4, 165.2 (2C=O); ESI-MS 431.0 $(M-H)^-$; elemental analysis (calcd., found for $C_{24}H_{16}O_8 \cdot 2/3H_2O$): C (64.87, 64.92), H (3.83, 4.06).

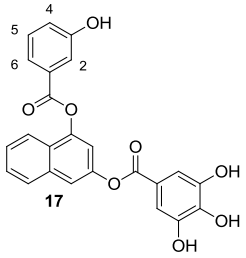

17

4-[(3-Hydroxybenzoyl)oxy]-2-naphthyl 3,4,5-trihydroxybenzoate (17). Obtained from silyl ether **73** (81 mg, 0.09 mmol) in 15% yield. R_f (DCM/MeOH, 95:5) 0.24; mp 128-130 ºC; IR (ATR) ν 3005 (OH), 1713 (C=O); ^{1}H NMR (300 MHz, acetone-d_6) δ 7.25 (ddd, *J* = 8.1, 2.6, 1.0, 1H, H_4), 7.33 (s, 2H, $2CH_{gal.}$), 7.48 (d, *J* = 2.1, 1H, $CH_{naph.}$), 7.49 (t, *J* = 8.0, 1H, H_5), 7.55-7.66 (m, 2H, $2CH_{naph.}$), 7.76-7.78 (m, 2H, $CH_{naph.}$, H_2), 7.82 (dt, *J* = 7.7, 1.3, 1H, H_6), 7.98 (dd, *J* = 8.1, 1.1, 1H, $CH_{naph.}$), 8.03 (dd, *J* = 8.1, 1.1, 1H, $CH_{naph.}$), 8.66 (br s, 4H, 4OH); ^{13}C NMR (75 MHz, acetone-d_6) δ 110.6 ($2CH_{gal.}$), 115.9 ($CH_{naph.}$), 117.4, 117.9 ($CH_{m\text{-}sal.}$, $CH_{naph.}$), 120.8 ($C_{gal.}$), 122.1, 122.2, 122.3 ($CH_{naph.}$, $2CH_{m\text{-}sal.}$), 126.0 ($C_{naph.}$), 127.2, 128.3, 128.8 ($3CH_{naph.}$), 131.1 ($CH_{m\text{-}sal.}$), 131.4 ($C_{m\text{-}sal.}$), 135.4 ($C_{naph.}$), 139.8 (C-$O_{gal.}$ *para*), 146.3 (2C-$O_{gal.}$ *meta*), 148.5, 149.4 (2C-$O_{naph.}$), 158.7 (C-$O_{m\text{-}sal.}$), 165.3, 165.4 (2C=O); ESI-MS 431.0 $(M-H)^-$; elemental analysis (calcd., found for $C_{24}H_{16}O_8 \cdot H_2O$): C (64.00, 64.24), H (4.03, 4.07).

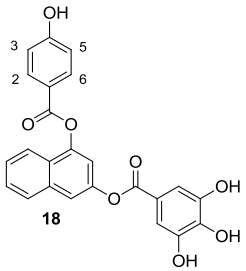

18

4-[(4-Hydroxybenzoyl)oxy]-2-naphthyl 3,4,5-trihydroxybenzoate (18). Obtained from silyl ether **74** (60 mg, 0.07 mmol) in 69% yield. R_f (DCM/MeOH, 95:5) 0.60; mp 146-148 ºC; IR (ATR) ν 3352 (OH), 1730 (C=O), 1607, 1514 (Ar); ^{1}H NMR (300 MHz, acetone-d_6) δ 7.07 (d, *J* = 8.6, 2H, H_3,

H_5), 7.33 (s, 2H, $2CH_{gal.}$), 7.44 (d, *J* = 2.2, 1H, $CH_{naph.}$), 7.53-7.65 (m, 2H, $2CH_{naph.}$), 7.75 (d, *J* = 2.0, 1H, $CH_{naph.}$), 7.98 (d, *J* = 8.7, 1H, $CH_{naph.}$), 8.02 (d, *J* = 7.7, 1H, $CH_{naph.}$), 8.21 (d, *J* = 8.8, 2H, H_2, H_6), 8.29 (br s, 1H, OH), 8.40 (br s, 2H, 2OH), 9.43 (br s, 1H, OH); ^{13}C NMR (75 MHz, acetone-d_6) δ 110.5 ($2CH_{p\text{-}sal.}$), 115.9 ($CH_{naph.}$), 116.6 ($2CH_{gal.}$), 117.6 ($CH_{naph.}$), 120.7 ($C_{gal.}$), 121.1 ($C_{p\text{-}sal.}$), 122.3 ($CH_{naph.}$), 126.2 ($C_{naph.}$), 127.1, 128.2, 128.7 ($3CH_{naph.}$), 133.4 ($2CH_{p\text{-}sal.}$), 135.3 ($C_{naph.}$), 139.7 (C-$O_{gal.}$ *para*), 146.3 (2C-$O_{gal.}$ *meta*), 148.7, 149.4 (2C-$O_{naph.}$), 160.3 (C-$O_{p\text{-}sal.}$), 163.6, 165.4 (2C=O); ESI-MS 431.0 $(M-H)^-$; elemental analysis (calcd., found for $C_{24}H_{16}O_8 \cdot H_2O$): C (64.00, 64.12), H (4.03, 4.13).

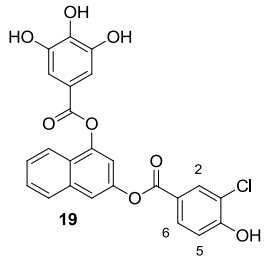

19

3-[(3-Chloro-4-hydroxybenzoyl)oxy]-1-naphthyl 3,4,5-trihydroxybenzoate (19). Obtained from silyl ether **75** (162 mg, 0.18 mmol) in 50% yield. R_f (DCM/MeOH, 95:5) 0.23; mp 138-139 ºC; IR (ATR) ν 3398 (OH), 1725 (C=O), 1603, 1504 (Ar); ^{1}H NMR (300 MHz, acetone-d_6) δ 7.22 (d, *J* = 8.5, 1H, H_5), 7.42 (s, 2H, $2CH_{gal.}$), 7.47 (d, *J* = 2.2, 1H, $CH_{naph.}$), 7.55-7.65 (m, 2H, $2CH_{naph.}$), 7.79 (d, *J* = 2.0, 1H, $CH_{naph.}$), 7.96-8.03 (m, 2H, $2CH_{naph.}$), 8.05 (dd, *J* = 8.6, 2.1, 1H, H_6), 8.20 (d, *J* = 2.1, 1H, H_2), 8.56 (br s, 4H, 4OH); ^{13}C NMR (75 MHz, acetone-d_6) δ 110.6 ($2CH_{gal.}$), 115.7 ($CH_{naph.}$), 117.5, 117.6 ($CH_{Clbenz.}$, $CH_{naph.}$), 120.3, 121.5 ($C_{gal.}$, $C_{Clbenz.}$), 122.3 ($CH_{naph.}$), 122.7 ($C_{Clbenz.}$), 126.3 ($C_{naph.}$), 127.2, 128.2, 128.8 ($3CH_{naph.}$), 131.4, 133.0 ($2CH_{Clbenz.}$), 135.2 ($C_{naph.}$), 139.9 (C-$O_{gal.}$ *para*), 146.4 (2C-$O_{gal.}$ *meta*), 148.8, 149.1 (2C-$O_{naph.}$), 158.9 (C-$O_{Clbenz.}$), 164.3, 165.2 (2C=O); ESI-MS 465.0 $(M-H)^-$; elemental analysis (calcd., found for $C_{24}H_{15}ClO_8 \cdot H_2O$): C (59.45, 59.80), H (3.53, 3.65).

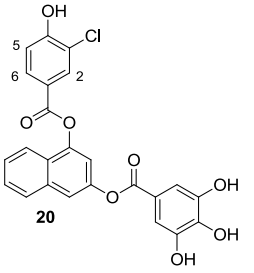

20

4-[(3-Chloro-4-hydroxybenzoyl)oxy]-2-naphthyl 3,4,5-trihydroxybenzoate (20). Obtained from silyl ether **76** (162 mg, 0.18 mmol) in 57% yield. R_f (DCM/MeOH, 95:5) 0.25; mp 143-145 ºC;

IR (ATR) ν 3383 (OH), 1721 (C=O), 1609, 1512 (Ar); ^{1}H NMR (300 MHz, acetone-d_6) δ 7.26 (d, J = 8.4, 1H, H_5), 7.33 (s, 2H, $2CH_{gal.}$), 7.46 (d, J = 2.2, 1H, $CH_{naph.}$), 7.54-7.65 (m, 2H, $2CH_{naph.}$), 7.77 (d, J = 1.8, 1H, $CH_{naph.}$), 7.99 (d, J = 8.2, 1H, $CH_{naph.}$), 8.02 (d, J = 7.5, 1H, $CH_{naph.}$), 8.15 (dd, J = 8.5, 2.1, 1H, H_6), 8.28 (d, J = 2.1, 1H, H_2), 8.41 (br s, 4H, 4OH); ^{13}C NMR (75 MHz, acetone-d_6) δ 110.5 ($2CH_{gal.}$), 115.9 ($CH_{naph.}$), 117.7, 117.8 ($CH_{Clbenz.}$, $CH_{naph.}$), 120.7, 121.7 ($C_{gal.}$, $C_{Clbenz.}$), 122.3 ($CH_{naph.}$), 122.5 ($C_{Clbenz.}$), 126.1 ($C_{naph.}$), 127.2, 128.3, 128.8 ($3CH_{naph.}$), 131.6, 133.1 ($2CH_{Clbenz.}$), 135.3 ($C_{naph.}$), 140.3 (C-$O_{gal.}$ *para*), 146.3 (2C-$O_{gal.}$ *meta*), 148.5, 149.4 (2C-$O_{naph.}$), 159.0 (C-$O_{Clbenz.}$), 164.2, 165.4 (2C=O); ESI-MS 465.0 $(M-H)^-$; elemental analysis (calcd., found for $C_{24}H_{15}ClO_8 \cdot H_2O$): C (59.45, 59.56), H (3.53, 3.60).

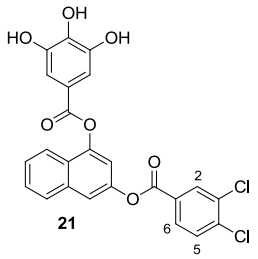

21

3-[(3,4-Dichlorobenzoyl)oxy]-1-naphthyl 3,4,5-trihydroxybenzoate (21). Obtained from silyl ether **77** (198 mg, 0.24 mmol) in 84% yield. mp 218-220 ºC; IR (ATR) ν 3393 (OH), 1735 (C=O), 1614, 1537 (Ar); ^{1}H NMR (300 MHz, acetone-d_6) δ 7.42 (s, 2H, $2CH_{gal.}$), 7.50-7.52 (m, 1H, $CH_{naph.}$), 7.58-7.67 (m, 2H, $2CH_{naph.}$), 7.84-7.87 (m, 2H, $CH_{naph.}$, H_5), 7.96-8.05 (m, 2H, $2CH_{naph.}$), 8.19 (d, J = 8.4, 1H, H_6), 8.37-8.38 (m, 1H, H_2), 8.49 (br s, 3H, 3OH); ^{13}C NMR (75 MHz, acetone-d_6) δ 110.6 ($2CH_{gal.}$), 115.4, 117.5 ($2CH_{naph.}$), 120.3 ($C_{gal.}$), 122.4 ($CH_{naph.}$), 126.5 ($C_{naph.}$), 127.4, 128.4, 128.8 ($3CH_{naph.}$), 130.6 ($CH_{Cl2benz.}$), 130.9 ($C_{Cl2benz.}$), 132.1, 132.7 ($2CH_{Cl2benz.}$), 133.5 ($C_{Cl2benz.}$), 135.2 ($C_{naph.}$), 138.5 ($C_{Cl2benz.}$), 146.4 (2C-$O_{gal.}$ *meta*), 148.9 (2C-$O_{naph.}$), 149.0 (C-$O_{gal.}$ *para*), 163.8, 165.2 (2C=O); ESI-MS 483.0 $(M-H)^-$; elemental analysis (calcd., found for $C_{24}H_{14}Cl_2O_7 \cdot 3/2H_2O$): C (56.27, 56.00), H (3.34, 3.01).

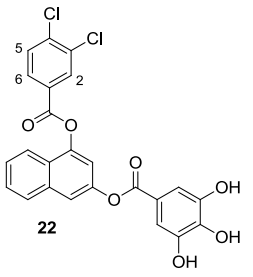

22

4-[(3,4-Dichlorobenzoyl)oxy]-2-naphthyl 3,4,5-trihydroxybenzoate (22). Obtained from silyl ether **78** (266 mg, 0.32 mmol) in 86% yield. mp 249-251 ºC; IR (ATR) ν 3373 (OH), 1734 (C=O), 1609, 1512 (Ar); ^{1}H NMR (300 MHz, acetone-d_6) δ 7.16 (s, 2H, $2CH_{gal.}$), 7.55-7.67 (m, 3H, $3CH_{naph.}$), 7.83 (s, 1H, $CH_{naph.}$), 7.92-7.97 (m, 2H, $CH_{naph.}$, H_5), 8.05 (d, *J* = 8.0, 1H, $CH_{naph.}$), 8.21 (d, *J* = 8.4, 1H, H_6), 8.43 (s, 1H, H_2), 9.23 (br s, 1H, OH *para*), 9.48 (br s, 2H, 2OH *meta*); ^{13}C NMR (75 MHz, acetone-d_6) δ 109.2 ($2CH_{gal.}$), 115.1, 117.4 ($2CH_{naph.}$), 117.9 ($C_{gal.}$), 121.3 ($CH_{naph.}$), 124.3 ($C_{naph.}$), 126.7, 127.6, 127.8 ($3CH_{naph.}$), 129.1 ($C_{Cl2benz.}$), 130.0, 131.5, 131.7 ($3CH_{Cl2benz.}$), 132.1 ($C_{Cl2benz.}$), 133.9 ($C_{naph.}$), 137.3 ($C_{Cl2benz.}$), 145.8 ($2C\text{-}O_{gal.}$ *meta*), 146.7 ($2C\text{-}O_{naph.}$), 147.9 ($C\text{-}O_{gal.}$ *para*), 162.9, 164.6 (2C=O); ESI-MS 483.0 $(M-H)^-$; elemental analysis (calcd., found for $C_{24}H_{14}Cl_2O_7 \cdot H_2O$): C (57.28, 56.99), H (3.20, 3.02).

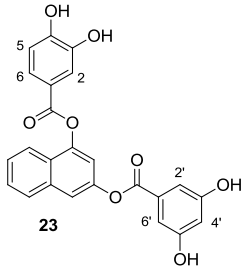

23

3-[(3,5-Dihydroxybenzoyl)oxy]-1-naphthyl 3,4-dihydroxybenzoate (23). Obtained from silyl ether **79** (167 mg, 0.39 mmol) in 85% yield. mp 252 ºC (decomposed); IR (ATR) ν 3310 (OH), 1741 (C=O), 1699, 1605 (Ar); ^{1}H NMR (300 MHz, acetone-d_6) δ 6.60 (t, *J* = 2.3, 1H, $H_{4'}$), 6.88 (d, *J* = 8.6, 1H, H_5), 7.17 (d, *J* = 2.3, 2H, $H_{2'}$, $H_{6'}$), 7.35 (d, *J* = 2.2, 1H, $CH_{naph.}$), 7.40-7.53 (m, 2H, $2CH_{naph.}$), 7.54-7.57 (m, 2H, H_2, H_6), 7.65 (d, *J* = 2.2, 1H, $CH_{naph.}$), 7.75-7.87 (m, 1H, $CH_{naph.}$), 7.87-7.93 (m, 1H, $CH_{naph.}$); ^{13}C NMR (75 MHz, acetone-d_6) δ 109.0 ($CH_{α\text{-}res.}$), 109.3 ($2CH_{α\text{-}res.}$), 115.9, 116.1, 117.7, 117.8 ($2CH_{naph.}$, $2CH_{prot.}$), 121.8 ($C_{prot.}$), 122.2 ($CH_{naph.}$), 124.4 ($CH_{prot.}$), 126.0 ($C_{naph.}$), 127.2, 128.3, 128.8 ($3CH_{naph.}$), 131.9 ($C_{α\text{-}res.}$), 135.3 ($C_{naph.}$), 145.9 ($C\text{-}O_{prot.}$), 148.5, 149.4 ($2C\text{-}O_{naph.}$), 151.7 ($C\text{-}O_{prot.}$), 159.9 ($2C\text{-}O_{α\text{-}res.}$), 165.3 (2C=O); ESI-MS 431.0 $(M-H)^-$; elemental analysis (calcd., found for $C_{24}H_{16}O_8 \cdot 2H_2O$): C (61.54, 61.57), H (4.30, 4.03).

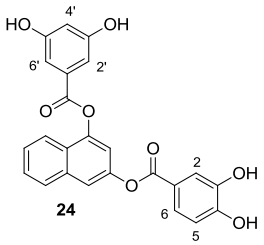

24

4-[(3,5-Dihydroxybenzoyl)oxy]-2-naphthyl 3,4-dihydroxybenzoate (24). Obtained from silyl ether **80** (187 mg, 0.43 mmol) in 92% yield. mp 254 ºC (decomposed); IR (ATR) ν 3315 (OH), 1702 (C=O), 1605 (Ar); ^{1}H NMR (300 MHz, acetone-d_6) δ 6.70 (t, J = 2.1, 1H, $H_{4'}$), 7.06 (d, J = 8.7, 1H, H_5), 7.22 (d, J = 2.1, 2H, $H_{2'}$, $H_{6'}$), 7.47 (d, J = 2.1, 1H, $CH_{naph.}$), 7.55-7.65 (m, 2H, $2CH_{naph.}$), 7.77-7.80 (m, 3H, H_2, H_6, $CH_{naph.}$), 7.98 (d, J = 8.1, 1H, $CH_{naph.}$), 8.02 (d, J = 7.5, 1H, $CH_{naph.}$), 8.60 (br s, 1H, OH), 8.78 (br s, 2H, 2OH), 8.95 (br s, 1H, OH); ^{13}C-NMR (75 MHz, acetone-d_6) δ 108.4 ($CH_{α-res.}$), 108.8 ($2CH_{α-res.}$), 115.2, 116.8, 117.1, 117.3 ($2CH_{naph.}$, $2CH_{prot.}$), 120.9 ($C_{prot.}$), 121.9 ($CH_{naph.}$), 124.0 ($CH_{prot.}$), 125.8 ($C_{naph.}$), 126.7, 127.8, 128.3 ($3CH_{naph.}$), 131.7 ($C_{α-res.}$), 134.8 ($C_{naph.}$), 145.6 (C-$O_{prot.}$), 148.3, 148.7 (2C-$O_{naph.}$), 151.5 (C-$O_{prot.}$), 159.9 (2C-$O_{α-res.}$), 164.6, 164.9 (2C=O); ESI-MS 431.0 $(M-H)^-$; elemental analysis (calcd., found for $C_{24}H_{16}O_8 \cdot H_2O$): C (62.88, 62.45), H (3.96, 4.02).

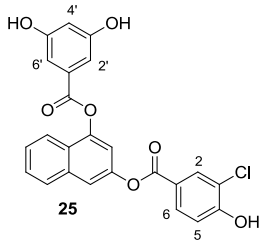

25

4-[(3,5-Dihydroxybenzoyl)oxy]-2-naphthyl 3-chloro-4-hydroxybenzoate (25). Obtained from silyl ether **81** (55 mg, 0.07 mmol) in 90% yield. R_f (DCM) 0.20; mp 228-229 ºC; IR (ATR) ν 3434 (OH), 1693 (C=O), 1465 (Ar); ^{1}H NMR (300 MHz, acetone-d_6) δ 6.73 (t, J = 2.2, 1H, $H_{4'}$), 7.22 (d, J = 8.5, 1H, H_5), 7.30 (d, J = 2.2, 2H, $H_{2'}$, $H_{6'}$), 7.51 (d, J = 2.2, 1H, $CH_{naph.}$), 7.61 (tt, J = 8.3, 3.4, 2H, $2CH_{naph.}$), 7.81 (d, J = 2.0, 1H, $CH_{naph.}$), 7.98 (d, J = 8.3, 1H, $CH_{naph.}$), 8.02-8.08 (m, 2H, $CH_{naph.}$, H_6), 8.21 (d, J = 2.1, 1H, H_2), 9.00 (br s, 3H, 3OH); ^{13}C NMR (75 MHz, acetone-d_6) δ 109.0 ($CH_{α-res.}$), 109.3 ($2CH_{α-res.}$), 115.7 ($CH_{naph.}$), 117.6, 117.8 (CH_{Clbenz}, $CH_{naph.}$), 121.5 (C_{Clbenz}), 122.2 ($CH_{naph.}$), 122.7 ($C_{Clbenz.}$), 126.1 ($C_{naph.}$), 127.3, 128.3, 128.8 ($3CH_{naph.}$), 131.5 (CH_{Clbenz}), 131.8 ($C_{α-res.}$), 133.0 ($CH_{Clbenz.}$), 135.3 ($C_{naph.}$), 148.5, 149.1 (2C-$O_{naph.}$), 158.9 (C-$O_{Clbenz.}$), 159.8 (2C-$O_{α-res.}$), 164.3, 165.2 (2C=O); ESI-MS 449.0 $(M-H)^-$; elemental analysis (calcd., found for $C_{24}H_{15}ClO_7 \cdot 1/2H_2O$): C (62.69, 63.08), H (3.51, 4.00).

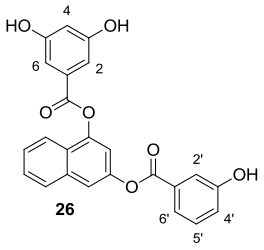

26

3-[(3-Hydroxybenzoyl)oxy]-1-naphthyl 3,5-dihydroxybenzoate (26). Obtained from silyl ether **82** (203 mg, 0.27 mmol) in 82% yield. R_f (DCM/MeOH, 95:5) 0.51; mp 118-121 ºC; IR (ATR) ν 3392 (OH), 1731 (C=O), 1602, 1453 (Ar); ^{1}H NMR (300 MHz, acetone-d_6) δ 6.74 (t, J = 2.2, 1H, H_4), 7.21 (ddd, J = 8.2, 2.5, 0.9, 1H, $H_{4'}$), 7.31 (d, J = 2.3, 2H, H_2, H_6), 7.45 (t, J = 7.9, 1H, $H_{5'}$), 7.52 (d, J = 2.2, 1H, $CH_{naph.}$), 7.57-7.65 (m, 2H, $2CH_{naph.}$), 7.69 (app t, J = 2.0, 1H, $H_{2'}$), 7.73 (dt, J = 7.8, 1.2, 1H, $H_{6'}$), 7.82 (d, J = 2.0, 1H, $CH_{naph.}$), 7.99 (d, J = 7.5, 1H, $CH_{naph.}$), 8.03 (d, J = 7.5, 1H, $CH_{naph.}$), 8.84 (br s, 3H, 3OH); ^{13}C NMR (75 MHz, acetone-d_6) δ 109.0 ($CH_{α\text{-}res.}$), 109.3 ($2CH_{α\text{-}res.}$), 115.7 ($CH_{naph.}$), 117.3, 117.8 ($CH_{m\text{-}sal.}$, $CH_{naph.}$), 121.8, 122.0, 122.2 ($2CH_{m\text{-}sal.}$, $CH_{naph.}$), 126.1 ($C_{naph.}$), 127.3, 128.3, 128.8 ($3CH_{naph.}$), 130.8 ($CH_{m\text{-}sal.}$), 131.6, 131.8 ($C_{α\text{-}res.}$, $C_{m\text{-}sal.}$), 135.3 ($C_{naph.}$), 148.5, 149.1 ($2C\text{-}O_{naph.}$), 158.5 ($C\text{-}O_{m\text{-}sal.}$), 159.8 ($2C\text{-}O_{α\text{-}res.}$), 165.2, 165.4 (2C=O); ESI-MS 415.0 $(M-H)^-$; elemental analysis (calcd., found for $C_{24}H_{16}O_7 \cdot 3/2H_2O$): C (65.01, 65.37), H (4.32, 4.27).

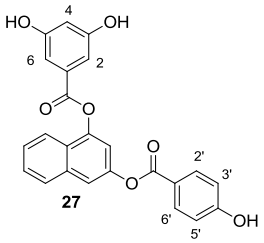

27

3-[(4-Hydroxybenzoyl)oxy]-1-naphthyl 3,5-dihydroxybenzoate (27). Obtained from silyl ether **83** (175 mg, 0.23 mmol) in 71% yield. R_f (DCM/MeOH, 95:5) 0.30; mp 208 ºC; IR (ATR) ν 3386 (OH), 1713 (C=O), 1603, 1511 (Ar); ^{1}H NMR (300 MHz, acetone-d_6) δ 6.73 (t, J = 2.3, 1H, H_4), 7.03 (d, J = 8.8, 2H, $H_{3'}$, $H_{5'}$), 7.31 (d, J = 2.3, 2H, H_2, H_6), 7.49 (d, J = 2.2, 1H, $CH_{naph.}$), 7.55-7.67 (m, 2H, $2CH_{naph.}$), 7.79 (d, J = 2.1, 1H, $CH_{naph.}$), 7.99 (dd, J = 7.9, 1.1, 1H, $CH_{naph.}$), 8.03 (d, J = 7.4, 1H, $CH_{naph.}$), 8.12 (d, J = 8.8, 2H, $H_{2'}$, $H_{6'}$), 9.01 (br s, 3H, 3OH); ^{13}C NMR (75 MHz, acetone-d_6) δ 109.0 ($CH_{α\text{-}res.}$), 109.3 ($2CH_{α\text{-}res.}$), 115.9 ($CH_{naph.}$), 116.4 ($2CH_{p\text{-}sal.}$), 117.8 ($CH_{naph.}$), 121.3 ($C_{p\text{-}sal.}$), 122.2 ($CH_{naph.}$), 126.0 ($C_{naph.}$), 127.2, 128.3, 128.8 ($3CH_{naph.}$), 131.8 ($C_{α\text{-}res.}$), 133.3 ($2CH_{p\text{-}sal.}$), 135.3 ($C_{naph.}$), 148.5, 149.3 ($2C\text{-}O_{naph.}$), 159.8 ($2C\text{-}O_{α\text{-}res.}$), 163.5 ($C\text{-}O_{p\text{-}sal.}$), 165.2, 165.3 (2C=O); ESI-MS 415.0 $(M-H)^-$; elemental analysis (calcd., found for $C_{24}H_{16}O_7 \cdot 3/2H_2O$): C (65.01, 65.08), H (4.32, 4.24).

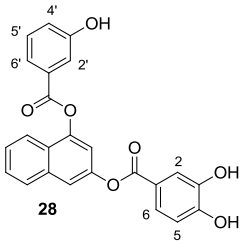

28

4-[(3-Hydroxybenzoyl)oxy]-2-naphthyl 3,4-dihydroxybenzoate (28). Obtained from silyl ether **84** (175 mg, 0.23 mmol) in 63% yield. R_f (DCM/MeOH, 95:5) 0.60; mp 99-102 ºC; IR (ATR) ν 3386 (OH), 1732 (C=O), 1600, 1499 (Ar); ^{1}H NMR (300 MHz, acetone-d_6) δ 7.01 (d, J = 8.8, 1H, H_5), 7.25 (ddd, J = 8.2, 2.5, 0.9, 1H, $H_{4'}$), 7.47-7.52 (m, 2H, $CH_{naph.}$, $H_{5'}$), 7.55-7.64 (m, 2H, $2CH_{naph.}$), 7.67-7.71 (m, 2H, H_2, H_6), 7.77 (app t, J = 2.0, 1H, $H_{2'}$), 7.79 (d, J = 2.1, 1H, $CH_{naph.}$), 7.82 (dt, J = 7.7, 1.3, 1H, $H_{6'}$), 7.99 (d, J = 8.0, 1H, $CH_{naph.}$), 8.03 (d, J = 8.0, 1H, $CH_{naph.}$), 8.80 (br s, 3H, 3OH); ^{13}C NMR (75 MHz, acetone-d_6) δ 115.9 ($CH_{naph.}$), 116.1 ($CH_{prot.}$), 117.4, 117.7, 117.9 ($CH_{naph.}$, $CH_{m\text{-}sal.}$, $CH_{prot.}$), 121.7 ($C_{prot.}$), 122.0, 122.2 ($CH_{naph.}$, $2CH_{m\text{-}sal.}$), 124.3 ($CH_{prot.}$), 126.0 ($C_{naph.}$), 127.2, 128.3, 128.8 ($3CH_{naph.}$), 131.0 ($CH_{m\text{-}sal.}$), 131.3 ($C_{m\text{-}sal.}$), 135.3 ($C_{naph.}$), 145.9 (C-$O_{prot.}$), 148.5, 149.4 (2C-$O_{naph.}$), 151.8 (C-$O_{prot.}$), 158.7 (C-$O_{m\text{-}sal.}$), 165.2, 165.3 (2C=O); ESI-MS 415.0 $(M-H)^-$; elemental analysis (calcd., found for $C_{24}H_{16}O_7 \cdot H_2O$): C (66.36, 66.58), H (4.18, 4.15).

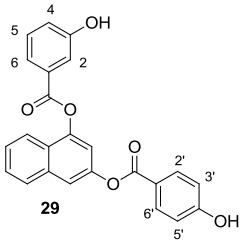

29

3-[(4-Hydroxybenzoyl)oxy]-1-naphthyl 3-hydroxybenzoate (29). Obtained from silyl ether **85** (202 mg, 0.32 mmol) in 51% yield. R_f (DCM/MeOH, 95:5) 0.45; mp 209 ºC; IR (ATR) ν 3383 (OH), 1711 (C=O), 1599, 1512 (Ar); ^{1}H NMR (300 MHz, acetone-d_6) δ 7.03 (d, J = 8.8, 2H, $H_{3'}$, $H_{5'}$), 7.25 (ddd, J = 8.2, 2.5, 0.8, 1H, H_4), 7.50 (t, J = 7.9, 1H, H_5), 7.51 (d, J = 2.2, 1H, $CH_{naph.}$), 7.55-7.67 (m, 2H, $2CH_{naph.}$), 7.76-7.84 (m, 3H, H_2, H_6, $CH_{naph.}$), 7.99 (d, J = 8.1, 1H, $CH_{naph.}$), 8.03 (d, J = 7.7, 1H, $CH_{naph.}$), 8.13 (d, J = 8.8, 2H, $H_{2'}$, $H_{6'}$), 9.14 (br s, 2H, 2OH); ^{13}C NMR (75 MHz, acetone-d_6) δ 115.9 ($CH_{naph.}$), 116.4 ($2CH_{p\text{-}sal.}$), 117.4, 117.9 ($CH_{m\text{-}sal.}$, $CH_{naph.}$), 121.4 ($C_{p\text{-}sal.}$), 122.0, 122.1, 122.2 ($CH_{naph.}$, $2CH_{m\text{-}sal.}$), 126.0 ($C_{naph.}$), 127.2, 128.3, 128.8 ($3CH_{naph.}$), 131.0 ($CH_{m\text{-}sal.}$), 131.3 ($C_{m\text{-}sal.}$), 133.3 ($2CH_{p\text{-}sal.}$), 135.3 ($C_{naph.}$), 148.5, 149.3 (2C-$O_{naph.}$), 158.7 (C-$O_{m\text{-}sal.}$), 163.4 (C-$O_{p\text{-}sal.}$), 165.2, 165.3 (2C=O); ESI-MS 399.0 $(M-H)^-$; elemental analysis (calcd., found for $C_{24}H_{16}O_6 \cdot H_2O$): C (69.33, 68.90), H (4.11, 4.34).

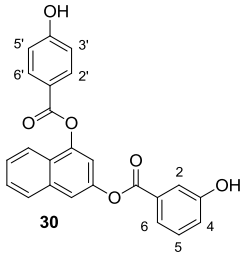

30

4-[(4-Hydroxybenzoyl)oxy]-2-naphthyl 3-hydroxybenzoate (30). Obtained from silyl ether **86** (188 mg, 0.30 mmol) in 45% yield. R_f (DCM/MeOH, 95:5) 0.50; mp 195-196 ºC; IR (ATR) ν 3369 (OH), 1729 (C=O), 1701, 1598, 1512 (Ar); ^{1}H NMR (300 MHz, acetone-d_6) δ 7.08 (d, J = 8.8, 2H, $H_{3'}$, $H_{5'}$), 7.21 (ddd, J = 8.1, 2.5, 0.9, 1H, H_4), 7.45 (t, J = 7.9, 1H, H_5), 7.50 (d, J = 2.2, 1H, $CH_{naph.}$), 7.55-7.66 (m, 2H, $2CH_{naph.}$), 7.68-7.70 (m, 1H, H_2), 7.73 (dt, J = 7.7, 1.3, 1H, H_6), 7.81 (d, J = 2.0, 1H, $CH_{naph.}$), 7.99 (d, J = 8.2, 1H, $CH_{naph.}$), 8.03 (d, J = 7.5, 1H, $CH_{naph.}$), 8.21 (d, J = 8.8, 2H, $H_{2'}$, $H_{6'}$), 9.17 (br s, 2H, 2OH); ^{13}C NMR (75 MHz, acetone-d_6) δ 115.7 ($CH_{naph.}$), 116.6 ($2CH_{p\text{-}sal.}$), 117.3, 117.6 ($CH_{m\text{-}sal.}$, $CH_{naph.}$), 121.1 ($C_{p\text{-}sal.}$), 121.8, 122.1, 122.4 ($CH_{naph.}$, $2CH_{m\text{-}sal.}$), 126.3 ($C_{naph.}$), 127.2, 128.3, 128.8 ($3CH_{naph.}$), 130.9 ($CH_{m\text{-}sal.}$), 131.6 ($C_{m\text{-}sal.}$), 133.4 ($2CH_{p\text{-}sal.}$), 135.2 ($C_{naph.}$), 148.7, 149.2 ($2C\text{-}O_{naph.}$), 158.6 ($C\text{-}O_{m\text{-}sal.}$), 163.6 ($C\text{-}O_{p\text{-}sal.}$), 165.1, 165.4 (2C=O); ESI-MS 399.0 $(M-H)^-$; elemental analysis (calcd., found for $C_{24}H_{16}O_6 \cdot 1/3H_2O$): C (70.93, 71.13), H (4.13, 4.35).

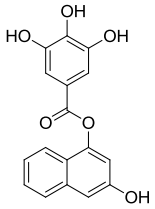

31

3-Hydroxy-1-naphthyl 3,4,5-trihydroxybenzoate (31). Obtained from silyl ether **59** (143 mg, 0.22 mmol) in 78% yield. R_f (DCM/MeOH, 9:1) 0.36; mp 168-170 ºC (decomposed); IR (ATR) ν 3361 (OH), 1703 (C=O), 1611 (Ar); ^{1}H NMR (300 MHz, acetone-d_6) δ 7.09 (d, J = 2.3, 1H, $CH_{naph.}$), 7.17 (d, J = 2.3, 1H, $CH_{naph.}$), 7.28-7.34 (m, 1H, $CH_{naph.}$), 7.40 (s, 2H, $2CH_{gal.}$), 7.41-7.47 (m, 1H, $CH_{naph.}$), 7.75 (d, J = 8.3, 1H, $CH_{naph.}$), 7.80 (d, J = 8.3, 1H, $CH_{naph.}$), 8.25 (br s, 1H, OH), 8.38 (br s, 2H, 2OH), 8.83 (br s, 1H, OH); ^{13}C NMR (75 MHz, acetone-d_6) δ 107.9 ($CH_{naph.}$), 110.6 ($2CH_{gal.}$), 112.3 ($CH_{naph.}$), 120.7 ($C_{gal.}$), 122.2 ($CH_{naph.}$), 123.1 ($C_{naph.}$), 124.3, 127.3, 127.7 ($3CH_{naph.}$), 136.5 ($C_{naph.}$), 139.7 ($C\text{-}O_{gal.}$ *para*), 146.4 ($2C\text{-}O_{gal.}$ *meta*), 149.2, 156.0 ($2C\text{-}O_{naph.}$), 165.3 (C=O); ESI-MS 311.1 $(M-H)^-$; elemental analysis (calcd., found for $C_{17}H_{12}O_6 \cdot H_2O$): C (61.82, 62.02), H, (4.27, 4.31).

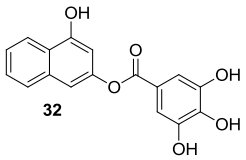

32

4-Hydroxy-2-naphthyl 3,4,5-trihydroxybenzoate (32). Obtained from silyl ether **62** (230 mg, 0.35 mmol) in 93% yield. R_f (DCM/MeOH, 9:1) 0.47; mp 188-190 ºC (decomposed); IR (ATR) ν 3369 (OH), 1701 (C=O), 1613 (Ar); ^{1}H NMR (300 MHz, acetone-d_6) δ 6.83 (d, J = 2.1, 1H, $CH_{naph.}$), 7.24 (d, J = 2.0, 1H, $CH_{naph.}$), 7.30 (s, 2H, $2CH_{gal.}$), 7.42-7.54 (m, 2H, $2CH_{naph.}$), 7.83 (d, J = 7.5, 1H, $CH_{naph.}$), 8.20 (br s, 1H, OH), 8.24 (d, J = 8.2, 1H, CH_{Ar}), 8.32 (br s, 2H, 2OH), 9.35 (br s, 1H, OH); ^{13}C NMR (75 MHz, acetone-d_6) δ 105.1 ($CH_{naph.}$), 110.5 ($2CH_{gal.}$), 110.9 ($CH_{naph.}$), 121.1 ($C_{gal.}$), 123.1 ($CH_{naph.}$), 124.1 ($C_{naph.}$), 125.2, 127.9, 128.2 ($3CH_{naph.}$), 135.7 ($C_{naph.}$), 139.5 (C-$O_{gal.}$ *para*), 143.3 (2C-$O_{gal.}$ *meta*), 150.4, 155.0 (2C-$O_{naph.}$), 165.5 (C=O); ESI-MS 311.1 $(M–H)^–$; elemental analysis (calcd., found for $C_{17}H_{12}O_6 \cdot 1/2H_2O$): C (63.55, 63.46), H, (4.08, 4.00).

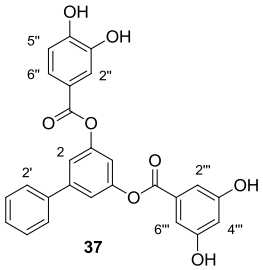

37

5-[(3,5-Dihydroxybenzoyl)oxy]biphenyl-3-yl 3,4-dihydroxybenzoate (37). Obtained from silyl ether **105** (75 mg, 0.08 mmol) in 83% yield. R_f (DCM/MeOH, 95:5) 0.27; mp 92-94 ºC; IR (ATR) ν 3378 (OH), 1708 (C=O), 1601, 1451 (Ar), 1207 (C-O); ^{1}H NMR (300 MHz, acetone-d_6) δ 6.69 (t, J = 2.2, 1H, $H_{4'''}$), 7.00 (d, J = 8.6, 1H, $H_{5''}$), 7.20 (d, J = 2.2, 2H, $H_{2'''}$, $H_{6'''}$), 7.25 (t, J = 2.1, 1H, H_4), 7.38-7.52 (m, 3H, $H_{3'}$, $H_{4'}$, $H_{5'}$), 7.53 (d, J = 2.0, 2H, H_2, H_6), 7.65-7.68 (m, 2H, $H_{2''}$, $H_{6''}$), 7.76 (d, J = 7.2, 2H, $H_{2'}$, $H_{6'}$), 8.75 (br s, 4H, 4OH); ^{13}C NMR (75 MHz, acetone-d_6) δ 108.9 ($CH_{α\text{-}res.}$), 109.3 ($2CH_{α\text{-}res.}$), 115.8 (C_4H), 116.1, 117.8 ($2CH_{prot.}$), 118.5, 118.8 (C_2H, C_6H), 121.8 ($C_{prot.}$), 124.3 ($CH_{prot.}$), 127.9 ($C_{2'}H$, $C_{6'}H$), 129.0 ($C_{4'}H$), 129.9 ($C_{3'}H$, $C_{5'}H$), 132.2 ($C_{α\text{-}res.}$), 140.1, 143.9 ($2C_{biph.}$), 145.9, 151.8, 153.0, 153.3 ($2C\text{-}O_{prot.}$, $2C\text{-}O_{biph.}$), 159.7 ($2C\text{-}O_{α\text{-}res.}$), 165.1, 165.3 (2C=O); ESI-MS 457.0 $(M–H)^–$; elemental analysis (calcd., found for $C_{26}H_{18}O_8 \cdot H_2O$): C (64.33, 64.33), H, (4.36, 4.55).

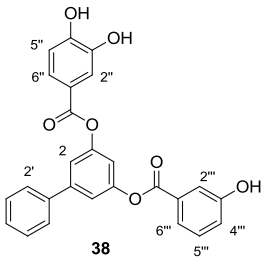

38

5-[(3-Hydroxybenzoyl)oxy]biphenyl-3-yl 3,4-dihydroxybenzoate (38). Obtained from silyl ether **106** (166 mg, 0.21 mmol) in 54% yield. R_f (DCM/MeOH, 95:5) 0.45; mp 110-112 ºC; IR (ATR) ν 3390 (OH), 1708 (C=O), 1603, 1451 (Ar), 1290, 1206 (C-O); ^{1}H NMR (300 MHz, acetone-d_6) δ 7.00 (d, J = 8.7, 1H, $H_{4'''}$), 7.20 (ddd, J = 8.1, 2.5, 0.8, 1H, $H_{5''}$), 7.27 (t, J = 2.0, 1H, H_4), 7.39-7.56 (m, 6H, H_2, H_6, $H_{3'}$, $H_{4'}$, H_5, $H_{5'''}$), 7.65-7.72 (m, 4H, $H_{2''}$, $H_{6''}$, $H_{2'''}$, $H_{6'''}$), 7.77 (d, J = 7.4, 2H, $H_{2'}$, $H_{6'}$), 8.77 (br s, 3H, 3OH); ^{13}C NMR (75 MHz, acetone-d_6) δ 115.9 (C_4H), 116.1 ($CH_{prot.}$), 117.4 ($CH_{m\text{-}sal.}$), 117.8 ($CH_{prot.}$), 118.5, 118.8 (C_2H, C_6H), 121.7 ($C_{prot.}$), 121.8, 122.1 (2$CH_{m\text{-}sal.}$), 124.4 ($CH_{prot.}$), 127.9 ($C_{2'}$H, $C_{6'}$H), 129.0 ($C_{4'}$H), 129.9 ($C_{3'}$H, $C_{5'}$H), 130.8 ($CH_{m\text{-}sal.}$), 131.7 ($C_{m\text{-}sal.}$), 140.1, 143.9 (2$C_{biph.}$), 145.9, 151.7, 153.0, 153.3 (2C-$O_{prot.}$, 2C-$O_{biph.}$), 158.6 (C-$O_{m\text{-}sal.}$), 165.1, 165.3 (2C=O); ESI-MS 441.1 $(M–H)^-$; elemental analysis (calcd., found for $C_{26}H_{18}O_7 \cdot 2/3H_2O$): C (68.72, 69.06), H, (4.29, 4.78).

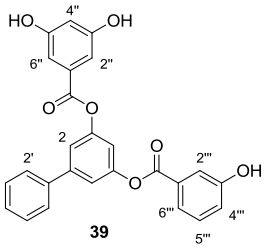

39

5-[(3-Hydroxybenzoyl)oxy]biphenyl-3-yl 3,5-dihydroxybenzoate (39). Obtained from silyl ether **107** (71 mg, 0.09 mmol) in 95% yield. R_f (DCM/MeOH, 95:5) 0.44; mp 93-94 ºC; IR (ATR) ν 3406 (OH), 1713 (C=O), 1601, 1454 (Ar), 1208 (C-O); ^{1}H NMR (300 MHz, acetone-d_6) δ 6.69 (t, J = 2.3, 1H, $H_{4''}$), 7.17-7.23 (m, 3H, $H_{2''}$, $H_{6''}$, $H_{4'''}$), 7.30 (t, J = 2.1, 1H, H_4), 7.44 (t, J = 7.8, 2H, $H_{4'}$, $H_{5'''}$), 7.50 (t, J = 7.3, 2H, $H_{3'}$, $H_{5'}$), 7.56-7.59 (m, 2H, H_2, H_6), 7.67 (t, J = 2.0, 1H, $H_{2'''}$), 7.71 (dt, J = 7.8, 1.3, 1H, $H_{6'''}$), 7.77 (d, J = 7.1, 2H, $H_{2'}$, $H_{6'}$), 8.81 (br s, 3H, 3OH); ^{13}C NMR (75 MHz, acetone-d_6) δ 108.8 ($CH_{\alpha\text{-}res.}$), 109.2 (2$CH_{\alpha\text{-}res.}$), 115.8 (C_4H), 117.3 ($CH_{m\text{-}sal.}$), 118.7 (C_2H, C_6H), 121.8 ($CH_{m\text{-}sal.}$), 122.1 ($CH_{m\text{-}sal.}$), 127.8 ($C_{2'}$H, $C_{6'}$H), 129.1 ($C_{4'}$H), 129.9 ($C_{3'}$H, $C_{5'}$H), 130.8 ($CH_{m\text{-}sal.}$), 131.6, 132.2 ($C_{m\text{-}sal}$, $C_{\alpha\text{-}res.}$), 139.9, 144.0 (2$C_{biph.}$), 153.0 (2C-$O_{biph.}$), 158.6 (C-$O_{m\text{-}sal.}$), 159.7 (2C-$O_{\alpha\text{-}res.}$), 165.3 (2C=O); ESI-MS 440.7 $(M–H)^-$; elemental analysis (calcd., found for $C_{26}H_{18}O_7 \cdot 1/2H_2O$): C (69.18, 69.00), H, (4.24, 4.60).

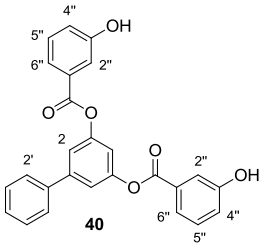

40

Biphenyl-3,5-diyl bis(3-hydroxybenzoate) (40). Obtained from silyl ether **99** (58 mg, 0.09 mmol) in 56% yield. R_f (DCM/MeOH, 95:5) 0.92; mp 95-96 ºC; IR (ATR) ν 3434 (OH), 1701 (C=O), 1464, 1364 (Ar), 1214, 1181 (C-O); ^{1}H NMR (300 MHz, acetone-d_6) δ 7.20 (ddd, J = 8.1, 2.5, 0.9, 2H, 2H$_{4''}$), 7.32 (t, J = 2.1, 1H, H$_4$), 7.39-7.47 (m, 3H, H$_{4'}$, 2H$_{5''}$), 7.51 (t, J = 7.3, 2H, H$_{3'}$, H$_{5'}$), 7.58 (t, J = 2.1, 2H, H$_2$, H$_6$), 7.67 (t, J = 1.9, 2H, 2H$_{2''}$), 7.71 (dt, J = 7.7, 1.3, 2H, 2H$_{6''}$), 7.77 (d, J = 7.1, 2H, H$_{2'}$, H$_{6'}$), 8.86 (br s, 2H, 2OH); ^{13}C NMR (75 MHz, acetone-d_6) δ 115.8 (C$_4$H), 117.3 (C$_2$H, C$_6$H), 118.7 (2CH$_{m\text{-sal.}}$), 121.8 (2CH$_{m\text{-sal.}}$), 122.1 (2CH$_{m\text{-sal.}}$), 127.8 (C$_{2'}$H, C$_{6'}$H), 129.1 (C$_{4'}$H), 129.9 (C$_{3'}$H, C$_{5'}$H), 130.8 (2CH$_{m\text{-sal.}}$), 131.6 (2C$_{m\text{-sal.}}$), 139.9, 144.0 (2C$_{biph.}$), 153.0 (2C-O$_{biph.}$), 158.6 (2C-O$_{m\text{-sal.}}$), 165.3 (2C=O); ESI-MS 424.7 (M–H)$^-$; elemental analysis (calcd., found for C$_{26}$H$_{18}$O$_6$·1/2H$_2$O): C (71.72, 72.18), H, (4.40, 4.81).

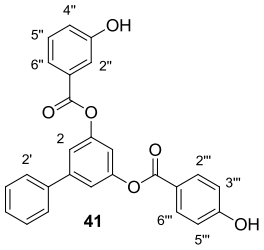

41

5-[(4-Hydroxybenzoyl)oxy]biphenyl-3-yl 3-hydroxybenzoate (41). Obtained from silyl ether **108** (104 mg, 0.16 mmol) in 77% yield. R_f (DCM/MeOH, 95:5) 0.48; mp 74-75 ºC; IR (ATR) ν 3392 (OH), 1707 (C=O), 1597, 1483 (Ar), 1283, 1264 (C-O); ^{1}H NMR (300 MHz, acetone-d_6) δ 7.03 (d, J = 8.8, 2H, H$_{3'''}$, H$_{5'''}$), 7.20 (ddd, J = 8.1, 2.5, 1.0, 1H, H$_{4''}$), 7.28 (t, J = 2.1, 1H, H$_4$), 7.37-7.54 (m, 4H, H$_{3'}$, H$_{4'}$, H$_{5'}$, H$_{5''}$), 7.56 (t, J = 1.9, 2H, H$_2$, H$_6$), 7.67 (t, J = 2.0, 1H, H$_{2''}$), 7.71 (dt, J = 7.7, 1.3, 1H, H$_{6''}$), 7.76 (d, J = 7.1, 2H, H$_{2'}$, H$_{6'}$), 8.10 (d, J = 8.8, 2H, H$_{2'''}$, H$_{6'''}$), 9.09 (br s, 2H, 2OH); ^{13}C NMR (75 MHz, acetone-d_6) δ 115.9 (C$_4$H), 116.4 (2CH$_{p\text{-sal.}}$), 117.3, 118.5, 118.8 (C$_2$H, C$_6$H, CH$_{m\text{-sal.}}$), 121.4 (C$_{p\text{-sal.}}$), 121.8, 122.1 (2CH$_{m\text{-sal.}}$), 127.8 (C$_{3'}$H, C$_{5'}$H), 129.0 (C$_{4'}$H), 129.9 (C$_{2'}$H, C$_{6'}$H), 130.8 (CH$_{m\text{-sal.}}$), 131.6 (C$_{m\text{-sal.}}$), 133.3 (2CH$_{p\text{-sal.}}$), 140.0, 143.9 (2C$_{biph.}$), 153.0, 153.2 (2C-O$_{biph.}$), 158.5 (C-OH$_{p\text{-sal.}}$), 163.4 (C-OH$_{m\text{-sal.}}$), 165.0, 165.3 (2C=O); ESI-MS 424.7 (M–H)$^-$; elemental analysis (calcd., found for C$_{26}$H$_{18}$O$_6$·1/2H$_2$O): C (71.72, 71.29), H, (4.40, 4.76).

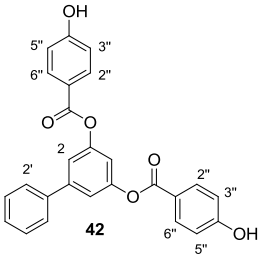

42

Biphenyl-3,5-diyl bis(4-hydroxybenzoate) (42). Obtained from silyl ether **100** (43 mg, 0.07 mmol) in 96% yield. R_f (DCM/MeOH, 95:5) 0.13; mp 230 ºC (decomposed); IR (ATR) ν 3362 (OH), 1704 (C=O), 1605, 1513, 1450 (Ar), 1262 (C-O); ^{1}H NMR (300 MHz, acetone-d_6) δ 7.02 (d, J = 8.8, 4H, 2H$_{3''}$, 2H$_{5''}$), 7.25 (t, J = 2.1, 1H, H$_4$), 7.41 (t, J = 7.3, 1H, H$_{4'}$), 7.50 (t, J = 7.7, 2H, H$_{3'}$, H$_{5'}$), 7.53 (d, J = 2.1, 2H, H$_2$, H$_6$), 7.76 (d, J = 7.2, 2H, H$_{2'}$, H$_{6'}$), 8.10 (d, J = 8.8, 4H, 2H$_{2''}$, 2H$_{6''}$), 9.40 (br s, 2H, 2OH); ^{13}C NMR (75 MHz, acetone-d_6) δ 115.9 (C$_4$H), 116.4 (4CH$_{p\text{-sal.}}$), 118.6 (C$_2$H, C$_6$H), 121.4 (2C$_{p\text{-sal.}}$), 127.8 (C$_{2'}$H, C$_{6'}$H), 129.0 (C$_{4'}$H), 129.9 (C$_{3'}$H, C$_{5'}$H), 133.3 (4CH$_{p\text{-sal.}}$), 140.1, 143.8 (2C$_{biph.}$), 153.1 (2C-O$_{biph.}$), 163.4 (2C-OH), 165.0 (2C=O); ESI-MS 424.9 (M–H)$^-$; elemental analysis (calcd., found for C$_{26}$H$_{18}$O$_6$·1/2H$_2$O): C (71.72, 71.75), H, (4.40, 4.72).

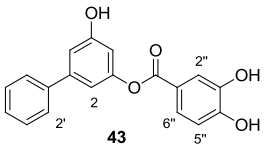

43

5-Hydroxybiphenyl-3-yl 3,4-dihydroxybenzoate (43). Obtained from silyl ether **101** (70 mg, 0.13 mmol) in 51% yield. R_f (DCM/MeOH, 97:3) 0.21; mp 174-175 ºC; IR (ATR) ν 3368 (OH), 1701 (C=O), 1608, 1523, 1447 (Ar), 1294, 1214 (C-O); ^{1}H NMR (300 MHz, acetone-d_6) δ 6.75 (t, J = 2.1, 1H, H$_4$), 6.99 (d, J = 8.1, 1H, H$_{5''}$), 7.02 (t, J = 1.7, 1H, H$_6$), 7.05 (t, J = 1.7, 1H, H$_2$), 7.36 (t, J = 7.3, 1H, H$_{4'}$), 7.45 (t, J = 7.4, 2H, H$_{3'}$, H$_{5'}$), 7.62-7.70 (m, 4H, H$_{2'}$, H$_{6'}$, H$_{2''}$, H$_{6''}$), 8.75 (br s, 3H, 3OH); ^{13}C NMR (75 MHz, acetone-d_6) δ 109.2 (C$_4$H), 112.0, 112.6 (CH$_{prot.}$, C$_6$H), 116.1 (C$_2$H), 117.7 (CH$_{prot.}$), 122.1 (C$_{prot.}$), 124.2 (CH$_{prot.}$), 127.7 (C$_{2'}$H, C$_{6'}$H), 128.6 (C$_{4'}$H), 129.7 (C$_{3'}$H, C$_{5'}$H), 141.1, 144.0 (2C$_{biph.}$), 145.9, 151.5 (2C-OH$_{prot.}$), 153.7 (C-O$_{biph.}$), 159.5 (C-OH$_{biph.}$), 165.2 (C=O); ESI-MS 321.0 (M–H)$^-$; elemental analysis (calcd., found for C$_{19}$H$_{14}$O$_5$·H$_2$O): C (67.05, 66.88), H, (4.74, 5.01).

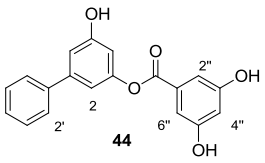

44

5-Hydroxybiphenyl-3-yl 3,5-dihydroxybenzoate (44). Obtained from silyl ether **102** (65 mg, 0.12 mmol) in 57% yield. R_f (DCM/MeOH, 95:5) 0.27; mp 200-203 ºC; IR (ATR) ν 3366 (OH), 1703 (C=O), 1601, 1483, 1456, 1425, 1346 (Ar), 1225 (C-O); ^{1}H NMR (300 MHz, acetone-d_6) δ 6.67 (t, J = 2.2, 1H, $H_{4''}$), 6.76 (t, J = 2.0, 1H, H_4), 7.04 (t, J = 1.9, 1H, H_6), 7.06 (t, J = 2.0, 1H, H_2), 7.17 (d, J = 2.2, 2H, $H_{2''}$, $H_{6''}$), 7.37 (t, J = 7.3, 1H, $H_{4'}$), 7.46 (t, J = 7.4, 2H, $H_{3'}$, $H_{5'}$), 7.66 (d, J =7.1, 2H, $H_{2'}$, $H_{6'}$), 8.72 (br s, 2H, 2OH), 8.84 (br s, 1H, 1OH); ^{13}C NMR (75 MHz, acetone-d_6) δ 108.7 ($C_{4''}$H), 109.1 (C_4H), 109.2 (2$CH_{α\text{-res.}}$), 112.2 (C_2H), 112.5 (C_6H), 127.7 ($C_{2'}$H, $C_{6'}$H), 128.6 ($C_{4'}$H), 129.7 ($C_{3'}$H, $C_{5'}$H), 132.5 ($C_{α\text{-res.}}$), 141.0, 144.1 (2$C_{biph.}$), 153.6 (C-$O_{biph.}$), 159.5 (C-$OH_{biph.}$), 159.7 (2C-$OH_{α\text{-res.}}$), 165.3 (C=O); ESI-MS 321.0 $(M–H)^–$; elemental analysis (calcd., found for $C_{19}H_{14}O_5 \cdot 1/2H_2O$): C (69.51, 69.28), H, (4.50, 4.87).

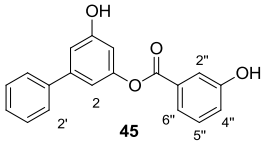

45

5-Hydroxybiphenyl-3-yl 3-hydroxybenzoate (45). Obtained from silyl ether **103** (82 mg, 0.20 mmol) in 84% yield. R_f (DCM/MeOH, 95:5) 0.30; mp 62-63 ºC; IR (ATR) ν 3363 (OH), 1709 (C=O), 1590, 1455 (Ar), 1286, 1205 (C-O); ^{1}H NMR (300 MHz, acetone-d_6) δ 6.78 (t, J = 2.1, 1H, H_4), 7.05-7.08 (m, 2H, H_2, H_6), 7.19 (ddd, J = 8.2, 2.6, 1.0, 1H, $H_{4''}$), 7.35-7.49 (m, 4H, $H_{3'}$, $H_{4'}$, $H_{5'}$, $H_{5''}$), 7.64-7.70 (m, 4H, $H_{2'}$, $H_{6'}$, $H_{2''}$, $H_{6''}$), 8.83 (br s, 2H, 2OH); ^{13}C NMR (75 MHz, acetone-d_6) δ 109.1 (C_4H), 112.2, 112.5 ($CH_{m\text{-sal.}}$, C_6H), 117.3 (C_2H), 121.6, 122.0 (2$CH_{m\text{-sal.}}$), 127.7 ($C_{2'}$H, $C_{6'}$H), 128.6 ($C_{4'}$H), 129.7 ($C_{3'}$H, $C_{5'}$H), 130.8 ($CH_{m\text{-sal.}}$), 131.9 ($C_{m\text{-sal.}}$), 141.0, 144.1 (2$C_{biph.}$), 153.5 (C-$O_{biph.}$), 158.6 (C-$OH_{m\text{-sal.}}$), 159.5 (C-$OH_{biph.}$), 165.3 (C=O); ESI-MS 304.8 $(M–H)^–$; elemental analysis (calcd., found for $C_{19}H_{14}O_4 \cdot 1/2H_2O$): C (72.37, 72.66), H, (4.79, 5.15).

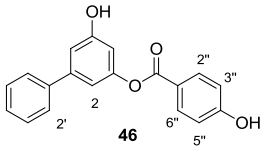

46

5-Hydroxybiphenyl-3-yl 4-hydroxybenzoate (46). Obtained from silyl ether **104** (32 mg, 0.08 mmol) in 90% yield. R_f (DCM/MeOH, 95:5) 0.19; mp 55-56 ºC; IR (ATR) ν 3354 (OH), 1696 (C=O), 1594, 1511, 1483, 1453 (Ar), 1263, 1164 (C-O); ^{1}H NMR (300 MHz, acetone-d_6) δ 6.76 (t, J = 2.2, 1H, H_4), 6.97-7.06 (m, 4H, H_2, H_6, $H_{3''}$, $H_{5''}$), 7.36 (t, J = 7.3, 1H, $H_{4'}$), 7.46 (t, J = 7.4, 2H, $H_{3'}$, $H_{5'}$), 7.65 (d, J = 7.1, 2H, $H_{2'}$, $H_{6'}$), 8.07 (d, J = 8.8, 2H, $H_{2''}$,$H_{6''}$), 8.84 (br s, 1H, OH), 9.39 (br s, 1H, OH); ^{13}C NMR (75 MHz, acetone-d_6) δ 109.2 (C_4H), 112.0 (C_6H), 112.6 (C_2H), 116.3 (2$CH_{p\text{-sal.}}$), 121.7 ($C_{p\text{-sal.}}$), 127.7 ($C_{2'}$H, $C_{6'}$H), 128.6 ($C_{4'}$H), 129.7 ($C_{3'}$H, $C_{5'}$H), 133.2 (2$CH_{p\text{-sal.}}$), 141.0, 144.0

($2CH_{biph.}$), 153.6 ($C\text{-}O_{biph.}$), 159.5 ($C\text{-}OH_{biph.}$), 163.3($C\text{-}OH_{p\text{-}sal.}$), 165.1 (C=O); ESI-MS 304.8 $(M–H)^-$; elemental analysis (calcd., found for $C_{19}H_{14}O_4 \cdot 4/3H_2O$): C (69.08, 69.35), H, (5.09, 5.26).

4.1.3. Synthesis of 33-36 and 47-50

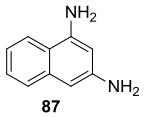

87

Naphthalene-1,3-diamine (87). To a solution of 1,3-dinitronaphthalene (1.0 g, 4.6 mmol) in MeOH (40 mL), 10% Pd/C (100 mg) was added and the reaction was stirred in a Parr hydrogenator under an initial hydrogen pressure of 40 psi at room temperature for 3.5 h. The mixture was filtered through a short column of Celite® and the solvent was evaporated under reduced pressure. The crude was purified by chromatography (from DCM to DCM/MeOH, 95:5) to afford diamine **87** as an oil in 60% yield. R_f (DCM) 0.14; IR (ATR) ν 3356 (NH_2), 1659, 1621 (Ar); ^{1}H NMR (300 MHz, DMSO-d_6) δ 4.99 (br s, 2H, NH_2), 5.42 (br s, 2H, NH_2), 6.11-6.12 (m, 2H, 2CH), 6.91 (t, J = 7.5, 1H, CH), 7.15 (t, J = 7.5, CH), 7.30 (d, J = 8.2, 1H, CH), 7.76 (d, J = 8.2, 1H, CH); ^{13}C NMR (75 MHz, DMSO-d_6) δ 96.5, 99.4 (2CH), 117.2 (C), 118.7, 122.1, 125.1, 125.5 (4CH), 136.2 (C), 145.1 (C-N), 147.3 (C-N); ESI-MS 159.0 $(M+H)^+$.

General Procedure for the Synthesis of Protected Amides 88 and 89. To a solution of **87** (1 equiv) and triethylamine (4 equiv) in anhydrous DCM (10 mL/mmol acid chloride **52**) under an argon atmosphere, a solution of the corresponding acid chloride **52a** or **f** (4 equiv) in anhydrous DCM (2.0 mL/mmol) was added dropwise. The reaction was stirred at room temperature overnight. Then, the crude was washed with a saturated aqueous solution of $NaHCO_3$ and with H_2O, the organic layer was dried (Na_2SO_4) and the solvent was evaporated under reduced pressure. The crude was purified by chromatography (from hexane to DCM) to afford protected amide **88** or **89**.

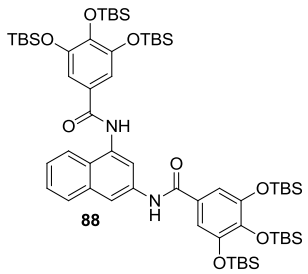

88

***N*,*N*'-Naphthalene-1,3-diylbis(3,4,5-tris{[*tert*-butyl(dimethyl)silyl]oxy}benzamide) (88).** Obtained from acid chloride **52a** (4.0 g, 7.6 mmol) and diamine **87** (300 mg, 1.9 mmol) in 33% yield. R_f (hexane/DCM, 1:1) 0.70; mp 170-172 ºC; IR (ATR) ν 3307 (NH), 1661 (C=O), 1572, 1477 (Ar);

^{1}H NMR (300 MHz, $CDCl_3$) δ 0.17 (s, 6H, $(CH_3)_2$Si *para*), 0.18 (s, 6H, $(CH_3)_2$Si *para*), 0.26 (s, 12H, 2$(CH_3)_2$Si *meta*), 0.29 (s, 12H, 2$(CH_3)_2$Si *meta*), 0.97 (s, 18H, 2$(CH_3)_3$CSi *meta*), 0.99 (s, 18H, 2$(CH_3)_3$CSi *meta*), 1.01 (s, 9H, $(CH_3)_3$CSi *para*), 1.02 (s, 9H, $(CH_3)_3$CSi *para*), 7.06 (s, 2H, $2CH_{gal.}$), 7.15 (s, 2H, $2CH_{gal.}$), 7.43-7.56 (m, 2H, $2CH_{naph.}$), 7.75-7.83 (m, 2H, $CH_{naph.}$, NH), 7.89 (dd, *J* = 7.8, 1.5, 1H, $CH_{naph.}$), 8.15-8.23 (m, 2H, $CH_{naph.}$, NH), 8.48 (d, *J* = 1.2, 1H, $CH_{naph.}$); ^{13}C NMR (75 MHz, $CDCl_3$) δ −3.8, −3.7 (2$(CH_3)_2$Si *para*), −3.5 (2$(CH_3)_2$Si *meta*), −3.4 (2$(CH_3)_2$Si *meta*), 18.6, 18.7 (2$(CH_3)_3$CSi *para*), 18.9 (2$(CH_3)_3$CSi *meta*), 19.0 (2$(CH_3)_3$CSi *meta*), 26.3 ($(CH_3)_3$CSi *para*), 26.4 (4$(CH_3)_3$CSi *meta*, $(CH_3)_3$CSi *para*), 113.3 ($2CH_{gal.}$, $CH_{naph.}$), 113.5 ($2CH_{gal.}$), 114.4, 119.6 ($2CH_{naph.}$), 123.7 ($C_{naph.}$), 125.5 ($CH_{naph.}$), 126.8 ($C_{gal.}$), 126.9 ($CH_{naph.}$), 127.2 ($C_{gal.}$), 129.3 ($CH_{naph.}$), 133.4, 134.9, 135.5 ($3C_{naph.}$), 142.6, 142.7 (2C-$O_{gal.}$ *para*), 149.1 (2C-$O_{gal.}$ *meta*), 149.2 (2C-$O_{gal.}$ *meta*), 165.1, 165.9 (2C=O); ESI-MS 1169.5 $(M+Na)^+$.

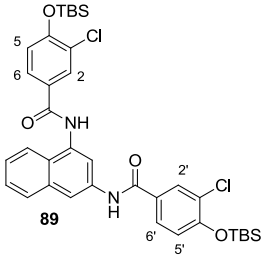

89

***N*,*N*'-Naphthalene-1,3-diylbis(4-{[*tert*-butyl(dimethyl)silyl]oxy}-3-chlorobenzamide) (89).** Obtained from acid chloride **52f** (700 mg, 2.3 mmol) and diamine **87** (90 mg, 0.57 mmol) in 36% yield. R_f (DCM) 0.34; mp 220-223 ºC; IR (ATR) ν 1645 (C=O), 1599, 1495 (Ar); ^{1}H NMR (300 MHz, $CDCl_3$) δ 0.26 (s, 6H, $(CH_3)_2$Si), 0.35 (s, 6H, $(CH_3)_2$Si), 1.08 (s, 9H, $(CH_3)_3$CSi), 1.13 (s, 9H, $(CH_3)_3$CSi), 6.72 (d, *J* = 8.4, 1H, H_5), 6.99 (d, *J* = 8.4, 1H, $H_{5'}$), 7.06 (t, *J* = 7.4, 1H, $CH_{naph.}$), 7.28-7.40 (m, 3H, $2CH_{naph.}$, H_6), 7.50 (d, *J* = 8.3, 1H, $H_{6'}$), 7.56 (s, 1H, $CH_{naph.}$), 7.66 (s, 2H, H_2, $H_{2'}$), 7.83 (d, *J* = 8.4, 1H, $CH_{naph.}$), 8.12 (d, *J* = 1.6, 1H, $CH_{naph.}$), 8.60 (s, 1H, NH), 8.67 (s, 1H, NH); ^{13}C NMR (75 MHz, $CDCl_3$) δ −4.2, −4.1 (2$(CH_3)_2$Si), 18.5, 18.6 (2$(CH_3)_3$CSi), 25.7, 25.8 (2$(CH_3)_3$CSi), 116.7, 118.4 ($2CH_{naph.}$), 119.9, 120.4 ($2CH_{Clbenz.}$), 120.8 ($C_{naph.}$), 125.1 ($CH_{naph.}$), 125.6, 125.8 ($2C_{Clbenz.}$), 126.2, 126.3, 127.1, 127.3 ($2CH_{Clbenz.}$, $2CH_{naph.}$), 128.0 ($C_{Clbenz.}$), 128.2 ($CH_{naph.}$), 128.3 ($C_{Clbenz.}$), 130.0, 130.3 ($2CH_{Clbenz.}$), 132.0, 134.0 (2C-N), 134.9 ($C_{naph.}$), 154.5, 155.1 (2C-O_{Clbenz}), 164.6, 165.9 (2C=O); ESI-MS 717.2 $(M+Na)^+$.

General Procedure for the Synthesis of Final Compounds 33 and 35. To a solution of TBS derivative **88** or **89** in a mixture of pyridine (0.96 mL/mmol of TBS group) and THF (2.0 mL/mmol of TBS group), HF·pyridine complex (0.96 mL/mmol of TBS group) was added, and the reaction was stirred at room temperature until the disappearance of the starting material (TLC analysis, approx. 15 min). Afterward, the mixture was diluted with water (50 mL/mmol) and extracted with ethyl

acetate. The organic layer was washed with a saturated aqueous solution of $CuSO_4$ and dried (Na_2SO_4). The solvent was evaporated under reduced pressure and the crude was purified by chromatography (DCM/MeOH, 95:5) to afford final compound **33** or **35**.

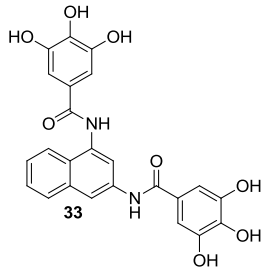

33

***N*,*N*'-Naphthalene-1,3-diylbis(3,4,5-trihydroxybenzamide) (33).** Obtained from silyl ether **88** (188 mg, 0.16 mmol) in 78% yield. R_f (DCM/MeOH, 95:5) 0.20; mp >250 ºC (decomposed); IR (ATR) ν 3297 (NH), 1600 (C=O), 1529, 1498 (Ar); ^{1}H NMR (300 MHz, methanol-d_4) δ 7.02 (s, 2H, $2CH_{gal.}$), 7.12 (s, 2H, $2CH_{gal.}$), 7.42-7.53 (m, 2H, $2CH_{naph.}$), 7.84-7.87 (m, 2H, $2CH_{naph.}$), 7.92 (d, *J* = 8.0, 1H, $CH_{naph.}$), 8.25 (d, *J* = 1.8, 1H, $CH_{naph.}$); ^{13}C NMR (75 MHz methanol-d_4) δ 108.2 ($2CH_{gal.}$), 108.4 ($2CH_{gal.}$), 117.7, 120.3, 123.8 ($3CH_{naph.}$), 126.2 ($C_{gal.}$), 126.3 ($CH_{naph.}$), 126.5 ($C_{gal.}$), 127.7 ($CH_{naph.}$), 128.3 ($C_{naph.}$), 129.1 ($CH_{naph.}$), 135.3, 136.0, 137.4 ($3C_{naph.}$), 138.5, 138.7 (2C-$O_{gal.}$ *para*), 146.8 (2C-$O_{gal.}$ *meta*), 146.8 (2C-$O_{gal.}$ *meta*), 169.3, 170.2 (2C=O); ESI-MS 460.7 $(M-H)^-$; elemental analysis (calcd., found for $C_{24}H_{18}N_2O_8 \cdot H_2O$): C (60.00, 59.97), H, (4.20, 4.02), N, (5.83, 6.06).

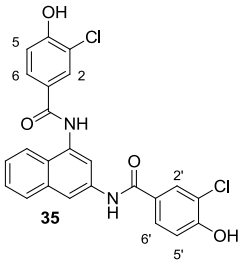

35

***N*,*N*'-Naphthalene-1,3-diylbis(3-chloro-4-hydroxybenzamide) (35).** Obtained from silyl ether **89** (36 mg, 0.05 mmol) in 75% yield. R_f (DCM/MeOH, 95:5) 0.42; mp 159-162 ºC (decomposed); IR (ATR) ν 3343 (OH), 1645 (C=O), 1546, 1492 (Ar); ^{1}H NMR (300 MHz, acetone-d_6) δ 7.13 (d, *J* = 8.5, 1H, H_5), 7.18 (d, *J* = 8.6, 1H, $H_{5'}$), 7.42 (ddd, *J* = 8.2, 6.9, 1.2, 1H, $CH_{naph.}$), 7.50 (ddd, *J* = 8.1, 7.4, 0.9, 1H, $CH_{naph.}$), 7.88 (d, *J* = 8.0, 1H, $CH_{naph.}$), 7.94 (dd, *J* = 8.5, 2.2, 1H, H_6), 8.02 (dd, *J* = 8.5, 2.2, 1H, $H_{6'}$), 8.06 (d, *J* = 8.5, 1H, $CH_{naph.}$), 8.12 (d, *J* = 2.2, 1H, H_2), 8.13 (d, *J* = 1.8, 1H, $CH_{naph.}$), 8.19 (d, *J* = 2.2, 1H, $H_{2'}$), 8.50 (d, *J* = 1.5, 1H, $CH_{naph.}$), 9.53 (br s, 2H, 2OH), 9.61 (br s, 1H, NH), 9.72 (br s, 1H, NH); ^{13}C NMR (75 MHz, acetone-d_6) δ 115.6, 117.2, 117.3, 118.1 ($2CH_{naph.}$,

$2CH_{Clbenz.}$), 121.1, 121.2 ($2C_{Clbenz.}$), 123.4, 125.5 ($2CH_{naph.}$), 126.8 ($C_{naph.}$), 127.3 ($CH_{naph.}$), 128.3, 128.5 ($2C_{Clbenz.}$), 128.9 ($2CH_{Clbenz.}$), 129.0 ($CH_{naph.}$), 130.5, 130.7 ($2CH_{Clbenz.}$), 135.1, 135.5, 137.5 ($3C_{naph.}$), 156.9, 157.0 ($2C\text{-}O_{Clbenz.}$), 164.9, 165.5 (2C=O); ESI-MS 465.0 $(M-H)^-$; elemental analysis (calcd., found for $C_{24}H_{16}N_2O_4 \cdot H_2O$): C (59.31, 59.40), H, (3.92, 3.74), N, (5.39, 5.77).

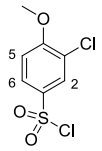

90

3-Chloro-4-methoxybenzenesulfonyl chloride (90).[96] To a solution of 2-chloroanisole (9.9 mL, 78 mmol) in chloroform (100 mL) at 0 ºC under an argon atmosphere, chlorosulfonic acid (10.5 mL, 156 mmol) was added dropwise and the reaction was stirred at room temperature overnight. The reaction mixture was then poured into ice-water (150 mL) and the aqueous phase was extracted with chloroform (2 x 50 mL). The combined organic phases were dried (Na_2SO_4) and concentrated under reduced pressure. The crude was purified by chromatography (from hexane to hexane/ethyl acetate, 9:1) to afford intermediate **90** as an oil in 61% yield. R_f (DCM) 0.41; IR (ATR) ν 1579, 1489 (Ar), 1375, 1173 (SO_2Cl); ^{1}H NMR (300 MHz, $CDCl_3$) δ 4.03 (s, 3H, CH_3), 7.08 (d, J = 8.9, 1H, H_5), 7.93 (d, J = 8.8, 2.4, 1H, H_6), 8.04 (d, J = 2.4, 1H, H_2); ^{13}C NMR (75 MHz, $CDCl_3$) δ 57.0 (CH_3), 111.9 (C_5H), 124.1 (C-Cl), 127.9, 129.3 (C_2H, C_6H), 136.5 ($C\text{-}SO_2$), 160.5 (C-O); ESI-MS 220.8 $(M_{SO_2H}-H)^-$. The spectroscopic data are in agreement with those previously described.[96]

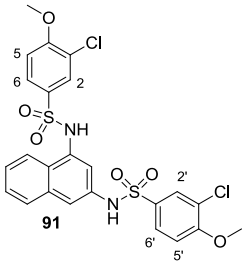

91

***N,N'*-Naphthalene-1,3-diylbis(3-chloro-4-methoxybenzenesulfonamide) (91).** To a solution of diamine **87** (150 mg, 0.95 mmol) and pyridine (0.31 mL, 3.8 mmol) in anhydrous DCM (20 mL) under an argon atmosphere, a solution of sulfonyl chloride **90** (500 mg, 1.6 mmol) in anhydrous DCM (8 mL) was added dropwise and the reaction was stirred at room temperature overnight. The crude was then washed with a saturated aqueous solution of $NaHCO_3$ and with water, and the organic layer was dried (Na_2SO_4) and concentrated under reduced pressure. The crude was purified by chromatography (from DCM to DCM/MeOH, 97:3) to afford compound **91** in 48% yield. R_f (DCM/MeOH, 95:5) 0.68; mp 131-133 ºC; IR (ATR) ν 3261 (NH), 1584, 1489 (Ar), 1161

(SO_2NH); ^1H NMR (300 MHz, acetone-d_6) δ 3.93 (s, 6H, $2CH_3$), 7.14 (d, J = 8.8, 1H, H_5), 7.18 (d, J = 8.8, 1H, $H_{5'}$), 7.34 (ddd, J = 8.2, 6.9, 1.2, 1H, $CH_{naph.}$), 7.43 (ddd, J = 8.1, 7.4, 1.0, 1H, $CH_{naph.}$), 7.53 (s, 2H, H_2, $H_{2'}$), 7.62 (dd, J = 8.7, 2.2, 1H, H_6), 7.73 (d, J = 2.3, 1H, $CH_{naph.}$), 7.74-7.77 (m, 2H, $CH_{naph.}$, $H_{6'}$), 7.83 (d, J = 2.3, 1H, $CH_{naph.}$), 8.00 (d, J = 8.4, 1H, $CH_{naph.}$), 9.10 (br s, 1H, NH), 9.27 (br s, 1H, NH); ^{13}C NMR (75 MHz, acetone-d_6) δ 57.1 ($2CH_3$), 113.1, 113.2 ($2CH_{Clbenz.}$), 116.1, 117.2, 123.1 ($3CH_{naph.}$), 123.2 ($2C_{Clbenz.}$), 126.2 ($CH_{naph.}$), 126.8 ($C_{naph.}$), 127.9, 128.6 ($2CH_{naph.}$), 128.8, 128.9 ($2CH_{Clbenz.}$), 129.7 ($2CH_{Clbenz.}$), 132.9, 133.3, 134.6, 135.4, 136.0 ($2C_{Clbenz.}$, $3C_{naph.}$), 159.3, 159.4 ($2C\text{-}O_{Clbenz.}$); ESI-MS 564.9 $(M-H)^-$.

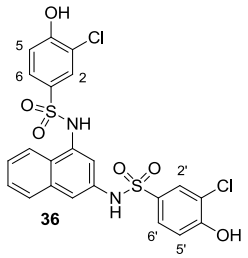

36

***N*,*N*'-Naphthalene-1,3-diylbis(3-chloro-4-hydroxybenzenesulfonamide) (36).** To a solution of sulfonamide **91** (100 mg, 0.18 mmol) in anhydrous DCM (5 mL) under an argon atmosphere, BBr_3 (0.1 mL, 1.1 mmol) was added at 0 ºC and the reaction was stirred at room temperature overnight. MeOH was then added dropwise to hydrolyze the remaining BBr_3 and the solvent was removed under reduced pressure. The residue was dissolved in diethyl ether, washed with water and dried (Na_2SO_4). The solvent was evaporated under reduced pressure and the crude was purified by chromatography (from DCM to DCM/MeOH, 95:5) to afford the title compound **36** in 38% yield. R_f (DCM/MeOH, 95:5) 0.35; mp 121-122 ºC; IR (ATR) ν 3346 (OH, NH), 1466, 1363 (Ar), 1180 (SO_2NH); ^1H NMR (300 MHz, $CDCl_3$) δ 7.02 (d, J = 8.6, 1H, H_5), 7.07 (d, J = 8.6, 1H, $H_{5'}$), 7.33 (ddd, J = 8.2, 6.9, 1.2, 1H, $CH_{naph.}$), 7.43 (ddd, J = 8.1, 7.0, 1.1, 1H, $CH_{naph.}$), 7.46 (dd, J = 8.5, 2.3, H_6), 7.50 (d, J = 2.1, 1H, $CH_{naph.}$), 7.53 (d, J = 1.9, 1H, $CH_{naph.}$), 7.60 (dd, J = 8.6, 2.2, 1H, $H_{6'}$), 7.70 (d, J = 2.2, 1H, H_2), 7.75 (d, J = 8.1, 1H, $CH_{naph.}$), 7.81 (d, J = 2.3, 1H, $H_{2'}$), 8.00 (d, J = 8.4, 1H, $CH_{naph.}$), 9.03 (br s, 1H, NH), 9.23 (br s, 1H, NH), 9.83 (br s, 2H, 2OH); ^{13}C NMR (75 MHz, $CDCl_3$) δ 116.2, 117.4 ($2CH_{naph.}$), 117.5 ($2CH_{Clbenz.}$), 121.5 ($2C_{Clbenz.}$), 123.2, 126.1 ($2CH_{naph.}$), 127.0 ($C_{naph.}$), 127.9, 128.5 ($2CH_{naph.}$), 128.6 ($2CH_{Clbenz.}$), 130.1, 130.2 ($2CH_{Clbenz.}$), 132.3, 132.7, 134.6, 135.4, 136.1 ($2C_{Clbenz.}$, $3C_{naph.}$), 157.7, 157.8 ($2C\text{-}O_{Clbenz.}$); ESI-MS 537.0 $(M-H)^-$; elemental analysis (calcd., found for $C_{22}H_{16}Cl_2N_2O_6S_2 \cdot H_2O$): C (47.40, 47.35), H, (3.25, 3.42), N, (5.03, 5.05), S, (11.50, 11.72).

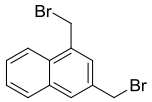

92

1,3-Bis(bromomethyl)naphthalene (92).[97] To a solution of a 1,3-dimethylnaphthalene (3.0 mL, 19 mmol) in anhydrous chloroform (30 mL) at 90 ºC under an argon atmosphere, NBS (8.0 g, 45 mmol) and AIBN (31 mg, 0.19 mmol) were added. The reaction was stirred at 90 ºC overnight. Then, the mixture was cooled to room temperature, filtered and the solvent was evaporated under reduced pressure. The crude was purified by chromatography (from hexane to hexane/ethyl acetate, 95:5) to afford intermediate **92** in 73% yield. mp 113-115 ºC (Lit.[98] 114-116 ºC); IR (ATR) ν 1508 (Ar), 783, 754 (C-Br); ^{1}H NMR (300 MHz, $CDCl_3$) δ 4.63 (s, 2H, CH_2), 4.94 (s, 2H, CH_2), 7.55 (t, *J* = 7.1, 1H, $CH_{naph.}$), 7.58 (s, 1H, $CH_{naph.}$), 7.63 (t, *J* = 7.3, 1H, $CH_{naph.}$), 7.83 (s, 1H, $CH_{naph.}$), 7.86 (d, *J* = 8.1, 1H, $CH_{naph.}$), 8.14 (d, *J* = 8.3, 1H, $CH_{naph.}$); ^{13}C NMR (75 MHz, $CDCl_3$) δ 31.4, 33.7 ($2CH_2$), 124.0, 127.2, 127.6, 128.8, 129.3, 129.8 ($6CH_{naph.}$), 131.0, 134.2, 134.6, 135.0 ($4C_{naph.}$); ESI-MS 331.9 $(M+NH_4)^+$. The spectroscopic data are in agreement with those previously described.[97]

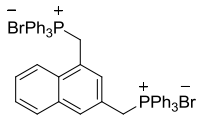

93

[Naphthalene-1,3-diyldi(methylene)]bis[bromo(triphenyl)phosphorane] (93). A mixture of bromo derivative **92** (390 mg, 1.2 mmol) and Ph_3P (720 mg, 2.7 mmol) in 10 mL of xylene was refluxed for 72 h under an argon atmosphere. The solvent was then evaporated under reduced pressure to afford the desired product in 96% yield. R_f (hexane) 0.31; mp 160-162 ºC; IR (ATR) ν 1437 (Ar); ^{1}H NMR (300 MHz, $CDCl_3$) δ 5.34 (d, *J* = 14.7, 2H, CH_2), 5.52 (d, *J* = 14.2, 2H, CH_2), 7.01 (t, *J* = 7.5, 1H, $CH_{naph.}$), 7.22 (t, *J* = 7.5, 1H, $CH_{naph.}$), 6.99-7.81 (m, 34H, $30CH_{Ph}$, $4CH_{naph.}$); ^{13}C NMR (75 MHz, $CDCl_3$) δ 28.1 (d, *J* = 47.3, CH_2), 30.6 (d, *J* = 47.3, CH_2), 116.8 (d, *J* = 17.7, $3C_{Ph}$), 118.0 (d, *J* = 18.3, $3C_{Ph}$), 123.4 (CH), 124.5, 124.6, 124.7 ($3C_{naph.}$), 126.5, 127.0 (2CH), 128.5 (d, *J* = 8.6, $4CH_{Ph}$) 128.6 (d, *J* = 10.5, $2CH_{Ph}$), 128.8 (d, *J* = 8.0, $2CH_{Ph}$) 130.2 (d, *J* = 10.3, $4CH_{Ph}$), 130.4 (d, *J* = 10.4, $4CH_{Ph}$), 131.9 (CH), 132.1 (d, *J* = 10.0, $2CH_{Ph}$), 133.0 ($C_{naph.}$), 133.6, 133.9 (2CH), 134.3 (d, *J* = 10.0, $4CH_{Ph}$), 134.4 (d, *J* = 9.9, $4CH_{Ph}$), 135.1 (CH), 135.2 (3CH); ESI-MS 339.2 $[(M+2H)/2]^+$.

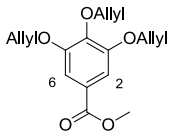

94

Methyl 3,4,5-tris(allyloxy)benzoate (94). To a suspension of methyl 3,4,5-trihydroxybenzoate (3.8 g, 21 mmol) and K_2CO_3 (26 g, 188 mmol) in anhydrous DMF (250 mL) at 65 ºC under an argon atmosphere, allyl bromide (7.2 mL, 83 mmol) was added dropwise and the reaction was stirred at 65 ºC for 4 h. Afterward, ice water (1 L) was added and the aqueous phase was extracted with ether (4 x 250 mL). The combined organic extracts were washed with water (3 x 500 mL) and brine (500 mL), dried (Na_2SO_4) and concentrated under reduced pressure to afford intermediate **94** as an oil in 99% yield. The compound was used in the next step without further purification. R_f (hexane/ethyl acetate, 9:1) 0.41; ^{1}H NMR (300 MHz, $CDCl_3$) δ 3.88 (s, 3H, CH_3), 4.60-4.62 (m, 6H, 3CH_2O), 5.18 (dq, *J* = 10.3, 1.9, 1H, CH=CHH *cis para*), 5.26-5.36 (m, 3H, CH=CHH *trans para*, 2CH=CHH *cis meta*), 5.43 (dq, *J* = 17.3, 1.6, 2H, 2CH=CHH *trans meta*), 6.00-6.15 (m, 3H, 3CH=CH_2), 7.28 (s, 2H, H_2, H_6); ESI-MS 305.1 $(M+H)^+$. The spectroscopic data are in agreement with those previously described.[99]

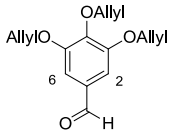

95

3,4,5-Tris(allyloxy)benzaldehyde (95). To a solution of Red-Al® (65% wt solution in toluene, 2.0 mL, 6.6 mmol) in anhydrous THF (1.4 mL) under an argon atmosphere, a solution of pyrrolidine (0.57 mL, 6.9 mmol) in THF (4.2 mL) was added at -10 ºC. The reaction was stirred for 1 h at room temperature and KO*t*-Bu (74 mg, 0.66 mmol) was then added. This mixture was added dropwise to a solution of methyl 3,4,5-tris(allyloxy)benzoate **94** (1.0 g, 3.3 mmol) in anhydrous THF (2 mL) at 0 ºC. The reaction mixture was stirred at this temperature for 10 min, after which a 1 M aqueous solution of HCl (80 mL) was slowly added. The reaction was then warmed to room temperature and extracted with ethyl acetate (120 mL). The organic layer was washed with water (50 mL) and with brine (50 mL), dried (Na_2SO_4) and evaporated under reduced pressure. The crude was purified by chromatography (hexane/ethyl acetate, 95:5) to afford aldehyde **95** as an oil in 78% yield. R_f (hexane/ethyl acetate, 9:1) 0.54; IR (ATR) ν 2870 (CHO), 1690 (C=O), 1581, 1494 (Ar); ^{1}H NMR (300 MHz, $CDCl_3$) δ 4.63-4.67 (m, 6H, 3CH_2O), 5.18 (dq, *J* = 10.3, 1.9, 1H, CH=CHH *cis para*), 5.28-5.37 (m, 3H, CH=CHH *trans para*, 2CH=CHH *cis meta*), 5.44 (dq, *J* = 17.3, 1.6, 2H, 2CH=CHH *trans meta*), 6.00-6.15 (m, 3H, 3CH=CH_2), 7.60 (s, 2H, H_2, H_6), 9.82 (s, 1H, CHO); ^{13}C

NMR (75 MHz, $CDCl_3$) δ 70.1 (2CH_2O *meta*), 74.3 (CH_2O *para*), 108.7 (C_2H, C_6H), 118.0 (2CH=$\underline{C}H_2$ *meta*), 118.3 (CH=$\underline{C}H_2$ *para*), 131.8 ($\underline{C}$-CHO), 132.9 (2$\underline{C}$H=CH_2 *meta*), 134.1 ($\underline{C}$H=CH_2 *para*), 143.4 (C-O *para*), 153.1 (2C-O *meta*), 191.2 (CHO); ESI-MS 275.1 $(M+H)^+$. The spectroscopic data are in agreement with those previously described.[100]

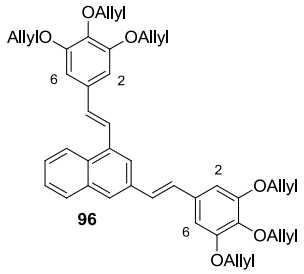

96

1,3-Bis{(*E*)-2-[3,4,5-tris(allyloxy)phenyl]vinyl}naphthalene (96). To a solution of **93** (710 mg, 0.84 mmol) in anhydrous THF (30 mL) under an argon atmosphere, *n*-butyllithium (1.6 M solution in hexane, 1.6 mL, 2.4 mmol) was added dropwise within a period of 1h at -78 ºC. The reaction mixture was stirred at this temperature for 1 h and a solution of aldehyde **95** (600 mg, 2.2 mmol) in anhydrous THF (10 mL) was slowly added. Then, the mixture was allowed to warm to room temperature and stirred for 18 h, before being quenched by addition of 2.0 mL of MeOH. The solvents were evaporated under reduced pressure and the crude was purified by chromatography (hexane/ethyl acetate, 97:3) to afford the desired (1*E*,3*E*)-**96** as an oil in 30% yield as well as the corresponding isomer (1*E*,3*Z*)-**96** in 18% yield.

(1*E*,3*E*)-96: R_f (hexane/ethyl acetate, 95:5) 0.33; IR (ATR) ν 1578, 1502 (C=C, Ar); ^{1}H NMR (300 MHz, $CDCl_3$) δ 4.60 (dt, *J* = 4.9, 1.2, 2H, CH_2O *para*), 4.62 (dt, *J* = 4.9, 1.3, 2H, CH_2O *para*), 4.65-4.70 (m, 8H, 4CH_2O *meta*), 5.21 (ddt, *J* = 10.3, 5.1, 1.8, 2H, 2CH=C$\underline{H}$H *cis para*), 5.29-5.40 (m, 6H, 2CH=CH$\underline{H}$ *trans para*, 4CH=C$\underline{H}$H *cis meta*), 5.41-5.44 (m, 4H, 4CH=CH$\underline{H}$ *trans meta*), 6.06-6.20 (m, 6H, 6C$\underline{H}$=CH_2), 6.82 (s, 2H, H_2, H_6), 6.86 (s, 2H, H_2, H_6), 7.10 (d, *J* = 15.9, 1H, C$\underline{H}$=CH), 7.14 (d, *J* = 16.3, 1H, C$\underline{H}$=CH), 7.20 (d, *J* = 16.3, 1H, CH=C$\underline{H}$), 7.48-7.54 (m, 2H, 2$CH_{naph.}$), 7.72 (d, *J* = 15.9, 1H, CH=C$\underline{H}$), 7.81 (s, 1H, $CH_{naph.}$), 7.86 (dd, *J* = 6.1, 3.4, 1H, $CH_{naph.}$), 7.91 (s, 1H, $CH_{naph.}$), 8.14 (dd, *J* = 6.2, 3.5, 1H, $CH_{naph.}$); ^{13}C NMR (75 MHz, $CDCl_3$) δ 70.2 (2CH_2O *meta*), 70.3 (2CH_2O *meta*), 74.4 (2CH_2O *para*), 106.2 (C_2H, C_6H), 106.4 (C_2H, C_6H), 117.5 (2CH=$\underline{C}H_2$ *meta*), 117.6 (2CH=$\underline{C}H_2$ *meta*), 117.7, 117.8 (2CH=$\underline{C}H_2$ *para*), 121.4, 123.9, 125.4, 126.2, 126.5, 126.6, 128.1, 128.8, 129.2 (9CH), 131.2 (C), 132.2 (CH), 133.0, 133.2 (2C), 133.5 (2$\underline{C}$H=CH_2 *meta*), 133.6 (2$\underline{C}$H=CH_2 *meta*), 134.2, 134.6 (2C), 134.7 (2$\underline{C}$H=CH_2 *para*), 135.6 (C), 138.1, 138.2 (2C-O *para*), 152.9 (2C-O *meta*), 153.0 (2C-O *meta*); ESI-MS 691.3 $(M+Na)^+$.

(1*E*,3*Z*)-96: R_f (hexane/ethyl acetate, 95:5) 0.27; IR (ATR) ν 1582, 1502 (C=C, Ar); ^{1}H NMR (300 MHz, $CDCl_3$) δ 4.11 (dt, *J* = 5.0, 1.5, 4H, $2CH_2O$ *meta*), 4.44 (d, *J* = 6.0, 2H, CH_2O *para*), 4.58 (d, *J* = 6.0, 2H, CH_2O *para*), 4.64 (dt, *J* = 5.1, 1.5, 4H, $2CH_2O$ *meta*), 5.04 (dq, *J* = 10.5, 5.4 , 2H, 2CH=CHH *cis*), 5.06-5.22 (m, 4H, 2CH=CHH *trans*, 2CH=CHH *cis*), 5.24-5.37 (m, 4H, 2CH=CHH *trans*, 2CH=CHH *cis*), 5.45 (dq, *J* = 17.3, 2.3 , 2H, 2CH=CHH *trans*), 5.75 (ddt, *J* = 17.2, 10.4, 5.1, 2H, 2CH=CH_2 *para*), 5.94-6.19 (m, 4H, 4CH=CH_2 *meta*), 6.34 (s, 2H, H_2, H_6), 6.73 (d, *J* = 12.2, 1H, CH=CH *cis*), 6.74 (s, 2H, H_2, H_6), 6.97 (d, *J* = 16.3, 1H, CH=CH *trans*), 6.98 (d, *J* = 11.5, 1H, CH=CH *cis*), 7.07 (d, *J* = 16.2, 1H, CH=CH *trans*), 7.39-7.51 (m, 2H, $2CH_{naph.}$), 7.65 (s, 1H, $CH_{naph.}$), 7.78 (s, 1H, $CH_{naph.}$), 7.84 (d, *J* = 7.7, 1H, $CH_{naph.}$), 7.98 (d, *J* = 8.1, 1H, $CH_{naph.}$); ^{13}C NMR (75 MHz, $CDCl_3$) δ 69.6 ($2CH_2O$ *meta*), 70.1 ($2CH_2O$ *meta*), 74.1, 74.3 ($2CH_2O$ *para*), 106.1 (C_2H, C_6H), 108.6 (C_2H, C_6H), 117.1 (2CH=CH_2 *meta*), 117.5 (2CH=CH_2 *meta*), 117.6, 117.7 (2CH=CH_2 *para*), 123.9, 125.3, 125.9, 126.3, 126.7, 127.7, 127.9, 128.5, 129.4 (9CH), 131.1, 131.9 (2C), 132.3 (CH), 132.9 (C), 133.3 (2CH=CH_2 *meta*), 133.5 (2CH=CH_2 *meta*), 134.2 (C), 134.6 (CH=CH_2 *para*), 134.7 (C, CH=CH_2 *para*), 135.6 (C), 137.2, 138.0 (2C-O *para*), 152.1 (2C-O *meta*), 152.9 (2C-O *meta*); ESI-MS 691.3 $(M+Na)^+$.

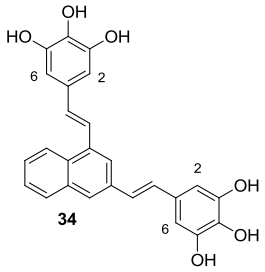

34

5,5'-{Naphthalene-1,3-diylbis[(*E*)ethene-2,1-diyl]}dibenzene-1,2,3-triol (34). A solution of (1*E*,3*E*)-**96** (76 mg, 0.11 mmol), *N,N'*-dimethylbarbituric acid (213 mg, 1.4 mmol) and $Pd(PPh_3)_4$ (39 mg, 0.03 mmol) in a 1:1 mixture of MeOH and anhydrous DCM (2 mL) was stirred for 1 h at room temperature under an argon atmosphere. Afterward, the solvent was evaporated under reduced pressure and DCM was added. The resulting solid was filtered and purified by chromatography (DCM/MeOH/acetic acid, 97:3:0.1) to afford the title compound **34** in 19% yield. R_f (DCM/MeOH/acetic acid, 97:3:0.1) 0.36; mp >300 ºC; IR (ATR) ν 1551, 1516 (C=C, Ar); ^{1}H NMR (300 MHz, acetone-d_6) δ 6.75 (s, 2H, H_2, H_6), 6.81 (s, 2H, H_2, H_6), 7.13 (d, *J* = 16.3, 1H, CH=CH), 7.15 (d, *J* = 15.9, 1H, CH=CH), 7.29 (d, *J* = 16.3, 1H, CH=CH), 7.47-7.52 (m, 2H, $2CH_{naph.}$), 7.74 (d, *J* = 16.0, 1H, CH=CH), 7.85 (s, 1H, $CH_{naph.}$), 7.89 (dd, *J* = 6.4, 3.1, 1H, $CH_{naph.}$), 7.95 (br s, 6H, 6OH), 8.06 (s, 1H, $CH_{naph.}$), 8.26 (dd, *J* = 6.2, 3.4, 1H, $CH_{naph.}$); ^{13}C NMR (75 MHz, acetone-d_6) δ 106.8 (C_2H, C_6H), 107.3 (C_2H, C_6H), 121.5, 123.3, 124.6, 126.2, 126.5, 126.7, 127.0, 129.4 (8CH), 130.0, 130.2 (2C), 130.6 (CH), 131.7 (C), 133.3 (CH), 134.2, 135.3, 136.1 (3C), 136.5 (2C-O *para*),

146.7 (4C-O *meta*); ESI-MS 427.0 $(M-H)^-$; elemental analysis (calcd., found for $C_{26}H_{20}O_6 \cdot H_2O$): C (68.56, 68.76), H, (5.06, 5.42).

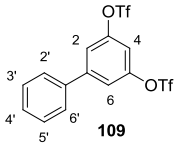

109

Biphenyl-3,5-diyl bis(trifluoromethanesulfonate) (109). To a solution of **97** (510 mg, 2.7 mmol) and triethylamine (0.77 mL, 5.8 mmol) in anhydrous DCM (9 mL) under an argon atmosphere, trifluoromethanesulfonic anhydride (Tf_2O) (1.2 mL, 6.9 mmol) was added dropwise at 0 ºC. The mixture was then warmed to room temperature and stirred for 2.5 h. Afterward, the reaction was cooled to 0 ºC and ice water was added to hydrolyze the remaining Tf_2O. A saturated aqueous solution of $NaHCO_3$ (5 mL) was added and the mixture was extracted with DCM (3 x 10 mL). The organic phases were dried over Na_2SO_4, filtered and the solvent was removed under reduced pressure. The crude was purified by chromatography (from hexane to hexane/ethyl acetate, 9:1) to afford the title compound **109** in 99% yield. R_f (hexane/ethyl acetate, 9:1) 0.57; mp 68-69 ºC; IR (ATR) ν 1459, 1428 (Ar), 1213 (SO_2); ^{1}H NMR (300 MHz, $CDCl_3$) δ 7.21 (t, *J* = 2.2, 1H, H_4), 7.47-7.57 (m, 7H, $7CH_{Ar}$); ^{13}C NMR (75 MHz, $CDCl_3$) δ 113.8 (C_4H), 118.9 (q, *J* = 321.1, $2CF_3$), 120.3 (C_2H, C_6H), 127.3 ($C_{3'}$H, $C_{5'}$H), 129.5 ($C_{2'}$H, $C_{6'}$H), 129.6 ($C_{4'}$H), 137.3, 146.0 ($2C_{biph.}$), 149.9 ($2C\text{-}O_{biph.}$); ESI-MS 317.0 $(M\text{-}SO_2CF_3-H)^-$.

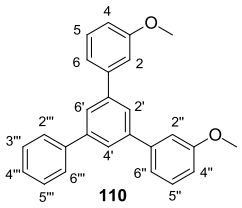

110

3,3''-Dimethoxy-5'-phenyl-1,1':3',1''-terphenyl (110). To a suspension of **109** (115 mg, 0.26 mmol), 3-methoxyphenylboronic acid (194 mg, 1.3 mmol) and Na_2CO_3 (118 mg, 2.1 mmol) in a 10:5:8 mixture of toluene, EtOH and water (5 mL) under an argon atmosphere, $Pd(PPh_3)_4$ (18 mg, 0.02 mmol) was added and the reaction was heated at 150 ºC in the microwave for 15 min. The mixture was extracted with ethyl acetate and the organic phase was dried (Na_2SO_4) and concentrated under reduced pressure. The crude was purified by chromatography (from hexane to DCM) to afford the title compound **110** in 75% yield. R_f (hexane/ethyl acetate, 1:1) 0.53; mp 114-116 ºC; IR (ATR) ν 1579, 1492, 1463, 1408 (Ar); ^{1}H NMR (300 MHz, $CDCl_3$) δ 3.89 (s, 6H, $2CH_3O$), 6.95 (dd, *J* = 8.1, 2.5, 2H, H_4, $H_{4''}$), 7.23 (t, *J* = 2.0, 2H, H_2, $H_{2''}$), 7.29 (d, *J* = 8.0, 2H, H_6, $H_{6''}$), 7.38-7.43 (m, 3H, $H_{3'''}$, $H_{4'''}$, $H_{5'''}$), 7.49 (t, *J* = 7.3, 2H, H_5, $H_{5''}$), 7.70 (d, *J* = 7.1, 2H, $H_{2'''}$, $H_{6'''}$), 7.78 (s, 3H,

$H_{2'}$, $H_{4'}$, $H_{6'}$); ^{13}C NMR (75 MHz, $CDCl_3$) δ 55.5 ($2CH_3O$), 113.1, 113.2, (C_2H, $C_{2''}H$, C_4H, $C_{4''}H$), 120.0 (C_6H, $C_{6''}H$), 125.4 ($C_{2'}H$), 125.5 ($C_{4'}H$, $C_{6'}H$), 127.5 ($C_{4'''}H$, $C_{6'''}H$), 127.7 ($C_{4'''}H$), 129.0 (C_5H, $C_{5''}H$), 130.0 ($C_{3'''}H$, $C_{5'''}H$), 142.4, 142.5, 142.8 (6C), 160.2 (2C-O); ESI-MS 367.1 $(M+H)^+$.

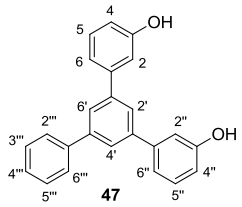

47

5'-Phenyl-1,1':3',1''-terphenyl-3,3''-diol (47). To a solution of intermediate **110** (70 mg, 0.19 mmol) in 5 mL of anhydrous DCM, BBr_3 (0.11 mL, 1.1 mmol) was added at 0 ºC under an argon atmosphere, and the reaction was stirred at room temperature for 3 h. Afterward, MeOH was added dropwise to hydrolyze the remaining BBr_3 and the mixture was concentrated under reduced pressure. The residue was dissolved in diethyl ether, washed with water and dried (Na_2SO_4). The solvent was evaporated under reduced pressure and the crude was purified by chromatography (from DCM to DCM/MeOH, 95:5) to afford the title compound **47** in 94% yield. R_f (DCM/MeOH, 95:5) 0.46; mp 270-272 ºC; IR (ATR) ν 3347 (OH), 1586, 1496, 1455, 1414 (Ar); ^{1}H NMR (300 MHz, acetone-d_6) δ 6.88 (app dt, J = 7.3, 1.7, 2H, H_4, $H_{4''}$), 7.26-7.27 (m, 2H, H_2, $H_{2''}$), 7.29-7.36 (m, 4H, $H_{3'''}$, $H_{5'''}$, H_6, $H_{6''}$), 7.41 (t, J = 7.3, 1H, $H_{4'''}$), 7.51 (t, J = 7.5, 2H, H_5, $H_{5''}$), 7.81-7.85 (m, 5H, $H_{2'}$, $H_{4'}$, $H_{6'}$, $H_{2'''}$, $H_{6'''}$), 8.58 (s, 2H, 2OH); ^{13}C NMR (75 MHz, acetone-d_6) δ 114.9 (C_2H, $C_{2''}H$), 115.4 (C_4H, $C_{4''}H$), 119.3 (C_6H, $C_{6''}H$), 125.4 ($C_{2'}H$), 125.5 ($C_{4'}H$, $C_{6'}H$), 128.1 ($C_{2'''}H$, $C_{6'''}H$), 128.5 ($C_{4'''}H$), 129.8 ($C_{5'}H$, $C_{5''}H$), 130.9 ($C_{3'''}H$, $C_{5'''}H$), 141.8, 143.1 (2C), 143.2, 143.3 (4C), 158.8 (2C-O); ESI-MS 337.1 $(M-H)^-$; elemental analysis (calcd., found for $C_{24}H_{18}O_2 \cdot 5/4H_2O$): C (79.87, 79.98), H, (5.73, 5.23).

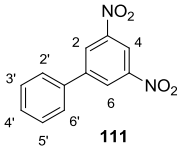

111

3,5-Dinitrobiphenyl (111). A suspension of 1-bromo-3,5-dinitrobenzene (500 mg, 2.3 mmol), phenylboronic acid (296 mg, 2.4 mmol), Na_2CO_3 (644 mg, 2.4 mmol) and $Pd(PPh_3)_4$ (117 mg, 0.10 mmol) in a 5:3 water of toluene and water (2 mL) was heated in the microwave at 150 ºC for 30 min. The mixture was extracted with ethyl acetate and the organic phase was dried (Na_2SO_4) and concentrated under reduced pressure. The crude was purified by chromatography (from hexane to DCM) to afford the desired product **111** in 83% yield. R_f (hexane/ethyl acetate, 9:1) 0.57; mp 151-153 ºC; IR (ATR) ν 1591, 1541, 1523, 1349 (Ar); ^{1}H NMR (300 MHz, $CDCl_3$) δ 7.53-7.60 (m, 3H,

$H_{3'}$, $H_{4'}$, $H_{5'}$), 7.69 (dd, *J* = 7.9, 1.5, 2H, $H_{2'}$, $H_{6'}$), 8.78 (d, *J* = 2.0, 2H, H_2, H_6), 9.02 (t, *J* = 2.0, 1H, H_4); ^{13}C NMR (75 MHz, $CDCl_3$) δ 117.2 ($C_{4'}H$), 127.1 (C_2H, C_6H), 127.4 ($C_{2'}H$, $C_{6'}H$), 129.8 ($C_{3'}H$, $C_{5'}H$), 130.0 ($C_{4'}H$), 136.6 (C_1), 145.0 ($C_{1'}$), 149.1 (2C-NO_2).

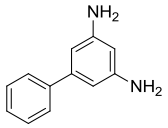

112

Biphenyl-3,5-diamine (112). A solution of dinitro derivative **111** (110 mg, 0.45 mmol) in anhydrous THF (10 mL) under an argon atmosphere was pumped through an H-Cube continuous-flow hydrogenation reactor at 1 mL/min using a 10% Pd/C CatCart® cartridge, under full-H_2 mode at room temperature. The resulting solution of diamine **112** was collected under an argon atmosphere protected from light to be directly used in the next reaction due to its unstability. The conversion into the diamino derivative was checked by TLC.

General Procedure for the Synthesis of Protected Diamide 113 and Sulfonamide 114. To the solution of diamine **112** (1 equiv) in anhydrous THF previously obtained, triethylamine (4 equiv) was added followed by dropwise addition of a solution of acid chloride **52d** or 3-methoxybenzenesulfonyl chloride (4 equiv) in anhydrous THF (2 mL/mmol) under an argon atmosphere. The reaction was protected from light and stirred at room temperature overnight. Then, the mixture was washed with a saturated aqueous solution of $NaHCO_3$ and with water, and the organic layer was dried (Na_2SO_4) and concentrated under reduced pressure. The crude was purified by chromatography using the appropriate eluent to afford the corresponding diamide **113** or disulfonamide **114**.

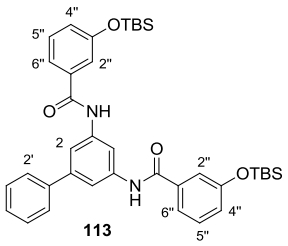

113

***N*,*N*'-Biphenyl-3,5-diylbis(3-{[*tert*-butyl(dimethyl)silyl]oxy}benzamide) (113).** Obtained from diamine **112** (0.45 mmol) and acid chloride **52d** (488 mg, 1.8 mmol) as an oil in 21% yield. Chromatography: hexane to DCM; R_f (DCM) 0.40; IR (ATR) ν 1652 (C=O), 1548, 1434 (Ar); ^{1}H NMR (300 MHz, $CDCl_3$) δ 0.23 (s, 12H, $2(CH_3)_2Si$), 1.01 (s, 18H, $2(CH_3)_3CSi$), 7.02 (ddd, *J* = 8.0, 1.5, 0.9, 2H, $2H_{4''}$), 7.30-7.44 (m, 9H, $H_{3'}$, $H_{4'}$, $H_{5'}$, $2H_{2''}$, $2H_{5''}$, $2H_{6''}$), 7.61 (d, *J* = 7.0, 2H, $H_{2'}$, $H_{6'}$), 7.73 (d, *J* = 1.7, 2H, H_2, H_6), 8.04-8.06 (m, 3H, H_4, 2NH); ^{13}C NMR (75 MHz, $CDCl_3$) δ −4.3

(2(CH_3)$_2$Si), 18.3 (2(CH_3)$_3$CSi), 25.8 (2(CH_3)$_3$CSi), 110.7 (C_4H), 115.0 (C_2H, C_6H), 119.3, 119.6, 123.9 (6$CH_{m\text{-sal.}}$), 127.4 ($C_{2'}$H, $C_{6'}$H), 127.9 ($C_{4'}$H), 128.9 ($C_{3'}$H, $C_{5'}$H), 130.0 (2$CH_{m\text{-sal.}}$), 136.4 (2$C_{m\text{-sal.}}$), 139.1 (2C-NH), 140.4 (C_1), 143.1 ($C_{1'}$), 156.3 (2C-$O_{m\text{-sal.}}$), 165.8 (2C=O); ESI-MS 651.3 $(M-H)^-$.

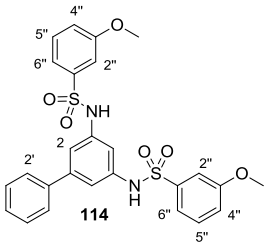

114

***N*,*N*'-Biphenyl-3,5-diylbis(3-methoxybenzenesulfonamide) (114).** Obtained from **112** (0.45 mmol) and 3-methoxybenzenesulfonyl chloride (372 mg, 1.8 mmol) in 45% yield. Chromatography: DCM to DCM/MeOH, 95:5; R_f (DCM/MeOH, 95:5) 0.58; mp 79-82 ºC; IR (ATR) ν 3253 (NH), 1483, 1439 (Ar), 1152 (SO_2); ^{1}H NMR (300 MHz, C_6D_6) δ 3.16 (s, 6H, 2CH_3O), 6.54 (br s, 2H, 2NH), 6.60 (ddd, J = 8.4, 2.6, 0.8, 2H, 2$H_{4''}$), 6.63 (d, J = 2.0, 2H, 2$H_{2''}$), 6.81 (t, J = 8.0, 2H, 2$H_{5''}$), 7.05-7.20 (m, 5H, $H_{2'}$, $H_{3'}$, $H_{4'}$, $H_{5'}$, $H_{6'}$), 7.34 (t, J = 1.9, 1H, H_4), 7.44 (d, J = 8.3, 2H, 2$H_{6''}$), 7.50 (t, J = 2.0, 2H, H_2, H_6); ^{13}C NMR (75 MHz, $CDCl_3$) δ 55.7 (2CH_3O), 111.6 (C_4H), 111.8 (C_2H, C_6H), 116.0, 119.5, 120.1 (6$CH_{m\text{-sal.}}$), 127.1 ($C_{2'}$H, $C_{6'}$H), 128.3 ($C_{4'}$H), 129.0 ($C_{3'}$H, $C_{5'}$H), 130.3 (2$CH_{m\text{-sal.}}$), 138.2 (2$C_{1''}$), 139.4 (C_1), 140.0 (2C-NH), 143.6 ($C_{1'}$), 160.0 (2C-$O_{m\text{-sal.}}$); ESI-MS 547.2 $(M+Na)^+$.

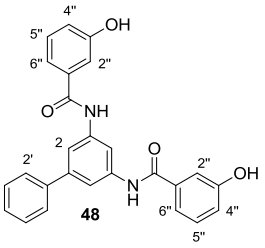

48

***N*,*N*'-Biphenyl-3,5-diylbis(3-hydroxybenzamide) (48).** To a solution of amide **113** (35 mg, 0.05 mmol) in a mixture of pyridine (0.10 mL, 0.96 mL/mmol of TBS group) and anhydrous THF (5 mL), HF·pyridine complex (0.10 mL, 0.96 mL/mmol of TBS group) was added and the reaction was stirred at room temperature until complete disappearance of the starting material (TLC, approx. 15 min). Then, the mixture was diluted with water (15 mL) and extracted with ethyl acetate. The organic layer was washed with a saturated aqueous solution of $CuSO_4$ and dried (Na_2SO_4). The solvent was evaporated under reduced pressure and the crude was purified by chromatography (from DCM to DCM/MeOH, 95:5) to afford pure final product **48** in 66% yield. R_f (DCM/MeOH, 95:5) 0.57; mp 95-96 ºC; IR (ATR) ν 3425 (OH), 1698 (C=O), 1422, 1363 (Ar); ^{1}H NMR (300 MHz,

acetone-d_6) δ 6.99 (dd, J = 8.1, 1.8, 2H, 2H$_{4''}$), 7.32 (t, J = 7.9, 2H, 2H$_{5''}$), 7.34-7.36 (m, 3H, 2H$_{2''}$, H$_{4'}$), 7.40 (d, J = 7.7, 2H, 2H$_{6''}$), 7.44 (t, J = 7.7, 2H, H$_{3'}$, H$_{5'}$), 7.66 (d, J = 7.3, 2H, H$_{2'}$, H$_{6'}$), 7.77 (d, J = 1.6, 2H, H$_2$, H$_6$), 8.08 (s, 1H, H$_4$); ^{13}C NMR (75 MHz, acetone-d_6) δ 114.1 (C$_4$H), 115.6 (2C$_{2''}$H), 117.1 (C$_2$H, C$_6$H), 119.5 (2C$_{6''}$H), 119.9 (2C$_{4''}$H), 128.1 (C$_{2'}$H, C$_{6'}$H), 128.7 (C$_{4'}$H), 129.9 (C$_{3'}$H, C$_{5'}$H), 130.7 (2C$_{5''}$H), 137.7 (2C$_{m\text{-sal.}}$), 140.7 (2C-NH), 141.9 (C$_1$), 143.5 (C$_{1'}$), 160.0 (2C-O$_{m\text{-sal.}}$), 169.1 (2C=O); ESI-MS 423.1 (M−H)$^-$; elemental analysis (calcd., found for C$_{26}$H$_{20}$N$_2$O$_4$·2/3H$_2$O): C (71.55, 71.93), H, (4.93, 4.96), N, (6.42, 6.23).

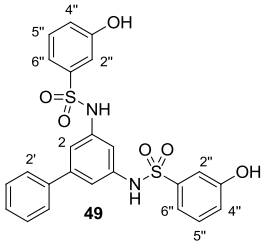

49

***N*,*N*'-Biphenyl-3,5-diylbis(3-hydroxybenzenesulfonamide) (49).** To a solution of sulfonamide **114** (50 mg, 0.10 mmol) in 5 mL of anhydrous DCM, BBr_3 (50 µL, 0.57 mmol) was added at 0 ºC under an argon atmosphere and the reaction was then stirred at room temperature for 3 h. Afterward, MeOH was added dropwise to hydrolyze the remaining BBr_3 and the mixture was concentrated under reduced pressure. The crude was dissolved in diethyl ether, washed with water and dried (Na_2SO_4). The solvent was evaporated under reduced pressure and the residue was purified by chromatography (from DCM to DCM/MeOH, 95:5) to afford the title compound **49** in 21% yield. R_f (DCM/MeOH, 95:5) 0.29; mp 154-157 ºC; IR (ATR) ν 3249 (NH, OH), 1480, 1448 (Ar), 1148 (SO_2); ^{1}H NMR (300 MHz, CD_3OD) δ 7.05 (ddd, J = 8.1, 2.4, 0.8, 2H, 2H$_{4''}$), 7.17 (d, J = 2.0, 2H, H$_2$, H$_6$), 7.25 (t, J = 2.0, 2H, H$_4$), 7.27 (dd, J = 6.7, 1.2, 2H, 2H$_{6''}$), 7.31 (t, J = 2.0, 2H, 2H$_{2''}$), 7.33 (t, J = 7.9, 2H, 2H$_{5''}$), 7.34-7.36 (m, 1H, H$_{4'}$), 7.41-7.44 (m, 4H, H$_{2'}$, H$_{3'}$, H$_{5'}$, H$_{6'}$,), 9.01, 9.12 (br s, 4H, 2OH, 2NH); ^{13}C NMR (75 MHz, CD_3OD) δ 111.5 (C$_4$H), 114.5 (2C$_{6''}$H), 115.2 (2C$_{2''}$H), 119.1 (C$_2$H, C$_6$H), 120.9 (2C$_{4''}$H), 127.5 (C$_{2'}$H, C$_{6'}$H), 128.8 (C$_{4'}$H), 129.8 (C$_{3'}$H, C$_{5'}$H), 131.1 (2C$_{5''}$H), 140.2 (2C$_{m\text{-sal.}}$), 140.7 (C$_1$), 141.8 (2C-NH), 143.5 (C$_{1'}$), 158.8 (2C-OH); ESI-MS 495.0 (M−H)$^-$; elemental analysis (calcd., found for C$_{24}$H$_{20}$N$_2$O$_6$S$_2$·H$_2$O): C (56.02, 55.86), H, (4.31, 4.55), N, (5.44, 5.20), S, (12.46, 12.60).

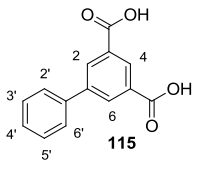

115

Biphenyl-3,5-dicarboxylic acid (115). A suspension of dimethyl 5-bromoisophthalate (500 mg, 1.8 mmol), phenylboronic acid (780 mg, 6.4 mmol), Na_2CO_3 (970 mg, 9.2 mmol) and $Pd(PPh_3)_4$ (106 mg, 0.09 mmol) in a 5:3 mixture of toluene and water (16 mL) under an argon atmosphere was heated at 150 ºC in the microwave for 30 min. The mixture was extracted with ethyl acetate and the organic phase was dried (Na_2SO_4) and evaporated under reduced pressure. The crude was purified by chromatography (from hexane to DCM) to afford dimethyl biphenyl-3,5-dicarboxylate in 90% yield. R_f (hexane/DCM, 3:7) 0.45; mp 94-96 ºC (Lit.[101] 90.9-92.4 ºC); IR (ATR) ν 1726 (C=O), 1435, 1339 (Ar); ^{1}H NMR (300 MHz, $CDCl_3$) δ 3.98 (s, 6H, $2CH_3O$), 7.41 (t, J = 7.2, 1H, $H_{4'}$), 7.49 (t, J = 7.4, 2H, $H_{3'}$, $H_{5'}$), 7.66 (d, J = 7.1, 2H, $H_{2'}$, $H_{6'}$), 8.47 (d, J = 1.5, 2H, H_2, H_6), 8.66 (t, J = 1.5, 1H, H_4); ^{13}C NMR (75 MHz, $CDCl_3$) δ 52.6 ($2CH_3O$), 127.3 ($C_{2'}H$, $C_{6'}H$), 128.4 ($C_{4'}H$), 129.2 ($C_{3'}H$, $C_{5'}H$), 129.5 (C_4H), 131.3 (C_3, C_5), 132.5 (C_2H, C_6H), 139.2 (C_1), 142.1 ($C_{1'}$), 166.4 (2CO); ESI-MS 293.1 $(M+Na)^+$. The spectroscopic data are in agreement with those previously described.[101]

Dimethyl biphenyl-3,5-dicarboxylate (440 mg, 1.6 mmol) was dissolved in THF (20 mL), a solution of NaOH (1.0 g, 26 mmol) in 25 mL of water was added and the mixture was refluxed for 1.5 h. Afterward, the organic solvent was evaporated under reduced pressure and the reaction was cooled to 0 ºC and acidified with concentrated HCl. The resulting precipitate was filtered, washed with water and dried under vacuum to obtain the title compound **115** in 85% yield. R_f (DCM) 0.05; mp >304 ºC (decomposed); IR (ATR) ν 1694 (C=O), 1461, 1431, 1406 (Ar); ^{1}H NMR (300 MHz, DMSO-d_6) δ 7.44 (t, J = 7.2, 1H, $H_{4'}$), 7.52 (t, J = 7.3, 2H, $H_{3'}$, $H_{5'}$), 7.74 (d, J = 7.2, 2H, $H_{2'}$, $H_{6'}$), 8.37 (d, J = 1.5, 2H, H_2, H_6), 8.46 (t, J = 1.4, 1H, H_4); ^{13}C NMR (75 MHz, DMSO-d_6) δ 126.9 ($C_{2'}H$, $C_{6'}H$), 128.4 ($C_{4'}H$), 128.8 (C_4H), 129.3 ($C_{3'}H$, $C_{5'}H$), 131.3 (C_2H, C_6H), 132.1 (C_3, C_5), 138.4 (C_1), 141.1 ($C_{1'}$), 166.5 (2CO); ESI-MS 241.1 $(M-H)^-$.

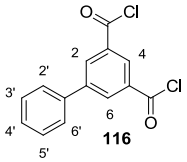

116

Biphenyl-3,5-dicarboxylic chloride (116). Thionyl chloride (0.34 ml, 4.6 mmol) was added dropwise to a solution of dicarboxylic acid **115** (140 mg, 0.58 mmol) in anhydrous THF (10 mL) under an argon atmosphere, and the mixture was refluxed for 3 h. Then it was cooled to room temperature and the solvent was removed under reduced pressure. Excess of thionyl chloride was removed by azeotropic destilation with toluene (4 x 10 mL) to afford the corresponding acid chloride **116** in quantitative yield which was used in the next step without further purification.

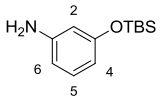

117

(3-{[*tert*-Butyl(dimethyl)silyl]oxy}phenyl)amine (117).[102] To a solution of imidazole (2.0 g, 29.3 mmol) and 3-hydroxyaniline (2.0 g, 18 mmol) in anhydrous DMF (40 mL) under an argon atmosphere, TBS chloride (3.6 g, 24 mmol) was added and reaction was stirred at room temperature overnight. Then, water (80 mL) was added and the mixture was extracted with ether (3 x 60 mL). The combined organic extracts were washed with brine, dried (Na_2SO_4) and concertrated under reduced pressure. The crude was purified by chromatography (from hexane to DCM) to afford amine **117** as an oil in 48% yield. R_f (hexane/DCM, 1:1) 0.36; IR (ATR) ν 3379 (NH), 1493, 1472, 1463 (Ar); ^{1}H NMR (300 MHz, $CDCl_3$) δ 0.21 (s, 6H, $(CH_3)_2Si$), 1.00 (s, 9H, $(CH_3)_3CSi$), 6.21 (t, J = 2.2, 1H, H_2), 6.27 (ddd, J = 8.1, 2.2, 0.8, 1H, H_6), 6.30 (ddd, J = 8.1, 2.2, 0.8, 1H, H_4), 7.00 (t, J = 8.0, 1H, H_5); ^{13}C NMR (75 MHz, $CDCl_3$) δ −4.3 ($(CH_3)_2Si$), 18.3 ($(CH_3)_3\underline{C}Si$), 25.8 ($(\underline{C}H_3)_3CSi$), 107.2, 108.6, 110.5 (C_2H, C_4H, C_6H), 130.1 (C_5H), 147.8 (C-N), 156.8 (C-O); ESI-MS 224.1 $(M+H)^+$. The spectroscopic data are in agreement with those previously described.[102]

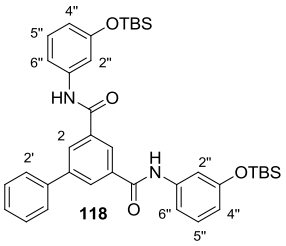

118

***N*,*N*'-Bis(3-{[*tert*-butyl(dimethyl)silyl]oxy}phenyl)biphenyl-3,5-dicarboxamide (118).** A solution of **116** (150 mg, 0.54 mmol) in THF (4.4 mL) was added dropwise to a solution of amine **117** (480 mg, 2.2 mmol) and triethylamine (0.30 mL, 2.2 mmol) in anhydrous THF (22 mL) under an argon atmosphere. The mixture was stirred at room temperature overnight. Afterward, the reaction mixture was washed with a saturated aqueous solution of $NaHCO_3$ and water, and the organic phase was dried (Na_2SO_4), filtered and concentrated under reduced pressure. The crude was purified by chromatography (from hexane to DCM) to afford the title compound **118** in 89% yield. R_f (hexane/DCM, 8:2) 0.23; mp 218-220 ºC; IR (ATR) ν 3292 (OH), 1651 (C=O), 1542, 1494, 1448 (Ar); ^{1}H NMR (300 MHz, $CDCl_3$) δ 0.26 (s, 12H, $2(CH_3)_2Si$), 1.01 (s, 18H, $2(CH_3)_3CSi$), 6.67 (ddd, J = 8.0, 2.3, 0.8, 2H, $2H_{4''}$), 7.24 (t, J = 8.1, 2H, $2H_{5''}$), 7.43-7.47 (m, 3H, $H_{4'}$, $2H_{6''}$), 7.55 (t, J = 7.4, 2H, $H_{3'}$, $H_{5'}$), 7.63 (t, J = 2.1, 2H, $2H_{2''}$), 7.81 (d, J = 7.2, 2H, $H_{2'}$, $H_{6'}$), 8.40 (d, J = 1.6, 2H, H_2, H_6), 8.48 (t, J = 1.6, 1H, H_4), 9.83 (s, 2H, NH); ^{13}C NMR (75 MHz, $CDCl_3$) δ −4.2 ($2(CH_3)_2Si$), 18.8 ($2(CH_3)_3\underline{C}Si$), 26.1 ($2(\underline{C}H_3)_3CSi$), 112.8 ($2C_{2''}H$), 114.0 ($2C_{6''}H$), 116.4 ($2C_{4''}H$), 126.3 (C_4H), 128.1 ($C_{2'}H$, $C_{6'}H$), 129.0 ($C_{4'}H$), 129.6 ($C_{3'}H$, $C_{5'}H$), 130.0 (C_2H, C_6H), 130.3 ($2C_{5''}H$), 137.3 (C_3, C_5), 140.4 (C_1), 141.3 (2C-NH), 142.5 ($C_{1'}$), 156.9 (2C-O), 165.6 (2C=O); ESI-MS 651.5 $(M+H)^+$.

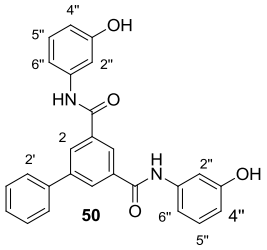

50

***N*,*N*'-Bis(3-hydroxyphenyl)biphenyl-3,5-dicarboxamide (50).** To a solution of silyl derivative **118** (150 mg, 0.23 mmol) in a mixture of pyridine (0.44 mL, 0.96 mL/mmol of TBS group) and anhydrous THF (10 mL) under an argon atmosphere, HF·pyridine complex (0.44 mL, 0.96 mL/mmol of TBS group) was added and the reaction mixture was stirred at room temperature. After the complete disappearance of the starting material (TLC, approx. 15 min), the reaction mixture was diluted with water (15 mL) and extracted with ethyl acetate. The organic layer was washed with a saturated aqueous solution of $CuSO_4$, dried (Na_2SO_4) and evaporated under reduced pressure and the resulting solid was purified by chromatography (DCM/MeOH, 95:5) to afford final compound **50** in 89% yield. R_f (DCM/MeOH, 95:5) 0.36; IR (ATR) ν 3379 (NH), 1493, 1472, 1463 (Ar); ^{1}H NMR (300 MHz, $CDCl_3$) δ 6.64 (ddd, J = 8.0, 2.3, 0.9, 2H, 2H$_{4''}$), 7.18 (t, J = 8.1, 2H, 2H$_{5''}$), 7.29 (d, J = 8.1, 2H, 2H$_{6''}$), 7.45 (t, J = 7.3, 1H, H$_{4'}$), 7.54 (t, J = 7.4, 2H, H$_{3'}$, H$_{5'}$), 7.58 (t, J = 2.1, 2H, 2H$_{2''}$), 7.81 (d, J = 7.3, 2H, H$_{2'}$, H$_{6'}$), 8.38 (d, J = 1.6, 2H, H$_2$, H$_6$), 8.47 (t, J = 1.5, 1H, H$_4$), 9.76 (s, 2H, OH); ^{13}C NMR (75 MHz, $CDCl_3$) δ 108.3 (2C$_{2''}$H), 111.9 (2C$_{4''}$H), 112.2 (2C$_{6''}$H), 126.4 (C$_4$H), 128.1 (C$_{2'}$H, C$_{6'}$H), 129.0 (C$_{4'}$H), 129.5 (C$_{3'}$H, C$_{5'}$H), 130.0 (C$_2$H, C$_6$H), 130.3 (2C$_{5''}$H), 137.4 (C$_3$, C$_5$), 140.4 (C$_1$), 141.3 (2C-NH), 142.4 (C$_{1'}$), 158.7 (2C-OH), 165.7 (2C=O); ESI-MS 423.1 $(M-H)^-$; elemental analysis (calcd., found for $C_{26}H_{20}N_2O_4 \cdot 5/4H_2O$): C (69.87, 70.02), H, (4.93, 5.07), N, (6.27, 6.01).

4.1.4. Synthesis of PC190723

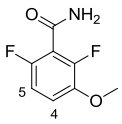

126

2,6-Difluoro-3-hydroxybenzamide (126).[70] To a suspension of 2,6-difluoro-3-methoxy benzoic acid (5.8 g, 31 mmol) in anhydrous toluene (40 mL) at room temperature under an argon atmosphere, thionyl chloride (3.4 mL, 46 mmol) was added dropwise and the reaction was refluxed for 5 h. Afterward, the reaction was cooled to room temperature and concentrated under reduced pressure. Then, a 28% aqueous ammonia solution (25 mL, 706 mmol) was added dropwise at 0 ºC and the reaction mixture was stirred at room temperature for 16 h. The solvent was evaporated under reduced pressure and the resulting solid was suspended in water and filtered. The collected solid was dried under vacuum to give intermediate **126** as a white solid (99% yield) that was used

without further purification. R_f (hexane/ethyl acetate, 3:7) 0.40; mp 167-169 ºC; IR (ATR) ν 3381, 3183 (NH_2), 1649 (C=O), 1591, 1490, 1451 (Ar); ^{1}H NMR (300 MHz, acetone-d_6) δ 3.88 (s, 3H, OCH_3), 6.97 (app td, J = 9.0, 2.0, 1H, C_5H), 7.18 (app td, J = 9.3, 5.1, 2H, C_4H), 7.18 (br s, $CONH_2$), 7.44 (br s, 1H, $CONH_2$); ^{13}C NMR (75 MHz, acetone-d_6) δ 57.1 (OCH_3), 111.4 (dd, J = 23.1, 4.2, C_5H), 115.1 (dd, J = 9.4, 2.8, C_4H), 117.3 (t, J = 21.6, C_1), 145.3 (dd, J = 11.0, 3.2, C_3), 149.5 (dd, J = 250.1, 8.1, CF), 153.4 (dd, J = 241.6, 6.5, CF), 162.2 ($CONH_2$); ESI-MS 188.1 $(M+H)^+$. The spectroscopic data are in agreement with those previously described.[70]

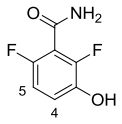

127

2,6-Difluoro-3-hydroxybenzamide (127).[71] To a suspension of methoxy derivative **126** (5.8 g, 31 mmol) in anhydrous DCM (60 mL) under an argon atmosphere, a 1 M solution of BBr_3 in DCM (62 mL, 62 mmol) was added dropwise. The reaction was stirred 3 days at room temperature. Then, the solvent was evaporated under reduced pressure and the residue was dissolved in ethyl acetate and washed with water (100 mL). The aqueous phase was extracted with ethyl acetate (3 x 100 mL) and the combined organic extracts were dried (Na_2SO_4) and concentrated under reduced pressure. The crude was purified by chromatography (from hexane to hexane/ethyl acetate, 3:7) to afford intermediate **127** in 79% yield. R_f (hexane/ethyl acetate, 2:8) 0.50; mp 123-124 ºC; IR (ATR) ν 3193 (NH_2), 1666 (C=O), 1596, 1493, 1396 (Ar); ^{1}H NMR (300 MHz, acetone-d_6) δ 6.87 (app td, J = 8.8, 1.8, 1H, C_5H), 7.01 (app td, J = 9.2, 5.4, 1H, C_4H), 7.17 (br s, 1H, $CONH_2$), 7.41 (br s, 1H, $CONH_2$), 8.79 (s, 1H, OH); ^{13}C NMR (75 MHz, acetone-d_6) δ 111.7 (dd, J = 23.3, 4.0, C_5H), 117.0 (t, J = 21.6, C_1), 118.7 (dd, J = 9.1, 3.7, C_4H), 142.3 (dd, J = 13.5, 3.2, C_3), 148.5 (dd, J = 245.4, 7.9, CF), 152.6 (dd, J = 240.3, 6.2, CF), 162.4 ($CONH_2$); ESI-MS 172.0 $(M-H)^-$. The spectroscopic data are in agreement with those previously described.[71]

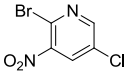

128

2-Bromo-5-chloro-3-nitropyridine (128).[70] To a solution of a 5-chloro-2-hydroxy-3-nitropyridine (1.5 g, 8.6 mmol) in a mixture of anhydrous toluene (15 mL) and DMF (2.5 mL) under an argon atmosphere, PBr_3 (1.2 mL, 13 mmol) was added dropwise and the reaction was heated at 130 ºC for 3 h. Afterward, the mixture was cooled to room temperature, water (50 mL) was added and the mixture was extracted with ethyl acetate (2 x 50 mL). The combined organic extracts were dried (Na_2SO_4) and concentrated under reduced pressure. The crude was purified by chromatography (from hexane to hexane/ethyl acetate, 9:1) to afford intermediate **128** in 42% yield.

R_f (hexane/ethyl acetate, 9:1) 0.48; ^{1}H NMR (300 MHz, $CDCl_3$) δ 8.14 (d, *J* = 2.3, 1H, CH), 8.57 (d, *J* = 2.3, 1H, CH). The spectroscopic data are in agreement with those previously described.[70]

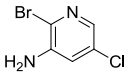

129

2-Bromo-5-chloropyridin-3-amine (129).[70] To a solution of **128** (854 mg, 3.6 mmol) in Et_2O (7 mL), a solution of $SnCl_2 \cdot 2H_2O$ (4.1 g, 18 mmol) in HCl (5.6 mL) was added dropwise and the reaction was heated at 50 ºC for 30 min. Then, the solvent was evaporated and the residue was dissolved in water (25 mL). A 28% aqueous ammonia solution was added until pH 10 and the mixture was extracted with ethyl acetate (2 x 50 mL). The combined organic extracts were dried (Na_2SO_4) and concentrated under reduced pressure. The crude was purified by chromatography (from hexane to hexane/ethyl acetate, 9:1) to afford intermediate **129** in 98% yield. R_f (hexane/ethyl acetate, 9:1) 0.31; ^{1}H NMR (300 MHz, $CDCl_3$) δ 7.00 (d, *J* = 2.2, 1H, CH), 7.75 (d, *J* = 2.3, 1H, CH). The spectroscopic data are in agreement with those previously described.[70]

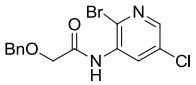

130

2-(Benzyloxy)-*N*-(2-bromo-5-chloropyridin-3-yl)acetamide (130).[70] To a solution of **129** (730 mg, 3.5 mmol) and Et_3N (0.54 mL, 3.9 mmol) in anhydrous DCM (11 mL) at 0 ºC under an argon atmosphere, a solution of benzyloxyacetyl chloride (0.66 mL, 4.2 mmol) in anhydrous DCM (4 mL) was added dropwise and the reaction was stirred at room temperature for 14 h. Then, the mixture was concentrated under reduced pressure and the residue was purified by chromatography (from hexane to hexane/ethyl acetate, 9:1) to afford intermediate **130** in 80% yield. R_f (hexane/ethyl acetate, 9:1) 0.32; ^{1}H NMR (300 MHz, $CDCl_3$) δ 4.15 (s, 2H, CH_2), 4.72 (s, 2H, CH_2), 7.35-7.41 (s, 5H, CH_{Bn}), 8.09 (d, *J* = 2.4, 1H, CH), 8.83 (d, *J* = 2.4, 1H, CH), 9.11 (br s, 1H, NH). The spectroscopic data are in agreement with those previously described.[70]

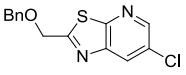

131

2-[(Benzyloxy)methyl]-6-chloro[1,3]thiazolo[5,4-*b*]pyridine (131).[71] To a solution of **130** (1.0 g, 2.8 mmol) in anhydrous toluene (20 mL) under an argon atmosphere, Lawesson's reagent (682 mg, 4.2 mmol) was added and the reaction was heated at 120 ºC for 3 h. Then, the mixture was concentrated under reduced pressure and the residue was purified by chromatography (from hexane to hexane/ethyl acetate, 9:1) to afford intermediate **131** in 79% yield. R_f (hexane/ethyl

acetate, 9:1) 0.50; ^{1}H NMR (300 MHz, $CDCl_3$) δ 4.74 (s, 2H, CH_2), 4.91 (s, 2H, CH_2), 7.35-7.41 (s, 5H, CH_{Bn}), 8.19 (d, *J* = 2.2, 1H, CH), 8.55 (d, *J* = 2.2, 1H, CH). The spectroscopic data are in agreement with those previously described.[71]

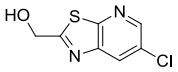

132

6-Chloro[1,3]thiazolo[5,4-*b*]pyridin-2-yl)methanol (132).[70] To a solution of **131** (647 mg, 2.2 mmol) in anhydrous DCM (3 mL) at -78 ºC under an argon atmosphere, a 1 M solution of BBr_3 in DCM (11 mL, 11 mmol) was added dropwise. The reaction was warmed to room temperature and stirred for 2 h. After this time, a saturated aqueous solution of $NaHCO_3$ (25 mL) was added and the mixture was extracted with ethyl acetate (3 x 25 mL). The combined organic extracts were dried over Na_2SO_4 and concentrated under reduced pressure. The crude was purified by chromatography (from hexane to hexane/ethyl acetate, 8:2) to afford intermediate **132** in 88% yield. R_f (hexane/ethyl acetate, 9:1) 0.15; ^{1}H NMR (300 MHz, DMSO-d_6) δ 4.88 (d, *J* = 5.9, 2H, CH_2), 6.46 (t, *J* = 5.9, 1H, OH), 8.54 (d, *J* = 2.3, 1H, CH), 8.66 (d, *J* = 2.2, 1H, CH). The spectroscopic data are in agreement with those previously described.[70]

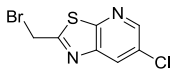

133

2-(Bromomethyl)-6-chloro[1,3]thiazolo[5,4-*b*]pyridine (133).[71] To a suspension of **132** (184 mg, 0.92 mmol) and Ph_3P (290 mg, 1.1 mmol) in anhydrous DCM (5 mL) under an argon atmosphere, NBS (240 mg, 1.3 mmol) was slowly added and the reaction was stirred at room temperature for 2.5 h. Then, a saturated aqueous solution of $NaHCO_3$ (25 mL) was added and the mixture was extracted with ethyl acetate (3 x 25 mL). The combined organic extracts were dried over Na_2SO_4 and concentrated under reduced pressure. The crude was purified by chromatography (from hexane to hexane/ethyl acetate, 95:5) to afford intermediate **133** in 68% yield. R_f (hexane/ethyl acetate, 9:1) 0.68; ^{1}H NMR (300 MHz, $CDCl_3$) δ 4.78 (s, 2H, CH_2), 8.24 (d, *J* = 2.2, 1H, CH), 8.58 (d, *J* = 1.8, 1H, CH). The spectroscopic data are in agreement with those previously described.[70]

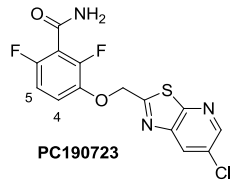

PC190723

3-[(6-Chloro[1,3]thiazolo[5,4-*b*]pyridin-2-yl)methoxy]-2,6-difluorobenzamide (PC190723).[71] To a suspension of hydroxybenzamide **127** (137 mg, 0.79 mmol), NaI (136 mg, 0.91 mmol), and K_2CO_3 (436 mg, 3.2 mmol) in anhydrous DMF (5 mL) under an argon atmosphere, bromo derivative **133** (240 mg, 0.91 mmol) was added. The reaction was stirred at room temperature overnight. Then, the mixture was concentrated under reduced pressure and the residue was purified by chromatography (hexane/ethyl acetate, from 6:4 to 1:1) to afford **PC190723** in 33% yield. R_f (hexane/ethyl acetate, 6:4) 0.52; mp 217-218 ºC (Lit.[71] 218 °C); ^{1}H NMR (300 MHz, DMSO-d_6) δ 5.73 (s, 2H, CH_2), 7.12 (app td, J = 9.1, 1.8, 1H, C_5H), 7.41 (app td, J = 9.4, 5.2, 1H, C_4H), 7.92 (br s, 1H, $CONH_2$), 8.19 (br s, 1H, $CONH_2$), 8.69 (d, J = 2.2, 1H, CH), 8.73 (d, J = 2.2, 1H, CH); elemental analysis (calcd., found for $C_{14}H_8ClF_2N_3O_2S$): C (47.27, 47.34), H, (2.27, 2.28), N (11.81, 11.59), S (9.01, 9.08). The spectroscopic data are in agreement with those previously described.[71]

4.1.5. Synthesis of 119-122

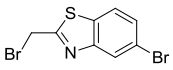

134

5-Bromo-2-(bromomethyl)-1,3-benzothiazole (134).[70] To a solution of a 2-methyl-5-bromobenzothiazole (5.0 g, 22 mmol) in CCl_4 (90 mL), NBS (7.8 g, 44 mmol) and AIBN (750 mg, 4.6 mmol) were added. The reaction was heated at 90 ºC for 3 h. After this time, the solvent was evaporated and the residue was purified by chromatography (from hexane to hexane/ethyl acetate, 95:5) to afford bromo derivative **134** in 13% yield. R_f (hexane/ethyl acetate, 1:1) 0.12; mp 110-112 ºC (Lit.[70] 116-117 °C); IR (ATR) ν 1730, 1583, 1542, 1507, 1435 (Ar); ^{1}H NMR (300 MHz, $CDCl_3$) δ 4.79 (s, 2H, CH_2), 7.54 (dd, J = 8.6, 1.8, 1H, C_6H), 7.74 (d, J = 8.6, 1H, C_7H), 8.17 (d, J = 1.8, 1H, C_4H); ^{13}C NMR (75 MHz, acetone-d_6) δ 27.0 (CH_2), 120.3 (C_5), 123.0 (C_7H), 126.6 (C_4H), 129.1 (C_6H), 135.3 (C_{7a}), 154.2 (C_{3a}), 168.3 (C_2); ESI-MS 307.8 $(M+H)^+$. The spectroscopic data are in agreement with those previously described.[70]

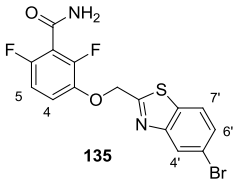

135

3-[(5-Bromo-1,3-benzothiazol-2-yl)methoxy]-2,6-difluorobenzamide (135).[71] To a suspension of **127** (532 mg, 3.1 mmol) and K_2CO_3 (1.3 g, 9.2 mmol) in anhydrous DMF (15 mL) under an argon atmosphere, bromo derivative **134** (943 mg, 3.1 mmol) was added and the reaction

was stirred at room temperature overnight. Then, the mixture was concentrated under reduced pressure and the residue was purified by chromatography (hexane/ethyl acetate, from 7:3 to 3:7) to afford intermediate **135** in 82% yield. R_f (hexane/ethyl acetate, 1:1) 0.25; mp 242-244 ºC; IR (ATR) ν 3373 (NH_2), 1669 (C=O), 1591, 1524, 1490 (Ar); ^{1}H NMR (300 MHz, DMSO-d_6) δ 5.70 (s, 2H, CH_2), 7.10 (app td, J = 9.0, 1.8, 1H, C_5H), 7.39 (app td, J = 9.4, 5.2, 1H, C_4H), 7.64 (dd, J = 8.6, 1.9 , 1H, $C_{6'}$H), 7.87 (br s, 1H, $CONH_2$), 8.13 (d, J = 8.6, 1H, $C_{7'}$H), 8.15 (br s, 1H, $CONH_2$), 8.25 (d, J = 1.9, 1H, $C_{4'}$H); ^{13}C NMR (75 MHz, DMSO-d_6) δ 68.6 (CH_2), 111.1 (dd, J = 23.4, 4.1, C_5H), 116.3 (dd, J = 9.4, 1.9, C_4H), 116.8 (dd, J = 24.8, 20.3, C_1), 119.2 ($C_{5'}$), 124.4 ($C_{7'}$H), 125.3 ($C_{4'}$H), 128.3 ($C_{6'}$H), 133.7 ($C_{7'a}$), 141.9 (dd, J = 11.0, 3.3, C_3), 148.1 (dd, J = 248.9, 9.1, CF), 152.5 (dd, J = 242.2, 7.1, CF), 153.7 ($C_{3'a}$), 161.1 ($C_{2'}$), 169.9 ($CONH_2$); ESI-MS 400.8 $(M+H)^+$. The spectroscopic data are in agreement with those previously described.[71]

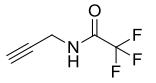

136

2,2,2-Trifluoro-*N*-prop-2-ynylacetamide (136).[103] To a solution of propargylamine (2.0 g, 36 mmol) in MeOH (30 mL), ethyl trifluoroacetate (4.3 mL, 36 mmol) was added dropwise and the reaction was stirred at room temperature overnight. Then, the solvent was evaporated under reduced pressure and the crude was purified by chromatography (DCM) to afford intermediate **136** in 60% yield. R_f (DCM) 0.37; IR (ATR) ν 3305 (NH), 1711 (C=O) ; ^{1}H NMR (300 MHz, $CDCl_3$) δ 2.32 (t, J = 2.6, 1H, CH), 4.13 (dd, J = 5.3, 2.5, 2H, CH_2), 6.80 (br s, 1H, NH); ^{13}C NMR (75 MHz, acetone-d_6) δ 29.8 (CH_2), 73.3 (CH), 77.4 (C), 115.7 (q, J = 288.0, CF_3), 157.1 (q, J = 37.4, CO); ESI-MS 150.0 $(M+H)^+$. The spectroscopic data are in agreement with those previously described.[103]

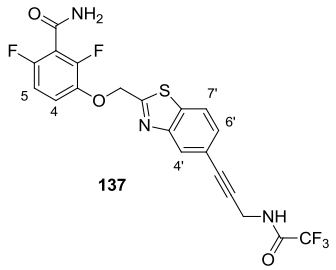

137

2,6-Difluoro-3-[(5-{3-[(trifluoroacetyl)amino]prop-1-ynyl}-1,3-benzothiazol-2-yl) methoxy]benzamide (137). A suspension of bromo derivative **135** (300 mg, 0.75 mmol), alkyne **136** (341 mg, 2.3 mmol), triethylamine (0.16 mL, 1.1 mmol), CuI (74 mg, 0.075 mmol) and $Pd(PPh_3)_4$ (87 mg, 0.075 mmol) in anhydrous DMF (15 mL) under an argon atmosphere was heated in the microwave at 100 ºC for 45 min. Then, the mixture was concentrated under reduced pressure and the residue was purified by chromatography (from hexane to ethyl acetate) to afford

intermediate **137** in 86% yield. R_f (hexane/ethyl acetate, 1:1) 0.16; mp 187-189 ºC; IR (ATR) ν 3301 (NH_2), 1716, 1679 (C=O), 1553, 1489, 1439 (Ar); ^{1}H NMR (300 MHz, DMSO-d_6) δ 4.32 (d, J = 5.6, 2H, C$\underline{H}_2$NH), 5.70 (s, 2H, CH_2O), 7.11 (app td, J = 8.9, 1.8, 1H, C_5H), 7.39 (app td, J = 9.3, 5.2, 1H, C_4H), 7.51 (dd, J = 8.4, 1.5, 1H, $C_{6'}$H), 7.88 (br s, 1H, $CONH_2$), 8.08 (d, J = 1.0, 1H, $C_{4'}$H), 8.16-8.18 (m, 2H, $C_{7'}$H, $CONH_2$), 10.10 (t, J = 5.3, 1H, NH); ^{13}C NMR (75 MHz, DMSO-d_6) δ 29.4 (CH_2NH), 68.6 (CH_2O), 82.1, 85.3 (C≡C), 111.1 (dd, J = 23.2, 4.0, C_5H), 116.2 (d, J = 9.3, C_4H), 116.6-117.0 (m, C_1, CF_3), 119.9 ($C_{5'}$), 123.1 ($C_{7'}$H), 125.5 ($C_{4'}$H), 128.3 ($C_{6'}$H), 135.1 ($C_{7'a}$), 141.9 (dd, J = 11.0, 3.2, C_3), 148.3 (dd, J = 248.7, 8.4, CF), 152.3 (dd, J = 242.2, 7.1, CF), 152.7 ($C_{3'a}$), 156.2 (d, J = 37.0, $\underline{C}OCF_3$), 161.1 ($C_{2'}$), 169.3 ($CONH_2$); ESI-MS 469.6 $(M+H)^+$.

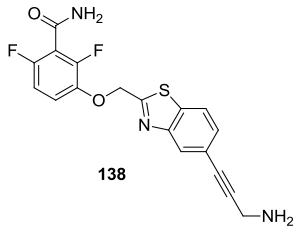

138

3-{[5-(3-Aminoprop-1-yn-1-yl)-1,3-benzothiazol-2-yl]methoxy}-2,6-difluorobenzamide (138). To a solution of intermediate **137** (70 mg, 0.15 mmol) in MeOH (15 mL), a 28% aqueous ammonia solution (10 mL, 282 mmol) was added and the reaction was stirred at room temperature overnight. Then, the solvent was evaporated under reduced pressure and the crude was triturated with Et_2O to afford amine **138** (99% yield) which was used in the next step without purification. ESI-MS 374.1 $(M+H)^+$.

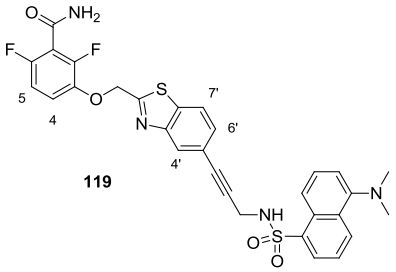

119

3-({5-[3-({[5-(Dimethylamino)-1-naphthyl]sulfonyl}amino)prop-1-ynyl]-1,3-benzothiazol-2-yl}methoxy)-2,6-difluorobenzamide (119). To a solution of the amine **138** (55 mg, 0.15 mmol) and triethylamine (62 μL, 0.44 mmol) in a 2:1 mixture of anhydrous DCM and DMF (3 mL) under an argon atmosphere, a solution of dansyl chloride (60 mg, 0.22 mmol) in anhydrous DCM (1 mL) was added. The reaction was stirred at room temperature for 24 h. Afterward, the solvent was evaporated under reduced pressure and the crude was purified by chromatography (from DCM to

ethyl acetate) to afford final compound **119** in 28% yield. R_f (ethyl acetate) 0.65; mp 194-196 ºC; IR (ATR) ν 1739 (C=O), 1489, 1461 (Ar); ^{1}H NMR (700 MHz, DMSO-d_6) δ 2.67 (s, 6H, $2CH_3$), 4.04 (d, J = 4.9, 2H, CH_2N), 5.67 (s, 2H, CH_2O), 6.79 (dd, J = 8.3, 1.4, 1H, CH_{DS}), 7.12 (app t, J = 9.0, 1H, C_5H), 7.21 (d, J = 7.4, 1H, CH_{DS}), 7.27 (d, J = 0.8, 1H, $C_{4'}H$), 7.38 (app td, J = 9.2, 5.1, 1H, C_4H), 7.58-7.63 (m, 2H, $C_{6'}H$, CH_{DS}), 7.90 (br s, 1H, $CONH_2$), 7.96 (d, J = 8.3, 1H, $C_{7'}H$), 8.17 (br s, 1H, $CONH_2$), 8.22 (dd, J = 7.2, 1.0, 1H, CH_{DS}), 8.32 (d, J = 8.6, 1H, CH_{DS}), 8.36 (d, J = 8.6, 1H, CH_{DS}), 8.53 (t, J = 5.0, 1H, $NHSO_2$); ^{13}C NMR (175 MHz, DMSO-d_6) δ 32.4 (CH_2N), 44.9 ($2CH_3$), 68.5 (CH_2O), 82.2, 86.3 (C≡C), 111.2 (dd, J = 25.0, 2.9, C_5H), 115.0 (CH_{DS}), 116.2 (d, J = 8.7, C_4H), 116.9 (dd, J = 25.5, 20.0, C_1), 119.2 (CH_{DS}), 119.6 ($C_{5'}$), 122.6 ($C_{7'}H$), 123.6 ($C_{4'}H$), 124.9 ($C_{6'}H$), 127.7, 127.8, 129.0 ($3CH_{DS}$), 129.4 (C_{DS}), 129.8 (CH_{DS}), 132.1 ($C_{7'a}$), 134.7, 136.0 ($2C_{DS}$), 142.3 (dd, J = 10.8, 2.4, C_3), 148.0 (dd, J = 248.8, 8.4, CF), 151.4 (C_{DS}), 152.1 ($C_{3'a}$), 152.5 (dd, J = 243.1, 6.7, CF), 161.1 ($C_{2'}$), 169.0 ($CONH_2$); ESI-MS 607.1 $(M+H)^+$; elemental analysis (calcd., found for $C_{30}H_{24}F_2N_4O_4S_2$): C (59.39, 59.57), H, (3.99, 4.27), N (9.27, 8.93), S (10.57, 10.77).

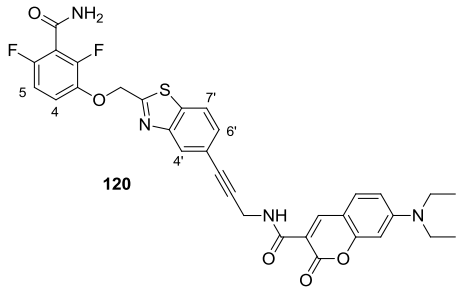

120

***N*-(3-(2-((3-Carbamoyl-2,4-difluorophenoxy)methyl)benzo[*d*]thiazol-5-yl)prop-2-ynyl)-7-(diethylamino)-2-oxo-2*H*-chromene-3-carboxamide (120).** To a solution of amine **138** (119 mg, 0.32 mmol), PyBroP® (268 mg, 0.57 mmol) and DIPEA (111 μL, 0.64 mmol) in anhydrous DMF (5 mL) under an argon atmosphere, a solution of 7-diethylaminocoumarin-3-carboxylic acid (100 mg, 0.38 mmol) in anhydrous DMF (1 mL) was added. The reaction was stirred at room temperature for 4 h. Afterward, the solvent was evaporated under reduced pressure and the crude was purified by chromatography (from DCM to ethyl acetate) to afford final compound **120** in 5% yield. R_f (ethyl acetate) 0.70; mp 248-249 ºC; ^{1}H NMR (700 MHz, DMSO-d_6) δ 1.17 (t, J = 7.0, 6H, $2CH_3$), 3.50 (q, J = 6.9, 4H, $2CH_2$), 4.43 (d, J = 5.5, 2H, $C\underline{H}_2NH$), 5.71 (s, 2H, CH_2O), 6.64 (d, J = 2.0, 1H, $CH_{coum.}$), 6.83 (dd, J = 8.9, 2.1, 1H, $CH_{coum.}$), 7.13 (app t, J = 8.8, 1H, C_5H), 7.40 (app td, J = 9.1, 5.1, 1H, C_4H), 7.52 (dd, J = 8.3, 1.1, 1H, $C_{6'}H$), 7.72 (d, J = 9.1, 1H, $CH_{coum.}$), 7.90 (s, 1H, $CONH_2$), 8.08 (s, 1H, $CH_{4'}$), 8.16 (d, J = 8.4, 1H, $C_{7'}H$), 8.18 (s, 1H, $CONH_2$), 8.72 (s, 1H, $CH_{coum.}$), 9.00 (t, J = 5.5, 1H, NH); ^{13}C NMR (175 MHz, DMSO-d_6) δ 12.3 ($2CH_3$), 29.2 (CH_2NH), 44.4 ($2CH_2$), 68.8 (CH_2O), 81.1, 87.5 (2C≡C), 95.9 ($CH_{coum.}$), 107.7, 108.8 ($2C_{coum.}$), 110.2 ($CH_{coum.}$), 111.1 (dd, J = 24.3, 4.2, C_5H), 116.2 (d, J = 9.9, C_4H), 117.1-117.0 (m, C_1), 120.4 ($C_{5'}$), 123.0 ($C_{7'}H$), 125.4 ($C_{4'}H$) 128.4

($CH_{coum.}$), 132.0 ($C_{6'}H$), 134.8 ($C_{7'a}$), 141.8-142.1 (m, C_3), 148.2 ($CH_{coum.}$), 149.2 (d, J = 265.5, CF), 152.4 (d, J = 242.0, CF), 152.5 ($C_{3'a}$), 152.6, 157.4 ($2C_{coum.}$), 161.1 (CONH), 161.7 ($C_{2'}$), 162.2 ($C{=}O_{coum.}$), 169.2 ($CONH_2$); ESI-MS 617.2 $(M+H)^+$; elemental analysis (calcd., found for $C_{32}H_{26}F_2N_4O_5S{\cdot}3H_2O$): C (57.31, 57.21), H, (4.81, 4.55), N (8.35, 7.96), S (4.78, 4.58).

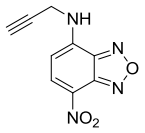

139

7-Nitro-*N*-prop-2-yn-1-yl-2,1,3-benzoxadiazol-4-amine (139).[104] To a solution of Cl-NBD (1.0 g, 5.0 mmol) in anhydrous acetonitrile (40 mL) under an argon atmosphere, propargylamine (0.64 mL, 10 mmol) was added and the reaction was stirred for 2 h at room temperature. Then, the solvent was evaporated under reduced pressure and the crude was purified by chromatography (from hexane to ethyl acetate) to afford intermediate **139** in 35% yield. mp 145-146 ºC (Lit.[104] 145-147 ºC) ^{1}H NMR (300 MHz, acetone-d_6) δ 2.47 (t, J = 2.5, 1H, C≡CH), 4.34 (dd, J = 5.9, 2.5, 2H, CH_2), 6.41 (d, J = 8.7, 1H, CH_{NBD}), 8.06 (br s, 1H, NH), 8.49 (d, J = 8.6, 1H, CH_{NBD}). The spectroscopic data are in agreement with those previously described.[104]

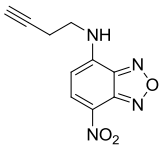

140

***N*-But-3-yn-1-yl-7-nitro-2,1,3-benzoxadiazol-4-amine (140).** To a solution of Cl-NBD (1.1 g, 5.3 mmol) and DIPEA (4.8 mL, 27 mmol) in MeOH (50 mL) under an argon atmosphere, a solution of 1-amino-3-butyne (0.64 mL, 5.3 mmol) in MeOH (50 mL) was added and the reaction was stirred for 15 h at room temperature. Then, the solvent was evaporated under reduced pressure and the crude was purified by chromatography (from hexane to DCM) to afford intermediate **140** in 77% yield. R_f (DCM) 0.59; mp 134-136 ºC; IR (ATR) ν 3286 (NH), 1582, 1496 (Ar), 1299 (NO_2); ^{1}H NMR (300 MHz, acetone-d_6) δ 2.50 (t, J = 2.6, 1H, C≡CH), 2.74 (td, J = 7.0, 2.7, 2H, CH_2), 3.83-3.86 (m, CH_2N), 6.54 (d, J = 8.8, 1H CH_{NBD}), 8.28 (s, 1H, NH), 8.51 (d, J = 8.8, 1H, CH_{NBD}); ^{13}C NMR (75 MHz, acetone-d_6) δ 18.9 (CH_2), 43.4 (CH_2N), 71.9 (<u>C</u>H≡C), 81.6 (CH≡<u>C</u>), 100.2 (br s, CH_{NBD}), 123.9 (C_{NBD}), 137.6 (CH_{NBD}), 145.1(C_{NBD}), 145.5 ($2C_{NBD}$); ESI-MS 233.0 $(M+H)^+$.

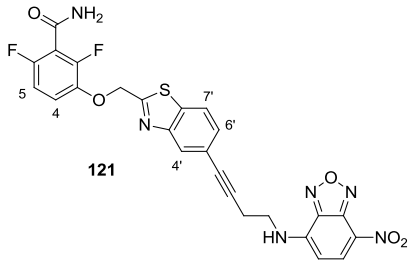

121

2,6-Difluoro-3-[(5-{4-[(7-nitro-2,1,3-benzoxadiazol-4-yl)amino]but-1-yn-1-yl}-1,3-benzothiazol-2-yl)methoxy]benzamide (121). A suspension of bromo derivative **135** (150 mg, 0.38 mmol), alkyne **140** (262 mg, 1.13 mmol), $Pd(PPh_3)_4$ (37 mg, 0.02 mmol), CuI (43 mg, 0.04 mmol) and triethylamine (79 µL, 0.56 mmol) in anhydrous DMF (8 mL) under an argon atmosphere was heated in the microwave at 100 ºC for 1 h. Then, the mixture was concentrated under reduced pressure and the residue was purified by chromatography (from hexane to ethyl acetate) to afford final compound **121** in 41% yield. R_f (hexane/ethyl acetate, 1:1) 0.29; mp 189-192 ºC; IR (ATR) ν 3405 (NH_2), 1684 (C=O), 1623, 1584, 1489 (Ar); ^{1}H NMR (700 MHz, DMSO-d_6) δ 2.46-2.55 (m, 2H, CH_2N), 2.91 (t, J = 6.7, 2H, CH_2), 5.68 (s, 2H, CH_2O), 6.59 (d, J = 9.0, 1H, CH_{NBD}), 7.11 (app td, J = 9.1, 1.7, 1H, C_5H), 7.28-7.46 (m, 2H, C_4H, $C_{6'}H$), 7.89 (br s, 1H, $CONH_2$), 7.97 (s, 1H, $C_{4'}H$), 8.10 (d, J = 8.4, 1H, $C_{7'}H$), 8.18 (br s, 1H, $CONH_2$), 8.52 (d, J = 8.7, 1H, CH_{NBD}), 9.62 (br s, 1H, NH_{NBD}); ^{13}C NMR (175 MHz, DMSO-d_6) δ 19.0 (CH_2), 42.2 (CH_2N), 68.6 (CH_2O), 81.5, 88.1 (C≡C), 99.7 (br s, CH_{NBD}), 111.1 (dd, J = 23.0, 3.8, C_5H), 116.2 (d, J = 9.4, C_4H), 116.6 (dd, J = 25.3, 20.3, C_1), 120.9 ($C_{5'}$), 122.9 ($C_{7'}H$), 125.3 ($C_{4'}H$), 128.2 ($C_{6'}H$), 128.7 (C_{NBD}), 134.5 ($C_{7'a}$), 137.7 (br s, CH_{NBD}), 141.9 (dd, J = 11.1, 3.2, C_3), 144.1, 144.3, 144.4 ($3C_{NBD}$), 148.0 (dd, J = 248.6, 8.2, CF), 152.4 ($C_{3'a}$), 152.5 (dd, J = 242.6, 7.7, CF), 161.1 ($C_{2'}$), 169.0 ($CONH_2$); ESI-MS 551.1 $(M+H)^+$; elemental analysis (calcd., found for $C_{25}H_{16}F_2N_6O_5S$): C (54.55, 54.45), H, (2.93, 3.32), N (15.27, 14.98), S (5.82, 5.71).

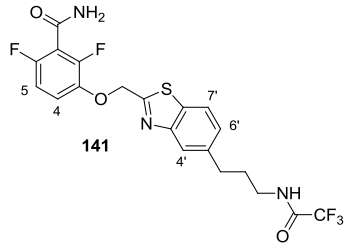

141

2,6-Difluoro-3-[(5-{3-[(trifluoroacetyl)amino]propyl}-1,3-benzothiazol-2-yl)methoxy] benzamide (141). To a suspension of alkyne **137** (250 mg, 0.53 mmol) in a mixture of anhydrous THF (20 mL) and MeOH (40 mL) under an argon atmosphere, Raney-Ni (1 mL, slurry in water) was added. The reaction was stirred under hydrogen atmosphere (1 bar) at room temperature for 3 h.

Then, the mixture was filtered through Celite® and concentrated under reduced pressure. The crude was purified by chromatography (from hexane to ethyl acetate) to afford intermediate **141** in 22% yield. R_f (hexane/ethyl acetate, 1:1) 0.16; mp 102-104 ºC; IR (ATR) ν 3303 (NH), 1710, 1680 (C=O), 1489 (Ar); ^{1}H NMR (300 MHz, DMSO-d_6) δ 1.96 (qt, J = 7.5, 2H, $CH_2C\underline{H}_2CH_2$), 2.82 (t, J = 7.7, 2H, CH_2Ar), 3.34 (t, J = 7.2, 2H, CH_2N), 5.57 (s, 2H, CH_2O), 6.97 (app td, J = 8.9, 1.8, 1H, C_5H), 7.32 (app td, J = 9.2, 5.0, 1H, C_4H), 7.35 (dd, J = 8.3, 1.3, 1H, $C_{6'}H$), 7.54-7.64 (m, 3H, $CONH_2$, CONH), 7.84 (s, 1H, $C_{4'}H$), 7.92 (d, J = 8.3, 1H, $C_{7'}H$); ^{13}C NMR (75 MHz, DMSO-d_6) δ 31.7, 33.9 (CH_2CH_2Ar), 40.3 (CH_2NH), 70.4 (CH_2O), 112.1 (dd, J = 23.7, 3.7, C_5H), 117.0-117.2 (m, C_1), 117.6 (q, J = 286.0, CF_3) 118.7 (d, J = 9.2, C_4H), 123.2 ($C_{7'}H$), 127.8 ($C_{4'}H$), 130.0 ($C_{6'}H$), 133.9 ($C_{5'}$), 141.7 ($C_{7'a}$), 143.8 (dd, J = 11.2, 2.4, C_3), 150.7 (dd, J = 252.3, 8.2, CF), 154.2 ($C_{3'a}$), 154.9 (dd, J = 244.5, 6.6, CF), 159.0 (d, J = 36.8, $\underline{C}OCF_3$), 165.0 ($C_{2'}$), 169.7 ($CONH_2$); ESI-MS 473.7 $(M+H)^+$.

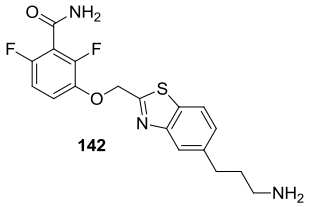

142

3-{[5-(3-Aminopropyl)-1,3-benzothiazol-2-yl]methoxy}-2,6-difluorobenzamide (142). To a solution of intermediate **141** (60 mg, 0.13 mmol) in MeOH (20 mL), a 28% aqueous ammonia solution (7.8 mL) was added and the reaction was stirred at room temperature overnight. Then, the solvent was evaporated under reduced pressure to afford amine **142** (99% yield) which was used without purification. ESI-MS 378.1 $(M+H)^+$.

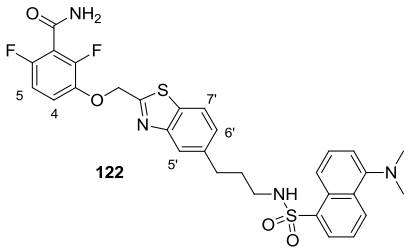

122

3-({5-[3-({[5-(Dimethylamino)-1-naphthyl]sulfonyl}amino)propyl]-1,3-benzothiazol-2-yl}methoxy)-2,6-difluorobenzamide (122). To a solution of amine **142** (50 mg, 0.13 mmol) and triethylamine (58 μL, 0.41 mmol) in a 2:1 mixture of anhydrous DCM and DMF (3 mL) under an argon atmosphere, a solution of dansyl chloride (56 mg, 0.21 mmol) in anhydrous DCM (1 mL) was added. The reaction was stirred at room temperature for 24 h. Afterward, the solvent was evaporated under reduced pressure and the crude was purified by chromatography (from DCM to

ethyl acetate) to afford final compound **122** in 26% yield. R_f (DCM/ethyl acetate, 1:4) 0.64; mp 185-186 ºC; IR (ATR) ν 3435 (NH), 1670 (C=O), 1604, 1486, 1450 (Ar); ^{1}H NMR (700 MHz, DMSO-d_6) δ 1.58 (qt, J = 7.2, 2H, $CH_2C\underline{H}_2CH_2$), 2.55 (t, J = 7.7, 2H, CH_2Ar), 2.82 (s, 6H, $2CH_3$), 2.83 (t, J = 7.3, 2H, CH_2N), 5.66 (s, 2H, CH_2O), 7.02 (dd, J = 8.2, 1.5, 1H, CH_{DS}), 7.10 (app t, J = 9.0, 1H, C_5H), 7.26 (d, J = 7.3, 1H, CH_{DS}), 7.38 (app td, J = 9.2, 5.1, 1H, C_4H), 7.57-7.62 (m, 3H, CH_{DS}, $C_{4'}H$, $C_{6'}H$), 7.89 (br s, 1H, $CONH_2$), 7.92 (d, J = 8.2, 1H, $C_{7'}H$), 8.01 (t, J = 5.9, 1H, $NHSO_2$), 8.07 (dd, J = 7.1, 1.1, 1H, CH_{DS}), 8.18 (br s, 1H, $CONH_2$), 8.33 (d, J = 8.7, 1H, CH_{DS}), 8.45 (d, J = 8.4, 1H, CH_{DS}); ^{13}C NMR (175 MHz, DMSO-d_6) δ 31.1, 31.8 (CH_2CH_2Ar), 41.8 (CH_2N), 45.1 ($2CH_3$), 68.5 (CH_2O), 111.1 (d, J = 21.6, C_5H), 115.1 (CH_{DS}), 116.2 (d, J = 8.5, C_4H), 116.8 (t, J = 23.4, C_1), 119.1 (CH_{DS}), 122.0 ($C_{7'}H$), 123.6 ($C_{4'}H$), 126.2 ($C_{6'}H$), 127.9 ($2CH_{DS}$), 128.3 (CH_{DS}), 129.1 (C_{DS}, $C_{5'}$), 129.4 (CH_{DS}), 131.9 ($C_{7'a}$), 136.1, 140.1 ($2C_{DS}$), 142.0 (d, J = 9.0, C_3), 148.0 (dd, J = 249.5, 7.7, CF), 151.4 (C_{DS}), 152.4 (d, J = 240.4, CF), 152.9 ($C_{3a'}$), 161.1 ($C_{2'}$), 167.4 ($CONH_2$); ESI-MS 611.2 $(M+H)^+$; elemental analysis (calcd., found for $C_{30}H_{28}F_2N_4O_4S_2$): C (59.00, 58.71), H, (4.62, 4.63), N (9.17, 9.17), S (10.50, 10.19).

4.1.6. Synthesis of 123-125, 149, and 150

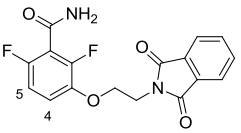

143

3-[2-(1,3-Dioxo-1,3-dihydro-2*H*-isoindol-2-yl)ethoxy]-2,6-difluorobenzamide (143). To a solution of hydroxybenzamide **127** (300 mg, 1.7 mmol), *N*-(2-hydroxyethyl)phthalimide (480 mg, 2.5 mmol) and Ph_3P (870 mg, 3.3 mmol) in anhydrous THF (10 mL) under an argon atmosphere, diethyl azodicarboxylate (DEAD) (0.61 mL, 3.3 mmol) was added and the reaction was refluxed for 24 h. Then, the solvent was evaporated under reduced pressure and the crude was purified by chromatography (from hexane to hexane/ethyl acetate, 1:1) to afford protected amine **143** in 67% yield. R_f (hexane/ethyl acetate, 1:1) 0.25; mp 169-171 ºC; IR (ATR) ν 3397 (NH_2), 1710 (C=O), 1654 (C=O), 1492 (Ar); ^{1}H NMR (300 MHz, acetone-d_6) δ 4.01 (t, J = 5.7, 2H, CH_2N), 4.29 (t, J = 5.7, 2H, CH_2O), 5.82 (br s, 1H, $CONH_2$), 5.97 (br s, 1H, $CONH_2$), 6.85 (app td, J = 9.1, 1.8, 1H, C_5H), 7.05 (app td, J = 9.0, 5.1, 1H, C_4H), 7.74 (dd, J = 5.4, 3.0, 2H, $2CH_{pht.}$), 7.87 (dd, J = 5.5, 2.9, 2H, $2CH_{pht.}$); ^{13}C NMR (75 MHz, acetone-d_6) δ 37.9 (CH_2N), 67.7 (OCH_2), 111.6 (dd, J = 23.5, 3.9, C_5H), 116.9 (t, J = 23.5, C_1), 117.1 (d, J = 7.1, C_4H), 123.9 ($2CH_{pht.}$), 133.0 ($2C_{pht.}$), 135.2 ($2CH_{pht.}$), 144.0 (dd, J = 10.8, 3.2, C_3), 150.6 (dd, J = 251.0, 8.9, CF), 153.0 (dd, J = 242.0, 6.5, CF), 162.0 (d, J = 6.7, $CONH_2$), 168.6 ($2CO_{pht.}$); ESI-MS 347.1 $(M+H)^+$.

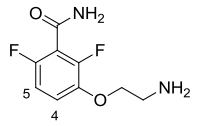

144

3-(2-Aminoethoxy)-2,6-difluorobenzamide (144). To a solution of phthalimide **143** (180 mg, 0.52 mmol) in EtOH (15 mL), hydrazine monohydrate (51 µL, 1.0 mmol) was added and the reaction was refluxed for 2 h. Then, the solvent was evaporated under reduced pressure and the crude was purified by chromatography (from DCM to DCM/MeOH, 95:5) to afford amine **144** in 67% yield. R_f (ethyl acetate/EtOH, 1:1) 0.01; mp 98-100 ºC; IR (ATR) ν 3310 (NH_2), 1675 (C=O), 1489 (Ar); ^{1}H NMR (500 MHz, methanol-d_4) δ 3.22 (t, J = 5.1, 2H, C$\underline{H_2}$NH$_2$), 4.20 (t, J = 5.1, 2H, CH_2O), 6.99 (app td, J = 8.9, 1.9, 1H, C_5H), 7.23 (app td, J = 9.2, 5.2, 1H, C_4H); ^{13}C NMR (125 MHz, methanol-d_4) δ 40.8 (CH_2NH_2), 70.1 (OCH_2), 112.1 (dd, J = 22.4, 4.5, C_5H), 117.1 (t, J = 23.8, C_1), 118.3 (dd, J = 9.4, 2.4, C_4H), 144.1 (dd, J = 11.0, 3.3, C_3), 150.7 (dd, J = 252.8, 9.0, CF), 154.6 (dd, J = 244.0, 5.8, CF), 165.1 ($CONH_2$); ESI-MS 216.9 $(M+H)^+$.

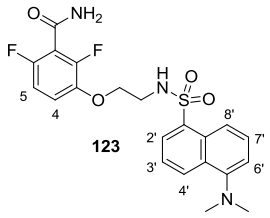

123

3-[2-({[5-(Dimethylamino)-1-naphthyl]sulfonyl}amino)ethoxy]-2,6-difluorobenzamide (123). To a solution of amine **144** (98 mg, 0.45 mmol) and triethylamine (0.19 mL, 1.4 mmol) in a 6:1 mixture of anhydrous DCM and DMF (3.5 mL) under an argon atmosphere, a solution of dansyl chloride (183 mg, 0.68 mmol) in anhydrous DCM (1 mL) was added. The reaction was stirred at room temperature for 24 h. Afterward, the solvent was evaporated under reduced pressure and the crude was purified by chromatography (DCM) to afford final compound **123** in 8% yield. R_f (DCM/ethyl acetate, 95:5) 0.67; mp 130-132 ºC; IR (ATR) ν 3316 (NH_2), 1744 (C=O), 1581, 1502, 1459 (Ar); ^{1}H NMR (300 MHz, $CDCl_3$) δ 2.89 (s, 6H, 2CH_3), 3.38 (app q, J = 5.5, 2H, CH_2N), 3.85 (t, J = 5.0, 2H, CH_2O), 5.25 (t, J = 6.0, 1H, NH), 6.77-6.85 (m, 2H, C_4H, C_5H), 7.17 (d, J = 7.2, 1H, $C_{6'}H$), 7.52 (t, J = 7.9, 1H, $C_{3'}H$/$C_{7'}H$), 7.57 (t, J = 8.0, 1H, $C_{3'}H$/$C_{7'}H$), 8.24-8.27 (m, 2H, $C_{4'}H$, $C_{8'}H$), 8.54 (d, J = 7.2, 1H, $C_{2'}H$); ^{13}C NMR (125 MHz, $CDCl_3$) δ 43.2 (CH_2N), 45.6 (2CH_3), 68.9 (OCH_2), 111.3 (dd, J = 20.6, 4.5, C_5H), 115.5 (CH_{DS}), 118.6 (br s, C_1), 120.4 (dd, J = 9.1, 3.5, C_4H), 128.8 (2CH_{DS}), 129.5 (2C_{DS}), 129.6 (2CH_{DS}), 129.1 (C_{DS}), 130.8 (CH_{DS}), 135.1 (C_{DS}), 142.9 (dd, J = 9.3, 3.5, C_3), 153.0 (dd, J = 262.9, 4.6, CF), 156.7 (dd, J = 255.0, 2.9, CF), 164.7 ($CONH_2$); ESI-MS

432.1 $(M+H)^+$; elemental analysis (calcd., found for $C_{21}H_{21}F_2N_3O_4S$): C (56.12, 56.17), H, (4.71, 5.16), N (9.35, 9.29), S (7.13, 6.83).

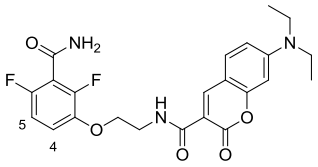

124

***N*-{2-[3-(Aminocarbonyl)-2,4-difluorophenoxy]ethyl}-7-(diethylamino)-2-oxo-2*H*-chromene-3-carboxamide (124).** To a solution of amine **144** (80 mg, 0.37 mmol), PyBroP® (311 mg, 0.66 mmol) and DIPEA (0.13 mL, 0.74 mmol) in anhydrous DMF (4 mL) under an argon atmosphere, a solution of 7-diethylaminocoumarin-3-carboxylic acid (100 mg, 0.38 mmol) in anhydrous DMF (1 mL) was added. The reaction was stirred at room temperature for 4 h. Afterward, the solvent was evaporated under reduced pressure and the crude was purified by chromatography (from DCM to DCM/ethyl acetate, 1:1) to afford final compound **124** in 27% yield. R_f (ethyl acetate) 0.4; mp 155-158 ºC; IR (ATR) ν 3366 (NH_2), 1709, 1663 (C=O), 1618, 1583, 1537 (Ar); ^{1}H NMR (700 MHz, DMSO-d_6) δ 1.14 (t, J = 7.0, 6H, $2CH_3$), 3.48 (q, J = 7.0, 4H, $2CH_2$), 3.70 (app q, J = 5.7, 2H, $C\underline{H}_2NH$), 4.18 (t, J = 5.7, 2H, CH_2O), 6.61 (d, J = 2.0, 1H, $CH_{coum.}$), 6.81 (dd, J = 9.0, 2.2, 1H, $CH_{coum.}$), 7.07 (app t, J = 8.8, 1H, C_5H), 7.29 (app td, J = 9.3, 5.3, 1H, C_4H), 7.69 (d, J = 9.0, 1H, $CH_{coum.}$), 7.85 (br s, 1H, $CONH_2$), 8.13 (br s, 1H, $CONH_2$), 8.69 (s, 1H, $CH_{coum.}$), 8.93 (t, J = 5.7, 1H, NH); ^{13}C NMR (175 MHz, DMSO-d_6) δ 12.3 ($2CH_3$), 38.3 (CH_2NH), 44.3 ($2CH_2$), 68.3 (OCH_2), 95.9 ($CH_{coum.}$), 107.7, 109.0 ($2C_{coum.}$), 110.2 ($CH_{coum.}$), 111.0 (dd, J = 22.6, 4.0, C_5H), 115.6 (d, J = 9.4, C_4H), 116.7 (dd, J = 25.1, 20.3, C_1), 131.7 ($CH_{coum.}$), 142.8 (dd, J = 10.6, 2.7, C_3), 147.9 ($CH_{coum.}$), 148.0 (dd, J = 248.5, 9.0, CF), 152.0 (dd, J = 241.7, 7.2, CF), 152.5, 157.3 ($2C_{coum.}$), 161.3, 161.8, 162.6 (3CO); ESI-MS 459.6 $(M+H)^+$; elemental analysis (calcd., found for $C_{23}H_{23}F_2N_3O_5$): C (60.13, 60.23), H, (5.05, 5.41), N (9.15, 9.44).

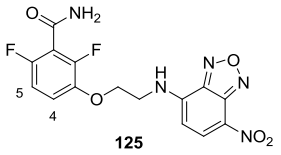

125

2,6-Difluoro-3-{2-[(7-nitro-2,1,3-benzoxadiazol-4-yl)amino]ethoxy}benzamide (125). To a solution of amine **144** (101 mg, 0.47 mmol) and triethylamine (71 μL, 0.51 mmol) in anhydrous DMF (3 mL) under an argon atmosphere, a solution of Cl-NBD (93 mg, 0.47 mmol) in anhydrous DMF (1 mL) was added. The reaction was stirred at room temperature for 20 h. Afterward, the solvent was evaporated under reduced pressure and the crude was purified by chromatography

(from DCM to DCM/ethyl acetate, 1:1) to afford final compound **125** in 13% yield. R_f (DCM/ethyl acetate, 8:2) 0.16; mp 169-172 ºC; IR (ATR) ν 3354 (NH_2), 1676 (C=O), 1586, 1491 (Ar); ^{1}H NMR (500 MHz, acetone-d_6) δ 4.15 (m, 2H, CH_2N), 4.52 (t, *J* = 5.2, 2H, CH_2O), 6.65 (d, *J* = 8.7, 1H, CH_{NBD}), 6.96 (app td, *J* = 8.9, 2.1, 1H, C_5H), 7.15 (br s, 1H, $CONH_2$), 7.24 (app td, *J* = 9.1, 5.1, 1H, C_4H), 7.39 (br s, 1H, $CONH_2$), 8.44 (br s, 1H, NH), 8.56 (d, *J* = 8.7, 1H, CH_{NBD}); ^{13}C NMR (125 MHz, acetone-d_6) δ 43.8 (br s, CH_2N), 68.5 (OCH_2), 100.0 (br s, CH_{NBD}), 111.1 (dd, *J* = 23.2, 4.1, C_5H), 116.3 (d, *J* = 9.6, C_4H), 116.9 (t, *J* = 25.7, C_1), 123.5 (C_{NBD}), 137.2 (CH_{NBD}), 143.6 (dd, *J* = 11.2, 3.4, C_3), 144.7, 145.1, 145.4 ($3C_{NBD}$), 149.3 (dd, *J* = 248.6, 8.3, CF), 153.3 (dd, *J* = 242.4, 6.3, CF), 161.6 ($CONH_2$); ESI-MS 379.7 $(M+H)^+$; elemental analysis (calcd., found for $C_{15}H_{11}F_2N_5O_5$): C (47.50, 47.40), H, (2.92, 3.29), N (18.47, 18.13).

General Procedure for the Synthesis of Final Compounds 149 and 150. To a solution of amine **144** (1 equiv) and Et_3N (5 equiv) in anhydrous DMF (50 mL/mmol) under an argon atmosphere, a solution of the succinimidyl ester of the corresponding fluorophore (1 equiv) in anhydrous DMF (25 mL/mmol) was added and the reaction was stirred for 4 h at room temperature protected from light. Then, the solvent was evaporated under reduced pressure and the crude was purified by chromatography (from ethyl acetate to ethyl acetate/MeOH/NH_3, 8:2:0.01) to afford the corresponding final compound **149** or **150**.

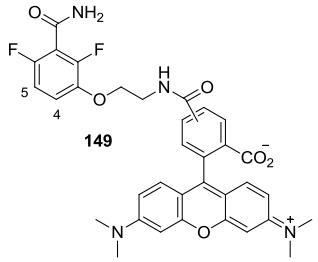

Mixture of 4- and 5-[({2-[3-(aminocarbonyl)-2,4-difluorophenoxy]ethyl}amino)carbonyl]-2-[6-(dimethylamino)-3-(dimethyliminio)-3*H*-xanthen-9-yl]benzoate (149). Obtained from amine **144** (4.1 mg, 19 μmol) and 4- and 5-TAMRA succinimidyl ester (mixed isomers, 10 mg, 19 μmol) in 99% yield as a 1:0.5 mixture of 4- and 5-TAMRA regioisomers. R_f (DCM/MeOH/NH_3, 8:2:0.01) 0.29; IR (ATR) ν 3321 (NH, NH_2), 1596 (N=C), 1365, 1348 (Ar); ^{1}H NMR (700 MHz, MeOD) δ 3.27 (s, 18H, $4CH3_{(5\text{-TAMRA})}$, $4x0.5CH3_{(6\text{-TAMRA})}$), 3.76 (t, *J* = 5.5, 1H, $0.5C\underline{H}_2NH_{(6\text{-TAMRA})}$), 3.85 (t, *J* = 5.5, 2H, $C\underline{H}_2NH_{(5\text{-TAMRA})}$), 4.22 (t, *J* = 5.5, 1H, $0.5CH_2O_{(6\text{-TAMRA})}$), 4.31 (t, *J* = 5.5, 2H, $CH_2O_{(5\text{-TAMRA})}$), 6.90-6.91 (m, 2.5H, $2CH_{Ar}$, $0.5C_5H_{(6\text{-TAMRA})}$), 6.97 (app td, *J* = 9.0, 1.6, 1H, $C_5H_{(5\text{-TAMRA})}$), 6.99-7.02 (m, 2.5H, $2.5CH_{Ar}$), 7.18 (app td, *J* = 9.2, 5.0, 1H, $C_4H_{(5\text{-TAMRA})}$), 7.23-7.28 (m, 3.5H, $3CH_{Ar}$, $0.5C_4H_{(6\text{-TAMRA})}$), 7.36 (d, *J* = 7.8, 1H, CH_{Ar}), 7.72 (d, *J* = 1.6, 1H, CH_{Ar}), 7.77 (s, 0.5H, $0.5CH_{Ar}$), 8.05 (dd, *J* = 7.8, 1.8, 1H, CH_{Ar}), 8.08-8.10 (m, 0.5H, $0.5CH_{Ar}$), 8.13-8.14 (m, 0.5H, $0.5CH_{Ar}$), 8.52 (d, *J* = 1.7, 1H,

CH_{Ar}), 8.57 (d, *J* = 1.7, 0.5H, 0.5CH_{Ar}). ESI-HRMS (calcd., found for $C_{34}H_{31}F_2N_4O_6$ $[M+H]^+$): 629.2206, 629.2185.

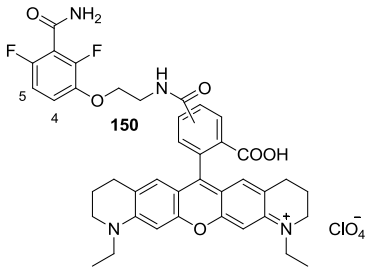

150

Mixture of 6-{4- and 6-{5- [({2-[3-(aminocarbonyl)-2,4-difluorophenoxy]ethyl}amino) carbonyl]-2-carboxyphenyl}-1,11-diethyl-1,2,3,4,9,10-hexahydro-8*H*-pyrano[3,2-*g*:5,6-*g*']diquinolin-11-ium perchlorate (150). Obtained from amine **144** (3.6 mg, 16 μmol) and 4- and 5-ATTO565 succinimidyl ester (mixed isomers, 10 mg, 16 μmol) in 66% yield as a 7:3 mixture of 4- and 5-ATTO565 regioisomers. R_f (DCM/MeOH/NH_3 1:1:0.01) 0.18; IR (ATR) ν 3358 (NH, NH_2), 1602 (N=C), 11499 (Ar); ^{1}H NMR (700 MHz, MeOD) δ 1.33 (t, *J* = 7.1, 6H, 2CH_3), 1.94 (br s, 4H, 2CH_2), 2.68-2.72 (m, 4H, 2CH_2), 3.57 (t, *J* = 5.3, 4H, 2$CH_2C\underline{H_2}N$), 3.62-3.70 (m, 4H, 2$CH_3C\underline{H_2}N$), 3.78 (t, *J* = 5.5, 2H, $C\underline{H_2}NHCO$), 4.24 (t, *J* = 5.5, 2H, CH_2O), 6.87-6.90 (m, 4H, 4CH_{Ar}), 6.93 (app td, *J* = 9.0, 1.4, 1H, C_5H), 7.21 (app td, *J* = 9.2, 5.1, 1H, C_4H), 7.70 (d, *J* = 1.1, 0.7H, 0.7CH_{Ar}), 7.74 (d, *J* = 1.1, 0.3H, 0.3CH_{Ar}), 8.07-8.13 (m, 2H, 2CH_{Ar}). ESI-HRMS (calcd., found for $C_{40}H_{40}F_2N_4O_6$ $[M+H]^+$): 710.2910, 710.2826.

4.1.7. Synthesis of 145-148 and 161

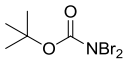

157

***tert*-Butyl *N,N*-dibromocarbamate (157).**[89] To a solution of *t*-butyl carbamate (1.3 g, 11 mmol) and K_2CO_3 (1.5 g, 22 mmol) in water (20 mL), bromine (1.2 mL, 22 mmol) was added dropwise. The reaction was stirred at room temperature for 2 h. Afterward, DCM (10 mL) was added and stirring was continued for 15 min. Then, the organic layer was separated and the aqueous phase was extracted with DCM (3 x 10 mL). The combined organic phases were washed with water (40 mL), dried (Na_2SO_4) and evaporated under reduced pressure to afford intermediate **157** as an orange solid in 79% yield. ^{1}H NMR (300 MHz, $CDCl_3$) δ 1.49 (s, 9H, 3CH_3). The spectroscopic data are in agreement with those previously described.[89]

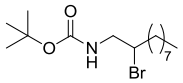

158

***tert*-Butyl (2-bromodecyl)carbamate (158).** To a solution of 1-decene (860 mg, 6.1 mmol) in refluxing anhydrous DCM (10 mL) under an argon atmosphere, a solution of dibromocarbamate **157** (1.7 g, 6.1 mmol) in anhydrous DCM (10 mL) was added dropwise.The reaction was refluxed for 3 h and then it was stirred at room temperature overnight (during this time the solution turned from orange to yellow). Afterward, the reaction was cooled to 5-10 ºC and a 12% aqueous solution of Na_2SO_3 (7 mL) was slowly added and the mixture was stirred for 15 min. After this time, the mixture was extracted with DCM (10 mL) and the organic phase was washed with water (20 mL), dried (Na_2SO_4) and evaporated under reduced pressure. The crude was purified by chromatography (DCM) to afford intermediate **158** as an oil in 56 % yield. R_f (hexane/ethyl acetate, 1:1) 0.38; IR (ATR) ν 3360 (NH), 1703 (C=O); ^{1}H NMR (300 MHz, $CDCl_3$) δ 0.87 (t, *J* = 6.6, 3H, CH_3), 1.26 (br s, 10H, $5CH_2$), 1.44-1.48 (m, 11H, CH_2, $(CH_3)_3C$), 1.75-1.83 (m, 2H, C$\underline{H}_2$CHBr), 3.29-3.36 (m, 1H, 1/2C$\underline{H}_2$NH), 3.60-3.62 (m, 1H, 1/2C$\underline{H}_2$NH), 4.08 (br s, 1H, CHBr), 4.98 (br s, 1H, NH); ^{13}C NMR (75 MHz, $CDCl_3$) δ 14.2 (CH_3), 22.8, 27.5 ($2CH_2$), 28.5 (($\underline{C}H_3)_3$C), 29.1, 29.3, 29.5, 32.0 ($4CH_2$), 36.3 ($\underline{C}H_2$CHBr), 47.7 (CH_2NH), 57.8 (CHBr), 79.9 ($(CH_3)_3\underline{C}$), 155.9 (CO); ESI-MS 360.0 $(M+H)^+$.

General Procedure for the Synthesis of Intermediates 151, 152, 155, and 159. To a solution of hydroxybenzamide **127** (1 equiv), K_2CO_3 (3 equiv) and NaI (0.2 equiv) in anhydrous DMF (10 mL/mmol **127**) under an argon atmosphere, the corresponding commercial bromo derivative or intermediate **158** (1 equiv) was added dropwise. The reaction mixture was stirred at room temperature overnight. Then, the reaction was concentrated under reduced pressure and the residue was dissolved in ethyl acetate and washed with a saturated aqueous solution of $NaHCO_3$ and with water. The organic layer was dried (Na_2SO_4) and the solvent was evaporated under reduced pressure. The crude was purified by chromatography (from hexane to ethyl acetate) to afford the corresponding intermediate **151**, **152**, **155**, or **159**.

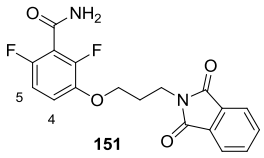

151

3-[3-(1,3-Dioxo-1,3-dihydro-2*H*-isoindol-2-yl)propoxy]-2,6-difluorobenzamide (151). Obtained from **127** (250 mg, 1.4 mmol) and *N*-(3-bromopropyl)phthalimide (387 mg, 1.4 mmol) in 57% yield. R_f (hexane/ethyl acetate, 1:3) 0.54; mp 200-203 ºC; IR (ATR) ν 3404 (NH_2), 1707, 1679 (C=O), 1611, 1494 (Ar); ^{1}H NMR (300 MHz, acetone-d_6) δ 1.62 (m, 2H, CH_2), 3.31 (t, *J* = 6.7, 2H,

CH_2N), 3.63 (t, *J* = 5.9, 2H, CH_2O), 6.59 (app td, *J* = 9.0, 1.8, 1H, C_5H), 6.71 (app td, *J* = 9.3, 5.3, 1H, C_4H), 7.34-7.43 (m, 4H, $4CH_{pht.}$), 7.50 (br s, 1H, $CONH_2$), 7.65 (br s, 1H, $CONH_2$); ^{13}C NMR (75 MHz, acetone-d_6) δ 27.7 (CH_2), 34.8 (CH_2N), 67.4 (OCH_2), 110.8 (dd, *J* = 24.2, 5.4, C_5H), 115.3 (d, *J* = 9.2, C_4H), 117.9 (br s, C_1), 122.9 ($2CH_{pht.}$), 131.8 ($2C_{pht.}$), 134.3 ($2CH_{pht.}$), 143.0 (dd, *J* = 13.9, 3.3, C_3), 148.0 (d, *J* = 231.6, CF), 153.7 (d, *J* = 224.7, CF), 161.3 ($CONH_2$), 168.1 ($2CO_{pht.}$); ESI-MS 361.0 $(M+H)^+$.

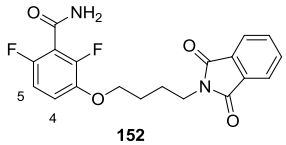

152

3-[4-(1,3-Dioxo-1,3-dihydro-2*H*-isoindol-2-yl)butoxy]-2,6-difluorobenzamide (152). Obtained from **127** (221 mg, 1.2 mmol) and *N*-(4-bromobutyl)phthalimide (344 mg, 1.2 mmol) in 87% yield. R_f (hexane/ethyl acetate, 1:1) 0.29; mp 155-157 ºC; IR (ATR) ν 3397 (NH_2), 1710, 1654 (C=O), 1492 (Ar); ^1H NMR (300 MHz, acetone-d_6) δ 1.84-1.88 (m, 4H, $2CH_2$), 3.74 (t, *J* = 6.7, 2H, CH_2N), 4.14 (t, *J* = 5.9, 2H, CH_2O), 6.93 (app td, *J* = 9.0, 2.0, 1H, C_5H), 7.14-7.22 (m, 2H, $CONH_2$, C_4H), 7.41 (br s, 1H, $CONH_2$), 7.83-7.87 (m, 4H, $4CH_{pht.}$); ^{13}C NMR (75 MHz, acetone-d_6) δ 25.8, 27.3 ($2CH_2$), 38.1 (CH_2N), 70.2 (OCH_2), 111.5 (dd, *J* = 23.2, 4.1, C_5H), 116.6 (dd, *J* = 9.3, 2.9, C_4H), 117.4 (br s, C_1), 123.7 ($2CH_{pht.}$), 133.1 ($2C_{pht.}$), 135.0 ($2CH_{pht.}$), 144.6 (dd, *J* = 11.0, 3.1, C_3), 147.6 (d, *J* = 261.3, CF), 153.5 (dd, *J* = 243.2, CF), 162.2 ($CONH_2$), 168.9 ($2CO_{pht.}$); ESI-MS 375.0 $(M+H)^+$.

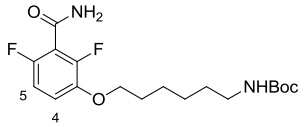

155

***tert*-Butyl {6-[3-(aminocarbonyl)-2,4-difluorophenoxy]hexyl}carbamate (155).** Obtained from **127** (250 mg, 1.4 mmol) and 6-(Boc-amino)hexyl bromide (405 mg, 1.4 mmol) as an oil in 77% yield. R_f (hexane/ethyl acetate, 1:3) 0.66; IR (ATR) ν 3326 (NH_2), 3193 (NH), 1669 (C=O), 1490, 1366 (Ar); ^1H NMR (300 MHz, $CDCl_3$) δ 1.37-1.52 (m, 15H, $3CH_2$, $(CH_3)_3C$), 1.79 (qt, *J* = 6.8, 2H, CH_2), 3.10 (m, 2H, CH_2NH), 3.99 (t, *J* = 6.4, 2H, CH_2O), 4.61 (br s, 1H, NH), 6.25 (br s, 1H, $CONH_2$), 6.48 (br s, 1H, $CONH_2$), 6.85 (app td, *J* = 9.1, 1.8, 1H, C_5H), 6.97 (app td, *J* = 9.1, 5.2, 1H, C_4H); ^{13}C NMR (75 MHz, $CDCl_3$) 25.6, 26.5 ($2CH_2$), 28.5 ($(\underline{C}H_3)_3C$), 29.1, 30.1 ($2CH_2$), 40.5 (CH_2N), 70.4 (OCH_2), 79.2 ($(CH_3)_3\underline{C}$), 111.1 (dd, *J* = 23.5, 4.3, C_5H), 114.2 (dd, *J* = 20.4, 16.8, C_1), 117.0 (dd, *J* = 9.6, 3.5, C_4H), 144.0 (dd, *J* = 11.4, 3.3, C_3), 150.1 (dd, *J* = 254.1, 6.8, CF), 153.4 (dd, *J* = 246.1, 5.8, CF), 156.1 (NHCO), 162.5 ($CONH_2$); ESI-MS 395.2 $(M+Na)^+$.

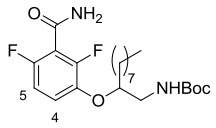

159

***tert*-Butyl {2-[3-(aminocarbonyl)-2,4-difluorophenoxy]decyl}carbamate (159).** Obtained from **127** (300 mg, 1.7 mmol) and bromo derivative **159** (344 mg, 1.2 mmol) as an oil in 23% yield. R_f (hexane/ethyl acetate, 6:4) 0.53; IR (ATR) ν 3356 (NH), 1681 (C=O), 1489, 1367 (Ar); ^{1}H NMR (300 MHz, $CDCl_3$) δ 0.85 (t, *J* = 6.7, 3H, CH_3), 1.24 (br s, 10H, $5CH_2$), 1.41-1.42 (m, 11H, CH_2, $(CH_3)_3C$), 1.54-1.69 (m, 2H, $OCHC\underline{H}_2$), 3.22-3.29 (m, 1H, $1/2C\underline{H}_2NH$), 3.39-3.43 (m, 1H, $1/2C\underline{H}_2NH$), 4.25 (br s, 1H, OCH), 4.96 (br s, 1H, NH), 6.16 (br s, 1H, $CONH_2$), 6.58 (br s, 1H, $CONH_2$), 6.84 (app td, *J* = 9.1, 1.8, 1H, C_5H), 7.38 (app td, *J* = 8.9, 5.3 1H, C_4H); ^{13}C NMR (75 MHz, $CDCl_3$) δ 14.5 (CH_3), 23.0, 25.5 ($2CH_2$), 28.7 ($(\underline{C}H_3)_3C$), 29.6, 29.8, 30.0 ($3CH_2$), 32.2 ($2CH_2$), 44.1 (CH_2NH), 80.0 ($(CH_3)_3\underline{C}$), 81.1 (OCH), 111.7 (dd, *J* = 23.3, 4.3, C_5H), 114.6 (dd, *J* = 20.5, 16.8, C_1), 120.5 (dd, *J* = 9.9, 2.3, C_4H), 143.3 (dd, *J* = 11.2, 3.3, C_3), 151.3 (dd, *J* = 253.9, 6.9, CF), 154.7 (dd, *J* = 256.6, 7.1, CF), 156.5 (NHCO), 162.8 ($CONH_2$); ESI-MS 328.2 $(M+H)^+$.

General Procedure for the Synthesis of Amines 153 and 154. To a solution of phthalimide **151** or **152** (1 equiv) in EtOH (15 mL/mmol), hydrazine monohydrate (2 equiv) was added dropwise and the reaction mixture was refluxed for 2 h. Then, the solvent was evaporated under reduced pressure and the crude was purified by chromatography (from ethyl acetate to ethyl acetate/MeOH, 95:5) to afford the corresponding amine **153** or **154**.

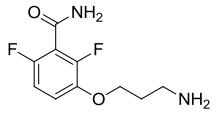

153

3-(3-Aminopropoxy)-2,6-difluorobenzamide (153). Obtained from **151** (290 mg, 0.81 mmol) in 64% yield. ESI-MS 231.1 $(M+H)^+$.

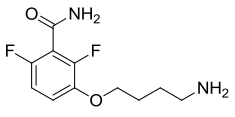

154

3-(4-Aminobutoxy)-2,6-difluorobenzamide (154). Obtained from **152** (350 mg, 0.93 mmol) in 55% yield. ESI-MS 245.1 $(M+H)^+$.

General Procedure for the Synthesis of Amines 156 and 160. To a solution of Boc derivative **155** or **159** (1 equiv) in anhydrous DCM (10 mL/mmol), trifluoroacetic acid (TFA) (20 equiv) was added dropwise and the reaction mixture was stirred at room temperature for 1 h. Then, the mixture was concentrated under reduced pressure and the residue was redissolved in DCM and neutralized with a saturated aqueous solution of $NaHCO_3$. The aqueous phase was then extracted with DCM and the organic layer was dried (Na_2SO_4) and concentrated under reduced pressure to afford amine **156** or **160** in quantitative yield, that was used in the next step without further purification.

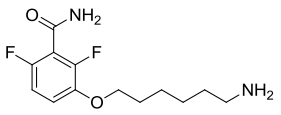

156

3-[(6-Aminohexyl)oxy]-2,6-difluorobenzamide (156). Obtained from **155** (350 mg, 0.94 mmol) in 99% yield. ESI-MS 273.1 $(M+H)^+$.

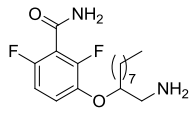

160

3-{[1-(Aminomethyl)nonyl]oxy}-2,6-difluorobenzamide (160). Obtained from **159** (110 mg, 0.26 mmol) in 99% yield. ESI-MS 329.2 $(M+H)^+$.

General Procedure for the Synthesis of Final Compounds 145-148. To a solution of amine **153**, **154**, **156** or **160** (1 equiv), and Et_3N (3 equiv) or DIPEA (1.2 equiv) in anhydrous DMF (15 mL/mmol) under an argon atmosphere, a solution of Cl-NBD (1.2 equiv) in anhydrous DMF (2 mL/mmol) was added and the reaction was stirred at room temperature overnight. Then, the solvent was evaporated under reduced pressure and the crude was purified by chromatography (from hexane to ethyl acetate) to afford final compounds **145**-**148**.

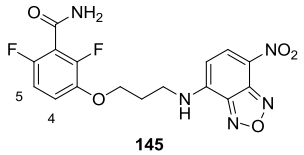

145

2,6-Difluoro-3-{3-[(7-nitro-2,1,3-benzoxadiazol-4-yl)amino]propoxy}benzamide (145). Obtained from amine **153** (184 mg, 0.51 mmol), Cl-NBD (123 mg, 0.62 mmol) and DIPEA (0.11 mL,

0.62 mmol) as an oil in 5% yield. R_f (DCM/ethyl acetate, 95:5) 0.29; IR (ATR) ν 3343 (NH_2), 1701 (C=O), 1378, 1364 (Ar); ^{1}H NMR (700 MHz, acetone-d_6) δ 2.35 (q, J = 6.4, 2H, CH_2), 3.90 (br s, 2H, CH_2N), 4.30 (t, J = 5.9, 2H, CH_2O), 6.50 (d, J = 8.8, 1H, CH_{NBD}), 6.96 (app td, J = 9.0, 2.0, 1H, C_5H), 7.17-7.22 (m, 2H, $CONH_2$, C_4H), 7.43 (br s, 1H, $CONH_2$), 8.40 (br s, 1H, NH), 8.53 (d, J = 8.7, 1H, CH_{NBD}); ^{13}C NMR (175 MHz, acetone-d_6) δ 32.6 (CH_2), 39.7(CH_2N), 68.8 (OCH_2), 99.6 (br s, CH_{NBD}), 111.5 (dd, J = 22.8, 4.1, C_5H), 116.5 (dd, J = 9.4, 2.7, C_4H), 117.4 (dd, J = 24.9, 19.5, C_1), 127.7 (C_{NBD}), 135.7 (br s, CH_{NBD}), 144.4 (dd, J = 10.7, 2.7, C_3), 145.1, 145.6, 147.0 ($3C_{NBD}$), 149.8 (dd, J = 248.8, 7.9, CF), 153.5 (dd, J = 242.2, 6.5, CF), 162.4 ($CONH_2$); ESI-HRMS (calcd., found for $C_{16}H_{13}F_2NaN_5O_5$ $[M+Na]^+$): 416.0782, 416.0777.

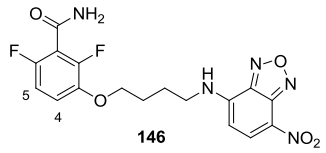

146

2,6-Difluoro-3-{4-[(7-nitro-2,1,3-benzoxadiazol-4-yl)amino]butoxy}benzamide (146). Obtained from amine **154** (188 mg, 0.50 mmol), Cl-NBD (121 mg, 0.60 mmol) and DIPEA (0.11 mL, 0.60 mmol) as an oil in 11% yield. R_f (DCM/ethyl acetate, 95:5) 0.34; IR (ATR) ν 3431 (NH_2), 1701 (CO), 1364 (Ar); ^{1}H NMR (300 MHz, acetone-d_6) δ 1.98-2.08 (m, 4H, $2CH_2$), 3.77 (br s, 2H, CH_2N), 4.17 (t, J = 5.9, 2H, CH_2O), 6.50 (d, J = 8.8, 1H, CH_{NBD}), 6.95 (app td, J = 9.0, 2.0, 1H, C_5H), 7.14-7.22 (m, 2H, $CONH_2$, C_4H), 7.45 (br s, 1H, $CONH_2$), 8.43 (br s, 1H, NH), 8.52 (d, J = 8.8, 1H, CH_{NBD}); ^{13}C NMR (175 MHz, acetone-d_6) δ 27.3, 30.2 ($2CH_2$), 44.1 (br s, CH_2N), 70.3 (OCH_2), 99.5 (br s, CH_{NBD}), 111.5 (dd, J = 23.2, 4.0, C_5H), 116.6 (br d, J = 8.7, C_4H), 117.3 (dd, J = 24.3, 20.0, C_1), 126.1 (C_{NBD}), 137.9 (CH_{NBD}), 144.5 (dd, J = 11.1, 3.2, C_3), 145.2 (C_{NBD}), 145.5 ($2C_{NBD}$), 149.8 (dd, J = 248.7, 8.0, CF), 153.5 (dd, J = 242.2, 6.4, CF), 162.8 ($CONH_2$); ESI-HRMS (calcd., found for $C_{17}H_{15}F_2NaN_5O_5$ $[M+Na]^+$): 430.0939, 430.0934.

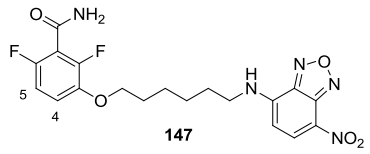

147

2,6-Difluoro-3-({6-[(7-nitro-2,1,3-benzoxadiazol-4-yl)amino]hexyl}oxy)benzamide (147). Obtained from amine **156** (328 mg, 0.88 mmol), Cl-NBD (211 mg, 1.1 mmol) and DIPEA (0.19 mL, 1.1 mmol) as an oil in 4% yield. R_f (ethyl acetate) 0.73; IR (ATR) ν 3335 (NH_2), 1678 (C=O), 1491, 1375, 1300 (Ar); ^{1}H NMR (700 MHz, acetone-d_6) δ 1.58 (qt, J = 3.6, 4H, $2CH_2$), 1.82 (qt, J = 6.8, 2H, CH_2), 1.89 (qt, J = 6.9, 2H, CH_2), 3.67 (br s, 2H, CH_2N), 4.08 (t, J = 6.4, 2H, CH_2O), 6.48 (d, J = 8.8, 1H, CH_{NBD}), 6.94 (app td, J = 9.0, 2.0, 1H, C_5H), 7.14-7.17 (m, 2H, $CONH_2$, C_4H), 7.41 (br s,

1H, $CONH_2$), 8.32 (br s, 1H, NH), 8.52 (d, *J* = 8.7, 1H, CH_{NBD}); ^{13}C NMR (175 MHz, acetone-d_6) δ 26.3, 27.3, 29.5, 30.2 ($4CH_2$), 44.5 (br s, CH_2N), 70.5 (OCH_2), 99.4 (br s, CH_{NBD}), 111.4 (dd, *J* = 23.2, 3.9, C_5H), 116.4 (dd, *J* = 9.3, 2.5, C_4H), 117.4 (dd, *J* = 24.4, 19.9, C_1), 123.3 (br s, C_{NBD}), 138.0 (CH_{NBD}), 144.7 (dd, *J* = 11.1, 3.1, C_3), 145.2, 145.6, 145.8 ($3C_{NBD}$), 149.8 (dd, *J* = 249.8, 8.0, CF), 153.4 (dd, *J* = 241.5, 6.6, CF), 162.3 ($CONH_2$); ESI-HRMS (calcd., found for $C_{19}H_{18}F_2N_5O_5$ $[M-H]^-$): 434.1289, 434,1276.

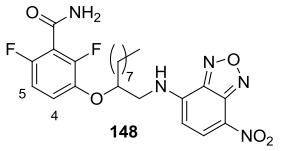

148

2,6-Difluoro-3-[(1-{[(7-nitro-2,1,3-benzoxadiazol-4-yl)amino]methyl}nonyl)oxy] benzamide (148). Obtained from amine **160** (110 mg, 0.26 mmol), Cl-NBD (62 mg, 0.31 mmol) and triethylamine (0.11 mL, 0.78 mmol) as an oil in 11% yield. R_f (hexane/ethyl acetate, 1:1) 0.42; IR (ATR) ν 3426 (NH, NH_2), 1700 (C=O), 1378, 1364 (Ar); ^1H NMR (700 MHz, acetone-d_6) δ 0.86 (t, *J* = 7.1, 3H, CH_3), 1.20-1.33 (m, 10H, $5CH_2$), 1.50-1.59 (m, 2H, CH_2), 1.86 (dt, *J* = 7.6, 6.4, 2H, $OCHC\underline{H_2}$), 4.01 (m, 2H, $C\underline{H_2}NH$), 4.82 (qt, *J* = 5.7, 2H, OCH), 6.61 (d, *J* = 8.8, 1H, CH_{NBD}), 6.90 (app td, *J* = 9.0, 1.8, 1H, C_5H), 7.15 (br s, 1H, $CONH_2$), 7.26 (app td, *J* = 9.2, 5.2, 1H, C_4H), 7.37 (br s, 1H, $CONH_2$), 8.31 (br s, 1H, NH), 8.53 (d, *J* = 8.7, 1H, CH_{NBD}).; ^{13}C NMR (175 MHz, acetone-d_6) δ 14.3 (CH_3), 23.3, 25.6, 29.5, 30.2, 30.3, 32.5, 32.8 ($7CH_2$), 47.8 (br s, CH_2NH), 80.1 (OCH), 100.2 (br s, CH_{NBD}), 111.7 (dd, *J* = 23.4, 3.9, C_5H), 116.7 (dd, *J* = 24.3, 20.4, C_1), 118.4 (dd, *J* = 9.0, 1.7, C_4H), 123.9 (br s, C_{NBD}), 137.7 (br s, CH_{NBD}), 143.4 (dd, *J* = 11.1, 3.2, C_3), 144.1 (C_{NBD}), 145.6 ($2C_{NBD}$), 150.7 (dd, *J* = 249.7, 8.6, CF), 153.9 (dd, *J* = 243.2, 6.5, CF), 161.1 ($CONH_2$); ESI-HRMS (calcd., found for $C_{23}H_{26}F_2N_5O_5$ $[M-H]^-$): 490.1902, 490.1891.

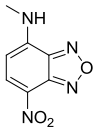

161

***N*-Methyl-7-nitro-2,1,3-benzoxadiazol-4-amine (161).**[90] To a solution of Cl-NBD (200 mg, 1.0 mmol) in MeOH (6 mL) under an argon atmosphere, methylamine hydrochloride (102 mg, 1.5 mmol) was added and the reaction was refluxed for 30 min protected from light. Then, a 0.75 M aqueous solution of sodium bicarbonate (4 mL) was added dropwise under stirring. The mixture was allowed to stand at 0 ºC for 1 h and the resulting red bright crystals were collected by filtration and dried under vacuum to afford pure compound **161** in 66% yield. R_f (DCM) 0.44; mp 259-261 ºC IR (ATR) ν 3307 (NH), 1618, 1597, 1482 (Ar); ^1H NMR (300 MHz, DMSO-d_6) δ 3.06 (d, *J* = 4.8, 3H,

CH_3), 6.30 (d, *J* = 8.9, 1H CH_{NBD}), 8.52 (d, *J* = 8.9, 1H, CH_{NBD}), 9.49 (s, 1H, NH); ^{13}C NMR (75 MHz, DMSO-d_6) δ 30.2 (CH_3), 99.1 (CH_{NBD}), 120.8 (C_{NBD}), 138.0 (CH_{NBD}), 144.4, 145.7, 145.8 ($3C_{NBD}$); ESI-MS 194.9 $(M+H)^+$; elemental analysis (calcd., found for $C_7H_6N_4O_3$): C (43.30, 43.29), H, (3.11, 3.19), N (28.83, 29.13). The spectroscopic data are in agreement with those previously described.[90]

4.2. Biological Experiments

The biological evaluation of the compounds synthesized in this thesis was carried out in collaboration with the research group of Dr. José Manuel Andreu at the Centro de Investigaciones Biológicas (CIB-CSIC), Spain. In addition, the antibacterial activity in pathogenic bacteria was assessed in the Prof. Sieber's laboratory at the Technische Universität München (TUM), Germany.

4.2.1. Protein Purification. FtsZ from *B. subtilis* was overproduced and purified as described.[84] Untagged, full length FtsZ from Bs-FtsZ was overproduced in *E. coli* C41(DE3) cells, purified and its concentration measured as described.[105] Bs-FtsZ was eluted from the hydrophobic chromatography at 99% electrophoretic purity and the gel-filtration chromatography was omitted. Instead, Bs-FtsZ was equilibrated in 50 mM Tris–HCl, 50 mM KCl, 1 mM ethylenediaminetetraacetic acid (EDTA), 10% glycerol at pH 7.5, employing a 5 mL HiTrap desalting column. It was concentrated to < 0.5 mL (about 1 mM Bs-FtsZ) and stored at -80 ºC. Bs-FtsZ preparations contained only 0.047 ± 0.044 guanine nucleotide bound per FtsZ, spectrophotometrically determined after perchloric acid extraction.[106] The Bs-FtsZ concentration was determined after subtracting the nucleotide contribution, employing a calculated extinction coefficient 2560 M^{-1} cm^{-1} at 280 nm (2 Tyr, 0 Trp residues) in 6 M guanidinium chloride.

Tubulin was purified from calf brain as described.[107] Prior to use, tubulin was equilibrated by gel chromatography in cold GAB buffer (3.4 M glycerol, 10 mM sodium phosphate, 1 mM EGTA, and 0.1 mM GTP, pH 6.8).

4.2.2. FtsZ Affinity Measurements: Ligand Competition with *mant*-GTP. The fluorescence anisotropy of *mant*-GTP was measured with a Fluoromax-4 (Horiba Jobin Yvon) photon-counting spectrofluorometer, with excitation at 357 nm (5 nm band pass) and emission at 445 nm (10 nm band pass) using 2x10 mm cells at 25 ºC. Ligand competition with *mant*-GTP for binding to FtsZ from *B. subtilis* was performed as described for *M. jannaschii* FtsZ[82] with modifications.[84] The binding of *mant*-GTP to FtsZ causes a significant increase in its fluorescence that if not taken into account can lead to the calculation of erroneous K_d values when employing anisotropy measurements. To avoid this error, the ratio between the fluorescence intensities of Bs-FtsZ-bound and free *mant*-GTP was determined R = 2.78 and used to correct all anisotropy-based binding calculations. To measure the equilibrium binding constant, *mant*-GTP (200 nM) was titrated with varying concentrations of Bs-FtsZ in experimental buffer at 25 ºC, which gave a reference

binding constant K_b of (9.85 ±1.05)·10^5 M^{-1}, an anisotropy value of free *mant*-GTP r = 0.025 ± 0.005 and the anisotropy of bound *mant*-GTP r = 0.213 ± 0.002. For the competition measurements, samples (0.5 mL) were prepared by mixing 0.25 mL of *mant*-GTP (1 µM) and binding sites (0.6 µM) with 0.25 mL buffer without or with competing ligand at varying concentrations, and measurements started 4 min after. The fractional of bound of *mant*-GTP and the affinity of the competing ligand were then determined from the fluorescence anisotropy values.[82] Controls include samples with GTP, without FtsZ, *mant*-GTP alone and test compound alone.

4.2.3. Antibacterial Activity: Minimum Inhibitory Concentration Determination. MIC values for each compound against *B. subtilis* 168 were determined in cation-adjusted Mueller-Hinton II broth (CAMHB) (Becton Dickinson) at 37 ºC with shaking, by the broth macrodilution method according to the recommendations of the Clinical and Laboratory Standards Institute (CLSI) for which the MIC was defined as the lowest concentration inhibiting growth determined by absorbance at 600 nm.[103]

MIC on a panel of bacterial pathogens measurements: overnight cultures of the bacteria were diluted in fresh brain-heart broth (BHB) medium or Luria Bertani broth (LB) to optical density at 600 nm, (OD_{600}) = 0.01, and 100 µL were taken to in Nunclon 96-well plates with round-shaped bottoms with 1 µL of the corresponding DMSO stock solutions of each compound at dilution ranges from 0.4 to 45 mg/L with 2% final concentration of DMSO. The samples were incubated for 12 h at 37 °C and the OD_{600} were obtained for MIC calculation. All experiments were conducted at least in triplicates, and DMSO served as control. Bacterial Strains: *S.aureus* strains: Mu50/ATCC 700699, USA300/ATCC Nr: BAA-1556 (both from Institute Pasteur, France); *L. monocytogenes* EGD-e and *E. faecalis* V583 ATCC700802 (both sequenced strains) were maintained in BHB medium at 37 °C, and *Escherichia coli* UTI89 and *Pseudomonas aeruginosa* PAO1 (both sequenced strains) were maintained in LB medium at 37 ºC.

4.2.4. Stability of Compounds 40, 47 and 48 in Bacterial Culture. Compounds **40**, **47** (5 µM), and **48** (25 µM) were incubated in bacterial culture of *Bacillus subtilis* SU570. Samples of 0.75 mL were taken from the culture at different times (1, 2, 4 and 18 h) and bacteria were pelleted in Eppendorf tubes with a microcentrifuge (Hettich Mikro 120, 12000 rpm, 10 min). Taxol (100 µM) was added as internal standard to 0.5 mL of the supernatant and the compounds were extracted with 0.75 mL of acetonitrile and dried under an argon stream. Samples were reconstituted in methanol, centrifuged and analyzed by HPLC-MS (see section 2.1 for analytical conditions). HPLC-MS measurements were made by selected ion monitoring (SIM), and fractions were quantified by measuring the area under the peak, relative to the internal standard.

4.2.5. FtsZ and Tubulin Polymerization Measured by Sedimentation. FtsZ polymerization was measured in Hepes/KOH (50 mM), KCl (50 mM), EDTA (1 mM), pH 6.8 at 25 ºC, to which the

compound or DMSO vehicle, $MgCl_2$ (10 mM) and GTP (1 mM) or GMPCPP (0.1 mM) were added. For the study of the compounds targeting the GTP-binding site, a GTP regeneration system was employed, consisting of acetyl phosphate (15 mM) and 1 unit/mL acetate kinase from *E. coli*, to which GTP (50 µM) was added. In the case of fluorescent derivatives, the slowly hydrolyzable GTP analogue GMPCPP (0.1 mM) was used. After incubation of 100 µL FtsZ (10 µM) in polycarbonate tubes, they were centrifuged at 386000*g* for 20 min in a TLA100 rotor (100000 rpm), at 25 ºC in a TLX ultracentrifuge (Beckman).

For tubulin polymerization, samples containing 100 µL of tubulin (15 µM), $MgCl_2$ (6 mM), GTP (1 mM) and compound or DMSO vehicle, were incubated for 30 min at 37 ºC, and centrifuged at 90000*g* for 10 min in a TLA100 rotor (50000 rpm) at 37 ºC.

Pellets were resuspended with 50 µL of SDS-containing electrophoresis sample solution plus 50 µL buffer, and supernatants were diluted with 50 µL sample solution. Pellet and supernatant aliquots were loaded with an electrophoretic shift between them into the same lanes of 12%-polyacrylamide gels with 0.1% SDS. Gels were stained with Coomassie blue, scanned with a CS-800 calibrated densitometer (BioRad) and analyzed with Quantity One software (BioRad). The inhibition of polymerization by each compound was calculated relative to polymerization with GTP alone (0% inhibition) and with GDP inhibitor (100% inhibition).

4.2.6. Bacterial Division Phenotype. *B. subtilis* 168 cells were grown in cation adjusted Mueller-Hinton broth (CAMHB) at 37 °C to an absorbance 0.1-0.2 at 600 nm and then the culture was divided into new flasks containing the compound at the desired concentration. Small aliquots (10 µL) were harvested at appropriate time intervals and bacterial cells visualized by phase-contrast light microscopy.

4.2.7. Fluorescent Microscopy. Experiments for cell visualization with the synthesized compounds targeting the GTP- binding site: A colony of *B. subtilis* strain SU570 (168 trpC2 ftsZ:ftsZ-gfp-Spec),[108,109] kindly donated by Dr. Elisabeth J. Harry, was resuspended in antibiotic medium no. 3 (Pennassay broth, Becton Dickinson) with 50 µg/mL spectinomycin and grown at 30 °C to an absorbance of 0.2 at 600 nm. Samples of the culture were mixed with an equal volume of medium containing twice the final desired concentration of compound. Aliquots (10 µL) were harvested at appropriate time intervals, combined with an equal volume of prewarmed Pennassay broth containing ~1% w/v agarose, and 10 µL of these samples were pipetted onto microscope slides, covered, and visualized through a 100X PlanApochromatic objective with a Zeiss Axioplan fluorescence microscope equipped with a Hamamatsu 4742-95 CCD camera. Nucleoids were stained with 4,6-diamino-2-phenylindole (DAPI, 0.25 µg/mL) and membranes with FM4-64 (1 µg/mL), which were added to the cells prior to visualization.

Experiments for cell visualization with the fluorescent probes targeting the PC- binding site: *B. subtilis* 168 cells were grown in cation adjusted Mueller-Hinton broth (CAMHB) at 37 °C to an absorbance 0.1-0.2 at 600 nm then the fluorescent probe (50 µM or 200 µM) was added and after 1 hour of incubation, 10 µL of the sample was pipetted onto microscope slides, covered, and visualized through the previously described fluorescence microscope. Membranes were stained with FM4-64 (1 µg/mL), which were added to the cells prior to visualization.

4.2.8. Fluorescence and Anisotropy Properties of Compounds 119-125 and 145-150. A Horiba-Jovin-Yvon Fluoromax-4 was used to measure the fluorescence intensity and the fluorescence anisotropy (r) values in different conditions, employing a solution of 500 µL in a 10 x 2 mm cuvette. Fluorescence emission spectra and anisotropy of fluorescent compounds (10 µM) were registered employing an excitation wavelength corresponding to the maximum absortion wavelength of each compound in Hepes buffer at pH 6.8 and 25 ºC. Then, Bs-FtsZ (10 µM), the slowly hydrozable GTP analogue GMPCPP (0.1 mM), $MgCl_2$ (10 mM) and PC190723 or **8j** (10 µM) were subsequently added. As negative controls, fluorescence emission spectra and anisotropy were registered with each compound and GMPCPP, $MgCl_2$ or PC190723 in the absence of FtsZ protein.

4.3. Docking and Virtual Screening

The virtual screening and molecular dynamics of this thesis were carried out in collaboration with the research group of Dr. Pablo Chacón of the Instituto de Química Física Rocasolano (IQFR-CSIC), Spain.

The ICM package[110] has been employed to give computational insights into the recognition of FtsZ sites by small molecules. Two slightly different ICM protocols were employed for virtual screening and for docking. For screening the large database compounds default parameters and procedures were used. Multiple receptor conformers as an extra dimension for the docking search as described[111] was considered for docking and for refinement of the best virtual screening poses. In either case, the ICM methodology utilizes internal coordinates to optimize flexible ligands in a grid-based receptor field. Energies are computed using MMFF partial charges with the ECEPP/3[112] force field. The ligand docking was also complemented by local energy minimization using a Biased Probability Monte Carlo method.[113]

- Preparation of receptor structures and binding pocket definition: For virtual screening we employed the same apo-FtsZ structure used for MD studies. For 4D docking, the conformational variability of the nucleotide-binding site was represented with seven conformers extracted from different snapshots of a long MD of the FtsZ unbound structure. All conformations were regularized using ICM standard procedures. The boundaries of the binding box of nucleotide site were derived from the GDP-crystallized ligand coordinate (PDB ID 2rhl).

- Preparation of ligand structures: Virtual screening was performed against a non-redundant collection of vendor compound database formed by 4 million of compounds. A small database was built with available compounds from UCM Medicinal Chemistry Laboratory. 3D atomic coordinates, tautomeric forms, stereochemistry, hydrogen atoms, and protonation states were assigned using standard procedures. Ligand molecules were prepared for docking by rotational search followed by a Cartesian minimization using MMFF[114] force field in the absence of the receptor. These free molecules were optimized with global energy in the internal coordinate space and the lowest-energy conformations were used for further studies. During docking, the ligand torsional or roto-translational variables are randomly changed.

5. RESUMEN

5.1. Introducción y objetivos

El descubrimiento y desarrollo de antibióticos puede considerarse como uno de los avances médicos más significativos del siglo XX. Sin embargo, la Organización Mundial de la Salud advierte de la gran amenaza que supone la resistencia a antibióticos para la salud pública mundial en el siglo XXI y de la extrema necesidad de nuevos tratamientos para combatir las cepas multiresistentes.[15,20] Una de las primeras causas del gran aumento de cepas multiresistentes es el hecho de que la mayoría de los antibióticos actuales están dirigidos a un número concreto de dianas terapéuticas, como las implicadas en la síntesis de proteínas, de ácidos nucleicos, de folato y de la pared bacteriana. Además, la mayoría de los nuevos antibióticos comercializados son simples variantes de fármacos anteriores, por lo que las bacterias pueden adquirir rápidamente resistencia a los tratamientos actuales. Estas limitaciones ponen de manifiesto la necesidad de nuevos agentes antibacterianos que posean un mecanismo de acción diferente.[3,30] En este sentido, el bloqueo de la división bacteriana impediría la proliferación descontrolada de bacterias y con ello, las septicemias letales en el caso de numerosos patógenos.[31,32] Sin embargo, no existe hasta la fecha ningún agente antibacteriano aprobado para su uso clínico por la Administración de Alimentos y Fármacos (*Food and Drug Administration*, FDA) que esté dirigido a la inhibición directa de la división bacteriana.

Recientemente, la proteína FtsZ ha sido propuesta como una diana terapéutica prometedora para el descubrimiento y desarrollo de nuevos antibióticos.[2,31-33] Esta proteína está presente en la mayoría de las bacterias conocidas y tiene un papel fundamental en la viabilidad de las bacterias debido a que es el primer eslabón dentro de una cascada de proteínas implicadas en el proceso de división bacteriana. Durante la división bacteriana, FtsZ sufre una polimerización reversible dependiente de GTP que da lugar a la formación del denominado anillo Z en la parte central de la bacteria. A continuación, el anillo Z actúa como plataforma para el ensamblaje de otras proteínas esenciales para el proceso de división, provocando la invaginación de la pared bacteriana y generando las dos células hijas.[35,36] Por tanto, teniendo en cuenta el mecanismo descrito para la división bacteriana, aquellos compuestos que sean capaces de interferir selectivamente en la polimerización de FtsZ, impedirán la proliferación y viabilidad de las bacterias.

En los últimos años se han identificado compuestos con una gran diversidad estructural que tienen algún efecto sobre la polimerización de FtsZ. En concreto, el compuesto PC190723, derivado de la 3-metoxibenzamida, ha sido descrito como el inhibidor más prometedor de FtsZ.[71,77] Este compuesto presenta una potente actividad antibacteriana [*e.g.* concentración mínima inhibitoria (CMI) (MRSA) = 2.8 μM] y es el primer inhibidor de FtsZ que ha demostrado eficacia en un modelo *in vivo* de infección.[71] La estructura de rayos X del complejo FtsZ-PC190723 ha revelado determinar que este inhibidor se une a la proteína en una región diferente a la del dominio de unión del GTP. Este hecho ha permitido identificar dos zonas en la proteína para la unión de moléculas pequeñas capaces de inhibir su función: el sitio de unión al nucleótido y el bolsillo al que se une PC190723.

Teniendo en cuenta estas consideraciones, el objetivo principal de esta tesis doctoral es el desarrollo de nuevos inhibidores de FtsZ con buenas propiedades antibacterianas. Para ello, hemos iniciado un proyecto dirigido a la identificación de nuevos compuestos capaces de inhibir FtsZ dirigidos a los dos sitios de unión de la proteína: (i) el sitio de unión de GTP y (ii) el bolsillo alostérico de PC (Figura 1).

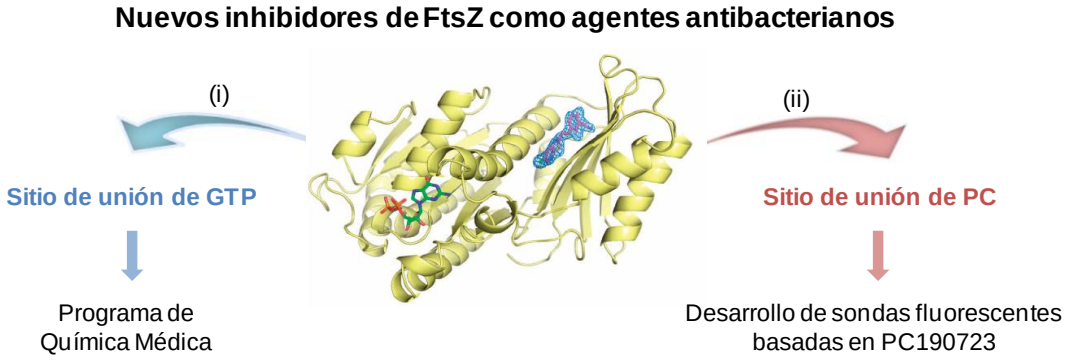

Figura 1. Estrategia dual para la búsqueda de nuevos inhibidores de FtsZ.

El desarrollo de moléculas pequeñas capaces de reemplazar al GTP e inhibir FtsZ de forma específica con el fin de bloquear la división bacteriana implica las siguientes etapas:

- Identificación de *hits*.
- Diseño, síntesis y evaluación biológica de una nueva serie de compuestos. La evaluación de cada compuesto consistirá en la determinación de su constante de afinidad por FtsZ, su actividad antibacteriana y la selectividad frente a tubilina.

- ❖ Caracterización más exhaustiva de los inhibidores optimizados en cuanto a propiedades antibacterianas frente a cepas patógenas Gram-positivas y -negativas, perfil citológico y mecanismo de acción.

Respecto al sitio de unión de PC, las interesantes propiedades antibacterianas que presentan los derivados de PC190723 y la falta de metodologías adecuadas para determinar la afinidad de posibles ligandos frente a este nuevo sitio de unión, nos llevó a desarrollar sondas fluorescentes basadas en este compuesto que permitan identificar nuevos inhibidores en este sitio de unión mediante un ensayo de afinidad basado en fluorescencia. Además, estas sondas podrían contribuir al estudio de este bolsillo alostérico que parece tener un papel fundamental en el ensamblaje de FtsZ. Por lo tanto, el segundo objetivo conlleva las siguientes etapas:

- ❖ Diseño y síntesis de derivados fluorescentes basado en PC190723.
- ❖ Evaluación biológica y caracterización de las propiedades fluorescentes de los compuestos sintetizados.
- ❖ Empleo de las mejores sondas fluorescentes identificadas como herramientas biológicas tanto para el estudio del proceso de division bacteriana como para el desarrollo de un ensayo de desplazamiento basado en fluorescencia que nos permita la identificación de nuevos inhibidores alostéricos de FtsZ.

5.2. Resultados y discusión

5.2.1. Desarrollo de inhibidores de FtsZ dirigidos al sitio de unión de GTP

La búsqueda de nuevos inhibidores de FtsZ se inició a partir de un cribado virtual de la quimioteca del Laboratorio de Química Médica de la Universidad Complutense de Madrid en el sitio de unión de GTP de FtsZ de *B. subtilis.*[84] A continuación, los *hits* obtenidos se confirmaron mediante un ensayo de competición con *mant*-GTP.[82] Los mejores inhibidores identificados poseen una estructura general definida por dos subunidades de ácido gálico unidas a un esqueleto central de naftaleno, bifenilo, benceno, ciclohexano o etileno. Entre ellos, los *hits* **1** y **2** presentaron las mejores constantes de afinidad (K_d = 2.3 y 0.8 μM, respectivamente) así como una moderada actividad antibacteriana en *B. subtilis* (CMI = 100 y 40 μM, respectivamente), y constituyen el primer ejemplo de inhibidores no-nucleótidos que compiten por el sitio de unión a GTP de FtsZ (Figura 2).[84]

Con el objetivo de llevar a cabo un estudio de estructura-afinidad-actividad a partir de los *hits* **1** y **2**, nos centramos en las dos subunidades susceptibles de modificaciones estructurales: los sistemas de polihidroxifenilo y los espaciadores entre dichos anillos y el esqueleto central (Figura 2). Así, se comenzó estudiando la influencia de los anillos de polihidroxifenilo y para ello se

consideró tanto la reducción en el número de grupos hidroxilo como la sustitución de estos grupos por átomos de cloro o grupos metoxi (**3**-**30**). Además, se propusieron los correspondientes monoésteres del *hit* **1** (**31** y **32**) para estudiar la influencia de las dos subunidades de polihidroxifenilo en la unión a FtsZ. Asimismo, se sintetizaron compuestos en los que los grupos éster de **1** fueron sustituidos por espaciadores tipo amida, sulfonamida o alqueno (**33**-**36**). Posteriormente, las mejores modificaciones obtenidas para el *hit* **1** fueron aplicadas al *hit* **2** y se sintetizaron derivados con un menor número de hidroxilos (**37**-**42**), monoésteres (**43**-**46**) y derivados con otros espaciadores (**47**-**50**).

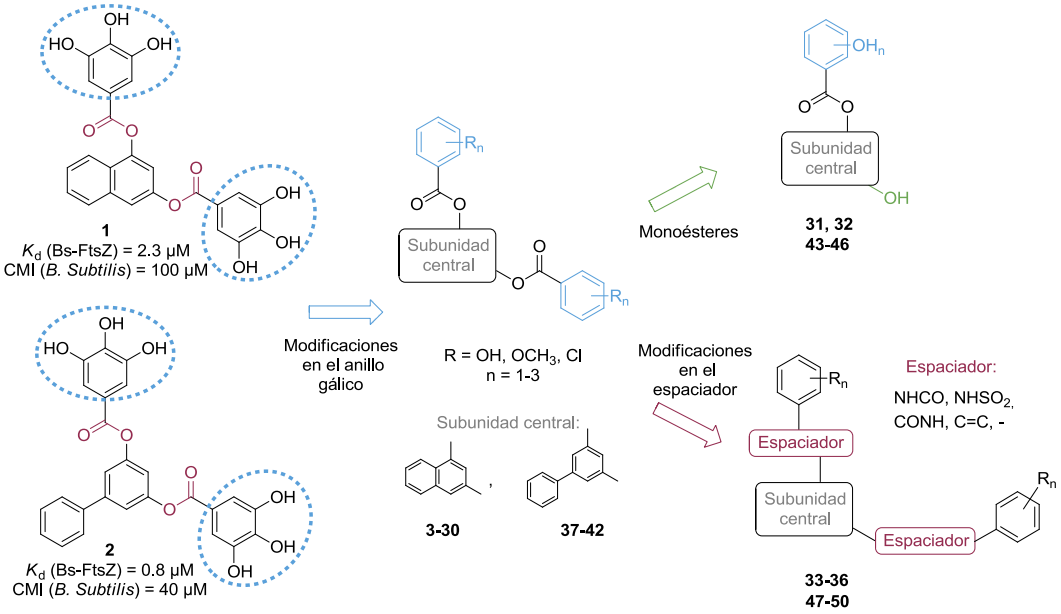

Figura 2. Compuestos **3**-**50** dirigidos al sitio de unión de GTP.

Los compuestos diseñados se sintetizaron mediante las rutas sintéticas optimizadas en el desarrollo de esta investigación (Esquemas 1-8).

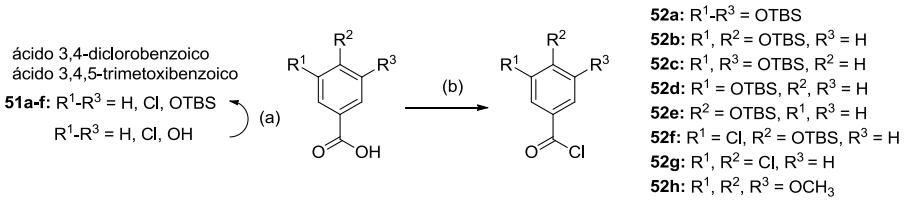

Esquema 1. Reactivos y condiciones: (a) (i) TBS-Cl, DIPEA, DMF, MW 100 ºC, 20 min or TBS-Cl, imidazol, DMF, t.a., 18 h; (ii) CH_3CO_2H, THF, t.a., 3 h, 74-81%; (b) cloruro de oxalilo, DMF, tolueno, 50 ºC, 1 h, cuantitativo.

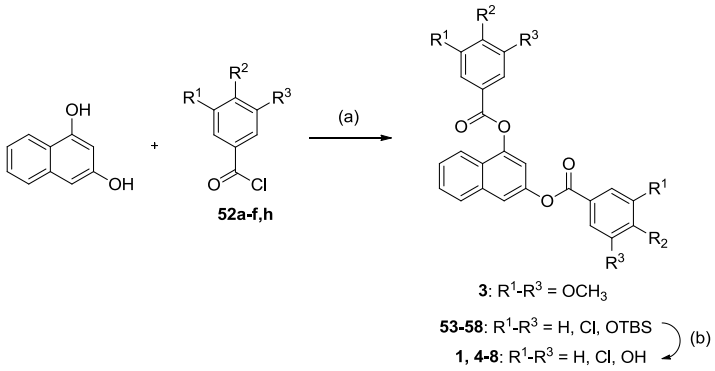

Esquema 2. Reactivos y condiciones: (a) Et_3N, DCM, t.a., 18 h, 54-71%; (b) HF·piridina, piridina, THF, t.a., 15 min, 26-88%.

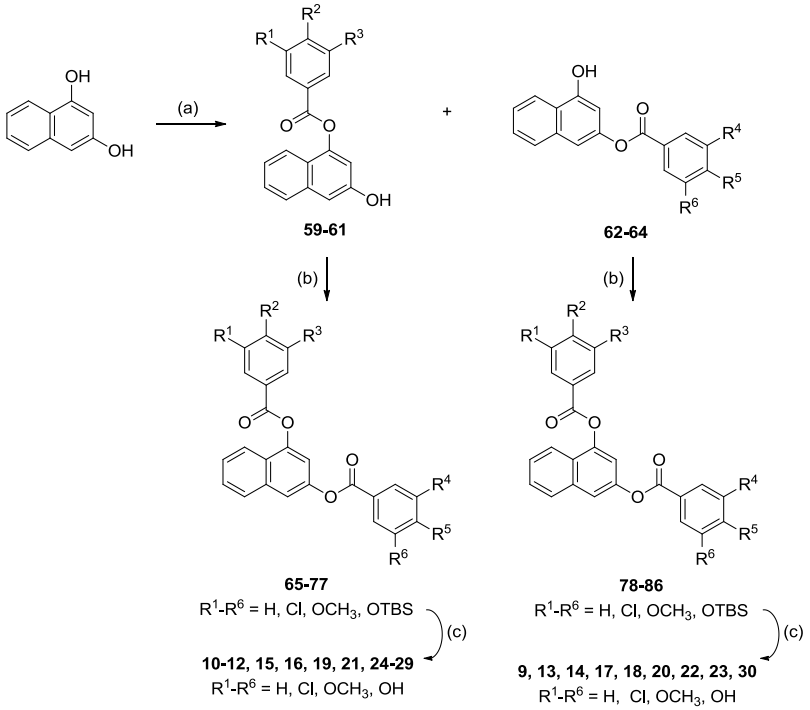

Esquema 3. Reactivos y condiciones: (a) **52a**,**c**, o **d** (0.25 equiv), Et_3N, DCM, t.a., 18 h, 22-38%; (b) **52b**-**h** (2 equiv), Et_3N, DCM, t.a., 18 h, 24-92%; (c) HF·piridina, piridina, THF, t.a., 15 min, 15-92%.

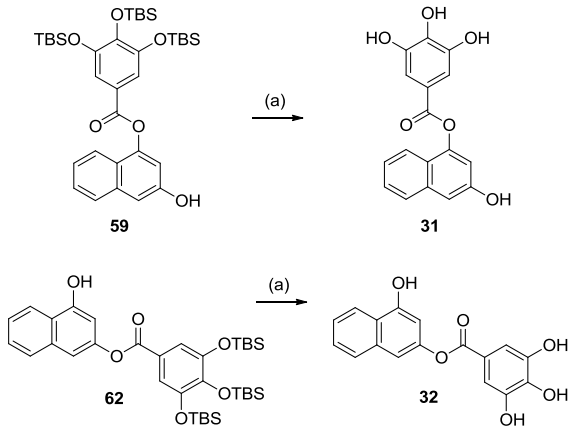

Esquema 4. Reactivos y condiciones: (a) HF·piridina, piridina, THF, t.a., 15 min, 78 y 93%.

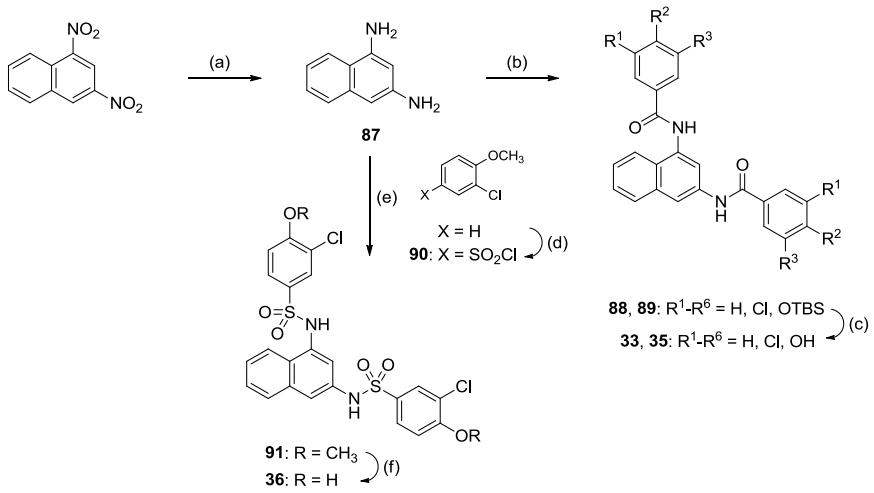

Esquema 5. Reactivos y condiciones: (a) H_2, 10% Pd/C, MeOH, t.a., 3.5 h, 60%; (b) **52a** o **f** (4 equiv), Et_3N, DCM, t.a., 18 h, 33-36%; (c) HF·piridina, piridina, THF, t.a., 15 min, 75-78%; (d) $ClSO_3H$, $CHCl_3$, 0 ºC a t.a., 16 h, 61%; (e) piridina, DCM, t.a., 18 h, 48%; (f) BBr_3, DCM, t.a., 18 h, 38%.

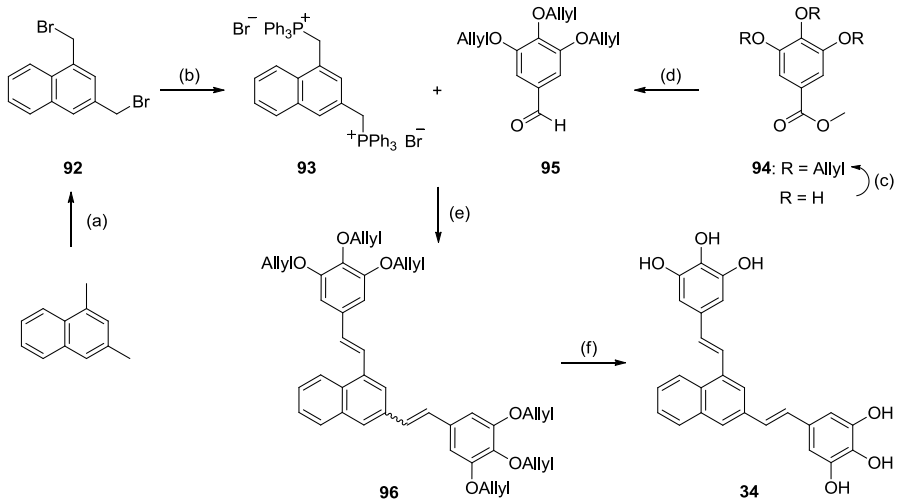

Esquema 6. Reativos y condiciones: (a) NBS, AIBN, CCl_4, 90 ºC, 16 h, 73%; (b) Ph_3P, xileno, reflujo, 72 h, 96%; (c) CH_2=$CHCH_2Br$, K_2CO_3, DMF, 65 ºC, 4 h, 99%; (d) Red-Al®, KO*t*-Bu, pirrolidina, THF, 0 ºC, 10 min, 78%; (e) *n*-BuLi, THF, -78 ºC a t.a., 18 h, 30% (1*E*,3*E*) y 18% (1*E*,3*Z*); (f) DMBA, $Pd(PPh_3)_4$, DCM/MeOH, t.a., 1 h, 19%.

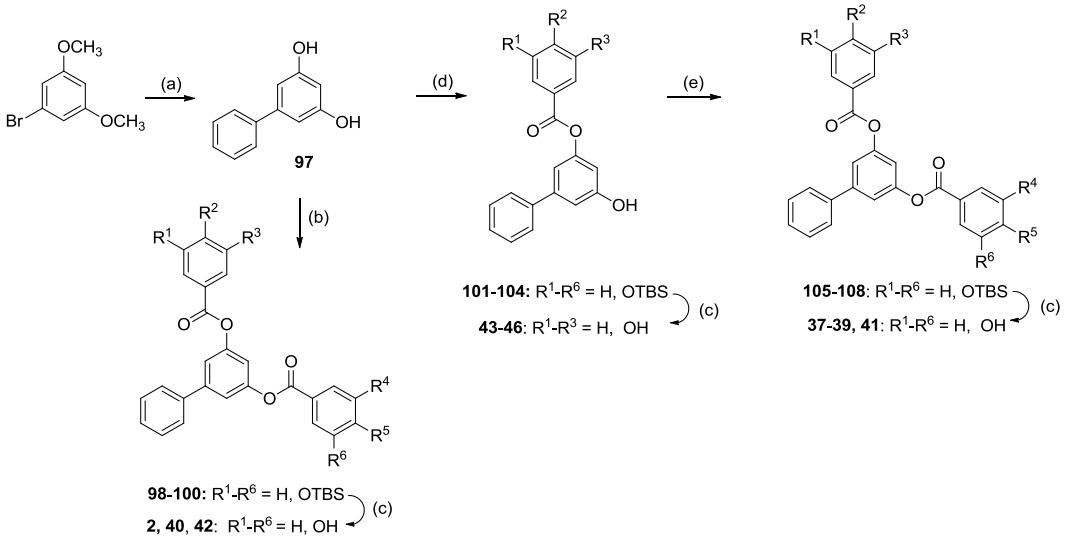

Esquema 7. Reactivos y condiciones: (a) (i) $PhB(OH)_2$, $Pd(PPh_3)_4$, Na_2CO_3, tolueno/H_2O, MW, 150 ºC, 30 min, 75%; (ii) BBr_3, DCM, t.a., 18 h, 97%; (b) **52a**,**d** o **e** (4 equiv), Et_3N, DCM, t.a., 18 h, 64-87%; (c) HF·piridina, piridina, THF, t.a., 15 min, 28-96%; (d) **52b**-**e** (0.25 equiv), Et_3N, DCM, t.a., 18 h, 46-69%; (e) **52c** o **d** (2 equiv), Et_3N, DCM, t.a., 18 h, 34-89%.

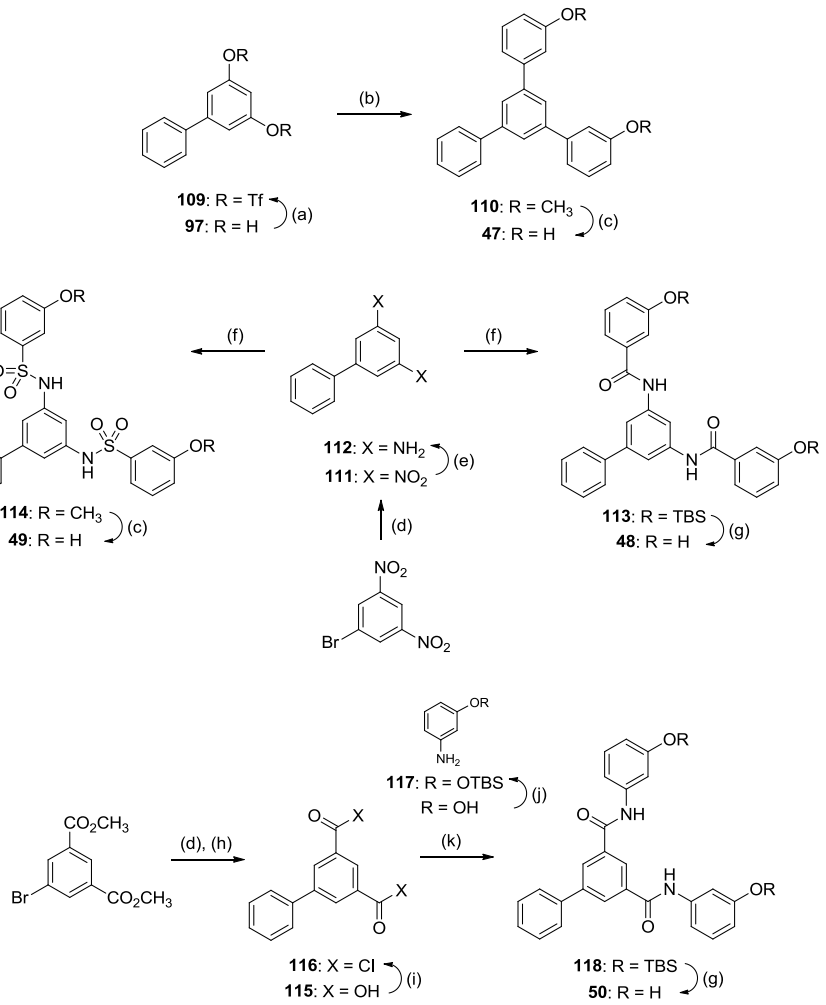

Esquema 8. Reactivos y condiciones: (a) anhídrido trifluorometanosulfónico, Et_3N, DCM, t.a., 2.5 h, 99%; (b) ácido 3-metoxifenilborónico, $Pd(PPh_3)_4$, Na_2CO_3, tolueno/EtOH/H_2O, MW, 150 ºC, 15 min, 75%; (c) BBr_3, DCM, t.a., 3 h, 21-94%; (d) $PhB(OH)_2$, $Pd(PPh_3)_4$, Na_2CO_3, tolueno/H_2O, MW, 150 ºC, 30 min, 83-90%; (e) H_2, 10% Pd/C (H-Cube), THF, t.a., 99%; (f) **52d** o cloruro de 3-metoxibencenosulfonilo, Et_3N, THF, t.a., 18 h, 20-45%; (g) HF·piridina, piridina, THF, t.a., 15 min, 66-89%; (h) NaOH, H_2O, THF, reflujo, 1.5 h, 85%; (i) $SOCl_2$, THF, reflujo, 3 h, 99%; (j) TBS-Cl, imidazol, 18 h, t.a., 48%; (k) Et_3N, THF, t.a., 18 h, 89%.

A continuación, se llevó a cabo la evaluación de la afinidad de los compuestos sintetizados **3**-**50** por la proteína FtsZ de *B. subtilis* mediante un ensayo de desplazamiento del ligando fluorescente *mant*-GTP. La mayoría de los compuestos sintetizados fueron capaces de desplazar *mant*-GTP en el rango micromolar (K_d = 0.5-2.2 µM). En general, la reducción en el número de grupos hidroxilo de las dos subunidades aromáticas aumenta la afinidad por FtsZ y los mejores resultados se

obtuvieron en aquellos compuestos con un hidroxilo en cada anillo (*e.g.* **29**, **40** y **41** K_d = 0.5-0.8 µM) (Figura 3). En cuanto a la actividad antibacteriana, todos los compuestos fueron activos en *B. subtilis* y MRSA USA 300 (como ejemplo representativo de cepa Gram-positiva patógena). La reducción en el número de hidroxilos parece ser también favorable para la actividad antibacteriana, lo que corrobora que estos compuestos ejercen su acción mediante la inhibición de FtsZ. De hecho, los mejores derivados fueron aquellos con dos grupos hidroxilo [*e.g.* **29** y **42**: CMI (MRSA) = 5 µM]. Otro patrón que parece ser importante en cuanto a la afinidad por FtsZ y la actividad antibacteriana es la introducción de átomos de cloro, como se puede observar en el compuesto **7** [K_d = 0.8 µM; CMI (MRSA) = 10 µM]. Además, se observó que en el caso de los monoésteres, la afinidad por FtsZ y la actividad antibacteriana se ven reducidas con respecto a los diésteres análogos, sugiriendo que ambas subunidades de polihidroxifenilo son necesarias para la unión a la proteína [*e.g.* **40**: K_d = 0.5 µM; CMI (MRSA) = 7 µM vs **45**: K_d = 3.8 µM; CMI (MRSA) = 50 µM]. En cuanto a los espaciadores entre la subunidad central y los anillos de polihidroxifenilo, la eliminación del espaciador dio lugar al compuesto **47**, que presentó la mayor afinidad obtenida hasta el momento (K_d = 0.5 µM) y una excelente actividad antibacteriana en MRSA (CMI = 3 µM). Sin embargo, la sustitución del éster por otros espaciadores produjo una disminución tanto en la afinidad como en la actividad antibacteriana [*e.g.* amida **48**: K_d = 4.3 µM; CMI (MRSA) = 50 µM].

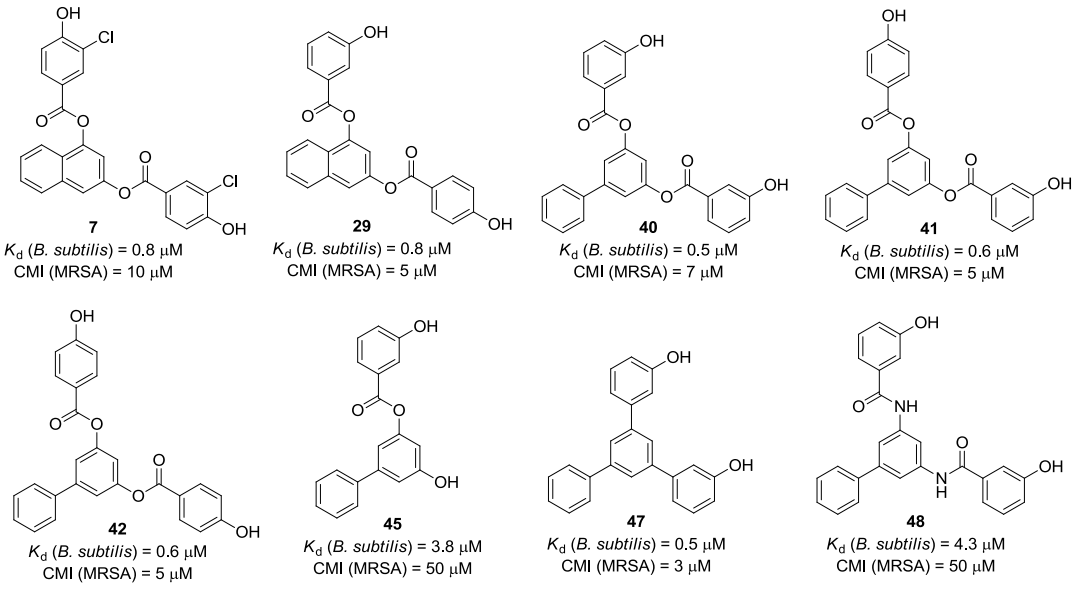

Figura 3. Inhibidores de FtsZ representativos dirigidos al sitio de unión de GTP en FtsZ.

La selectividad frente a tubulina −la homóloga eucariota de FtsZ− de los mejores compuestos se determinó mediante un estudio comparativo de la inhibición del ensamblaje de estas dos proteínas. Así, según se muestra en la Figura 4, los resultados de estos ensayos indicaron que la

introducción de átomos de cloro es perjudicial en cuanto a la selectividad, puesto que el compuesto **7** resultó ser el inhibidor más potente de tubulina. Además, la serie de bifenilos mostró en general una mayor inhibición de la polimerización de FtsZ y una mejor selectividad frente a tubulina, con excepción del monoéster **45**.

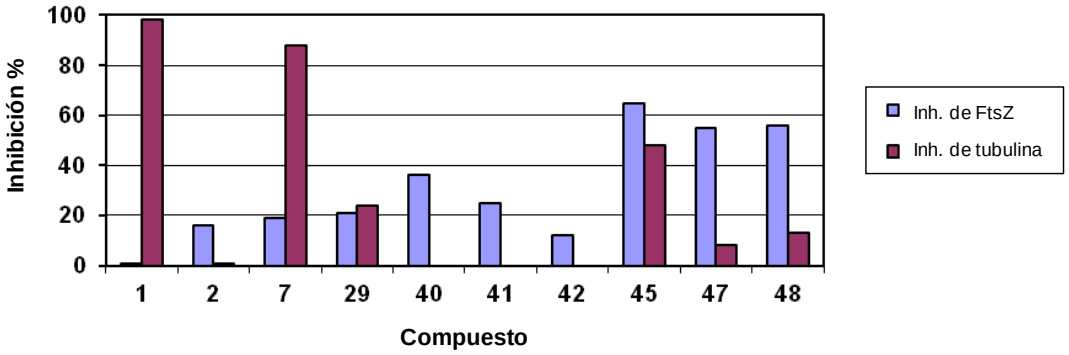

Figura 4. Porcentaje de inhibición de FtsZ (compuestos a 25 µM) y tubulina (compuestos a 100 µM).

A continuación, se estudió el perfil antibacteriano de los compuestos sintetizados en un panel de bacterias patógenas resistentes Gram-positivas y Gram-negativas. En general, todos los compuestos inhibieron el crecimiento de bacterias Gram-positivas, como por ejemplo MRSA (CMI = 3-50 µM) y *Listeria monocytogenes* (*L. monoc*., CMI = 5-50 µM); mientras que los derivados **29**, **40**-**42** y **45** también fueron capaces de inhibir el crecimiento de *Enterococcus faecalis* (*E. faecalis*) a 50 µM. En cuanto a las cepas Gram-negativas, a pesar de que el *hit* **2** fue activo en *Pseudomonas aeruginosa* y *Escherichia coli* resistentes (*P. aerug.* y *E. coli*, CMI = 50 µM), ninguno de sus derivados afectó al crecimiento de bacterias patógenas Gram-negativas a la concentración ensayada (100 µM), lo que parece indicar que la reducción en el número de hidroxilos en estos compuestos es perjudicial en términos de actividad antibacteriana frente a dichas cepas.

Tabla 1. Actividad antibacteriana de los compuestos seleccionados frente a bacterias patógenas resistentes.

Compuesto	K_d[a] FtsZ (μM)	CMI (μM)					
		MRSA		*E. faecalis*[d]	*L. monoc.*[e]	*P. aerug.*[f]	*E. coli*[g]
		USA 300[b]	Mu50[c]				
1	2.3 ± 0.1	60	80	>100	50	100	>100
2	0.8 ± 0.1	50	50	>100	50	50	50
29	0.8 ± 0.2	5	5	50	5	>100	>100
40	0.5 ± 0.1	7	7	50	7	>50	>100
41	0.6 ± 0.3	5	5	50	5	>50	>100
42	0.4 ± 0.1	5	5	50	5	>50	>100
45	3.8 ± 0.8	50	50	50	50	>50	>100
47	0.5 ± 0.1	3	3	>100	5	>50	>100
48	4.3 ± 1.0	50	50	>100	50	>50	>100

[a]Los valores son la media ± EEM. Cepas clínicamente aisladas de *S. aureus* provenientes del Instituto Pasteur de Francia [b]resistentes a meticilina (ATCC Nr: BAA-1556) o [c]resistentes a meticilina, kanamicina y ampicilina (ATCC 700699). [d]Cepas secuenciadas de *Enterococcus faecalis* resistente a gentamicina y vancomicina (V583 ATCC 700802). [e]Cepas secuenciadas de *Listeria* monocytogenes (EGDe). [f]Cepas secuenciadas de *Pseudomonas aeruginosa* resistente a imipenem (PAO1). [g]Cepas clínicamente aisladas de *Escherichia coli* proveniente de una infección de cistitis (UTI89).

Con el fin de identificar el inhibidor de la división bacteriana más efectivo entre los compuestos descritos, se llevó a cabo un estudio de sus efectos en la división celular de la bacteria *B. subtilis* 168 natural y en la localización subcelular de FtsZ en *B. subtilis* SU570. Estas últimas células expresan FtsZ fusionada a la proteína fluorescente verde (FtsZ-GFP) como única proteína FtsZ. Así, se caracterizaron los efectos celulares de los inhibidores más efectivos frente a FtsZ (**29**, **40**, **41**, **45**, **47** y **48**), observándose que las células de *B. subtilis* 168 tratadas con cada uno de estos compuestos exprimentaron un aumento de longitud respecto a las células control (Figura 5). Entre los compuestos ensayados, el derivado **40** mostró el efecto más claro en la división bacteriana y las bacterias tratadas con este inhibidor consistieron en células filamentosas sin dividir mucho más alargadas.

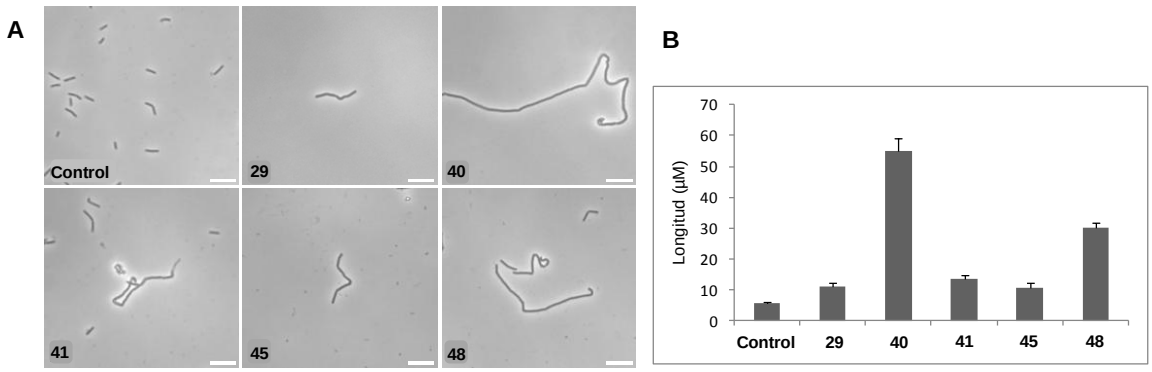

Figura 5. Efecto en la división celular de los inhibidores de FtsZ. (A) Células de *B. subtilis* 168 incubadas durante 3 h con los inhibidores de FtsZ **29** (5 µM), **40** (4 µM), **41** (5 µM), **45** (25 µM) y **48** (12 µM) y observadas mediante microscopía de contraste de fases. (B) Longitud de las células *B. subtilis* 168. La barra de la imagen se corresponde a una escala de 10 µm.

La visualización intracelular de FtsZ en células de *B. subtilis* SU570 indica que los compuestos **29**, **40** y **48** producen la deslocalización de la proteína, evitando la formación del anillo Z en la zona central y provocan la aparición de numerosos *foci* de FtsZ distribuidos aletoriamente en la célula. Dicha situación origina un defecto en la formación del anillo Z, lo que provoca la aparición de células alargadas incapaces de dividirse (Figura 6, fila FtsZ-GFP). Además, cuando se visualizó el nucleoide, se observó que éste tenía una apariencia fragmentada, por lo que estos compuestos parecen inducir la descondensación del ADN bacteriano (Figura 6, fila DAPI). Asimismo, la visualización de la membrana de las mismas células de *B. subtilis* SU570 con el colorante FM4-64 también permitió apreciar que los inhibidores tienen un efecto sobre la membrana celular, ya que se distinguen algunos agregados intracelulares.

En resumen, la mayoría de los compuestos descritos en esta primera parte del trabajo son capaces de inhibir la división bacteriana bloqueando el ensamblaje de la proteína FtsZ y por tanto la formación del anillo Z. Entre los compuestos desarrollados, el derivado **40** destaca como el inhibidor más efectivo de la división bacteriana. Este compuesto junto con **29** y **48** bloquea la polimerización de FtsZ, dando lugar a células filamentosas que no se dividen, impidiendo la viabilidad de la bacteria.

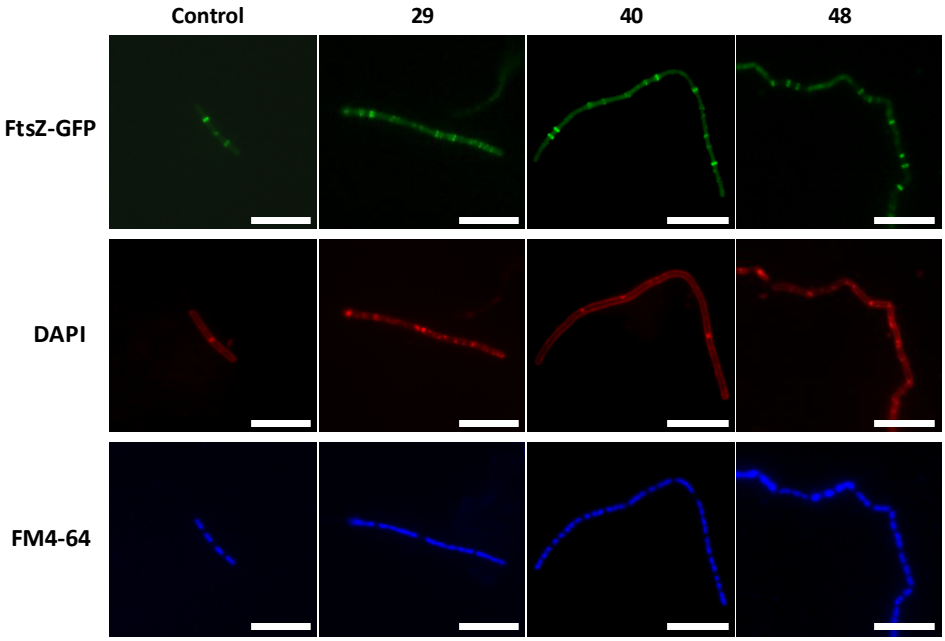

Figure 6. Localización subcelular de FtsZ en células de *B. subtilis* SU570 (FtsZ-GFP) incubadas durante 1 h con los compuestos **29** (5 µM), **40** (3 µM), y **48** (12 µM). El marcaje FtsZ-GFP y la tinción del nucleoide con colorante DAPI y de la membrana con colorante FM4-64 se visualizaron en el canal de fluorescencia correspondiente. La barra de la imagen se corresponde a una escala de 10 µm.

5.2.2. Desarrollo de sondas fluorescentes dirigidas al sitio de unión de PC

La falta de un ensayo de unión a FtsZ que permita medir la afinidad de moléculas pequeñas en el sitio de unión alostérico identificado para el inhibidor PC190723, dificulta el desarrollo de nuevos inhibidores alostéricos de FtsZ. De hecho, para identificar inhibidores que se unan al sitio de unión de PC sólo se han empleado hasta el momento experimentos fenotípicos como el ensayo de sedimentación de polímeros de FtsZ. Por lo tanto, el empleo de derivados fluorescentes de PC o de su análogo **8j** permitiría desarrollar un ensayo de desplazamiento basado en fluorescencia para el cribado de librerías de compuestos y la consiguiente identificación de inhibidores de FtsZ que se unan a este nuevo sitio alostérico.

En este contexto, hemos desarrollado un proyecto de investigación enfocado al diseño y síntesis de derivados de PC/**8j** fluorescentes siguiendo dos aproximaciones: (i) el anclaje de un fluoróforo a la estructura de **8j** mediante un espaciador rígido, como por ejemplo un alquino, o una cadena alifática flexible (**119**-**122**), y (ii) la substitución de la subunidad heterocíclica de PC/**8j** por un fluoróforo (**123**-**125**). Respecto a los fluoróforos empleados, inicialmente se seleccionaron

estructuras pequeñas como nitrobenzoxadiazol (NBD), un derivado de cumarina y dansilo (Figura 7).

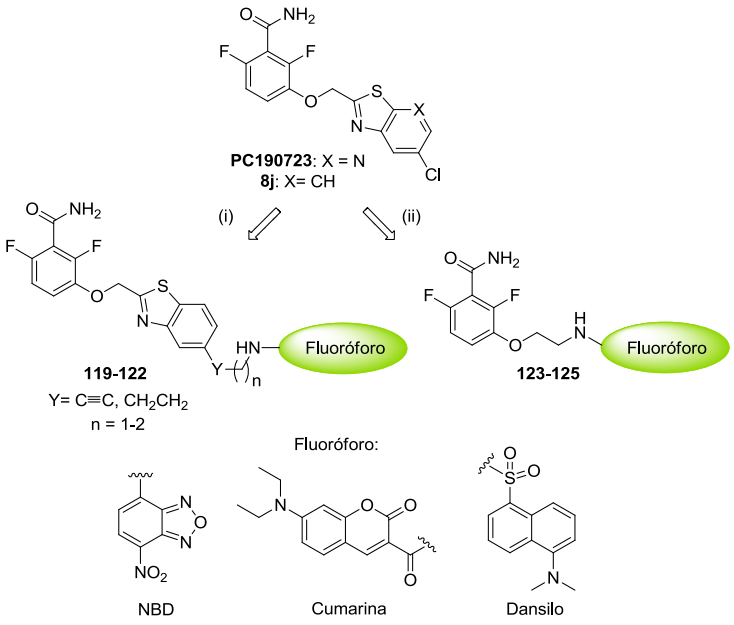

Figura 7. Diseño incial de derivados fluorescentes de PC190723/**8j**.

En primer lugar, se sintetizó PC190723 para su empleo como control positivo en la puesta a punto del ensayo de desplazamiento basado en fluorescencia. La síntesis se llevó a cabo siguiendo la metodología previamente descrita en la bibliografía (Esquema 9).[71]

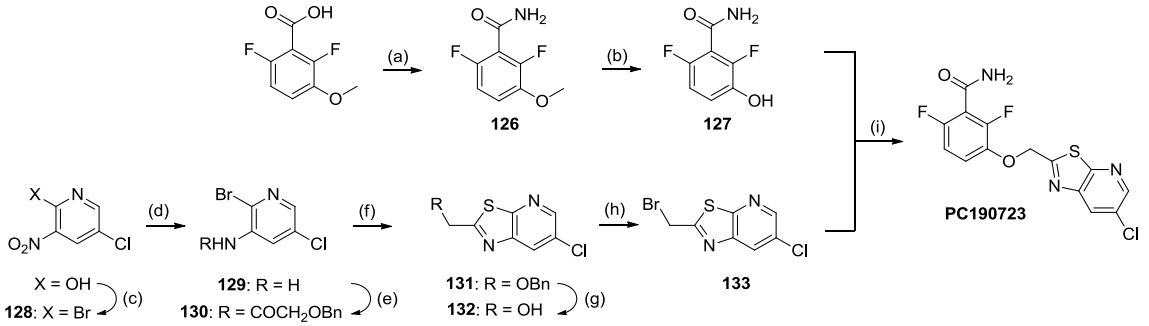

Esquema 9. Reactivos y condiciones: (a) i) $SOCl_2$, tolueno, reflujo, 5 h, cuantitativo; ii) NH_4OH, THF, t.a., 16 h, 80%; (b) BBr_3, DCM, t.a., 3 días, 79 %; (c) PBr_3, tolueno/DMF, 130 ºC, 3 h, 42%; (d) $SnCl_2{\cdot}H_2O$, HCl, Et_2O, 50 ºC, 30 min, 98%; (e) cloruro de benciloxiacetilo, Et_3N, DCM, t.a., 14 h, 80 %; (f) reactivo de Lawesson, tolueno, 120 ºC, 3 h, 79%; (g) BBr_3, DCM, t.a., 2 h, 88%; (h) NBS, Ph_3P, DCM, t.a., 2.5 h, 68%; (i) K_2CO_3, NaI, DMF, t.a., 16 h, 33%.

Los derivados fluorescentes **119**-**125** se sintetizaron mediante las secuencias de reacciones recogidas en los Esquemas 10-13 a partir de transformaciones que se pusieron a punto a lo largo de la tesis.

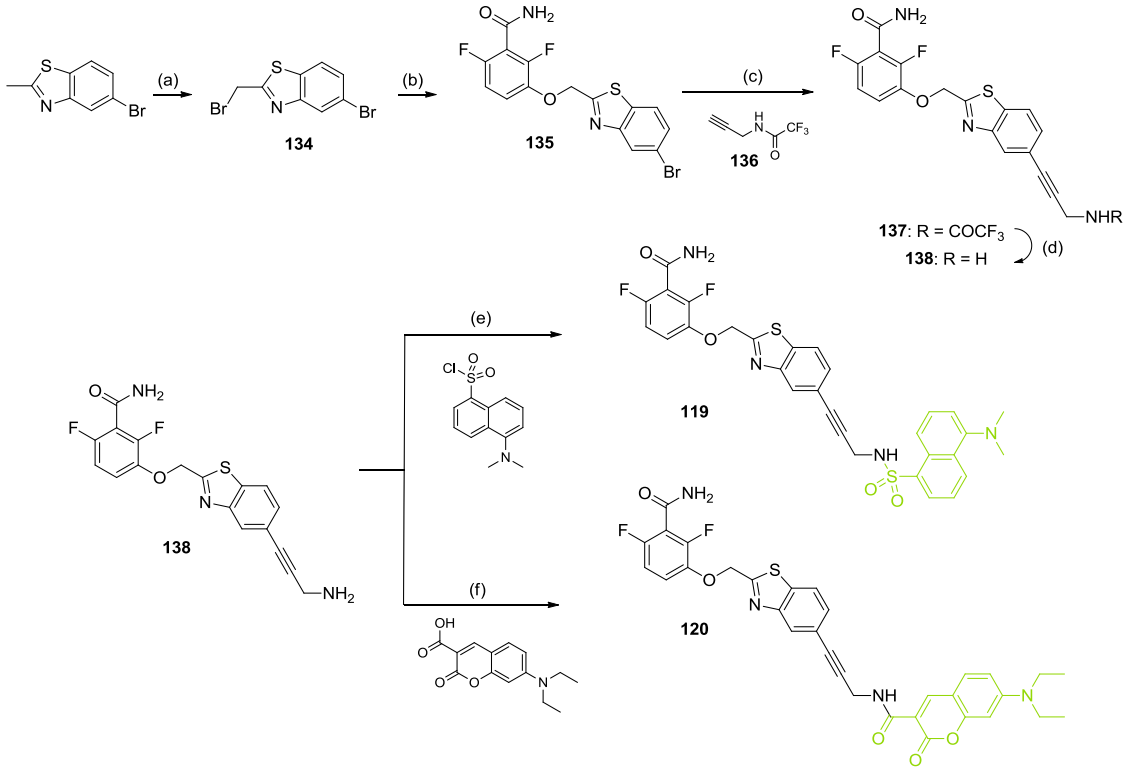

Esquema 10. Reactivos y condiciones: (a) NBS, AIBN, CCl_4, 90 ºC, 3 h, 13%; (b) **127**, K_2CO_3, DMF, t.a., 16 h, 82%; (c) $Pd(PPh_3)_4$, CuI, Et_3N, DMF, MW, 100 ºC, 45 min, 86%; (d) NH_4OH, MeOH, t.a., 17 h, 99%; (e) Et_3N, DCM/DMF, t.a., 24 h, 28%; (f) PyBroP®, DIPEA, DMF, t.a., 4 h, 5%.

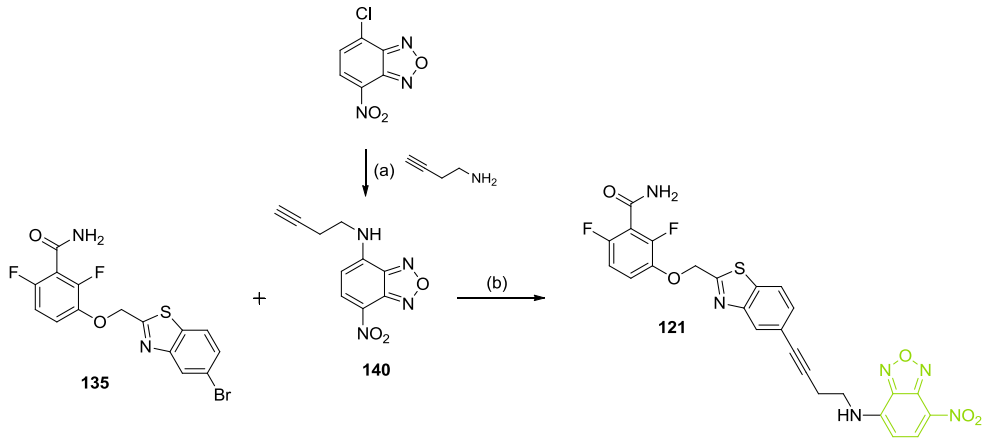

Esquema 11. Reactivos y condiciones: (a) DIPEA, MeOH, t.a., 15 h, 77%; (b) $Pd(PPh_3)_4$, CuI, Et_3N, DMF, MW, 100 ºC, 1 h, 41%.

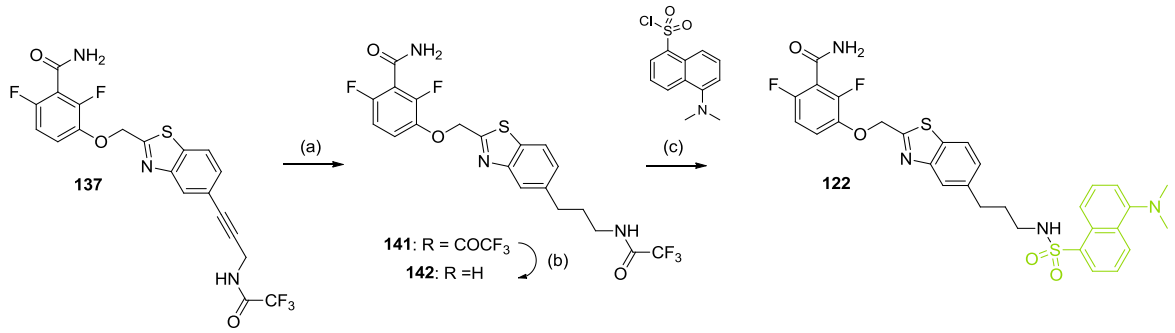

Esquema 12. Reactivos y condiciones: (a) H_2, Ni-Ra, THF/MeOH, t.a., 3 h, 22%; (b) NH_4OH, MeOH, t.a., 17 h, 99%; (c) Et_3N, DCM/DMF, t.a., 24 h, 26%.

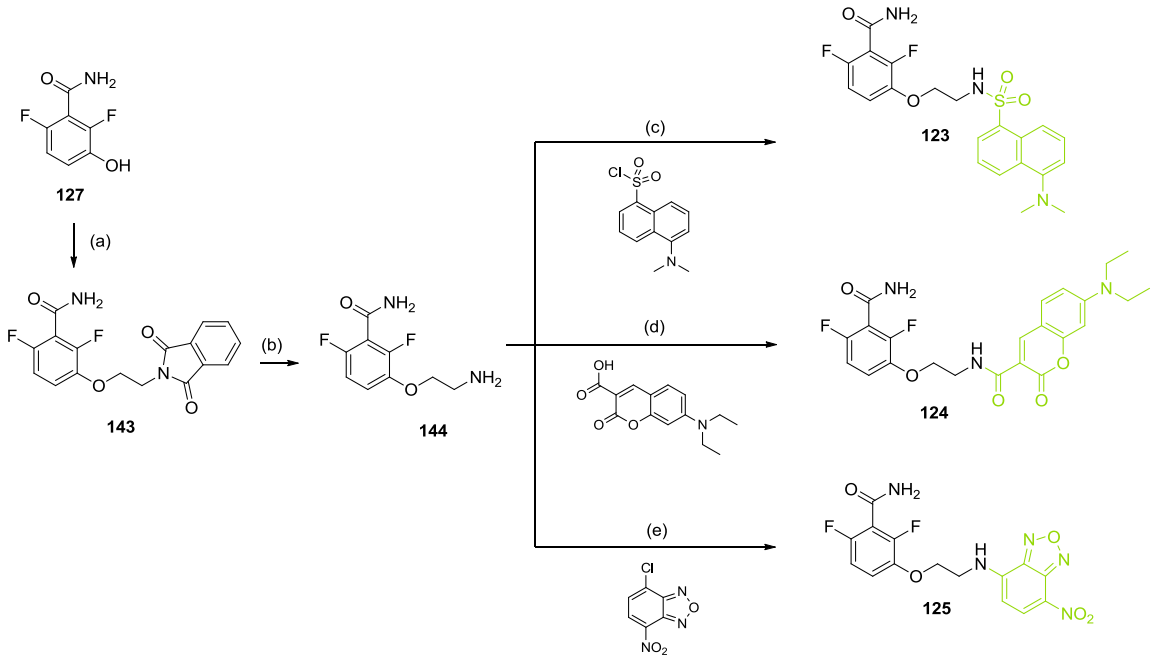

Esquema 13. Reactivos y condiciones: (a) *N*-(2-hidroxietil)ftalimida, DEAD, Ph_3P, THF, reflujo, 24 h, 67%; (b) $N_2H_4 \cdot H_2O$, EtOH, reflujo, 2 h, 67%; (c) Et_3N, DCM/DMF, t.a., 24 h, 8%; (d) PyBroP®, DIPEA, DMF, t.a., 4 h, 27%; (e) Et_3N, DMF, t.a., 20 h, 13%.

A continuación, se estudiaron las propiedades fluorescentes de los compuestos **119**-**125** con el fin de evaluar su potencial como sondas fluorescentes. En teoría un buen candidato a sonda fluorescente de FtsZ debería mostrar un cambio significativo en el espectro de emisión de fluorescencia [longitud de onda (λ) y/o intensidad de emisión (I_{em})], o en los valores de anisotropía (r) en presencia de la proteína. Dicho cambio debería poderse revertir a los valores iniciales mediante la adición del inhibidor PC190723 y consiguiente desplazamiento de la sonda del sitio de unión alostérico. Por tanto, para determinar si la fluorescencia de estos ligandos cambia al unirse a los monómeros o a los polímeros de FtsZ se registraron espectros de emisión de fluorescencia de cada compuesto (10 μM) en las condiciones de polimerización, excitando a la longitud de onda correspondiente al máximo de absorción de cada compuesto fluorescente. Los espectros de emisión y la anisotropía de fluorescencia se registraron en varias condiciones partiendo de una disolución del compuesto de interés en tampón Hepes pH 6.8 a 25 ºC a la que se le fueron añadiendo consecutivamente la proteína Bs-FtsZ (10 μM), GMPCPP (0.1 mM), $MgCl_2$ (10 mM), y PC190723 o **8j** (10 μM) para revertir finalmente el efecto.

En general, ninguno de los compuestos sintetizados mostró cambios significativos en la longitud de onda o intensidad de emisión de fluorescencia. En cambio, se observó que la anisotropía de

fluorescencia del derivado de NBD **125** aumenta en las condiciones de polimerización; es decir, en presencia de FtsZ (10 μM), GMPCPP (0.1 mM) y $MgCl_2$ (10 mM) (basal: r = 0.035; polimerización: r = 0.086). La adición de PC190723 produce una disminución de la anisotropía (r = 0.036), demostrando que es posible desplazar el ligando fluorescente (Tabla 2). Considerando los buenos resultados obtenidos con el derivado **125**, dicho compuesto fue seleccionado para estudiar el espaciador entre la difluorobenzamida y el fluoróforo NBD (**145**-**147**, Figura 8). Además, teniendo en cuenta la actividad frente a FtsZ de los compuestos derivados de 3-metoxibenzamida descritos en la bibliografía, consideramos interesante la introducción de una cadena de octilo en el espaciador (**148**, Figura 8). Llegados a este punto, también contemplamos la posibilidad de introducir fluoróforos adecuados para microscopía de super-resolución, como por ejemplo 4-(y-5)-carboxitetrametilrodamina (TAMRA) y ATTO 565, con el fin de obtener sondas con mejores propiedades fluorescentes para estudiar los procesos dinámicos de la división bacteriana (**149** y **150**, Figura 8).

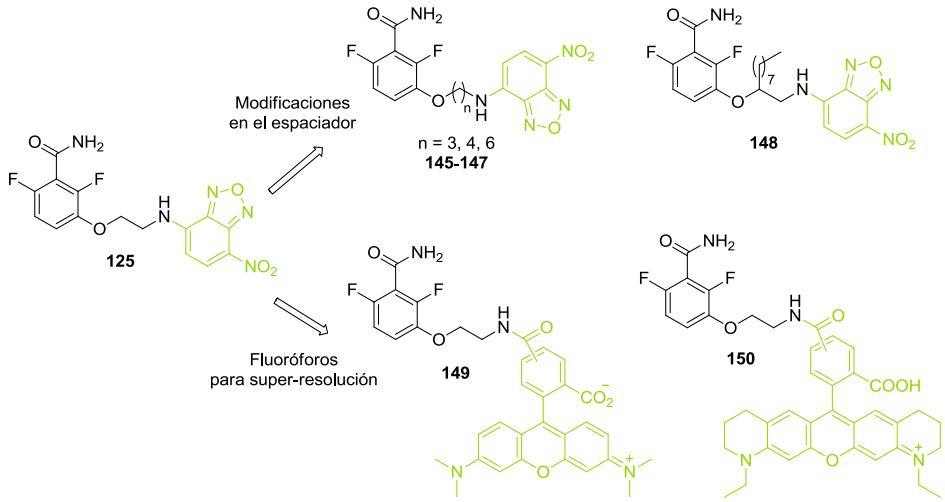

Figura 8. Diseño de nuevos derivados fluorescentes basados en el compuesto **125**.

La síntesis de los compuestos **145**-**150** se llevó a cabo siguiendo las rutas sintéticas representadas en los Esquemas 14-16.

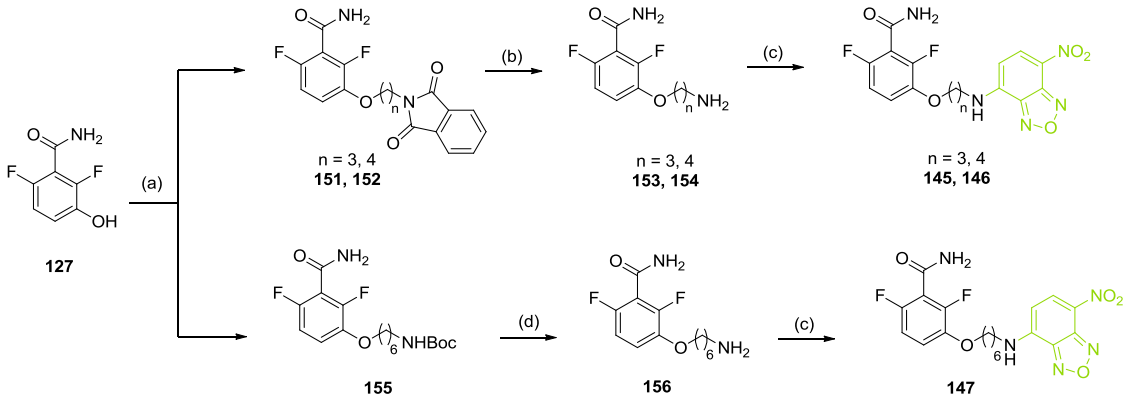

Esquema 14. Reactivos y condiciones: (a) *N*-(3-bromopropil)-, *N*-(4-bromobutil)ftalimida, o 6-bromo-*N*-Boc-1-hexanamina, K_2CO_3, NaI, DMF, t.a., 16 h, 57-87%; (b) $N_2H_4 \cdot H_2O$, EtOH, reflujo, 2 h, 55-64%; (c) Cl-NBD, DIPEA, DMF, t.a., 16 h, 4-11%; (d) TFA, DCM, t.a., 1 h, 99%.

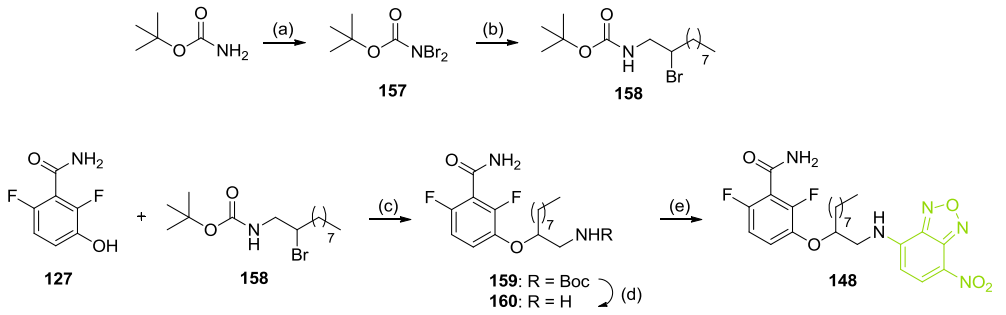

Esquema 15. Reactivos y condiciones: (a) Br_2, K_2CO_3, H_2O, t.a., 2 h, 79%; (b) i) 1-deceno, DCM, reflujo, 3 h; ii) Na_2SO_3, 5-10 ºC, 15 min, 56%; (c) K_2CO_3, NaI, DMF, t.a., 16 h, 23%; (d) TFA, DCM, t.a., 1 h, 99%; (e) Cl-NBD, Et_3N, DMF, t.a., 16 h, 11%.

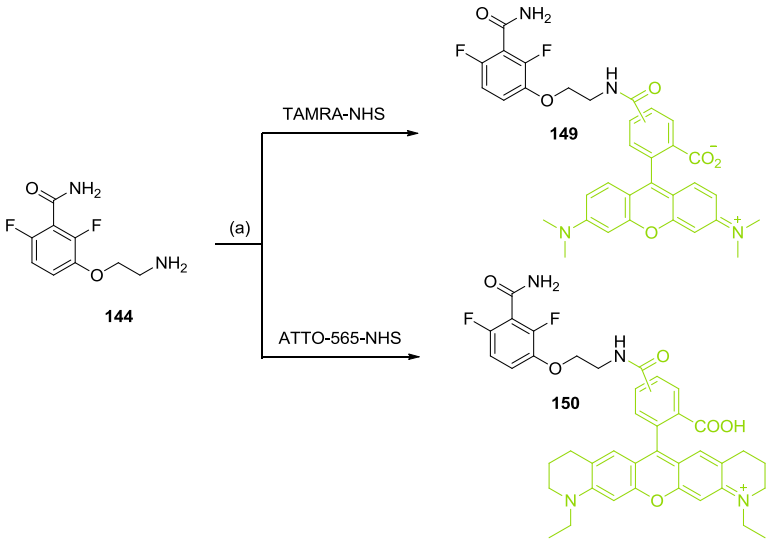

Esquema 16. Reactivos y condiciones: (a) Et_3N, DMF, t.a., 4 h, 66, 99%.

Una vez más, los derivados de NBD **145**-**148** experimentaron un incremento de anisotropía con la adición de $MgCl_2$, volviendo a los valores iniciales por desplazamiento de PC190723, excepto en el caso de **148** en el que no fue posible revertir el aumento de anisotropía (Tabla 2). En cuanto a los compuestos funcionalizados con TAMRA y ATTO 565, no se observaron cambios en la fluorescencia ni en la anisotropía en las condiciones de polimerización.

Tabla 2. Valores de anisotropía (r) de los derivados fluorescentes **125** y **145**-**150**.

	125	**145**	**146**	**147**	**148**	**149**	**150**
Compuesto (10 μM)	0.026	0.038	0.032	0.030	0.045	0.030	0.019
+ Bs-FtsZ (10 μM)	0.034	0.042	0.035	0.042	0.130	0.031	0.025
+ GMPCPP (0.1 mM)	0.035	0.040	0.039	0.042	0.186	0.030	0.022
+ $MgCl_2$ (10 mM)	0.086	0.078	0.078	0.127	0.317	0.032	0.025
+ PC190723 (10 μM)	0.036	0.057	0.046	0.067	0.324	0.030	0.023
+ PC190723 (10 μM)*	0.026	0.046	0.032	0.046	0.322	0.030	0.019
Compuesto + GMPCPP	0.034	0.038	0.028	0.038	0.053	0.029	0.019
Compuesto + $MgCl_2$	0.035	0.033	0.027	0.033	0.054	0.030	0.020
Compuesto + PC190723	0.038	0.032	0.028	0.032	0.052	0.030	0.020
Mezcla sin Bs-FtsZ	0.026	0.035	0.027	0.035	0.052	-	-

* Se añadió más PC190723 (10 μM), concentración final 20 μM.

Por tanto, se seleccionaron los derivados de NBD **125** y **145**-**147** como los mejores candidatos a sondas fluorescentes de la proteína FtsZ, estudiándose a continuación su efecto en la polimerización de FtsZ. El ensayo de sedimentación de polímeros de FtsZ indica que estos compuestos alteran la polimerización en función de la concentración. Así, los derivados **125**, **145** y **146** aumentaron el porcentaje de sedimento siguiendo el mismo patrón que PC190723, que actúa como un estabilizador de los protofilamentos de FtsZ. Por el contrario, el derivado **147** produjo una disminución del porcentaje de sedimento con respecto al control, actuando como un inhibidor de la polimerización de FtsZ (Figura 9).

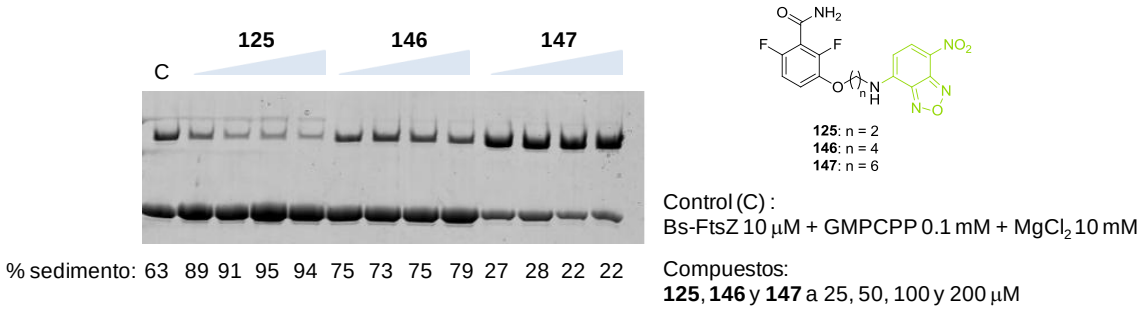

Figura 9. Ensayo de sedimentación de polímeros de FtsZ con los derivados **125**, **146** y **147**.

A continuación, se determinaron las curvas de desplazamiento de los compuestos **125** y **145**-**147** con PC190723 con el objetivo de evaluar el potencial de estas sondas fluorescentes en un ensayo que permita identificar nuevos inhibidores de FtsZ dirigidos al sitio alostérico de PC. Para ello, a partir de una disolución de FtsZ polimerizada (5 μM) en presencia de GMPCPP (0.1 mM), $MgCl_2$ (10 mM) y el correspondiente derivado fluorescente (5 μM), se fueron añadiendo concentraciones crecientes de PC190723 hasta recuperar los valores de anisotropía basales correspondientes a la sonda libre (Figura 10). Como se puede observar en la gráfica, los valores de anisotropía disminuyen a concentraciones crecientes de PC190723, lo que indica que estos derivados de NBD pueden utilizarse como sondas fluorescentes. Así, los derivados **125** y **146** han sido seleccionados para llevar a cabo un ensayo de desplazamiento basado en fluorescencia en el que se evaluarán compuestos descritos como inhibidores de FtsZ que no actúan sobre el sitio de unión de GTP junto con una librería de compuestos comerciales que ha sido previamente seleccionada por cribado virtual. Este ensayo se está llevando a cabo actualmente y permitirá la determinación de las constantes de afinidad por el sitio de unión de PC y la consiguiente identificación de nuevos inhibidores alostéricos de FtsZ.

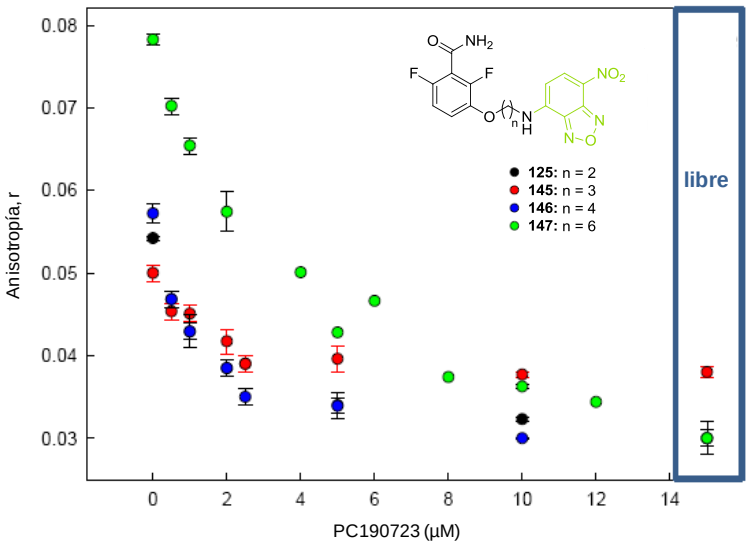

Figura 10. Curvas de desplazamiento de las sondas fluorescentes **125** y **145**-**147** con PC190723.

Finalmente, se realizaron experimentos *in vivo* en células de *B. subtilis* utilizando las sondas fluorescentes a distintas concentraciones con el fin de marcar FtsZ y visualizar el proceso de división bacteriana. Así, los derivados **125** y **145**-**147** fueron capaces de marcar FtsZ sin afectar a la división bacteriana a una concentración igual o menor de 50 µM (Figura 11A). La fluorescencia desaparece con la adición de PC190723 (25 µM), lo que indica que la sonda está siendo desplazada y demuestra la especificidad del marcaje (Figura 11B). Además, se observó que las sondas son capaces de afectar a la polimerización de FtsZ a una concentración de 200 µM, dando lugar a células filamentosas, efecto característico que también se observa con el inhibidor PC190723. Por lo tanto, estos experimentos confirman el potencial de las sondas fluorescentes descritas para la visualización de la proteína FtsZ y el estudio de su papel principal en el proceso de división bacteriana.

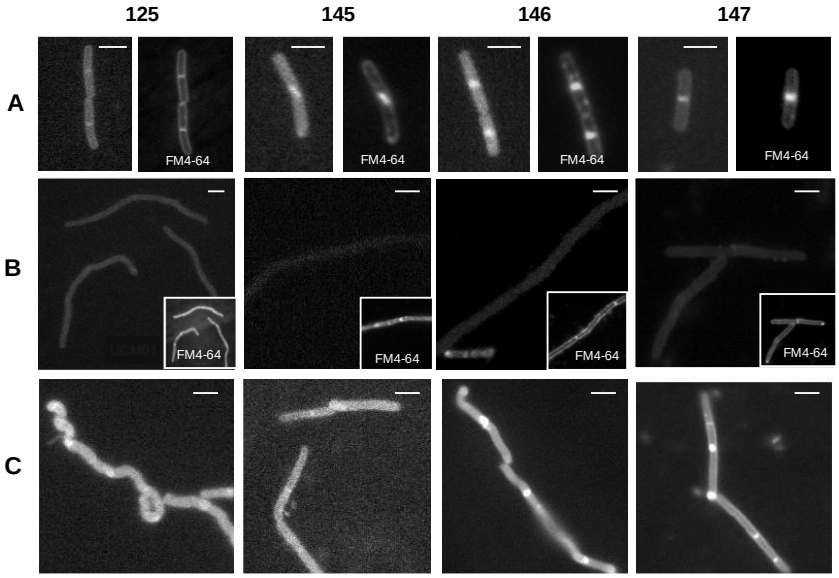

Figura 11. Estudios *in vivo* con las sondas fluorescentes **125** y **145**-**147** en células *B. subtilis* 168. (A) Marcaje de FtsZ con las sondas a 50 µM y visualización mediante microscopía de fluorescencia. (B) Para determinar la especificidad del marcaje, las células se marcaron en las condiciones anteriores en presencia de PC190723 (25 µM). (C) Células fluorescentes filamentosas observadas con las sondas a 200 µM.

5.3. Conclusiones

En el presente trabajo se ha llevado a cabo la identificación de agentes antibacterianos con un nuevo mecanismo de acción mediante el desarrollo de compuestos dirigidos a los dos sitios de unión descritos para la proteína de la división bacteriana FtsZ. Con respecto al sitio de unión de GTP, se han identificado los primeros derivados sintéticos no-nucleótidos que inhiben de manera específica la polimerización de FtsZ y bloquean la citoquinesis bacteriana. Estos compuestos presentan una buena actividad antibacteriana en bacterias Gram-positivas patógenas. Entre ellos, el derivado **40** destaca como un prometedor agente antibacteriano con buena afinidad (K_d = 0.5 µM) y actividad antibacteriana [CMI (MRSA) = 7 µM]. Este inhibidor, junto con **29**, **45** y **48** actúa como un agente que bloquea la polimerización de FtsZ y da lugar a células filamentosas que no son capaces de dividirse y finalmente mueren. En conclusión, estos compuestos contribuyen a ampliar el escaso número de miméticos de GTP que inhiben FtsZ y proporcionan la base para el desarrollo de agentes antibacterianos con un nuevo mecanismo de acción.

En cuanto al sitio de unión de PC, hemos desarrollado derivados fluorescentes de PC190723 como sondas para el marcaje de FtsZ que contribuyan al estudio *in vivo* de la función de FtsZ en la división bacteriana. En concreto, los derivados de NBD **125** y **145**-**147** han demostrado tener un

gran potencial para la visualización del anillo Z durante la división bacteriana. Asimismo, el empleo de estas sondas en ensayos de desplazamiento permitirá la identificación de nuevos inhibidores alostéricos de FtsZ, experimento que se está poniendo a punto actualmente.

6. SUMMARY

6.1. Introduction and Objectives

Antibacterial resistance is one of the biggest threat of the health system in the 21st century and new treatments to fight against multi-drug resistant infections are desperately necessary.[15,20] In this sense, FtsZ has been proposed as an attractive target for the identification of novel mode of action (MoA) agents, which could contribute to fight against the virulence and the speed in which bacteria adquire resistance to recently approved antibiotics.[33] FtsZ is a tubulin-like GTPase almost universally conserved throughout bacteria that plays a key role in the cell division process. This protein polymerizes into different shaped filaments leading to a highly dynamic structure known as the Z-ring, which together with other accessory proteins regulate and form the divisome.[39] This complex finally constricts and generates two daughter cells. Therefore, FtsZ could be an interesting therapeutic target to fight against bacterial infections since small molecules able to inhibit its activity will eventually disrupt bacterial viability.

Among the FtsZ inhibitors described so far, PC190723 is the most studied compound and its co-crystalization with FtsZ has allowed the identification of a long cleft as a new allosteric druggable site in the protein, known as the PC-binding site. This compound exhibits potent antibacterial activity [*e.g.* MIC (MRSA) = 2.8 μM] and is the first inhibitor shown to be efficacious in an *in vivo* model of bacterial infection.

In this context, the main objective of this thesis is the development of new FtsZ inhibitors with good antibacterial properties. For this purpose we have focused our efforts on the identification of new compounds targeting the two druggable binding sites of FtsZ: (i) the GTP- and (ii) the allosteric PC-binding pocket (Figure 1).

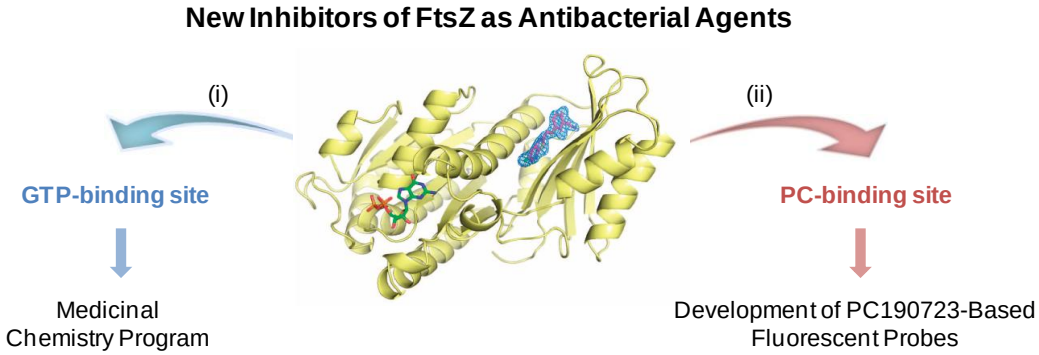

Figure 1. Dual strategy on the search for FtsZ inhibitors.

The development of new small molecules able to replace the natural regulator GTP and to specifically inhibit FtsZ in order to block the bacterial cell division process involves the following steps:

- Identification of hits.
- Design, synthesis, and biological evaluation of a new series of compounds. In this evaluation we will consider the assessment of the FtsZ binding affinity, the antibacterial activity and selectivity against tubulin.
- Further characterization of optimized inhibitors in terms of antibacterial properties against Gram-positive and Gram-negative pathogens, cytological profile, and mechanism of action.

Regarding the PC-binding pocket, the interesting antibacterial properties of PC190723 and the lack of a methodology to assess the binding affinity against this newly reported binding site in FtsZ, prompted us to develop fluorescent probes based on this inhibitor to set up a fluorescence-based binding assay for the identification of new inhibitors. In addition, these probes could contribute to study this allosteric site that seems to play a key role in the FtsZ assembly, in order to get a better understanding about this dynamic process. Therefore, the second goal of this project implies the following steps:

- Design and synthesis of fluorescent derivatives based on PC190723.
- Biological evaluation and fluorescent characterization of the synthesized compounds.
- Use of the best fluorescent probes as biological tools for the study of the bacterial cell division process and for the identification of new FtsZ inhibitors by a fluorescence-based displacement assay.

6.2. Results and Discussion

6.2.1. Development of FtsZ Inhibitors Targeting the GTP-Binding Site

In the search of new FtsZ inhibitors of the GTP-binding site, we docked our in-house library into the GTP-binding pocket of *B. subtilis* FtsZ and tested the hits with the highest scores in the *mant*-GTP fluorescence anisotropy competitive assay.[84] The best molecules obtained from this screening shared a general structure of two gallate subunits bound to a central core of differently substituted naphthalene, benzene, biphenyl and cyclohexane rings as well as an ethylene spacer. Among them, hits **1** and **2** showed the highest affinities for Bs-FtsZ (K_d = 2.3 and 0.8 μM, respectively), and moderate antibacterial activity in *B. subtilis* (MIC = 100 and 40 μM, respectively), being the first non-nucleotide synthetic molecules that effectively compete with GTP for binding to FtsZ (Figure 2).[84]

In order to carry out a structure-affinity-activity analysis around hits **1** and **2**, we focused our attention on two subunits susceptible to structural modifications: the galloyl rings and the ester bonds used as spacers (Figure 2). Variations in the central core were discarded since derivatives of our in-house library bearing other scaffolds displayed less affinity and/or antibacterial activity than the 1,3-naphthyl or 3,5-biphenyl counterparts. The structure of compound **1** was used as a starting point for chemical modifications. Thus, to study the influence of the hydroxy groups of the phenyl rings, we first considered the reduction of the number of these groups as well as their substitution pattern and their replacement by other substituents such as methoxy or chlorine, while keeping constant other parts of hit **1** (**3**-**30**). In addition, monoester derivatives **31** and **32** were synthesized in order to study the influence of both polyhydroxyphenyl rings in the binding to FtsZ. Furthermore, compounds in which the ester groups of **1** were replaced by other spacers such as amides, sulfonamides and double bonds were contemplated (**33**-**36**). After the biological evaluation of this series, the best modifications obtained for hit **1** were applied to biphenyl derivative **2** and compounds having a lower number of hydroxy groups (**37**-**42**), monoesters (**43**-**46**) and non-ester derivatives (**47**-**50**) were synthesized.

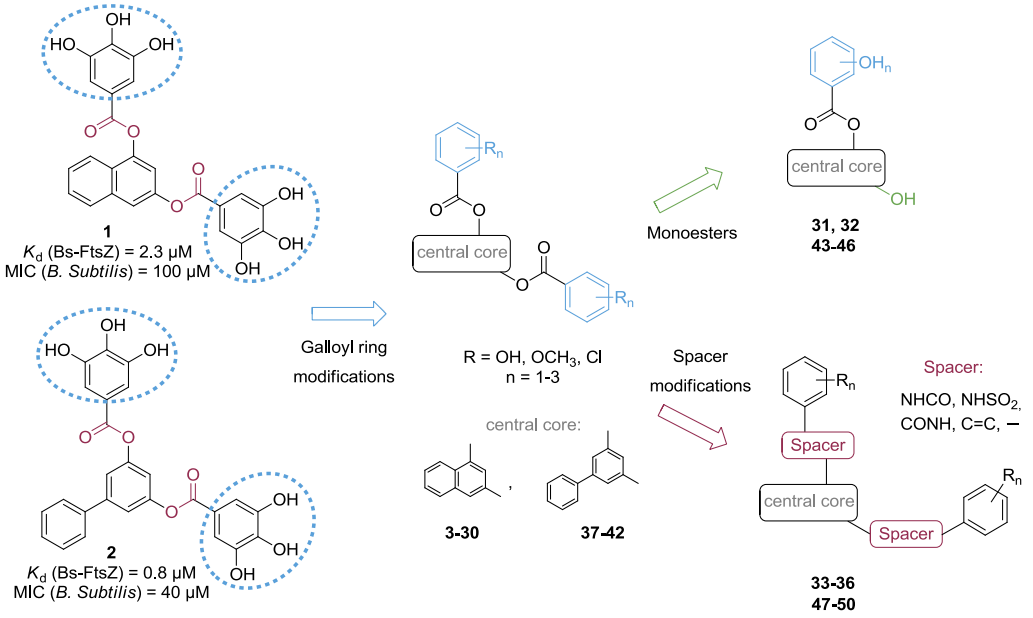

Figure 2. Synthesized compounds **3-50** targeting the GTP-binding site.

The synthesized compounds **3**-**50** were then evaluated using the *mant*-GTP fluorescence anisotropy competitive assay[82] to measure their binding affinities (dissociation constant, K_d) for FtsZ of *B. subtilis*. Most of the tested compounds were able to displace *mant*-GTP in the micromolar range (K_d = 0.5-2.2 µM). In general, the reduction in the number of hydroxy groups on both phenyl rings improves the binding affinity, and the best K_d values were obtained for those derivatives having only two hydroxy groups (*e.g.* **29**, **40** and **41** K_d = 0.5-0.8 µM) (Figure 3). Assesment of antibacterial activity of compounds **3**-**50** indicates that, in general, all compounds are active against *B. subtilis* and MRSA USA 300 (as a representative example of Gram-positive pathogenic bacteria). The reduction in the number of hydroxy groups seems to be favorable in terms of potency, which supports that these compounds exert their antibacterial activity through inhibition of FtsZ. In fact, the most potent derivatives were those with only two hydroxy groups [*e.g.* **29** and **42**: MIC (MRSA) = 5 µM]. Another structure-affinity-activity relationship that can be drawn for this series is that the introduction of chlorine atoms proved to be important for FtsZ affinity and antibacterial activity, as can be shown for compound **7** [K_d = 0.8 µM; MIC (MRSA) = 10 µM]. Moreover, FtsZ affinity and antibacterial activity of monoesters were reduced when compared with their corresponding diesters, suggesting that both polyhydroxyphenyl subunits are required for FtsZ binding and antibacterial activity [*e.g.* **40**: K_d = 0.5 µM; MIC (MRSA) = 7 µM vs **45**: K_d = 3.8 µM; MIC (MRSA) = 50 µM]. Regarding the influence of the spacer between the central core and the polyhydroxyphenyl rings, the replacement of the ester groups by

sulfonamides or alkenes did not provide higher FtsZ affinity nor good antibacterial activity [*e.g.* amide **48**: K_d = 4.3 μM; MIC (MRSA) = 50 μM]. However, submicromolar affinity (K_d = 0.5 μM) and excellent antibacterial activity against MRSA (MIC = 3 μM) were obtained when the linker between the biphenhyl central core and the phenyl subunits was removed in compound **47**.

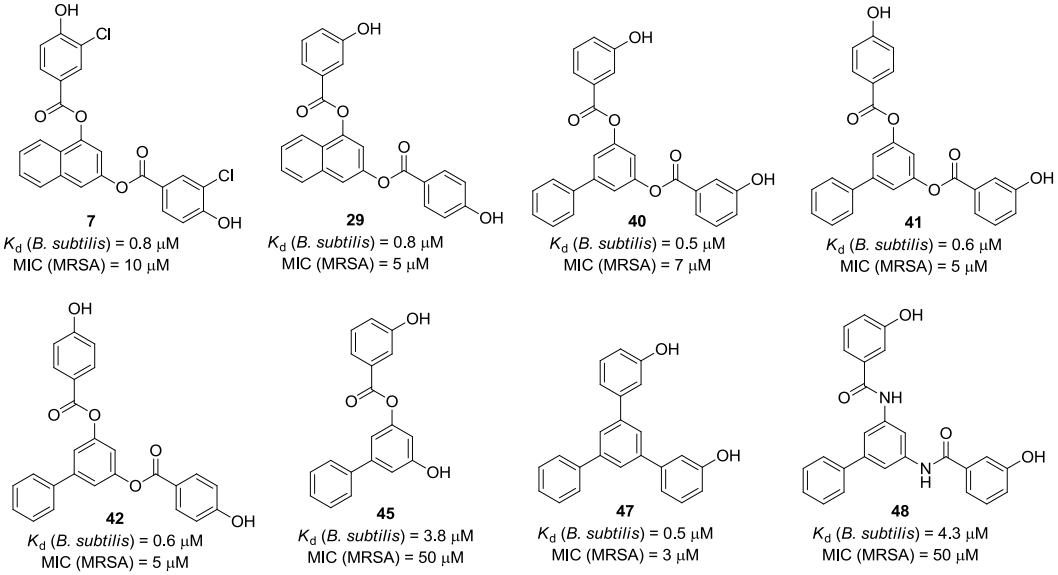

Figure 3. Representative FtsZ inhibitors targeting the GTP-binding site.

Afterward, tubulin and FtsZ assembly inhibition was determined as an assessment of FtsZ selectivity. As shown in Figure 4, the introduction of chlorine atoms was detrimental for selectivity, being compound **7** among the most potent tubulin inhibitors. In addition, most biphenyl derivatives exerted stronger FtsZ inhibition as well as good tubulin selectivity, with the exception of monoester **45**.

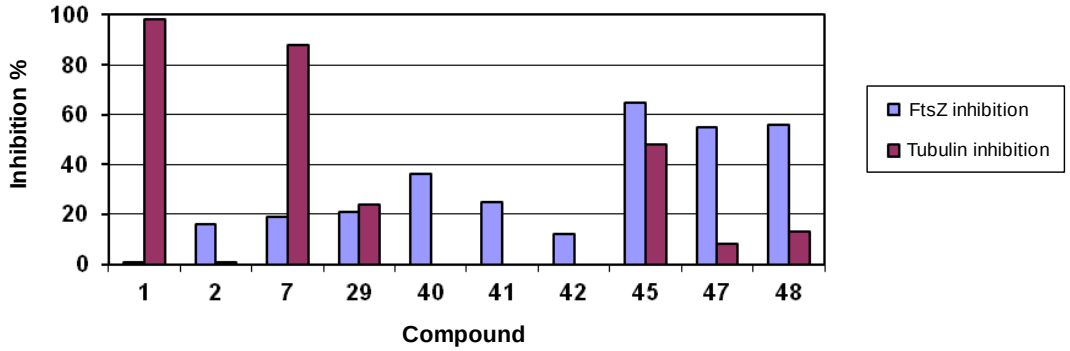

Figure 4. Percentage of FtsZ (25 μM of compound) and tubulin (100 μM of compound) inhibition.

Microbiological profile of selected compounds on a broader panel of antibiotic-resistant Gram-positive and Gram-negative pathogenic bacteria was also determined (Table 1). In general, all tested compounds inhibited the growth of Gram-positive resistant pathogenic bacteria such as MRSA (MIC = 3-50 μM) and *Listeria monocytogenes* (*L. monoc*., MIC = 5-50 μM), being **29**, **40**-**42** and **45** also able to inhibit *Enterococcus faecalis* (*E. faecalis*) growth at 50 μM. Regarding Gram-negative bacteria, although initial biphenyl hit **2** showed moderate activity in resistant *Pseudomonas aeruginosa* and *Escherichia coli* (*P. aerug.* and *E. coli*, MIC = 50 μM), none of its derivatives affected the growth of Gram-negative pathogens at the assayed concentration (100 μM), which indicates that removal of hydroxy groups was detrimental for the antibacterial activity against these strains.

Table 1. Antibacterial activity against pathogenic bacteria of selected compounds.

Compuesto	K_d[a] FtsZ (μM)	MIC (μM)					
		MRSA		*E. faecalis*[d]	*L. monoc.*[e]	*P. aerug.*[f]	*E. coli*[g]
		USA 300[b]	Mu50[c]				
1	2.3 ± 0.1	60	80	>100	50	100	>100
2	0.8 ± 0.1	50	50	>100	50	50	50
29	0.8 ± 0.2	5	5	50	5	>100	>100
40	0.5 ± 0.1	7	7	50	7	>50	>100
41	0.6 ± 0.3	5	5	50	5	>50	>100
42	0.4 ± 0.1	5	5	50	5	>50	>100
45	3.8 ± 0.8	50	50	50	50	>50	>100
47	0.5 ± 0.1	3	3	>100	5	>50	>100
48	4.3 ± 1.0	50	50	>100	50	>50	>100

[a]The values are the mean ± SEM. [b]*S. aureus* community acquired, methicillin resistant ATCC Nr: BAA-1556 (Institute Pasteur, France) and [c]Methicillin, ampicillin and kanamycin resistant Mu50/ATCC 700699 (Institute Pasteur, France). [c]*Enterococcus faecalis,* gentamicin and vancomycin resistant V583 ATCC700802 (sequenced strain). [d]*Listeria monocytogenes,* EGDe (sequenced strain). [e]*Pseudomonas aeruginosa,* imipenem resistant PAO1 (sequenced strain). [f] *Escherichia coli*, UTI89 from cystitis infection (sequenced strain).

In order to identify the most effective bacterial division blockers among the selected compounds, we examined their effects on the cell division of wild type *B. subtilis* 168 and on FtsZ subcellular localization in *B. subtilis* SU570, a strain that has FtsZ fused to green fluorescent protein (FtsZ-GFP) as the only FtsZ protein. First, we characterized the cellular effects of our most effective FtsZ inhibitors (**29**, **40**, **41**, **45**, **47**, and **48**). Cells of wild type *B. subtilis* 168 exposed to each of these compounds were longer than control cells (Figure 5). Among them, derivative **40** exhibited the clearest effect as bacterial division blocker. The phenotype of cells treated with biphenyl **40** (4 μM) consisted of long filamentous undivided cells. This effect was also observed

when the cells were incubated with the amide analogue **48** (12 μM) and weaker effects were found with **41** (5 μM) and fragment **45** (25 μM) as well as with the naphthyl compound **29** (5 μM).

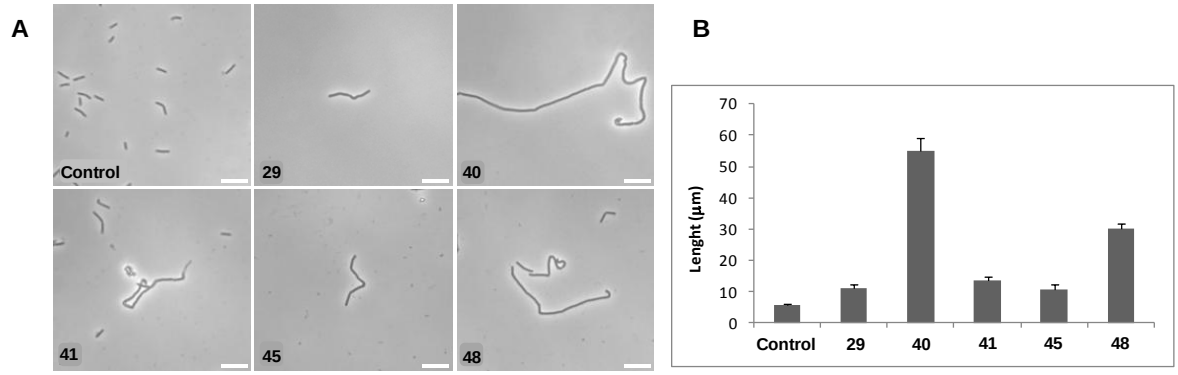

Figure 5. Cell division effect of FtsZ inhibitors. (A) *B. subtilis* 168 incubated during 3 h with FtsZ inhibitors **29** (5 μM), **40** (4 μM), **41** (5 μM), **45** (25 μM), and **48** (12 μM) and observed by phase contrast microscopy. Scale bar: 10 μm. (B) *B. subtilis* 168 cell length.

Moreover, these compounds impaired the normal assembly of FtsZ-GFP into the mid-cell Z-ring prior to division of *B. subtilis* SU570 at concentrations near their MIC values, further supporting FtsZ targeting. The observed effects consisted of a reduction in the proportion of cells with normal Z-rings at division sites with respect to controls and FtsZ delocalization into characteristic punctuate *foci* along the bacterial cells (Figure 6, FtsZ-GFP row). Z-rings along the filamented cells were very frequently observed abnormally close to each other with compounds **29**, **40**, and **48**, whereas FtsZ-GFP *foci* were more abundant in cells treated with compounds **29** and **40**. The impairment of the cell division ring is also reflected by abnormal nucleoid morphology. In contrast with the control cells, nucleoids frequently had a fragmenting appearance in cells treated with the FtsZ inhibitors (Figure 6, DAPI row). Membranes were visualized in the same *B. subtilis* SU570 treated cells with the vital stain FM4-64, and frequent extra membrane accumulations and patches were observed.

Therefore, the majority of the GTP-replacing compounds under study inhibited bacterial cell division by disrupting FtsZ assembly and impairment of the Z-ring. Among them, biphenyl derivative **40** stands out as the most effective bacterial cell division inhibitor. This compound together with compounds **29** and **48** acts as an effective FtsZ modifier and leads to filamentous undivided cells, finally disrupting bacterial viability.

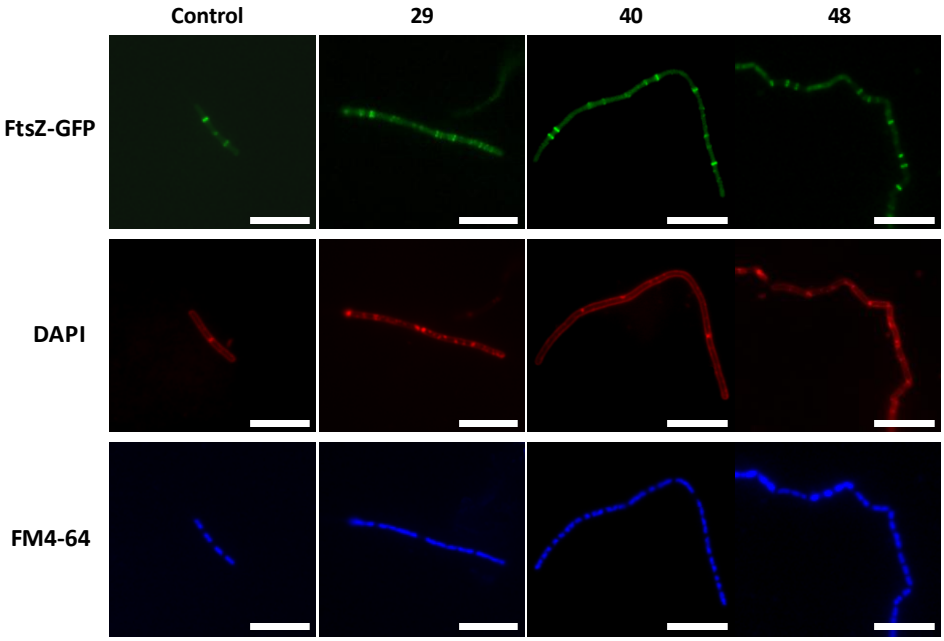

Figure 6. Effect of FtsZ inhibitors on FtsZ subcellular localization. Cells of *B. subtilis* SU570 (FtsZ-GFP) were incubated during 1 h with **29** (5 µM), **40** (3 µM), and **48** (12 µM). FtsZ-GFP, membrane stained with FM4-64, and DNA stained with DAPI were visualized through their corresponding channels with a fluorescence microscope. Scale bar: 10 µm.

6.2.2. Development of Fluorescent Probes for the PC190723 Binding Site of FtsZ

The lack of a binding assay to assess the affinity of small molecules for the new druggable pocket of FtsZ, known as the PC190723-binding site, hampers the development of new FtsZ inhibitors addressing this allosteric site as antibacterial agents. Indeed, only phenotypic experiments such as polymer pelleting assays have been used in order to identify new inhibitors. Therefore, fluorescent derivatives of PC or its analogue **8j** could be used as valuable tools to set up a fluorescence-based assay for the identification of FtsZ inhibitors by screening a library of compounds against this newly identified binding site.

This fact prompted us to carry out a project aimed at the design and synthesis of fluorescent probes based on PC/**8j** following two different approaches: (i) attachment of a fluorophore to the structure of **8j** through a rigid linker, such as an alkyne moiety, or a flexible aliphatic chain (**119**-**122**), and (ii) substitution of the heterocyclic subunit of PC/**8j** by a fluorescent tag (**123**-**125**). With respect to the fluorescent tag, we selected small fluorophores such as nitrobenzoxadiazole (NBD), a coumarin derivative, and dansyl (Figure 7).

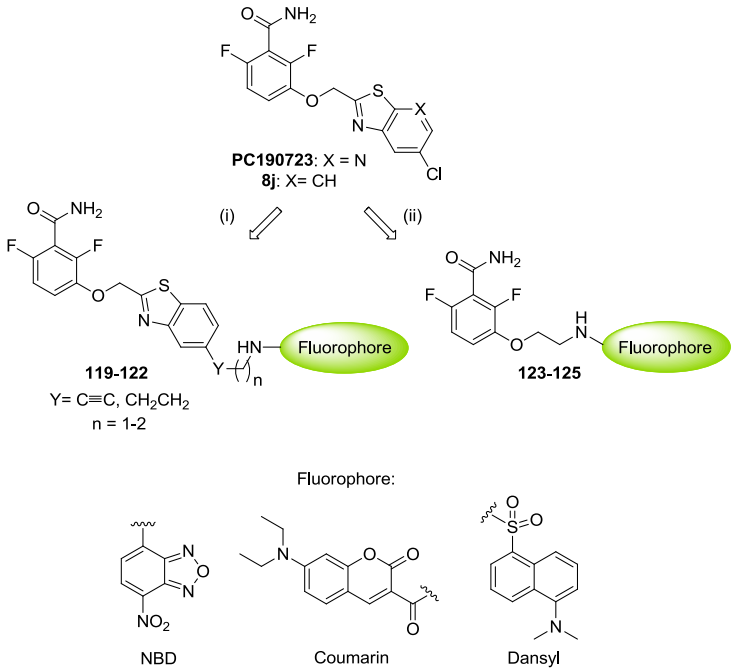

Figure 7. Initial design of PC190723/**8j** fluorescent derivatives.

Once fluorescent compounds **119**-**125** were synthesized, we assessed their fluorescent properties in order to evaluate their potential as chemical probes. In theory, a good candidate for a FtsZ fluorescent probe based on PC190723 should show a significant modification in the emission fluorescence spectrum [wavelength (λ) and/or emission intensity (I_{em})] or in the fluorescence anisotropy values (r) in the presence of the protein, that could be then reverted to the initial values by addition and displacement of the parent compound PC190723. Therefore, fluorescence emission spectra and anisotropy of compounds **119**-**125** (10 μM) were registered employing an excitation wavelength corresponding to the maximum absortion of each compound in Hepes buffer at pH 6.8 and 25 ºC. Then, Bs-FtsZ (10 μM) in Hepes buffer, the slowly hydrozable GTP analogue GMPCPP (0.1 mM) and $MgCl_2$ (10 mM) were subsequently added to set up the polymerization conditions. Finally, PC190723 or **8j** (10 μM) was added in order to displace and revert the possible effect of the fluorescent probes.

In general, the fluorescence emission spectra of the compounds did not show significant changes. However, fluorescence anisotropy of NBD derivative **125** (Table 2) increased when $MgCl_2$ was added and the polymerization was initiated (basal: r = 0.035; polymerization: r = 0.086), being then restored by displacement with PC190723 (r = 0.036), which indicates that this fluorescent compound binds to the protein at the same binding site than PC190723. Taking into

account the positive results obtained with **125**, we selected this compound to study the influence of the spacer between the difluorobenzamide and the NBD moiety by increasing the length of the alkyl chain (**145**-**147**, Figure 8). Moreover, based on the activity data of 3-methoxybenzamide derivatives in FtsZ previously reported, we also considered the introduction of an octyl chain in the linker (**148**). At this point, fluorophores for super-resolution microscopy such as 4-(and-5)-carboxytetramethylrhodamine (TAMRA) and ATTO 565 were also taken into account in order to obtain probes with optimized fluorescent properties for the study of the bacterial division process (**149** and **150**, Figure 8).

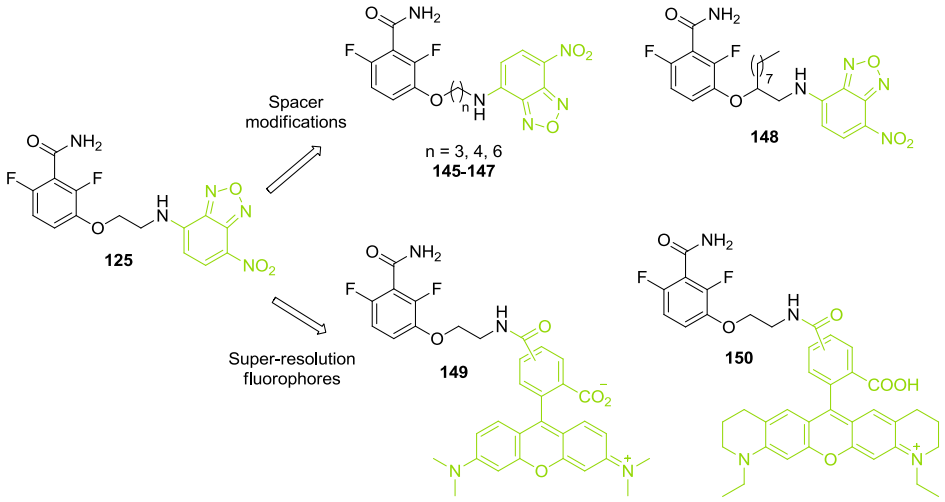

Figure 8. Design of new fluorescent derivatives based on compound **125**.

Once again, NBD derivatives displayed an increase in anisotropy when $MgCl_2$ was added and their basal values were restored by displacement with inhibitor PC190723, with exception of probe **148** (Table 2). Regarding TAMRA and ATTO-565 derivatives **149** and **150**, no anisotropy changes were observed under polymerization conditions.

Table 2. Anisotropy values (r) of fluorescent derivatives **125** and **145**-**150**.

	125	**145**	**146**	**147**	**148**	**149**	**150**
Compound (10 µM)	0.026	0.038	0.032	0.030	0.045	0.030	0.019
+ Bs-FtsZ (10 µM)	0.034	0.042	0.035	0.042	0.130	0.031	0.025
+ GMPCPP (0.1 mM)	0.035	0.040	0.039	0.042	0.186	0.030	0.022
+ $MgCl_2$ (10 mM)	0.086	0.078	0.078	0.127	0.317	0.032	0.025
+ PC190723 (10 µM)	0.036	0.057	0.046	0.067	0.324	0.030	0.023
+ PC190723*	0.026	0.046	0.032	0.046	0.322	0.030	0.019
Compound + GMPCPP	0.034	0.038	0.028	0.038	0.053	0.029	0.019
Compound + $MgCl_2$	0.035	0.033	0.027	0.033	0.054	0.030	0.020
Compound + PC190723	0.038	0.032	0.028	0.032	0.052	0.030	0.020
Mixture without Bs-FtsZ	0.026	0.035	0.027	0.035	0.052	-	-

* Additional 10 µM of PC190723 was added. Final 20 µM concentration.

Therefore, the best candidates to be used as fluorescent probes to set up a displacement binding assay against the PC-binding site seem to be NBD derivatives **125** and **145**-**147**. The study of the effect of these probes in FtsZ polymerization by polymer pelleting assay showed that they alter the polymerization in a concentration depending manner. Thus, compounds **125**, **145**, and **146** increased the pellet percentage of FtsZ protofilaments as their parent compound -PC190723- acting as FtsZ stabilizing agents, whereas derivative **147** reduced FtsZ polymerization as shown by the decrease in the pellet percentage with repect to the control (Figure 9). Hence, this latter inhibitor showed a different activity pattern, acting as an inhibitor of FtsZ polymerization instead of stabilizing the protofilaments.

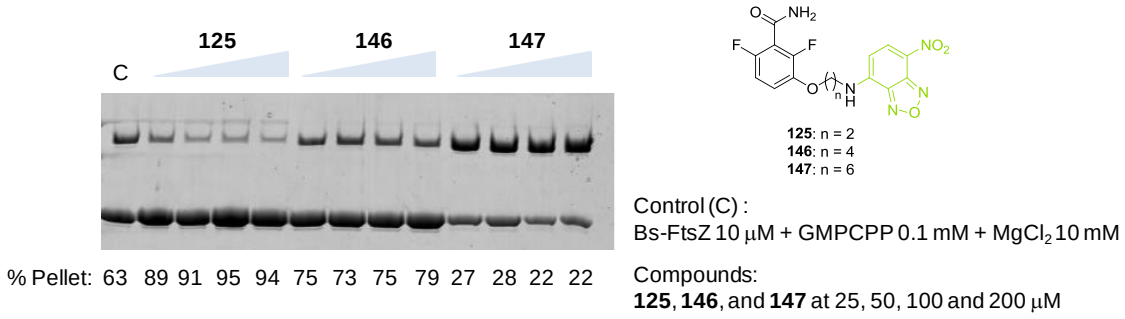

Figure 9. Effects of NBD derivatives **125**, **146**, and **147** in FtsZ polymerization.

In order to evaluate the potential of these probes, displacement anisotropy curves were carried out. Starting from a solution of polymerized FtsZ (5 µM) in the presence of GMPCPP (0.1 mM), $MgCl_2$ (10 mM) and the corresponding fluorescent probe (5 µM), increasing concentrations of the

inhibitor PC190723 were subsequently added until the anisotropy was restored to the basal value of the free compound (Figure 10). As it is shown in the graph, anisotropy values decrease with increasing concentrations of PC, which indicates that all these NBD derivatives can be used as fluorescent probes. Among them, **125** and **146** were selected to carry out a fluorescence-based displacement assay to screen a library of already described FtsZ inhibitors that do not target the GTP-binding site and a series of hits obtained by virtual screening of a commercial library against the PC-binding pocket. This assay, which is currently on going, will allow the assessment of affinity constants for the PC binding site and therefore, the possibility of performing a high-throughput screening in order to identify new FtsZ inhibitors targeting this allosteric binding site.

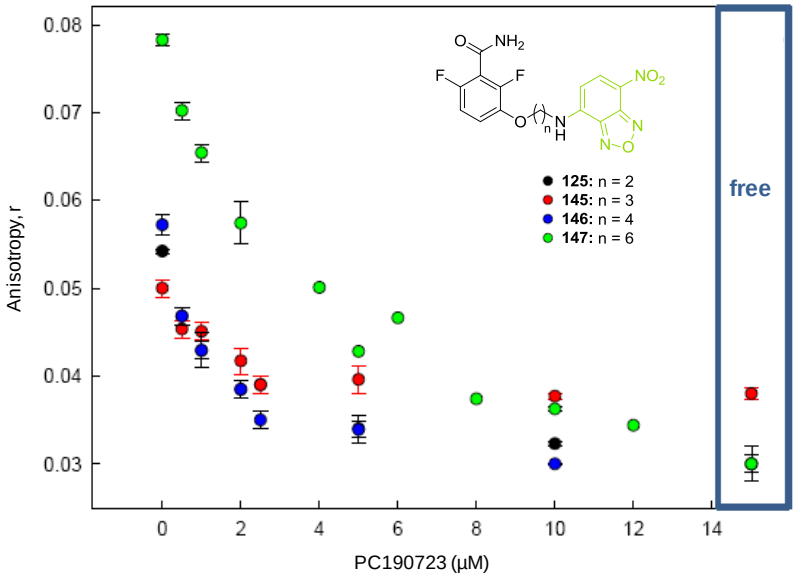

Figure 10. Displacement curves of fluorescent probes **125** and **145**-**147** by PC190723.

Finally, in order to confirm whether selected fluorescent probes would enable to stain FtsZ in cells allowing the monitorization of the division process, we carried out *in vivo* studies of the probes at different concentrations with *B. subtilis* cells. Thus, probes **125** and **145**-**147** were able to label FtsZ in the cells without affecting bacterial cell division at concentrations lower than 50 µM (Figure 11A). This fluorescence disappeared by addition of PC190723 (25 µM) and consequent displacement of the probe, which demonstrate the specificity of the labeling (Figure 11B). Moreover, at higher concentration (200 µM) the probes were able not only to stain the cells but also to alter FtsZ polymerization (Figure 11C).[87] These results show that fluorescent probes **125** and **145**-**147** can be used at 50 µM to visualize FtsZ protein *in vivo*, which demonstrates its ability to study the role of FtsZ in the bacterial division process.

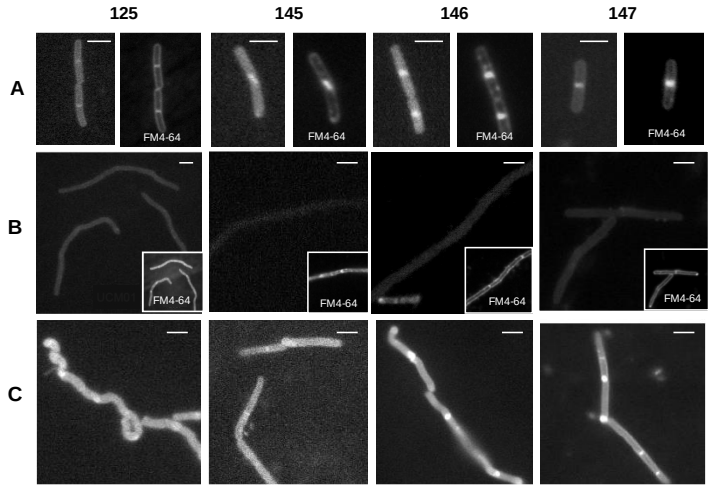

Figure 11. *In vivo* studies of fluorescent probes **125** and **145**-**147** in *B. subtilis*. (A) Labeling of FtsZ with the probes at 50 µM and visualization by fluorescent microscopy. (B) To assess specificity, cells were labeled under previous conditions and PC190723 (25 µM) was then added. (C) Fluorescent filamentous cells were observed at 200 µM of compound.

6.3. Conclusions

In this thesis we have addressed the development of antibacterial agents with a novel mode of action targeting FtsZ protein. We report the first series of synthetic non-nucleotide small molecules able to replace the natural regulator GTP. These inhibitors specifically perturb protein assembly rather than tubulin polymerization and block bacterial cytokinesis. Furthermore, they display high antibacterial activity against multidrug-resistant Gram-positive pathogenic bacteria. Among them, biphenyl **40** stands out as the most promising FtsZ inhibitor, with good affinity (K_d = 0.5 µM) and antibacterial activity [MIC (MRSA) = 7 µM]. This compound together with **29**, **45**, and **48**, acts as an effective FtsZ assembly modifier and leads to filamentous undivided cells, finally disrupting bacterial viability. Overall, these inhibitors contribute to expand the scarce number of GTP mimetics available and provide a compelling rationale for the development of antibacterial agents with novel modes of action.

Regarding the recently identified PC-binding site, we have developed fluorescent derivatives of PC190723 as chemical probes to label FtsZ, which will contribute to the *in vivo* study of the FtsZ role in bacterial division process. Among the synthesized fluorescent compounds, NBD derivatives **125** and **145**-**147** have demonstrated to be valuable tools for the visualization of the Z-ring during bacterial division process, and can be used as fluorescent probes in a displacement assay. This assay, which is currently on going, will allow the identification of new allosteric inhibitors of FtsZ as antibacterial agents.

7. BIBLIOGRAPHY

1. Reardon, S. Antibiotic resistance sweeping developing world. *Nature* **2014**, *509*, 141-142.

2. Silver, L. L. Challenges of antibacterial discovery. *Clin. Microbiol. Rev.* **2011**, *24*, 71-109.

3. Taiwo, S. S. Antibiotic-resistant bugs in the 21st century: a public health challenge. *World J. Clin. Infec. Dis.* **2011**, *1*, 11-16.

4. HHS CDC. Antibiotic resistance threats in the United States, 2013 http://www.cdc.gov/drugresistance/threat-report-2013/pdf/ar-threats-2013-508.pdf (US Centers for disease Control and Prevention, 2013).

5. Wunderink, R. G.; Waterer, G. W. Clinical practice. Community-acquired pneumonia. *New Engl. J. Med.* **2014**, *370*, 543-551.

6. O'Connell, K. M. G.; Hodgkinson, J. T.; Sore, H. F.; Welch, M.; Salmond, G. P. C.; Spring, D. R. Combating multidrug-resistant bacteria: current strategies for the discovery of novel antibacterials. *Angew. Chem. Int. Ed.* **2013**, *52*, 10706-10733.

7. Butler, M. S.; Cooper, M. A. Antibiotics in the clinical pipeline in 2011. *J. Antibiot.* **2011**, *64*, 413-425.

8. Wuite, J.; Davies, B. I.; Go, M. J.; Lambers, J. C.; Jackson, D.; Mellows, G.; Tasker, T. C. G. Pseudomonic acid, a new antibiotic for topical therapy. *J. Am. Acad. Dermatol.* **1985**, *12*, 1026-1031.

9. Butler, M. S.; Blaskovich, M. A.; Cooper, M. A. Antibiotics in the clinical pipeline in 2013. *J. Antibiot.* **2013**, *66*, 571-591.

10. Sirturo web page. http://www.sirturo.com.

11. Diacon, A. H.; Dawson, R.; von Groote-Bidlingmaier, F.; Symons, G.; Venter, A.; Donald, P. R.; van Niekerk, C.; Everitt, D.; Winter, H.; Becker, P.; Mendel, C. M.; Spigelman, M. K. 14-day bactericidal activity of PA-824, bedaquiline, pyrazinamide, and moxifloxacin combinations: a randomised trial. *Lancet* **2012**, *380*, 986-993.

12. Cooper, M. A.; Shlaes, D. Fix the antibiotics pipeline. *Nature* **2011**, *472*, 32.

13. Payne, D. J.; Gwynn, M. N.; Holmes, D. J.; Pompliano, D. L. Drugs for bad bugs: confronting the challenges of antibacterial discovery. *Nat. Rev. Drug. Discov.* **2007**, *6*, 29-40.

14. Projan, S. J.; Shlaes, D. M. Antibacterial drug discovery: is it all downhill from here? *Clin. Microbiol. Infec.* **2004**, *10*, 18-22.

15. Lewis, K. Platforms for antibiotic discovery. *Nat. Rev. Drug Discov.* **2013**, *12*, 371-387.

16. Bald, D.; Koul, A. Advances and strategies in discovery of new antibacterials for combating metabolically resting bacteria. *Drug Discov. Today* **2013**, *18*, 250-255.

17. Boggs, A. F.; Miller, G. H. Antibacterial drug discovery: is small pharma the solution? *Clin. Microbiol. Infec.* **2004**, *10*, 32-36.

18. Wright, G. D. Antibiotics: a new hope. *Chem. Biol.* **2012**, *19*, 3-10.

19. Hevener, K. E.; Cao, S. Y.; Zhu, T.; Su, P. C.; Mehboob, S.; Johnson, M. E. Special challenges to the rational design of antibacterial agents. *Ann. Rep. Med. Chem.* **2013**, *48*, 283-298.

20. WHO, drug resistance, antimicrobial resistance: global report on surveillance 2014. http://www.who.int/drugresistance/documents/surveillancereport/en/ (World Health Organization).

21. The antibiotic alarm. *Nature* **2013**, *495*, 141.

22. Leclercq, R. Epidemiological and resistance issues in multidrug-resistant staphylococci and enterococci. *Clin. Microbiol. Infect.* **2009**, *15*, 224-231.

23. Gould, I. M.; David, M. Z.; Esposito, S.; Garau, J.; Lina, G.; Mazzei, T.; Peters, G. New insights into meticillin-resistant *Staphylococcus aureus* (MRSA) pathogenesis, treatment and resistance. *Int. J. Antimicrob. Agents* **2012**, *39*, 96-104.

24. De Angelis, F.; Lee, J. K.; O'Connell, J. D., 3rd; Miercke, L. J.; Verschueren, K. H.; Srinivasan, V.; Bauvois, C.; Govaerts, C.; Robbins, R. A.; Ruysschaert, J. M.; Stroud, R. M.; Vandenbussche, G. Metal-induced conformational changes in ZneB suggest an active role of membrane fusion proteins in efflux resistance systems. *Proc. Natl. Acad. Sci. USA* **2010**, *107*, 11038-11043.

25. Davies, J.; Davies, D. Origins and evolution of antibiotic resistance. *Microbiol. Mol. Biol. Rev.* **2010**, *74*, 417-433.

26. Levy, S. B.; Marshall, B. Antibacterial resistance worldwide: causes, challenges and responses. *Nat. Med.* **2004**, *10*, S122-S129.

27. Pokrovskaya, V.; Belakhov, V.; Hainrichson, M.; Yaron, S.; Baasov, T. Design, synthesis, and evaluation of novel fluoroquinolone-aminoglycoside hybrid antibiotics. *J. Med. Chem.* **2009**, *52*, 2243-2254.

28. Zasloff, M. Antimicrobial peptides of multicellular organisms. *Nature* **2002**, *415*, 389-395.

29. Bumann, D. Has nature already identified all useful antibacterial targets? *Curr. Opin. Microbiol.* **2008**, *11*, 387-392.

30. Bassetti, M.; Merelli, M.; Temperoni, C.; Astilean, A. New antibiotics for bad bugs: where are we? *Ann. Clin. Microbiol. Antimicrob.* **2013**, *12*, 22.

31. Lock, R. L.; Harry, E. J. Cell-division inhibitors: new insights for future antibiotics. *Nat. Rev. Drug Discov.* **2008**, *7*, 324-338.

32. Vollmer, W. The prokaryotic cytoskeleton: a putative target for inhibitors and antibiotics? *Appl. Microbiol. Biotechnol.* **2006**, *73*, 37-47.

33. Sass, P.; Brotz-Oesterhelt, H. Bacterial cell division as a target for new antibiotics. *Curr. Opin. Microbiol.* **2013**, *16*, 522-530.

34. Erickson, H. P.; Anderson, D. E.; Osawa, M. FtsZ in bacterial cytokinesis: cytoskeleton and force generator all in one. *Microbiol. Mol. Biol. R.* **2010**, *74*, 504-528.

35. Oliva, M. A.; Cordell, S. C.; Lowe, J. Structural insights into FtsZ protofilament formation. *Nat. Struct. Mol. Biol.* **2004**, *11*, 1243-1250.

36. Adams, D. W.; Errington, J. Bacterial cell division: assembly, maintenance and disassembly of the Z ring. *Nat. Rev. Microbiol.* **2009**, *7*, 642-653.

37. Stricker, J.; Maddox, P.; Salmon, E. D.; Erickson, H. P. Rapid assembly dynamics of the *Escherichia coli* FtsZ-ring demonstrated by fluorescence recovery after photobleaching. *Proc. Natl. Acad. Sci. USA* **2002**, *99*, 3171-3175.

38. Anderson, D. E.; Gueiros-Filho, F. J.; Erickson, H. P. Assembly dynamics of FtsZ rings in *Bacillus subtilis* and *Escherichia coli* and effects of FtsZ-regulating proteins. *J. Bacteriol.* **2004**, *186*, 5775-5781.

39. Kirkpatrick, C. L.; Viollier, P. H. New(s) to the (Z-)ring. *Curr. Opin. Microbiol.* **2011**, *14*, 691-697.

40. Margolin, W. Bacterial division: another way to box in the ring. *Curr. Biol.* **2006**, *16*, R881-R884.

41. Sass, P.; Josten, M.; Famulla, K.; Schiffer, G.; Sahl, H. G.; Hamoen, L.; Brotz-Oesterhelt, H. Antibiotic acyldepsipeptides activate ClpP peptidase to degrade the cell division protein FtsZ. *Proc. Natl. Acad. Sci. USA* **2011**, *108*, 17474-17479.

42. Lowe, J.; Amos, L. A. Crystal structure of the bacterial cell-division protein FtsZ. *Nature* **1998**, *391*, 203-206.

43. Li, Y.; Hsin, J.; Zhao, L. Y.; Cheng, Y. W.; Shang, W. N.; Huang, K. C.; Wang, H. W.; Ye, S. FtsZ protofilaments use a hinge-opening mechanism for constrictive force generation. *Science* **2013**, *341*, 392-395.

44. Matsui, T.; Han, X. R.; Yu, J.; Yao, M.; Tanaka, I. Structural change in FtsZ induced by intermolecular interactions between bound GTP and the T7 loop. *J. Biol. Chem.* **2014**, *289*, 3501-3509.

45. Matsui, T.; Yamane, J.; Mogi, N.; Yamaguchi, H.; Takemoto, H.; Yao, M.; Tanaka, I. Structural reorganization of the bacterial cell-division protein FtsZ from *Staphylococcus aureus*. *Acta Crystallogr. Sect. D-Biol. Crystallogr.* **2012**, *68*, 1175-1188.

46. Lappchen, T.; Hartog, A. F.; Pinas, V. A.; Koomen, G. J.; den Blaauwen, T. GTP analogue inhibits polymerization and GTPase activity of the bacterial protein FtsZ without affecting its eukaryotic homologue tubulin. *Biochemistry* **2005**, *44*, 7879-7884.

47. Kumar, K.; Awasthi, D.; Berger, W. T.; Tonge, P. J.; Slayden, R. A.; Ojima, I. Discovery of anti-TB agents that target the cell-division protein FtsZ. *Future Med. Chem.* **2010**, *2*, 1305-1323.

48. Anderson, D. E.; Kim, M. B.; Moore, J. T.; O'Brien, T. E.; Sorto, N. A.; Grove, C. I.; Lackner, L. L.; Ames, J. B.; Shaw, J. T. Comparison of small molecule inhibitors of the bacterial cell division protein FtsZ and identification of a reliable cross-species inhibitor. *ACS Chem. Biol.* **2012**, *7*, 1918-1928.

49. Schaffner-Barbero, C.; Martín-Fontecha, M.; Chacón, P.; Andreu, J. M. Targeting the assembly of bacterial cell division protein FtsZ with small molecules. *ACS Chem. Biol.* **2012**, *7*, 269-277.

50. Foss, M. H.; Eun, Y. J.; Grove, C. I.; Pauw, D. A.; Sorto, N. A.; Rensvold, J. W.; Pagliarini, D. J.; Shaw, J. T.; Weibel, D. B. Inhibitors of bacterial tubulin target bacterial membranes *in vivo*. *MedChemComm* **2013**, *4*, 112-119.

51. Wang, J.; Galgoci, A.; Kodali, S.; Herath, K. B.; Jayasuriya, H.; Dorso, K.; Vicente, F.; Gonzalez, A.; Cully, D.; Bramhill, D.; Singh, S. Discovery of a small molecule that inhibits cell division by blocking FtsZ, a novel therapeutic target of antibiotics. *J. Biol. Chem.* **2003**, *278*, 44424-44428.

52. Plaza, A.; Keffer, J. L.; Bifulco, G.; Lloyd, J. R.; Bewley, C. A. Chrysophaentins A-H, antibacterial bisdiarylbutene macrocycles that inhibit the bacterial cell division protein FtsZ. *J. Am. Chem. Soc.* **2010**, *132*, 9069-9077.

53. Rai, D.; Singh, J. K.; Roy, N.; Panda, D. Curcumin inhibits FtsZ assembly: an attractive mechanism for its antibacterial activity. *Biochem. J.* **2008**, *410*, 147-155.

54. Kim, M. B.; Shaw, J. T. Synthesis of antimicrobial natural products targeting FtsZ: (+)-totarol and related totarane diterpenes. *Org. Lett.* **2010**, *12*, 3324-3327.

55. Jaiswal, R.; Beuria, T. K.; Mohan, R.; Mahajan, S. K.; Panda, D. Totarol inhibits bacterial cytokinesis by perturbing the assembly dynamics of FtsZ. *Biochemistry* **2007**, *46*, 4211-4220.

56. Margalit, D. N.; Romberg, L.; Mets, R. B.; Hebert, A. M.; Mitchison, T. J.; Kirschner, M. W.; RayChaudhuri, D. Targeting cell division: small-molecule inhibitors of FtsZ GTPase perturb cytokinetic ring assembly and induce bacterial lethality. *Proc. Natl. Acad. Sci. USA* **2004**, *101*, 11821-11826.

57. Beuria, T. K.; Santra, M. K.; Panda, D. Sanguinarine blocks cytokinesis in bacteria by inhibiting FtsZ assembly and bundling. *Biochemistry* **2005**, *44*, 16584-16593.

58. Domadia, P. N.; Bhunia, A.; Sivaraman, J.; Swarup, S.; Dasgupta, D. Berberine targets assembly of *Escherichia coli* cell division protein FtsZ. *Biochemistry* **2008**, *47*, 3225-3234.

59. Parhi, A.; Lu, S.; Kelley, C.; Kaul, M.; Pilch, D. S.; LaVoie, E. J. Antibacterial activity of substituted dibenzo[a,g]quinolizin-7-ium derivatives. *Bioorg. Med. Chem. Lett.* **2012**, *22*, 6962-6966.

60. Parhi, A.; Kelley, C.; Kaul, M.; Pilch, D. S.; LaVoie, E. J. Antibacterial activity of substituted 5-methylbenzo[c]phenanthridinium derivatives. *Bioorg. Med. Chem. Lett.* **2012**, *22*, 7080-7083.

61. Kelley, C.; Zhang, Y.; Parhi, A.; Kaul, M.; Pilch, D. S.; LaVoie, E. J. 3-Phenyl substituted 6,7-dimethoxyisoquinoline derivatives as FtsZ-targeting antibacterial agents. *Bioorg. Med. Chem.* **2012**, *20*, 7012-7029.

62. Kelley, C.; Lu, S.; Parhi, A.; Kaul, M.; Pilch, D. S.; Lavoie, E. J. Antimicrobial activity of various 4- and 5-substituted 1-phenylnaphthalenes. *Eur. J. Med. Chem.* **2012**, *60*, 395-409.

63. Kaul, M.; Parhi, A. K.; Zhang, Y.; LaVoie, E. J.; Tuske, S.; Arnold, E.; Kerrigan, J. E.; Pilch, D. S. A bactericidal guanidinomethyl biaryl that alters the dynamics of bacterial FtsZ polymerization. *J. Med. Chem.* **2012**, *55*, 10160-10176.

64. Huang, Q.; Kirikae, F.; Kirikae, T.; Pepe, A.; Amin, A.; Respicio, L.; Slayden, R. A.; Tonge, P. J.; Ojima, I. Targeting FtsZ for antituberculosis drug discovery: noncytotoxic taxanes as novel antituberculosis agents. *J. Med. Chem.* **2006**, *49*, 463-466.

65. Singh, D.; Bhattacharya, A.; Rai, A.; Dhaked, H. P.; Awasthi, D.; Ojima, I.; Panda, D. SB-RA-2001 inhibits bacterial proliferation by targeting FtsZ assembly. *Biochemistry* **2014**, *53*, 2979-2992.

66. Kumar, K.; Awasthi, D.; Lee, S. Y.; Zanardi, I.; Ruzsicska, B.; Knudson, S.; Tonge, P. J.; Slayden, R. A.; Ojima, I. Novel trisubstituted benzimidazoles, targeting Mtb FtsZ, as a new class of antitubercular agents. *J. Med. Chem.* **2011**, *54*, 374-381.

67. Stokes, N. R.; Sievers, J.; Barker, S.; Bennett, J. M.; Brown, D. R.; Collins, I.; Errington, V. M.; Foulger, D.; Hall, M.; Halsey, R.; Johnson, H.; Rose, V.; Thomaides, H. B.; Haydon, D. J.; Czaplewski, L. G.; Errington, J. Novel inhibitors of bacterial cytokinesis identified by a cell-based antibiotic screening assay. *J. Biol. Chem.* **2005**, *280*, 39709-39715.

68. Ohashi, Y.; Chijiiwa, Y.; Suzuki, K.; Takahashi, K.; Nanamiya, H.; Sato, T.; Hosoya, Y.; Ochi, K.; Kawamura, F. The lethal effect of a benzamide derivative, 3-methoxybenzamide, can be suppressed by mutations within a cell division gene, ftsZ, in *Bacillus subtilis*. *J. Bacteriol.* **1999**, *181*, 1348-1351.

69. Czaplewski, L. G.; Collins, I.; Boyd, E. A.; Brown, D.; East, S. P.; Gardiner, M.; Fletcher, R.; Haydon, D. J.; Henstock, V.; Ingram, P.; Jones, C.; Noula, C.; Kennison, L.; Rockley, C.; Rose, V.; Thomaides-Brears, H. B.; Ure, R.; Whittaker, M.; Stokes, N. R. Antibacterial alkoxybenzamide inhibitors of the essential bacterial cell division protein FtsZ. *Bioorg. Med. Chem. Lett.* **2009**, *19*, 524-527.

70. Brown, D. R. C., I.; Czaplewski, L. G; Haydon, D. J. Antibacterial agents. WO2007/107758 A1.

71. Haydon, D. J.; Bennett, J. M.; Brown, D.; Collins, I.; Galbraith, G.; Lancett, P.; Macdonald, R.; Stokes, N. R.; Chauhan, P. K.; Sutariya, J. K.; Nayal, N.; Srivastava, A.; Beanland, J.; Hall, R.; Henstock, V.; Noula, C.; Rockley, C.; Czaplewski, L. Creating an antibacterial with *in vivo* efficacy: synthesis and characterization of potent inhibitors of the bacterial cell division protein FtsZ with improved pharmaceutical properties. *J. Med. Chem.* **2010**, *53*, 3927-3936.

72. Haydon, D. J.; Stokes, N. R.; Ure, R.; Galbraith, G.; Bennett, J. M.; Brown, D. R.; Baker, P. J.; Barynin, V. V.; Rice, D. W.; Sedelnikova, S. E.; Heal, J. R.; Sheridan, J. M.; Aiwale, S. T.; Chauhan, P. K.; Srivastava, A.; Taneja, A.; Collins, I.; Errington, J.; Czaplewski, L. G. An inhibitor of FtsZ with potent and selective anti-staphylococcal activity. *Science* **2008**, *321*, 1673-1675.

73. Andreu, J. M.; Schaffner-Barbero, C.; Huecas, S.; Alonso, D.; Lopez-Rodriguez, M. L.; Ruiz-Avila, L. B.; Nunez-Ramirez, R.; Llorca, O.; Martin-Galiano, A. J. The antibacterial cell division inhibitor PC190723 is an FtsZ polymer-stabilizing agent that induces filament assembly and condensation. *J. Biol. Chem.* **2010**, *285*, 14239-14246.

74. Kaul, M.; Zhang, Y.; Parhi, A. K.; Lavoie, E. J.; Pilch, D. S. Inhibition of RND-type efflux pumps confers the FtsZ-directed prodrug TXY436 with activity against Gram-negative bacteria. *Biochem. Pharmacol.* **2014**, *89*, 321-328.

75. Kaul, M.; Mark, L.; Zhang, Y. Z.; Parhi, A. K.; LaVoie, E. J.; Pilch, D. S. Pharmacokinetics and *in vivo* antistaphylococcal efficacy of TXY541, a 1-methylpiperidine-4-carboxamide prodrug of PC190723. *Biochem. Pharmacol.* **2013**, *86*, 1699-1707.

76. Kaul, M.; Mark, L.; Zhang, Y. Z.; Parhi, A. K.; LaVoie, E. J.; Pilch, D. S. An FtsZ-targeting prodrug with oral antistaphylococcal efficacy *in vivo*. *Antimicrob. Agents Chemother.* **2013**, *57*, 5860-5869.

77. Haydon, D. J. C., L.G.; Stokes, N.R.; Davies, D.; Collins, I.; Palmer, J.T.; Mitchell, J.P; Pitt, G. R. W.; Offerman, D. Aromatic amides and uses thereof. WO2012/142671.

78. Stokes, N. R.; Baker, N.; Bennett, J. M.; Berry, J.; Collins, I.; Czaplewski, L. G.; Logan, A.; Macdonald, R.; Macleod, L.; Peasley, H.; Mitchell, J. P.; Nayal, N.; Yadav, A.; Srivastava, A.; Haydon, D. J. An improved small-molecule inhibitor of FtsZ with superior *in vitro* potency, drug-like properties, and *in vivo* efficacy. *Antimicrob. Agents Chemother.* **2013**, *57*, 317-325.

79. Stokes, N. R.; Baker, N.; Bennett, J. M.; Chauhan, P. K.; Collins, I.; Davies, D. T.; Gavade, M.; Kumar, D.; Lancett, P.; Macdonald, R.; MacLeod, L.; Mahajan, A.; Mitchell, J. P.; Nayal, N.; Nayal, Y. N.; Pitt, G. R. W.; Singh, M.; Yadav, A.; Srivastava, A.; Czaplewski, L. G.; Haydon, D. J. Design, synthesis and structure-activity relationships of substituted oxazole-benzamide antibacterial inhibitors of FtsZ. *Bioorg. Med. Chem. Lett.* **2014**, *24*, 353-359.

80. Elsen, N. L.; Lu, J.; Parthasarathy, G.; Reid, J. C.; Sharma, S.; Soisson, S. M.; Lumb, K. J. Mechanism of action of the cell-division inhibitor PC190723: modulation of FtsZ assembly cooperativity. *J. Am. Chem. Soc.* **2012**, *134*, 12342-12345.

81. Tan, C. M.; Therien, A. G.; Lu, J.; Lee, S. H.; Caron, A.; Gill, C. J.; Lebeau-Jacob, C.; Benton-Perdomo, L.; Monteiro, J. M.; Pereira, P. M.; Elsen, N. L.; Wu, J.; Deschamps, K.; Petcu, M.; Wong, S.; Daigneault, E.; Kramer, S.; Liang, L.; Maxwell, E.; Claveau, D.; Vaillancourt, J.; Skorey, K.; Tam, J.; Wang, H.; Meredith, T. C.; Sillaots, S.; Wang-Jarantow, L.; Ramtohul, Y.; Langlois, E.; Landry, F.; Reid, J. C.; Parthasarathy, G.; Sharma, S.; Baryshnikova, A.; Lumb, K. J.; Pinho, M. G.; Soisson, S. M.; Roemer, T. Restoring methicillin-resistant *Staphylococcus aureus* susceptibility to beta-lactam antibiotics. *Sci. Transl. Med.* **2012**, *4*, 126ra35.

82. Schaffner-Barbero, C.; Gil-Redondo, R.; Ruiz-Avila, L. B.; Huecas, S.; Lappchen, T.; den Blaauwen, T.; Diaz, J. F.; Morreale, A.; Andreu, J. M. Insights into nucleotide recognition by cell division protein FtsZ from a *mant*-GTP competition assay and molecular dynamics. *Biochemistry* **2010**, *49*, 10458-10472.

83. Turrado, C.; Puig, T.; García-Cárceles, J.; Artola, M.; Benhamú, B.; Ortega-Gutiérrez, S.; Relat, J.; Oliveras, G.; Blancafort, A.; Haro, D.; Marrero, P. F.; Colomer, R.; López-Rodríguez, M. L. New synthetic inhibitors of fatty acid synthase with anticancer activity. *J. Med. Chem.* **2012**, *55*, 5013-5023.

84. Ruiz-Avila, L. B.; Huecas, S.; Artola, M.; Vergoñós, A.; Ramírez-Aportela, E.; Cercenado, E.; Barasoain, I.; Vázquez-Villa, H.; Martín-Fontecha, M.; Chacón, P.; López-Rodríguez, M. L.;

Andreu, J. M. Synthetic inhibitors of bacterial cell division targeting the GTP-binding site of FtsZ. *ACS Chem. Biol.* **2013**, *8*, 2072-2083.

85. Nonejuie, P.; Burkart, M.; Pogliano, K.; Pogliano, J. Bacterial cytological profiling rapidly identifies the cellular pathways targeted by antibacterial molecules. *Proc. Natl. Acad. Sci. USA* **2013**, *110*, 16169-16174.

86. Lamsa, A.; Liu, W. T.; Dorrestein, P. C.; Pogliano, K. The *Bacillus subtilis* cannibalism toxin SDP collapses the proton motive force and induces autolysis. *Mol. Microbiol.* **2012**, *84*, 486-500.

87. Adams, D. W.; Wu, L. J.; Czaplewski, L. G.; Errington, J. Multiple effects of benzamide antibiotics on FtsZ function. *Mol. Microbiol.* **2011**, *80*, 68-84.

88. Heilemann, M.; van de Linde, S.; Mukherjee, A.; Sauer, M. Super-resolution imaging with small organic fluorophores. *Angew. Chem. Int. Ed.* **2009**, *48*, 6903-6908.

89. Sliwinska, A.; Zwierzak, A. Regioselective aminobromination of terminal alkenes. *Tetrahedron* **2003**, *59*, 5927-5934.

90. Heyne, B.; Beddie, C.; Scaiano, J. C. Synthesis and characterization of a new fluorescent probe for reactive oxygen species. *Org. Biomol. Chem.* **2007**, *5*, 1454-1458.

91. Huh, N. W.; Porter, N. A.; McIntosh, T. J.; Simon, S. A. The interaction of polyphenols with bilayers: conditions for increasing bilayer adhesion. *Biophys. J.* **1996**, *71*, 3261-3277.

92. Li, W. S.; Kim, K. S.; Jiang, D. L.; Tanaka, H.; Kawai, T.; Kwon, J. H.; Kim, D.; Aida, T. Construction of segregated arrays of multiple donor and acceptor units using a dendritic scaffold: remarkable dendrimer effects on photoinduced charge separation. *J. Am. Chem. Soc.* **2006**, *128*, 10527-10532.

93. Jung, M. E.; Koch, P. Mild, selective deprotection of PMB ethers with triflic acid/1,3-dimethoxybenzene. *Tetrahedron Lett.* **2011**, *52*, 6051-6054.

94. Fan, F. Y.; Culligan, S. W.; Mastrangelo, J. C.; Katsis, D.; Chen, S. H.; Blanton, T. N. Novel glass-forming liquid crystals. 6. High-temperature glassy nematics. *Chem. Mater.* **2001**, *13*, 4584-4594.

95. Puig, T.; Turrado, C.; Benhamú, B.; Aguilar, H.; Relat, J.; Ortega-Gutiérrez, S.; Casals, G.; Marrero, P. F.; Urruticoechea, A.; Haro, D.; López-Rodríguez, M. L.; Colomer, R. Novel inhibitors of fatty acid synthase with anticancer activity. *Clin. Cancer Res.* **2009**, *15*, 7608-7615.

96. Van Loevezijn, A. I. B., W. I.; Stoit, A.; Rensink, A. A. M.; Venhorst, J.; Van Der Neut, M. A. W.; De Haan, M.; Kruse, C. G. Arylsulfonyl pyrazoline carboxamidine derivatives as 5-HT_6 antagonists. WO2009115515.

97. Picraux, L. B.; Smeigh, A. L.; Guo, D.; McCusker, J. K. Intramolecular energy transfer involving heisenberg spin-coupled dinuclear iron-oxo complexes. *Inorg. Chem.* **2005**, *44*, 7846-7859.

98. Jones, P. G.; Kus, P. Secondary interactions in crystals of all ten isomers of di(bromomethyl)naphthalene. *J. Chem. Sci.* **2010**, *65*, 433-444.

99. Percec, V.; Wilson, D. A.; Leowanawat, P.; Wilson, C. J.; Hughes, A. D.; Kaucher, M. S.; Hammer, D. A.; Levine, D. H.; Kim, A. J.; Bates, F. S.; Davis, K. P.; Lodge, T. P.; Klein, M. L.; DeVane, R. H.; Aqad, E.; Rosen, B. M.; Argintaru, A. O.; Sienkowska, M. J.; Rissanen, K.; Nummelin, S.; Ropponen, J. Self-assembly of janus dendrimers into uniform dendrimersomes and other complex architectures. *Science* **2010**, *328*, 1009-1014.

100. Stembrecher, T.; Hrenn, A.; Dormann, K. L.; Merfort, I.; Labahn, A. Bornyl (3,4,5-trihydroxy)-cinnamate- An optimized human neutrophil elastase inhibitor designed by free energy calculations. *Bioorg. Med. Chem.* **2008**, *16*, 2385-2390.

101. Korn, T. J.; Schade, M. A.; Cheemala, M. N.; Wirth, S.; Guevara, S. A.; Cahiez, G.; Knochel, P. Cobalt-catalyzed cross-coupling reactions of heterocyclic chlorides with arylmagnesium halides and of polyfunctionalized arylcopper reagents with aryl bromides, chlorides, fluorides and tosylates. *Synthesis* **2006**, 3547-3574.

102. Petronijevic, F. R.; Wipf, P. Total synthesis of (+/-)-cycloclavine and (+/-)-5-epi-cycloclavine. *J. Am. Chem. Soc.* **2011**, *133*, 7704-7707.

103. Nilsson, B. M.; Ringdahl, B.; Hacksell, U. Derivatives of the muscarinic agent *N*-methyl-*N*-(1-methyl-4-pyrrolidino-2-butynyl)acetamide. *J. Med. Chem.* **1988**, *31*, 577-582.

104. McGill, N. W.; Williams, S. J. 2,6-Disubstituted benzoates as neighboring groups for enhanced diastereoselectivity in beta-galactosylation reactions: synthesis of beta-1,3-linked oligogalactosides related to arabinogalactan proteins. *J. Org. Chem.* **2009**, *74*, 9388-9398.

105. Andreu, J. M.; Schaffner-Barbero, C.; Huecas, S.; Alonso, D.; Lopez-Rodriguez, M. L.; Ruiz-Avila, L. B.; Nunez-Ramirez, R.; Llorca, O.; Martin-Galiano, A. J. The antibacterial cell division inhibitor PC190723 is a FtsZ polymer stabilizing agent which induces filament assembly and condensation. *J. Biol. Chem.* **2010**, *285*, 14239-14246.

106. Rivas, G.; Lopez, A.; Mingorance, J.; Ferrandiz, M. J.; Zorrilla, S.; Minton, A. P.; Vicente, M.; Andreu, J. M. Magnesium-induced linear self-association of the FtsZ bacterial cell division protein monomer - The primary steps for FtsZ assembly. *J. Biol. Chem.* **2000**, *275*, 11740-11749.

107. Andreu, J. M. Large scale purification of brain tubulin with the modified Weisenberg procedure. *Methods Mol. Med.* **2007**, *137*, 17-28.

108. Levin, P. A.; Kurtser, I. G.; Grossman, A. D. Identification and characterization of a negative regulator of FtsZ ring formation in *Bacillus subtilis*. *Proc. Natl. Acad. Sci. USA* **1999**, *96*, 9642-9647.

109. Strauss, M. P.; Liew, A. T. F.; Turnbull, L.; Whitchurch, C. B.; Monahan, L. G.; Harry, E. J. 3D-SIM super resolution microscopy reveals a bead-like arrangement for FtsZ and the division machinery: implications for triggering cytokinesis. *Plos Biol.* **2012**, *10*, e1001389.

110. Totrov, M.; Abagyan, R. Flexible protein-ligand docking by global energy optimization in internal coordinates. *Proteins* **1997**, *Suppl 1*, 215-220.

111. Bottegoni, G.; Kufareva, I.; Totrov, M.; Abagyan, R. Four-dimensional docking: a fast and accurate account of discrete receptor flexibility in ligand docking. *J. Med. Chem.* **2009**, *52*, 397-406.

112. Némethy, G.; Gibson, K. D.; Palmer, K. A.; Yoon, C. N.; Paterlini, G.; Zagari, A.; Rumsey, S.; Scheraga, H. A. Energy parameters in polypeptides. 10. Improved geometrical parameters and nonbonded interactions for use in the ECEPP/3 algorithm, with application to proline-containing peptides. *J. Phys. Chem.* **1992**, *96*, 6472-6484.

113. Abagyan, R.; Totrov, M.; Kuznetsov, D. ICM - A new method for protein modeling and design. Applications to docking and structure prediction from the distorted native conformation. *J. Comput. Chem.* **1994**, *15*, 488-506.

114. Halgren, T. A. Merck molecular force field. V. Extension of MMFF94 using experimental data, additional computational data, and empirical rules. *J. Comput. Chem.* **1996**, *17*, 616-641.